

Some pages of this thesis may have been removed for copyright restrictions.

If you have discovered material in AURA which is unlawful e.g. breaches copyright, (either yours or that of a third party) or any other law, including but not limited to those relating to patent, trademark, confidentiality, data protection, obscenity, defamation, libel, then please read our [Takedown Policy](#) and [contact the service](#) immediately

POLYMER MODIFIED CEMENT: HYDRATION, MICROSTRUCTURE AND DIFFUSION PROPERTIES

SHUNJIE ZENG

Submitted for the Degree of Doctor of Philosophy

**The University of Aston in Birmingham,
Civil Engineering Department**

June 1996

This copy of the thesis has been supplied on condition that anyone who consults it is understood to recognise that its copyright rests with its author and that no quotation from the thesis and no information derived from it may be published without the author's prior, written consent.

**Polymer Modified Cement:
Hydration, Microstructure and Diffusion Properties**

Shunjie Zeng

Submitted for the degree of Doctor of Philosophy, March 1996

Thesis Summary

Polymer modified cement (PMC) has been widely used in the construction industry e.g. in concrete repair and bridge deck overlay, but it is noted that theoretical studies of PMC are lagging far behind its engineering application. A fundamental investigation of polymer modified cement systems, covering hydration characteristics, microstructure and diffusion properties, has been carried out.

Investigations concentrated on the styrene butadiene rubber (SBR) latex and formulations included standard carboxylated and special carboxylated latexes. The aqueous component, containing the stabilisers and antifoaming agent but not the polymer solids, was also used. For comparison, limited investigations were carried out using other polymer types e.g. acrylic, ethylene-vinyl acetate (EVA), and redispersible powders rather than emulsions.

Experiments were conducted in four main areas:

- 1) influence of polymer dispersions on the kinetics of cement hydration
- 2) microstructure development in polymer modified cement pastes
- 3) nature of interactions between polymer dispersions and hydrating cementitious materials
- 4) role of polymer in modifying the diffusion resistance of cement materials

The major findings were:

- 1) All latex systems investigated acted as retarders for cement hydration. The extent of retardation depends on the type of polymer. The mechanism for cement hydration may be changed and excessive retardation influences properties.
- 2) Polymer modified cements exhibited either similar or coarser pore structures compared with unmodified cements. Results suggest that polymer mainly exists in a mixture of cement hydrates and polymer phase. Very little evidence was found for the formation of a distinct polymer film phase.
- 3) During the first few days of curing the polymer solids are removed from the pore solution and concentrations of OH^- , Na^+ and K^+ are reduced. These observations are probably a result of polymer-cement surface interactions since there was no evidence of any chemical reactions or degradation of the polymer.
- 4) Improved diffusional resistance of modified cements depends on the ability to achieve adequate workability at low w/c ratio, rather than modification of matrix structure.

Keywords: Cement, Latex, Styrene Butadiene Rubber, Acrylics, Ethylene-Vinyl Acetate, Hydration, Microstructure, Porosity, Diffusion

ACKNOWLEDGEMENTS

Dedication

To my wife and my son, Shaomi and Yangmin, for their love.

ACKNOWLEDGEMENTS

First of all, I wish to express sincere appreciation to my supervisor Dr. N. R. Short for his invaluable advice, enthusiastic encouragement and support throughout this research project.

I am very grateful to Professor C. L. Page, my associate supervisor, for his guidance and suggestion on this project.

Many thanks to Dr G. Sergi for his advice on Chapter 7 (Diffusion Properties of PMC).

During the course of this research, the technical staffs of Civil Engineering Department, in particular Mr C. Thompson and Mr R. Poole gave me lots of assistance in the laboratory work. I would like to thank them for their help.

I wish to thank my research colleagues and friends, Drs S. Yu, V. Ngala, M. Maleki and Mr Salbin for their stimulating discussions and help.

Finally, I am deeply indebted to Engineering Physical Science Research Council (EPSRC) and Civil Engineering Department for financial support.

LIST OF CONTENTS

	Page
Title Page	1
Thesis Summary	2
Dedication	3
Acknowledgements	4
List of Contents	5
List of Tables	11
List of Figures	12
List of Abbreviations and Symbols	16
CHAPTER 1 INTRODUCTION AND AIMS OF THE STUDY	18
1.1 Classification of Polymer Cement Composites	18
1.2 Aims of the Present Study	21
CHAPTER 2 BACKGROUND OF POLYMER MODIFIED/ CEMENTS/MORTARS/CONCRETE (PMC)	25
2.1 History	25
2.2 Polymer Latexes Used in PMC	26
2.2.1 Definition and Manufacture Process of Latexes	26
2.2.2 Types of Latexes	27
2.3 Basic Properties of Latexes	28
2.3.1 Polymer Composition	28
2.3.2 Surfactants and Compounding	29
2.3.3 Carboxylation	30
2.3.4 Stability	30
2.3.5 Particle Size	31
2.3.6 Film-forming Temperature	32
2.4 Physical and Mechanical Characteristics of PMC and Applications	32
2.4.1 Properties of Fresh Mortar and Concrete	32
2.4.2 Properties of Hardened Mortar and Concrete	34
2.4.2.1 Strength	34
2.4.2.2 Durability	37

	Page	
2.4.3	Application of PMC	39
2.5	Factors Affecting PMC Properties	40
2.5.1	Type of Polymer	40
2.5.2	Mix Design of PMC	41
2.5.3	Curing Regime	41
2.6	Hypothesis of Mechanism for Improvements	42
2.6.1	Equivalent Workability at Low w/c Ratio	42
2.6.2	Microcracks Held Together by Polymer Film Network	43
2.6.3	Chemical Reaction Theory	43
CHAPTER 3	MATERIALS AND EXPERIMENTAL TECHNIQUES	44
3.1	Choice of Materials	44
3.1.1	Cements	44
3.1.2	Polymers	44
3.1.2.1	Styrene-Butadiene Rubber Copolymers (SBR)	45
3.1.2.2	Acrylics	45
3.1.2.3	Ethylene-Vinyl Acetate Copolymers (EVA)	47
3.1.2.4	Other Polymers	48
3.2	Specimen Preparation	49
3.2.1	Mix Proportions and Casting	49
3.2.2	Curing Regime	49
3.2.3	Drying of Samples	50
3.2.4	Total Solid Content of Latex	50
3.2.5	Synthetic Pore Solution	51
3.2.6	Solution preparation for Selective Dissolution	51
3.2.7	Preparation of Polymer Films	52
3.3	Experimental Techniques	52
3.3.1	Conduction Calorimetry	52
3.3.2	Mercury Intrusion Porosimetry (MIP)	53
3.3.3	Solvent Exchange Porosity and Water Absorption Porosity	54
3.3.4	Helium Pycnometry	56
3.3.5	Differential Thermal Analysis (DTA) and Thermal Gravimetric Analysis (TGA)	56
3.3.6	Scanning Electron Microscopy (SEM)	57
3.3.7	Pore Solution Expression	57

	Page	
3.3.8	Analysis of Solution	58
3.3.8.1	Hydroxyl Ion	58
3.3.8.2	Chloride Ion	58
3.3.8.3	Sodium and Potassium Ions	59
3.3.9	Total Chloride Ion	59
3.3.10	Selective Dissolution of Cement	60
3.3.11	Infrared Spectroscopy (IR)	60
3.3.11.1	Sampling Techniques	61
3.3.11.2	Interpretation	61
3.3.12	X-Ray Diffraction	62
3.3.13	Steady-State Diffusion	63
3.3.14	Non-Steady State Diffusion	64
CHAPTER 4	HYDRATION KINETICS AND MECHANISMS	71
	OF POLYMER MODIFIED CEMENT	
4.1	General Aspects of Cement Chemistry	71
4.2	Previous Work	74
4.3	Calorimetry	77
4.3.1	Procedure	77
4.3.2	Theory of Calorimeter	78
4.4	Results and Discussion	80
4.4.1	Styrene Butadiene Rubber-Cement System	80
4.4.1.1	Polymer/Cement Ratio (P/C)	80
4.4.1.2	Water/Cement Ratio (W/C)	81
4.4.1.3	Alkali Content of Cement	82
4.4.1.4	Modification of Polymer (Carboxylation)	82
4.4.1.5	Aqueous Component of Latex and Defoamer	82
4.4.1.6	Hydration Temperature	83
4.4.2	Other Polymer-Cement Systems	83
4.4.2.1	Acrylic-Cement System	83
4.4.2.2	Ethylene Vinyl Acetate (EVA)-Cement System	84
4.4.2.3	Vinylacetate Vinylversatate Copolymer (VaVe)-Cement and Vinylacetate-Vinylversatate-Acrylic Terpolymer (VaVeAc)- Cement System	85
4.5	Analysis of Reaction Rates	86
4.5.1	Kinetics of Induction Period	86

	Page
4.5.2	Kinetics of Acceleratory Period 90
4.6	General Discussion 92
4.6.1	Initial Reaction and Induction Period 93
4.6.2	Acceleratory Period 94
4.6.3	Deceleratory Period 96
4.7	Conclusions 96
CHAPTER 5	MICROSTRUCTURE DEVELOPMENT OF 120
	POLYMER MODIFIED CEMENT
5.1	Previous Work 120
5.2	Pore Characteristics of PMC 123
5.2.1	Methods of Pore Structure Determination and Problems 123
5.2.2	Results and Discussion 126
5.2.2.1	Mercury Intrusion Porosity 126
5.2.2.2	Solvent Exchange Porosity and Water Absorption Porosity 129
5.2.2.3	Porosity from Helium Pycnometry 130
5.2.2.4	Comparison of Porosity Results Obtained by the Various 130
	Techniques
5.3	Morphology of Cement Hydrates and Polymer 131
	Film within Hardened Matrix
5.3.1	SEM Observation of Fracture Surfaces 132
5.3.2	SEM Observation of Etched Fracture Surfaces 133
5.3.3	Flocculation of Polymer Latexes with Hardened Matrix 133
5.3.3.1	Method Determining Polymer Contents in Pore Solution 134
5.3.3.2	Polymer Contents in Cement Pastes and Mortars 134
5.4	Conclusions 136
CHAPTER 6	STUDY OF POLYMER - CEMENT 155
	INTERACTIONS
6.1	Previous Work 155
6.2	Results and Discussion 159
6.2.1	Differential Thermal Analysis (DTA) and Thermal 159
	Gravimetric Analysis (TGA)
6.2.1.1	Characterisation of Unmodified Cement Pastes 159

	Page	
6.2.1.2	Characterisation of Polymers	160
6.2.1.3	Characteristics of Polymer Modified Cement Paste and Physical Mixes	161
6.2.1.4	Discussion on the Results of Thermal Analysis	162
6.2.2	Pore Solution Extraction and Analysis of PMC	163
6.2.2.1	SBR 1-OPC I and SBR 1-OPC II Systems	164
6.2.2.2	Ac 1-OPC I and Ac 1-OPC II Systems	165
6.2.3	Infrared Spectroscopy Analysis	165
6.2.3.1	SBR 1-OPC I System	166
6.2.3.2	Acrylic-OPC I Systems	166
6.2.3.3	Ethylene Vinyl Acetate-OPC I Systems	167
6.2.4	X-ray Diffraction Analysis	167
6.2.5	Discussion on the Possibility of Chemical Reaction	168
6.3	Conclusions	170

CHAPTER 7 DIFFUSION OF CHLORIDE IONS IN POLYMER MODIFIED CEMENT PASTES **192**

7.1	Previous Work	192
7.2	Mathematical Modelling of Diffusion Process	196
7.2.1	Steady-State Diffusion	196
7.2.2	Non-Steady State Diffusion	197
7.3	Diffusion Property of SBR-Cement Pastes	199
7.3.1	Results and Discussions of Steady-State Diffusion	199
7.3.1.1	SBR 1-OPC I Pastes	199
7.3.1.2	SBR 2-OPC I Pastes	201
7.3.1.3	Aqueous Component-OPC I Pastes	201
7.3.2	Results and Discussions of Non-Steady State Diffusion	202
7.3.2.1	Ionic Concentration Profile and Apparent Diffusivity D^*	202
7.3.2.2	Free and Bound Chloride Ions	203
7.3.2.3	Estimate of Service Life	205
7.4	Diffusion Properties of Other Polymer-Cement Systems	206
7.4.1	Acrylic-Cement Pastes	206
7.4.2	VaVeAc, VaVe, and EVA-OPC I Systems	207
7.4.3	Influence of Defoamer on Diffusion Property	207
7.4.4	Chloride Diffusion through Pure Polymer Films	208
7.5	Conclusions	209

	Page
CHAPTER 8 GENERAL DISCUSSION, CONCLUSIONS AND FURTHER WORK	221
8.1 Hydration Kinetics of PMC	221
8.2 Microstructure of PMC	223
8.3 A Model for Microstructure Development of PMC	225
8.4 Influence on Engineering Properties	228
8.4.1 Strength	228
8.4.2 Diffusion	
8.5 Conclusions	232
8.6 Further Work	233
REFER ENCES	235
APPEN DICES	
A: X-ray Powder Diffraction File of Cement-Based Materials	245
B: Calibration of Hydration Curves and Calculation of Total Hydration Heat	247
C: A Estimation of Polymer Layers Covered Cement Grains	250
D: Papers Published and Submitted from the Study	251

LIST OF TABLES

		page
Table 3.1	Chemical analysis of cements	65
Table 3.2	Properties of polymers used in the investigation	66
Table 4.1	Characteristic parameters for heat evolution of SBR modified pastes at 22°C	98
Table 4.2	Characteristic parameters for heat evolution of SBR 1 modified pastes at w/c=0.5 and different temperatures	99
Table 4.3	Characteristic parameters for heat evolution of other types of polymer modified pastes at 22°C	100
Table 4.4	Kinetic parameters of the induction period for new phase nuclei formation for SBR 1 modified OPC I at w/c=0.5	101
Table 4.5	Constant, n and reaction rate constant, $k(s^{-1})$, for SBR 1 modified OPC I, at w/c=0.5 and different temperatures	102
Table 4.6	Activation energy for the hydration of SBR 1 modified OPC I	103
Table 5.1	Porosity measured by mercury intrusion porosimetry for various polymer-cement system	137
Table 5.2	Porosity measured by solvent exchange and water absorption for SBR 1-cement system with w/c-0.5	138
Table 5.3	Porosity measured by helium pycnometer for SBR 1-OPC I and Ac 1-OPC I systems	139
Table 5.4	Porosities measured by MIP, solvent exchanged, water absorption and helium pycnometer for SBR 1-OPC I system, at w/c=0.5	140
Table 5.5	Polymer contents in the pore solution of acrylic-cement paste	141
Table 6.1	Chemical analysis of pore solution for SBR 1-OPC I and OPC II at w/c=0.5	171
Table 6.2	Chemical analysis of pore solution for Ac 1-OPC I and Ac 1-OPC II at w/c=0.5	172
Table 7.1	Effective diffusivity of chloride ion for SBR 1-OPC I paste	211
Table 7.2	Ionic concentration profiles for SBR 1-cement pastes at w/c=0.5	212
Table 7.3	Total, free and bound chloride concentration profile of SBR 1-OPC I paste in non-steady state diffusion	213
Table 7.4	Effective diffusivity of chloride ion for all polymer-cement pastes	214

LIST OF FIGURES

		Page
Figure 1.1	Summary of the numbers of PC, PMC and PIC papers published in 1-7th International Congress on Polymers in Concrete (ICPIC)	23
Figure 1.2	Interrelating aspect of the research	24
Figure 3.1	Conduction calorimeter interfaced with computer	68
Figure 3.2	Cross section of the press used to extract pore solution	69
Figure 3.3	Experimental set-up of diffusion cell	70
Figure 3.4	Location of disc cutting and analysis points along the depth of the cylinder	70
Figure 4.1	Mechanisms of Portland cement hydration	104
Figure 4.2	Typical heat evolution curve for Portland cement	105
Figure 4.3	Sectional diagram of large sample holder and assembled calorimeter	106
Figure 4.4	Sectional diagram of small sample holder and assembled calorimeter	106
Figure 4.5	Typical graph of dE/dt versus E	107
Figure 4.6	Calibrated of heat evolution curve	107
Figure 4.7	Heat evolution curves of SBR 1 modified OPC I at $w/c=0.3$ and 22°C	108
Figure 4.8	Heat evolution curves of SBR 1 modified OPC I at $w/c=0.5$ and 22°C	108
Figure 4.9	Influence of alkali content of cement on heat evolution curves for SBR 1-cement system at $w/c=0.5$ and 22°C	109
Figure 4.10	Scheme of polymer adsorbing or bonding to cement grains	110
Figure 4.11	Influence of carboxyl groups on heat evolution curves at $w/c=0.5$ and 22°C	111
Figure 4.12	Influence of aqueous component on heat evolution curves at $w/c=0.5$ and 22°C	112
Figure 4.13	Influence of defoamer on heat evolution curves at $w/c=0.5$ and 22°C	112
Figure 4.14	Heat evolution curves of SBR 1 modified OPC I at different hydration temperature	113
Figure 4.15	Heat evolution curves of Ac 1 modified OPC I at $w/c=0.5$ and 22°C	114

	Page	
Figure 4.16	Heat evolution curves of Ac 1 modified OPC II at w/c=0.5 and 22°C	114
Figure 4.17	Heat evolution curves of acrylics-OPC I at w/c=0.5 and 22°C	115
Figure 4.18	Heat evolution curves of ethylene vinyl acetate-OPC I at w/c=0.5 and 22°C	116
Figure 4.19	Heat evolution curves of vinylvesatate-vinylacetate-OPC I and vinylvesatate-vinylacetate-acrylic-OPC I at w/c=0.5 and 22°C	116
Figure 4.20	A typical relationship between induction time and polymer addition for SBR modified OPC I at w/c=0.5	117
Figure 4.21	Influence of polymer addition and hydration temperature on the rate constant (k)	117
Figure 4.22	Relationship between hydration degree and time under Jander's model and Avrami's model at w/c=0.5 and 22°C	118
Figure 4.23	Arrhenius plots for the determination of activation energy for the hydration kinetics of SBR 1 modified OPC I	119
Figure 5.1	Influence of different drying methods on MIP results of unmodified cement pastes aged 7 days	142
Figure 5.2	Pore size distribution curves for SBR 1-OPC I pastes at w/c=0.3	143
Figure 5.3	Pore size distribution curves for SBR 1-OPC I pastes at w/c=0.5	145
Figure 5.4	Pore size distribution curves for Ac 1-OPC I pastes at w/c=0.5	146
Figure 5.5	Change in pore structure for SBR 1-OPC I paste at w/c=0.3	147
Figure 5.6	Change in pore structure for SBR 1-OPC I paste at w/c=0.5	148
Figure 5.7	Influence of surfactant and carboxylate content on pore structure, at w/c=0.5	149
Figure 5.8	Relationship between porosity measured by water absorption, solvent exchange, helium pycnometer and MIP	150
Figure 5.9	A comparison of porosity measured by water absorption, solvent exchange and MIP	150

	Page	
Figure 5.10	SEM picture of fracture surface of OPC I paste, 90 days at w/c=0.5	151
Figure 5.11	SEM picture of fracture surface of SBR 1-OPC I paste, 90 days at w/c=0.5	151
Figure 5.12	SEM picture of fracture surface of Ac 1-OPC I paste, 90 days at w/c=0.5	152
Figure 5.13	SEM picture of fracture surface of SBR 2-OPC I paste, 90 days with w/c=0.5	152
Figure 5.14	SEM picture of etched fracture surface of OPC I paste, 90 days at w/c=0.5	153
Figure 5.15	SEM picture of etched fracture surface of SBR 1-OPC I paste, 90 days at w/c=0.5	153
Figure 5.16	Calibration curve of polymer content in solution	154
Figure 6.1	Thermal analysis of unmodified cement paste	173
Figure 6.2	DTA curves of cement-based compounds	174
Figure 6.3	A schematic representation of a DTA curve of polymer	175
Figure 6.4	Thermograms of polymers	176
Figure 6.5	Thermograms of SBR 1-OPC I pastes in argon, at w/c=0.5	177
Figure 6.6	Thermograms of SBR 1-OPC I and SBR 2-OPC I pastes in air	178
Figure 6.7	Thermograms of Ac 1-OPC I and Ac 1-OPC II pastes in air	179
Figure 6.8	Influence of curing time on thermograms of 10% SBR 1-OPC I	180
Figure 6.9	Pore solution analysis for SBR 1-OPC I system at w/c=0.5	181
Figure 6.10	Pore solution analysis for SBR 1-OPC II system at w/c=0.5	182
Figure 6.11	Pore solution analysis for Ac 1-OPC I system at w/c=0.5	183
Figure 6.12	Pore solution analysis for Ac 1-OPC II system at w/c=0.5	184
Figure 6.13	Infrared spectra of SBR 1-OPC I system	185
Figure 6.14	Infrared spectra of Ac 1-OPC I system	186
Figure 6.15	Infrared spectra of Ac 3-OPC I system	187
Figure 6.16	Infrared spectra of VaVeAc-OPC I system	188
Figure 6.17	Infrared spectra of EVA 1-OPC I system	189
Figure 6.18	Infrared spectra of EVA 3-OPC I system	190

		Page
Figure 6.19	X-ray diffraction pattern of hydrated OPC I paste, 90 day old and at w/c=0.5	191
Figure 6.20	X-ray diffraction pattern of 20%SBR 1-OPC I paste, 90 day old and at w/c=0.5	191
Figure 7.1	Chloride ion diffusion through unmodified cement paste and SBR 1-cement, at w/c=0.5 and 25 °C	215
Figure 7.2	Arrhenius plots for SBR 1-OPC I system at w/c=0.3	215
Figure 7.3	Arrhenius plots for SBR 1-OPC I system at w/c=0.5	216
Figure 7.4	Ionic concentration profile of pure cement at w/c=0.5	216
Figure 7.5	Ionic concentration profile of 10% SBR 1- cement at w/c=0.5	217
Figure 7.6	Ionic concentration profile of 20% SBR 1- cement at w/c=0.5	217
Figure 7.7	Total chloride concentration profile in SBR 1-OPC I paste	218
Figure 7.8	Relationship between bound chloride and chloride concentration in pore solution	218
Figure 7.9	Relationship between total chloride and x/\sqrt{t}	219
Figure 7.10	Relationship between cover thickness and induction time	219
Figure 7.11	Pore size distribution for 10%Ac 2-OPC I compared to unmodified and 10%SBR 1-OPC I paste, at w/c=0.3, 90 days	220
Figure 8.1	Microstructure development model of polymer modified cement	231

LIST OF ABBREVIATIONS AND SYMBOLS

Polymers

Ac	Acrylic
CR	Polychloroprene Rubber
VAI	Polyvinyl Alcohol
EVA	Ethylene-Vinylacetate
VaVe	Vinylacetate Versatate
SBR	Styrene Butadiene Rubber
S-Ac	Styrene Acrylic
VA	Polyvinyl Acetate
VdC	Vinylidene Chloride Copolymer
VP	Polyvinyl Propionate
EHA	Ethyl Hexyl Acrylate
MMA	Methyl Methacrylate
VaVeAc	Vinyl acetate-Vinylversatate-Butylacrylate Terpolymer
VdC-Ac	Polyvinylidene Chloride-Acrylic
Ac-VA	Acrylic-Vinyl Acetate
VpVC	Vinylpropionate-Vinylidene Chloride
PMMA	Polymethyl Methacrylate
VdC-VC-EAc	Vinylidene Chloride-Vinyl Chloride-Ethylacrylate
EAc-MMA	Ethylacrylate Methyl Methacrylate
PMMA/PAc	Polymethyl Methacrylate-butyl Acrylate

Miscellaneous

PMC	Polymer Modified Cement
PIC	Polymer Impregnated Concrete
PC	Polymer Concrete
p/c	Polymer Cement Ratio
w/c	Water Cement Ratio
d	Equivalent Diameter of the Intruded Pores
p	Pressure
g	Surface Tension of Mercury
θ	Angle of Contact between Mercury and Pore Walls
P	Porosity

W_1	Weight in Air
W_2	Weight after Solvent Exchange
W_{dry}	Weight after Dried in the Oven at 105°C
ρ_p, ρ_w	Specific Gravity of Propylene-2-ol and Water
D_r	Relative Density Measured by Helium Pycnometry
D_d	Bulk Density Measured by Mercury Pycnometer
ΔG^*	Gibbs Free Energy of Activation
k, K^*	Rate Constant and Equilibrium Constant
$Q(t)$	Hydration Heat at Time t
$Q(f)$	Final Hydration Heat
α	Degree of Hydration at Time t
E_a	Activation Energy
D	Diffusion Coefficient

CHAPTER 1

INTRODUCTION AND AIMS OF THE STUDY

1.1 CLASSIFICATION OF POLYMER CEMENT COMPOSITES

Traditional mortars and concretes are composed of hydraulic cement, fine/coarse aggregate and water. Whilst they have good compressive strength, their tensile/flexural strength, toughness and durability are often less than required, particularly for thin section work such as repairs and bridge decks. Deficiencies in the materials are to a large extent related to the presence of porosity and various microstructural defects such as shrinkage cracks.

Furthermore, conventional mortar and concrete are not very satisfactory as repair materials because of their poor bonding ability to old concrete, steel and other substrates. Efforts to overcome these problems have included modification of existing, and development of new, systems incorporating polymers.

The addition of polymers to cement systems began in the 1920's and many combinations have been investigated. According to the different ways of incorporating the polymer, composites may be divided into three principal classes (Feldman 1989; Swamy 1979; Aminabhavi 1982-3):

Polymer Modified Concrete (PMC) which has also been referred to as polymer-Portland cement-concrete (PPCC) and latex modified concrete (LMC). Portland cement and aggregate are combined at the time of mixing with organic polymers. These polymers may be in the form of a dispersed phase (latex) or redispersible powder in water. In these systems, cement hydration takes place first followed by the coalescence of polymer particles to form a polymer film. The resulting solid consists of interpenetrating hardened cement and polymer phases.

Polymer Impregnated Concrete (PIC) is manufactured by impregnating monomeric systems into hardened (normally precast) Portland cement concrete. Subsequently, the monomers are polymerised within the pore structure. In this system, the process of cement hydration and the monomer polymerisation are physically separated.

Polymer Concrete (PC) is prepared by mixing aggregate with a pure monomer which is subsequently cured. Thus, PC consists of an aggregate and a polymeric binder, instead of Portland cement and water.

The resultant properties of polymer-cement composites depend on the type of polymer used and the incorporation method.

In the case of PMC, the research has generally shown: an improvement of workability which allows a reduction of water/cement ratio; modification of the hardened cement matrix via a polymer-cement matrix which includes changes in the morphology of cement hydrates and pore structure; formation of a three dimensional network of interpenetrating polymer film binding the structure; and interactions between polymer and cement forming chemical anchors. These alterations result in PMC having good adhesion to existing substrates, higher tensile/flexural strength and improved durability including resistance to chloride penetration, carbonation and freezing/thawing. Its process technology is very similar to that for ordinary concrete and the cost is cheaper than that of PIC and PC. In addition, most latexes are nontoxic, non-flammable and are of reasonably low viscosity at high solid content level, e.g. 40-50%. With these advantages, the application of PMC has shown a steady growth in the construction industry.

PIC has good strength, stiffness and durability. However, PIC is now little used in current commercial applications, mainly since its process technology is complicated. Several factors influence the rate and degree of monomer loading in a concrete specimen. So far, there are no accurate, easy measuring methods for determining polymer

impregnation depth, which leads to difficulties in quality control and poor reliability in structural applications. In addition, high temperatures are required for drying the concrete and curing the polymer, consuming a great deal of thermal energy. An adverse balance between its performance and high cost has limited its practical applications (Okada 1990). In fact, at the present time, polymer impregnated concrete is not used in the UK, USA, Japan, Brazil and other countries.

The properties of PC are largely dependent on the characteristics and amount of polymer, since this phase forms a continuous matrix. In general, it has much higher compressive and flexural strength than conventional concrete and a greater ductility than both PIC and PMC. Currently, PC is used as repair materials, overlays of bridge decks and precast components, but its cost is much higher than PMC.

Figure 1.1 presents a summary of the numbers of papers on PMC, PIC and PC published in 1-7th International Congress on Polymers in Concrete (ICPIC). These figures reflect the research and development activity carried out internationally. It is observed that the overall research has been increasing since the first International Congress on Polymer in Concrete (ICPIC). The papers increased from 54 in the 1st ICPIC to 121 in the 6th ICPIC. It can also be noted that the research in PIC gradually decreases after having reached a peak in 1970's, while PMC and PC keep steadily increasing.

1.2 AIMS OF THE PRESENT STUDY

It should be noted that theoretical studies of PMC are lagging far behind its engineering application. Most of the reports dealing with PMC have been devoted to discussing the improved mechanical properties of uncharacterised systems and there are relatively few devoted to mechanisms. Little is known of the mechanisms of hydration in this system or how this influences microstructure, and in turn, engineering properties.

The aim of the study is to identify the fundamental nature of the interactions between the hydrating cement phases and polymer, and the role of these interactions in determining composite properties such as resistance to chloride ion diffusion. Figure 1.2 shows possible areas for research in PMC. The investigations reported in this thesis include:

1) A study of the influence of polymer dispersions on the kinetics of cement hydration. Isothermal calorimetry has been used to determine whether various latexes accelerate or retard cement hydration and which component e.g. latex solid, surfactant, defoamer, etc. is the most important in this respect.

2) Microstructure development in polymer modified cement pastes including characterisation of cement hydration products; formation of polymer film and determination of porosity and pore size distribution in hardened polymer modified cement pastes.

3) The nature of interactions between polymer dispersions and hydrating cementitious materials. Identification of any 'chemical anchor' and stability of polymer phase in a high alkalinity environment.

4) The role of polymer in modifying the diffusion resistance of cement materials. This involves the determination of intrinsic diffusion coefficients and activation energies for chloride ions by steady state and non-steady state techniques.

5) Failure investigations of PMC materials have often been hampered by a lack of information regarding the identity of the latex systems used. Thus, a further aim was to determine whether material characterisation methods such as thermal analysis, infrared spectroscopy, and pyrolysis techniques could be used to identify and quantify the latex used in an unknown PMC.

Note: A project running in parallel to the work described in this thesis has looked at rheology behaviour, curing conditions and adhesion of PMC to existing concrete substrates (Salbin 1996).

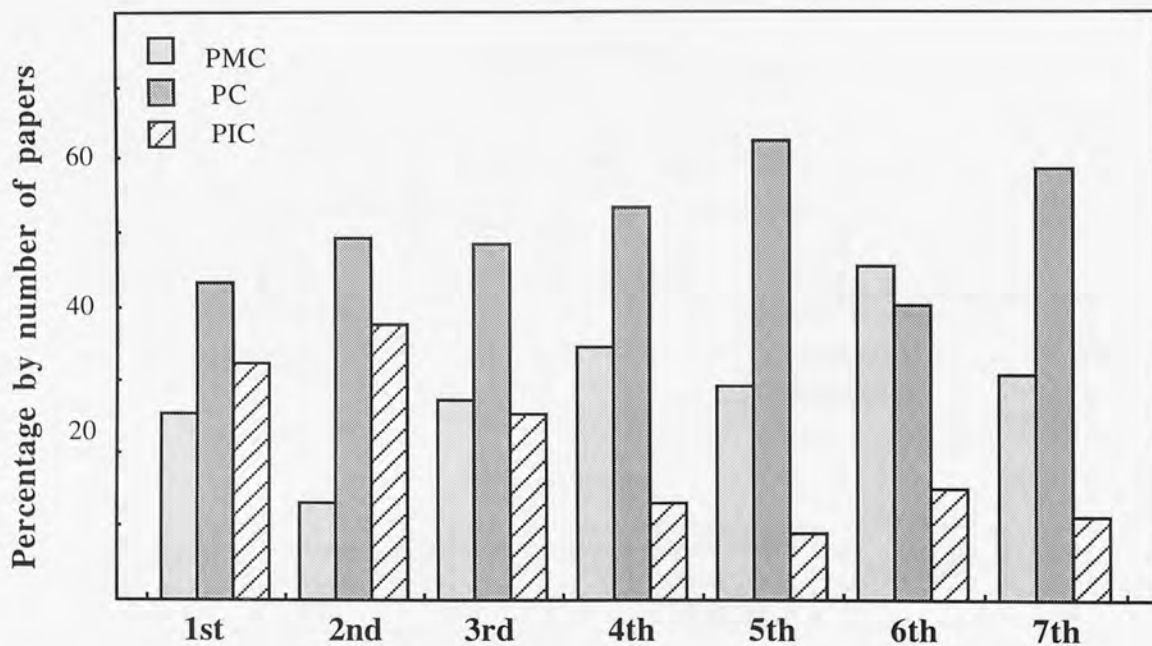
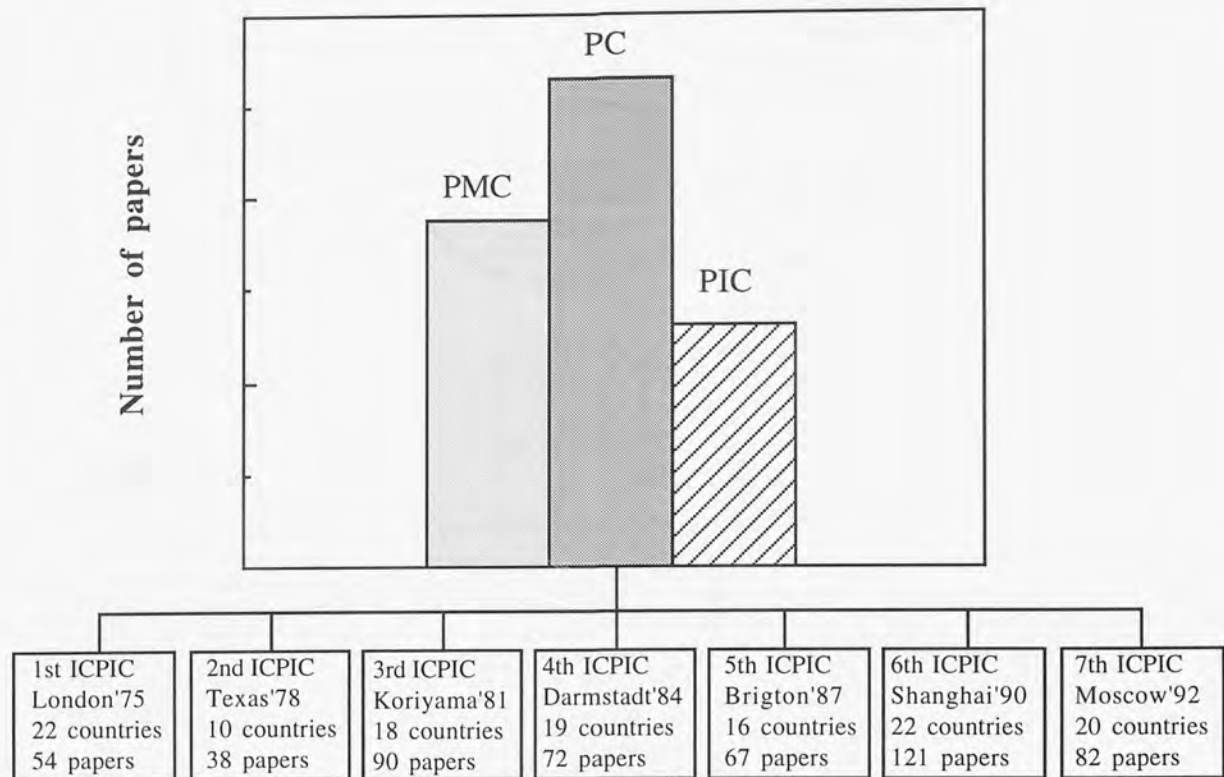


Fig.1.1 Summary of the numbers of PC, PMC and PIC papers published in 1-7th International Congress on Polymers in Concrete (ICPIC)

* Data of 1-5th ICPIIC after Bares (Bares and Czarnecki 1987)

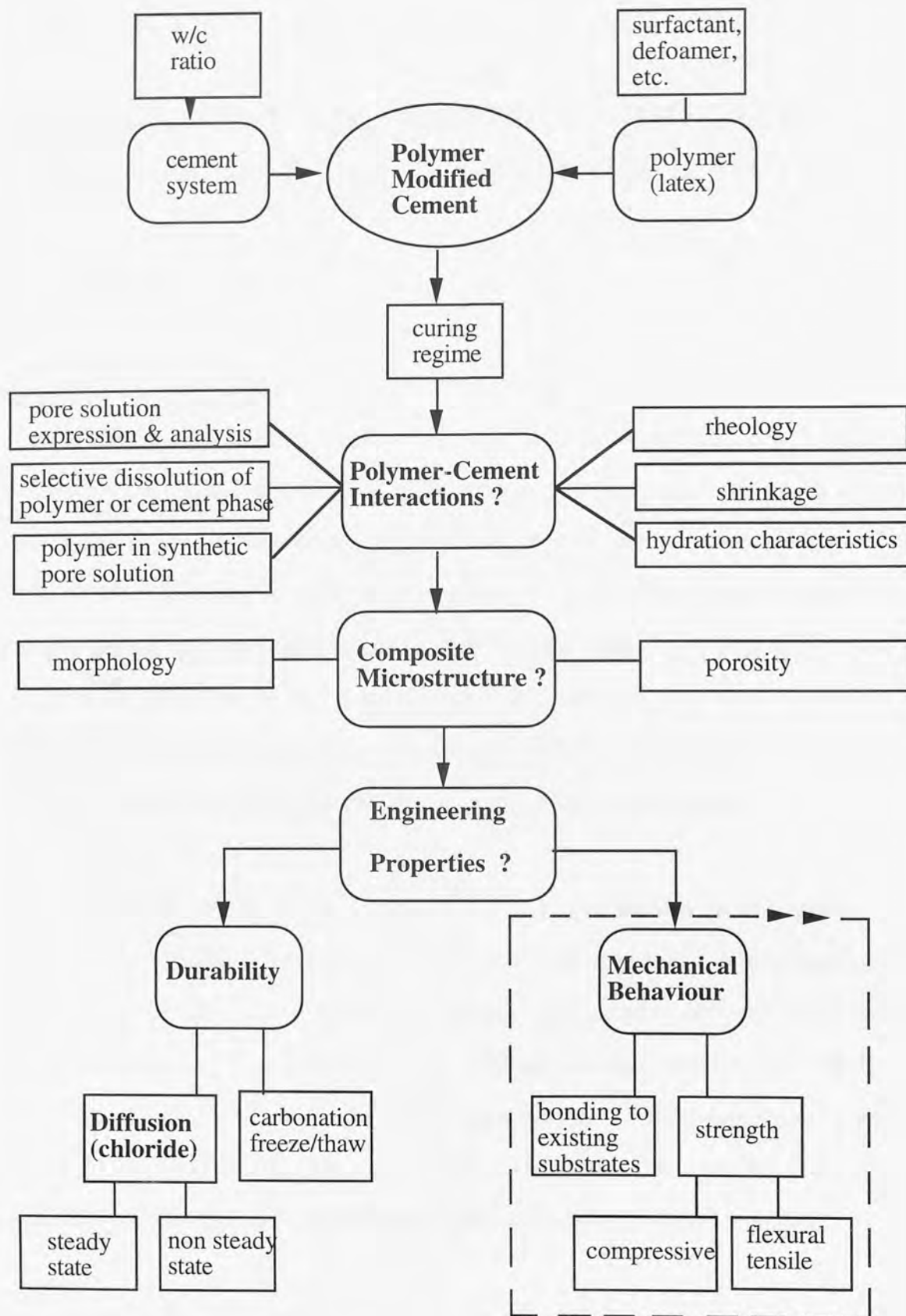


Fig. 1.2 Interrelating aspects of the research

CHAPTER 2

BACKGROUND OF POLYMER MODIFIED CEMENTS/MORTARS/CONCRETE (PMC)

2.1. HISTORY

According to a State-of-the-Art Report on Polymer-Modified Concrete by the American Concrete Institute (ACI 1991), the first concept of latex hydraulic cement systems started in the early 1920's. In 1923, Cresson produced a paving material by mixing cement with natural rubber latexes and obtained the first patent for this system. Some similar work had been done by Lefebure in 1924 and Kirkpatrick in 1925. Their interests were mainly focused on natural rubber latexes. In 1932 Bond used a synthetic rubber latex, instead of the natural rubber latex. Rodwell applied synthetic resin latexes to this system in 1933. Since then, various synthetic latexes, including polychloroprene rubber (CR), polyacrylic ester and polyvinyl acetate were used for modifying mortar and concrete.

In the 1950's, feasibility studies pursued by Griffiths and Sterens on the application of natural rubber modified systems and Geist's fundamental study on polyvinyl acetate modified mortar provided a number of valuable suggestions for later research and development of latex modified systems. Throughout the 1960's to 1980's, the development and application of latex modified mortar and concrete continually increased. Research included determination of chemical, physical and mechanical properties, durability and test methods and has been conducted actively in many countries.

2.2 POLYMER LATEXES USED IN PMC

The polymers used in polymer modified mortar/concrete are available in various physical forms including latex, redispersible powders and solution. When polymers are dissolved in organic solvents or water, the molecular chains open up and are dispersed throughout

the solvent to give a clear solution. Water-soluble polymers include polyelectrolytes such as polyacrylonitrile, polymethacrylic acid, polyvinyl acetate-maleic anhydride; polyvinyl alcohol (VAI), polyethylene oxide and cellulose ethers. Redispersible powdered emulsions often used include ethylene-vinylacetate (EVA) or vinyl acetate versatate (VaVe). The major form of addition is as a latex, and the following section considers this type in detail.

2.2.1 Definition and Manufacturing Process of Latex

A latex is sometimes referred to as an emulsion, and may be defined as a stable colloidal dispersion of organic polymer particles in water, giving a milky fluid that is generally white to off-white in colour. Since the polymer particles are very fine, their surface area/mass ratio is extremely high so that gravity has far less effect upon them than do surface energy forces. These surface energy forces provide a repulsion between the particles, enabling them to remain in suspension. However, permanence of the suspension may be dependent upon the presence of other surface-active chemicals within the dispersed phase.

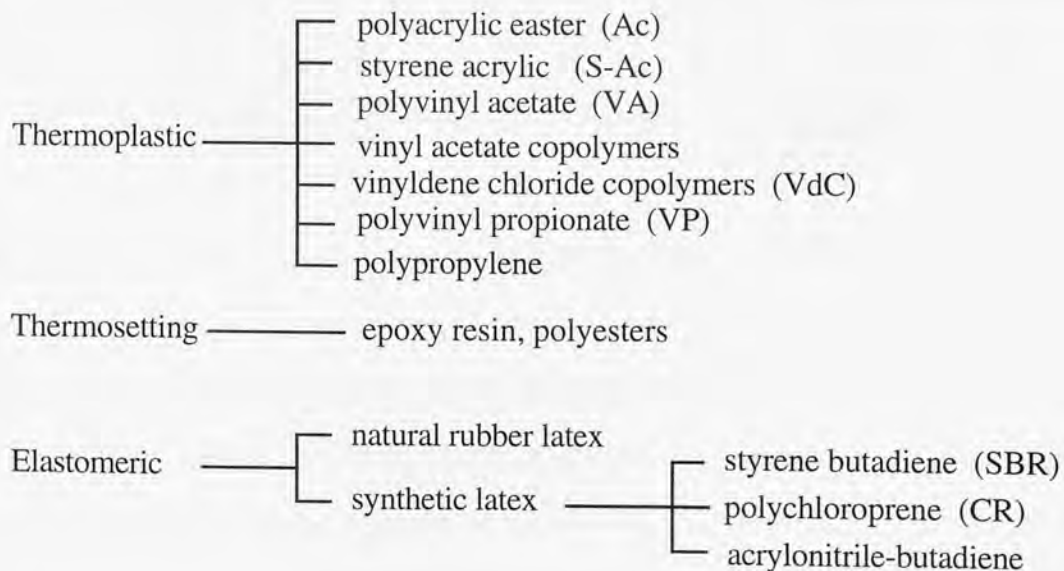
Almost all latexes are produced by a process known as emulsion polymerisation. In this process, the system consists of the monomers, water, a stabiliser, and a water soluble initiator. The initiator generates free radicals that cause the monomers to polymerise by chain addition. The stabiliser, including emulsifier or surface active agent which reduces surface tension, controls the rate of polymerisation and particle size, and increases the stability of the latex.

The method of manufacture is to add water, stabiliser, other ingredients and part of the monomer to an autoclave under agitation. When the temperature is increased to the desired point, the initiator and the remainder of the monomer is added. The reaction is terminated by removing residual monomers and conversion is normally about 90%. The "raw" latex is then compounded by raising the pH value, adjusting the solid content,

introducing preservatives and stabilisers etc.. The solid content is expressed as the percentage weight of polymer particles in the latex and this is typically around 50%, but the value may be in the range of 45-70% (Dennis 1984; Kuhlmann 1987; Walters 1987).

2.2.2 Types of Latexes

Latexes can be divided into three classes: cationic, anionic and non-ionic according to the type of electrical charge on the particle, which in turn is determined by the type of surfactant used as the stabiliser. According to their physical and thermal nature, they can be divided into thermoplastic, thermosetting and elastomeric. Even though a wide range of polymer latexes is available commercially, only about five per cent of them are suitable for use with hydraulic cements (ACI 1991). In general, latexes that are cationic or anionic are not suitable for hydraulic cements because they lack the necessary stability. Most of the latexes used with Portland cement utilised a surfactant that is non-ionic and are thermoplastic or elastomeric in nature. Various latexes that have been or are being used with hydraulic cements are listed below:



In the UK, popular polymers used in PMC are styrene butadiene rubber (SBR), pure acrylics (Ac) and ethylene vinyl acetate (EVA) (Concrete Society 1994; Dennis 1984; Plum 1990).

2.3 BASIC PROPERTIES OF LATEXES

Latexes are rather complex colloid systems, and many factors can influence their properties which, in turn, have varying impacts on the modified hydraulic cement mixes. It is worth understanding some fundamental characteristics to evaluate latex modified systems.

2.3.1 Polymer Composition

A polymer is a homopolymer if it is made of one type of monomer (e.g. **A** or **B**), and a copolymer when two different monomers are polymerised (**A+B**). Their molecules may be linear, branched, or crosslinked. If more than one unit is involved, a copolymer may be of the regular, random, block, or graft types:

A-A-A-A-A-A-A-A-A-A-A-A-A-A-A-A-A-	Homopolymer
A-B-A-B-A-B-A-B-A-B-A-B-A-B-A-B-	Copolymer-Regular type
A-B-B-A-A-A-B-B-A-B-A-B-B-B-A-A-A-A-	Copolymer-Random type
A-A-A-A-B-B-B-B-B-A-A-A-A-A-B-B-B-B-	Copolymer-Block type

The properties of polymers formed are very dependent on how the various monomers are put together. The weight fraction of the various monomers in a co-polymer play an important part in the properties of the formed latex. For example, SBR latex may be made by copolymerizing styrene and butadiene in any desired ratio from 100% polybutadiene to 100% polystyrene. However, a high styrene level produces a hard film whereas a high butadiene content produces a soft film. High styrene contents would improve compressive and tensile strengths, and reduce adhesion and flexibility. In contrast, a high butadiene level leads to decreased modulus and cohesive strength and increased

elongation and film formation. A styrene-butadiene copolymer latex with a styrene butadiene (S/B) ratio of 30/70 will give a modified concrete with a much lower compressive strength than a styrene-butadiene copolymer of similar molecular weight but with a S/B ratio of 70/30. For use with cement, a styrene content about 60-65% produces a good balance of properties (Dennis 1984). Similarly, acrylic latex consisting of ethyl hexyl acrylate (EHA) and methyl methacrylate (MMA) can give the required properties for PMC by adjusting their monomer ratio, since polymerised EHA is soft and polymerised MMA is relatively hard.

2.3.2 Surfactants and Compounding

Surfactants (also referred to as stabilisers) are added during the manufacture of latex. The type and level of surfactant influence stability and surface tension. In latex modified cement systems, it is supposed that the surfactant can act rather like a cement plasticiser and water-reducer, which enables workable mortars to be made at low water/cement ratios (Concrete Society 1994). However, it is not always beneficial to the hydration of Portland cement and excess surfactant may entrain more air leading to lowering of the performance of mortars exposed to wet conditions.

The latex must be compounded at the end of the polymerisation process for use; the main function being to improve the product properties. Compounding may involve one or more of the following additions: plasticiser, coalescent agent, alkali, antioxidant, bactericide, water, freeze/thaw stabiliser, additional surfactant. Antioxidants provide protection against ageing and light attack, surfactants improve workability and freeze thaw stability, and reduce the water-cement ratio. The levels of these added materials are relatively low, ranging from parts per million for bactericides to a few percent for surfactants. Other ingredients that may be added include defoaming or antifoaming agents. The defoamer reduces the air content entrained by polymer and is often added by the latex manufacturer. If the latex does not contain such a material, one must be added before use to avoid high air contents in the hardened cement mix.

2.3.3 Carboxylation

For additional stability, a small proportion of carboxylic acid, e.g. acrylic acid, is often incorporated into the latex particles. On raising the latex pH, carboxyl groups near the particle surface ionise and provide further negative charges. Since these charges are chemically bound to the latex particles they are excellent stabilisers.

The inclusion of bound carboxylic acid into a latex such as SBR can improve adhesion to damp and inorganic backgrounds and improve freeze/thaw resistance of the latex. On the other hand, high proportions of carboxylic acid increase the water absorption of the dried film. Therefore, the optimum proportion of carboxylic groups should be such to ensure that they are chemically bound onto the particle surface and not be locked inside the particle or left in solution (Dennis 1984). Furthermore, carboxylic acid may react with metal cations released during cement hydration to form carboxylates (Chandra 1987).

2.3.4 Stability

Stability is very important for latexes that are used with hydraulic cement mixes. It is a measure of resistance to change when subjected to a force or shock and has three basic forms: mechanical, chemical, and thermal. Mechanical stability is determined by subjecting latex to some mechanical motion, usually high speed agitation, for a specific period of time and then measuring the amount of coagulum that is formed. Chemical stability may be assessed by determining the amount of a certain chemical required to cause complete coagulation, or by adding a certain level of the chemical and then determining the mechanical stability. Thermal stability is generally determined by subjecting latex to specified temperatures for a specific period of time, and then determining the effect upon another property.

These stability properties are important for latexes that are used with hydraulic cement mixes. Good mechanical stability is required because latex modified systems are

frequently subjected to high shear. Good thermal stability is required because the latex may be subjected to wide variations in temperature. Good chemical stability is required because of the extremely active chemical nature of the hydraulic cements.

2.3.5 Particle Size

The particles contained in the latex are more or less spherical in shape. Their size can be controlled by the level of surfactant. The smaller the particle size, the larger the surface area of the particles and the more surfactant is needed to maintain the latex stability.

Large particles give latex which leads to readily trowellable mortar mixes whereas small particles aid adhesion and penetration. Particle size distribution is also important. A blend of small and large particles can give low viscosity at high solid concentration. While extra large particles cause "creaming" i.e. the process by which large particles float to the top on storage. A wide distribution of particle size benefits film forming as fewer gaps between the particles can be obtained. Usually, the particle size of latex varies between 0.05 to 5 μm , much smaller than the particle size of any aggregate. Natural rubber latex has mean particle sizes of about μm and a wide particle size distribution. SBR and acrylics are normally about 0.15 μm (Dennis 1984).

2.3.6 Film-Forming Temperature

Minimum film-forming temperature is defined as the lowest temperature at which the polymer particles of the latex have sufficient mobility and flexibility to coalesce into a continuous film. Below that temperature, only a powder deposit will form. The film-forming temperature is controlled by the type and level of monomer, addition of plasticizer, particle size and quality of dispersion, and chemical structure of polymer and physical structure. For successful application of latex-modified cement mortar, with a few exceptions, the film-forming temperature should be lower than the application temperature.

In polymer modified cement systems, it is considered that the latex particles coalesce to form a continuous film when the mixing water is consumed. The quality of the film depends largely on the mobility of latex particles. Efficient packing will be obtained only if the particles are deflocculated sufficiently to allow them to slide past each other easily. While with a poor dispersion, in which the particles are flocculated, a spongy film can result.

2.4 PHYSICAL AND MECHANICAL CHARACTERISTICS OF PMC AND ITS APPLICATIONS

2.4.1 Properties of Fresh Mortar and Concrete

Workability

The workability or flowability of fresh mortar and concrete is improved by addition of polymers. It has been reported that addition of SBR increased the initial slump of fresh concrete (ACI 1991). The final slump values at 3 hours for the control and SBR-cement ($w/c=0.52$) were respectively 80 and 124mm. Slump retention at $w/c=0.52$ is significantly better than that at $w/c=0.45$. At a higher w/c the mean particle distance is increased and the tendency for agglomeration of particles due to physical and chemical interaction is reduced. The addition of SBR enhances not only the initial slump of the paste but also the slump retention characteristics.

A set of similar results has been obtained by Oye (1989). The slump of a unmodified sample at $w/c=0.55$ was 70mm, but with 5% addition of latexes the slump was 100mm for SBR-cement, 80mm for polymethyl-methacrylate-butyl acrylate and 93mm for polyvinyl acetate-ethylene-vinyl chloride. The flow value of latex-cement before jiggling nearly reaches that of the unmodified sample after jiggling. Ohama (1973) reported that the flowability (ASTM C230) of the fresh mortar ($W/C=0.7$) is about 150 mm, but the flowability with 5% of SBR latex is 230mm.

As in the case of conventional concretes, there is a loss of slump with time in PMC. Based on a study by the FHWA (Clear 1978), it was reported that the slump loss with time was similar for both conventional concrete and polymer modified concrete.

Air content

The air content of latex modified mortar or concrete is usually larger than that of ordinary concrete. This is due to the action of surfactant contained in the latex, which stabilises air bubbles, thus entrains a larger quantity of air. Because excessive amounts of air decrease the compressive strength of concrete (approximately a 5% reduction in compressive strength for every 1% increase in the air content), a maximum air content of about 6.5 percent is recommended by ACI Committee (ACI 1991). The air content of most PMC is less than 2 percent (Ohama 1984).

The air content can be controlled by incorporating an anti-foamer into the latex. For SBR latex, the anti-foamer is usually a silicious product and often added by the latex supplier. For some latexes e.g. acrylics, the anti-foamer is added by the user prior to mixing. In addition, the composition of the cement and the type of aggregates can affect the air content. It is important to evaluate the actual mixture proportions before using them in the field.

Setting time

The setting times of latex modified concrete are affected by the types and addition of latexes. The data from two studies of this property indicated that the setting time of SBR-mortar or concrete is either equal to or slightly longer than ordinary concrete (Smutzer 1981). The setting time increases with an increase in latex addition. Natural rubber latex causes the maximum delay in setting time. It is suggested that the delay in setting time is due, in part, to the fact that surfactants contained in latexes inhibit the hydration of cement.

Dennis (1984), however, reported that a mortar consisting of 1 part of cement: 3 parts of sand, and containing a polymer concentration of about 20%, has a rather shorter setting time than an unmodified mix of similar initial consistency. Floor toppings based on some types of SBR latex can take light foot traffic 8 hours after laying, at air temperatures of 20°C.

2.4.2 Properties of Hardened Mortar and Concrete

2.4.2.1 Strength

Strength is a major property, which is significantly affected by the modification of mortar and concrete with polymers. In relation to polymer modified systems, strength is influenced in principle by: a) the nature of materials used, b) mix proportions, c) curing methods and d) methods of testing. In general, latex modified mortar and concrete show a noticeable increase in tensile and flexural strengths but no improvement in compressive strength, as compared with ordinary cement mortar and concrete.

Compressive Strength

From the work done by Lewis (1990), the compressive strength of SBR latex modified concrete with constant w/c is reduced for all contents of polymer. Dennis also reported a lower compressive strength for 20% SBR mortar.

Mortars modified with acrylics have shown similar results. The 28 day compressive strength of acrylic modified concrete, with 15% addition, is 51 N/mm² compared with the 66N/mm² for normal concrete (Lewis 1990). Emberson (1990) and Lavelle (1988) obtained lower compressive strength compared to unmodified mortar. Bhargava (1981), however, from tests on concrete samples cured in air using 4 types of acrylic polymers, with 10% addition, obtained an increase in compressive strength to the unmodified mortar, of the order of 5 to 45%.

For mortars modified with EVA polymers, a higher strength was reported than the unmodified mortar with increasing p/c ratio up to 20%. Strength also depended on bound ethylene content, with an optimum value between 12-17% (Ohama 1987).

Burge (1987) reported an increase in compressive strength at 28 days with increasing polymer content, when using a styrene acrylate polymer. However, Grosskuth(1987) observed a decrease in compressive strength. Other polymers which have been reported to result in increased compressive strength compared to unmodified sample, are natural rubber latex, polyvinyl sulfonic acid (Diab 1985) and vinylidene chloride (Aminabhavi 1982-83).

Tensile and Flexural Strengths

An increased tensile and flexural strength is a significant property contributed by latex modification of cement. Plain mortars and concretes are weak in tension, whereas polymers do possess an inherent ability to withstand tensile and flexural stress. Hence, the addition of polymer to a concrete should improve flexibility and this indeed is observed (Lavelle 1988; Lewis 1990; Nagaraj 1988; Ohama 1987). The strength increase has been reported to be between 40% and 200%. For example, with 55% bound styrene content and 20% p/c, styrene-butyl acrylate-cement has a 200% higher flexural strength than an unmodified one. This increase in strength, is attributed to the improved bond between the aggregates and the polymer modified matrix.

Tensile and flexural strengths will decrease when PMC are exposed to wet curing at early ages due to lack of proper film formation. This phenomenon is particularly significant when VA and VAl are used, because in wet cement the polyvinyl acetate converts to polyvinyl alcohol and calcium acetate which are soluble and leach out.

Adhesion and Bond Strength

In general, most polymers used in modifying mortars and concretes improve their bond strength to both concrete and steel substrates. A mortar modified with SBR latex (20%)

was tested for adhesion in tension by Michalyshin (1983). A conventional mortar was cut in half and the polymer modified mortar being tested was cast against the cut face. The tensile bond strengths of modified mortars were respectively 336 N/cm² in dry conditions and 217 N/cm² in wet conditions, while the bond strengths of the control mortar were about 49 and 42 N/cm².

From pull-out tests performed by Burge (1987), PVP, SBR and S-Ac polymer modified mortars exhibited bond strength increases of about 50, 150 and 400% respectively over control mortar.

Another test that measures adhesion by a direct tensile method has been used on PMC (Walters 1988; Kuhlmann1988). The results indicate that the bond strength of PMC exceeds 140 N/cm² at 2 days and 210 N/cm² at 28 days.

The shear bond strength of PMC has been measured by using a guillotine-type device to shear a cap of PMC off a cylinder of conventional concrete (ACI 1991). The PMC was made with 15% latex addition and cured first 1 day at 100 percent RH, and then at 50 percent RH at 20°C. The average values were 179 N / cm² after 7 days and 328 N/cm² at 28 days.

The bond of PMC to reinforcing steel has also been evaluated (ACi 1991). Epoxy-coated and uncoated steel bars were embedded in a PMC overlay on a conventional concrete base. The results showed that the design capacity of the bars was achieved in the PMC overlays.

Shrinkage

The addition of latexes to concrete does not increase its total shrinkage. This was demonstrated by Ohama (1982), where three latex contents were used in concrete specimens of three different sizes. The results showed that the shrinkage of concrete did not increase with the addition of SBR.

In a recent study, Evbuomwan (1992) investigated the drying shrinkage of a polymer modified mortar containing microsilica with or without steel fibres. The tests were carried out in two ways: free and restrained drying shrinkage tests in different curing regimes. The drying shrinkage of the specimens for free drying shrinkage test, was generally found to increase with age up to 84 days. Increasing the period of initial moist curing of the specimens with and without 5%SBR led to a reduction of about 17.2 and 30.5% of drying shrinkage respectively at 84 days. The mix which showed the most significant reduction of drying shrinkage of about 43% was the one which contained 5%SBR+1.0% steel fibres. In the restrained drying test, the specimens containing the combination of either 0.4% polypropylene, or 1.0% steel fibres and 5%SBR remained uncracked at 280 days after casting. The added 5%SBR and the fibres appears to be very important in reducing drying shrinkage and eliminating shrinkage cracking in the polymer modified concrete.

Some latexes such as VA, natural rubber and polychloroprene (CR) may cause a larger shrinkage than those of unmodified concretes.

Abrasion and Impact Resistance

Generally, abrasion and impact resistance of mortars and concretes are increased when suitable polymer latexes are used. Many investigators (Lavelle 1988; Teichman 1976; Gierloff 1982) have reported an increase in the abrasion resistance of PMC for several latexes. This is also reflected in the work of Burge (1987). The mortars modified by S-Ac, SBR and acrylic latex showed higher abrasion resistance.

2.4.2.2 Durability

It is suggested that the improved durability of the polymer modified system is associated with reduced porosity due to reduced w/c ratio and the partial filling of pores by the polymers. In addition to the modification of pore structure, the chemical resistance of the

polymers may also contribute to improvements in the impermeability, waterproofness, freeze-thaw, chloride diffusion, corrosion and carbonation resistance.

Permeability

Polymer modified concretes have low permeability, which have been demonstrated by several tests. For example, the water absorption and water vapour transmission tests exhibited that PMC has a good water impermeability (Marusin 1987; ACI 1991). Good water impermeability of the PMC also provides the high resistance to chloride penetration and chemical corrosion (Al-Qaser 1990; Lavelle 1988; ACI 1991). The main polymer types that have been investigated with respect to chloride diffusion include SBR, VA, EVA and acrylic system. They all exhibited excellent resistance to chloride diffusion.

Freeze and Thaw

The freeze-thaw resistance depends on the type of polymer and the number of freeze-thaw cycles which the modified systems are subject to. In general, polymer modified concretes have good freeze and thaw resistance, provided that they have been properly cured allowing the formation of the polymer film. Walters(1990) observed that SBR gave the highest freeze-thaw resistance among VA, VAE, S-Ac and SBR. Ohama(1987) reported that the freeze-thaw durability is improved at a p/c ratio 5% or more. Increasing the p/c ratio does not necessarily cause an improvement in the freeze-thaw durability. The reason for this improvement is due to the combination effects of water impermeability and air entrainment.

Carbonation Resistance

Carbonation resistance is an important property that influences of the durability of the concrete and corrosion of rebars. Researchers have studied the carbonation resistance of systems modified with various polymer types. For instance, mortars modified with S-Ac and VaVeAc increased the carbonation resistance by a factor of 4 to 7 compared to the control mortar (Hackel 1987). The carbonation resistance of SBR, EVA and Ac modified mortars were found to be greater than that of the plain mortar (Ohama 1987). Aimin

(1988) performed tests on modified cement pastes using polymers based on acrylic monomers. They observed that carbonation depths increased with exposure time but at different rates for each polymer content, and that the rate of carbonation increased with increase in polymer content compared with control paste reaching a maximum at 10-15%, and then decreased with further increase of polymer content.

2.4.3 Applications of PMC

PMC has been widely used in the construction industry for many years and has proved to be reliable not only for repairing deteriorated concrete, but also for protecting new concrete. Major applications include bonding, flooring, repairing, overlays of bridge decks and latex shotcrete.

A slurry of cement in latex is generally a better adhesive than either of the constituent materials used alone. Therefore, the slurries of latex-cement are widely used to promote the adhesion of cementitious mortars or concretes to existing hardened concrete, rock, quarry tiles and other substrates.

Slurries incorporating fine fillers such as silica flour are used as levelling compounds in the preparation of floors to provide a smooth levelled surface before laying sheet flooring materials. They are also used as protective coatings to steel reinforcement, or an all-over coating to provide a damp-proof membrane, or the resurfacing of airfield runways.

Polymer modified mortars and fine aggregate concretes are used as waterproof renders for lining cellars, swimming pools etc. As abrasion-resistant renderings, they are used to line industrial coal bunkers, and for sea defences.

In the field of concrete repairs, polymer modified mortars are widely used because the durability of conventional mortar had been found unreliable for a variety of reasons such as high porosity, rapid carbonation and poor bond. Polymer modified mortars are proving very beneficial and have largely replaced epoxy resin mortars. It should be

stressed that the mix proportion of mortar should be well designed to obtain optimum performance.

2.5 FACTORS AFFECTING PMC PROPERTIES

2.5.1 Type of Polymer

It is obvious that different polymers have different features, which impart polymer modified concrete with different properties. SBR, with an appropriate ratio of styrene/butadiene, gives a good performance in both wet and dry conditions because the two monomers are hydrophobic. Wear resistance is generally very good and SBR modified mortars are widely used in industrial flooring.

Acrylics generally have a good wear property and resistance to chemicals, but poor adhesion in wet conditions. S-Ac has fairly good wear and abrasion characteristics, and the improvement in strength is substantial in both wet and dry conditions.

VA can achieve good compatibility with cement and eliminate problems such as set retardation. It also produces good adhesion to existing substrates. The high molecular weight ensures good strength properties and wear resistance. However, VA readily absorbs water and is also readily hydrolysed, especially under alkaline conditions, to give polyvinyl alcohol and acetic acid, both of which are water-soluble. This causes significant weakening of the wet performance of a VA modified material.

VA and ethylene copolymerise at high pressure readily to give high molecular weight products. This results in a more hydrophobic co-polymer which shows a corresponding improvement in performance under wet conditions. Similarly, VaVe improves the wet performance and resistance to hydrolysis.

2.5.2 Mix Design of PMC

The mix design for incorporating polymers in mortars and concrete, is usually dependent on the needs of application and type of polymers. In practice, the levels of latex dosages (weight of polymer solids to weight of cement used) range from 5-20%, of which 15 has been found to yield optimum performance. An excessive dosage of polymer, in addition to being uneconomical, tends to have an adverse effect on the properties of latex modified concrete, e.g. low compressive strength and skinning problems. The reduction in strength may be due to the fact that at too a large ratio, polymer bonding creates discontinuities in the cement paste structure, or the cement may not hydrate adequately. Too little addition will increase the required water cement ratio and the desired properties may not be achieved.

2.5.3 Curing Regime

The curing conditions for latex modified mortar and concrete are different from those for ordinary concrete. Many authors (ACI 1991; Dennis 1988; Ohama 1987) have reported their investigations on this topic. For cement hydration and subsequent development of strength of the cement paste a wet cure is needed, but for film formation of the latex phase a dry cure is required. Consequently, a wet-dry curing procedure suitable for both processes is often recommended. That is that the specimens are first cured at 100% RH for one or two days and then cured in air at 50% RH for another 26 days. This curing regime provides suitable condition for the cement hydration and allows latex to dry out and form a film, thus, leading to better properties of the system.

2.6 HYPOTHESIS OF MECHANISM FOR IMPROVEMENTS

2.6.1 Equivalent Workability at Lower w/c Ratio

A common opinion on the improvement mechanism of PMC is that the polymers improve workability of fresh mortar and concrete, thereby reducing water content needed for a given flowability.

This is explained as the result of changes in the dispersion structure of particles in the slurry. The latex particles are spherical in shape. When they are added to concrete mixes, they tend to distribute among the cement particles providing a ball bearing action which lubricates the mix and minimises internal frictional forces, thus increasing the flow.

The aqueous components of the latex may also influence workability and could be more important than the polymer itself. For example, surfactant combinations, when they are well designed, have great benefits on the workability of concrete mixes. They adsorb onto the surfaces of the cement and lower surface tension in the mix, which gives a better cement distribution, resulting in decreases in both viscosity and yield stress and allowing the release of a little water from the mix under pressure from the trowel. Therefore, the surfactants act as a cement plasticiser and water-reducing admixture (Concrete Society 1994). In addition, lowering surface tension assists the cement paste or mortar to wet the substrate to which it is applied, promoting good adhesion.

As a result, the mixing water is reduced, thus a lower water cement ratio is required for given flowability. Consequently, higher compressive strength and better freezing and thawing characteristics of the mortar and concrete are obtained.

2.6.2 Microcracks Held Together by Polymer Film Network

Generally, when polymer latexes are mixed with fresh cement mortar or concrete, the polymer particles are uniformly dispersed. CSH gel is gradually formed by cement hydration and the water phase is saturated with calcium hydroxide, whereas the polymer particles deposit partially on the surfaces of the cement gel or unhydrated cement particles and partially on aggregates. With continuous water removal by further cement hydration, evaporation, or both, the polymer particles start to coalesce into a continuous polymer film or a network which binds cement phases and aggregates.

By using electron microscopy techniques some researchers (Wagner 1965, 1967; Isenburg 1974) have observed polymer films bridging in microcracks of concretes. Based on this fact, improvement in the properties of latex modified systems have been explained in the following way. The inherent micro-cracks in mortar or concrete are bridged by the polymer films. Under stress, these films prevent crack propagation and simultaneously a strong cement hydrate-aggregate bond is developed. The sealing effect due to the polymer films also provides a considerable increase in resistance to moisture, water penetration, chemical resistance, and freeze-thaw durability. The continuous film of polymer formed in a hardened concrete improves mechanical properties by preventing propagation of cracks.

2.6.3 Chemical Reaction Theory

The chemical reaction theory emphasises chemical interaction between the polymer phase and the hydration products of the cement. When the polymer is added to the cement, chemical reactions probably take place at the interfaces between polymer particles and hydrates. A typical chemical reaction is the saponification of lower acrylates. The carboxylate groups react with Ca^{2+} ions. These reactions may lead to crosslinking and insolubilization of polymers, which actually act as a chemical bonding or chemical anchors (Chandra 1987; Larbi 1990; Wagner 1978).

CHAPTER 3

MATERIALS AND EXPERIMENTAL TECHNIQUES

3.1 CHOICE OF MATERIALS

3.1.1 Cements

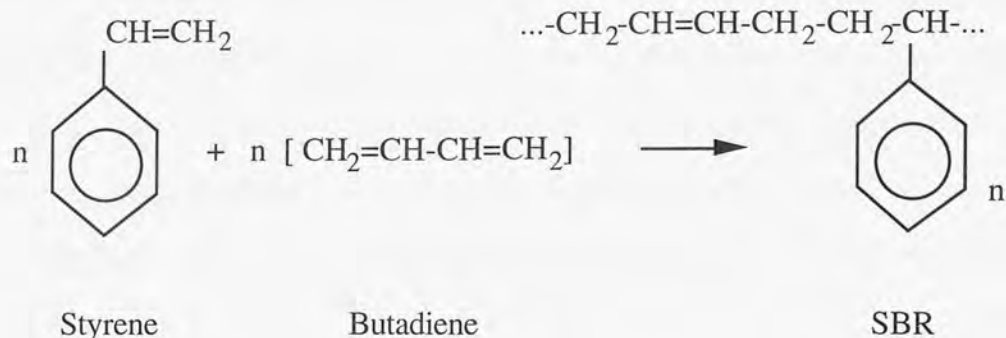
In order to carry out fundamental studies, polymer modified cement paste rather than mortar/concrete, was preferred for the investigations since the elimination of aggregate simplifies the systems. An ordinary Portland cement (OPC I) was used throughout this investigation and another ordinary Portland cement (OPC II), which contained a higher alkali content compared to OPC I, was selected for some experiments. Table 3.1 lists their chemical composition and Bogue compounds.

3.1.2 Polymers

The choice of the polymer latex was restricted to those which are manufactured and marketed under strict conditions of quality control and consequently possess well established material properties. Since styrene butadiene rubber (SBR), pure acrylics and ethylene vinyl acetate (EVA) are widely used in PMC, they were preferably chosen with the view of making the results of the investigations directly relevant and applicable to the UK construction industry. Other formulations were chosen to enable comparison between latex and redispersible powder forms, and study systematic changes in composition.

3.1.2.1 Styrene-Butadiene Rubber Copolymers (SBR)

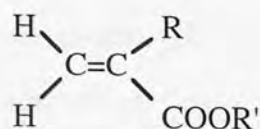
The polymer emulsions used were a standard carboxylated SBR (designated SBR 1), and a special SBR (designated SBR 2). Styrene:Butadiene is 60:40 and copolymerization results in a nearly random copolymer:



Both SBR 1 and SBR 2 contained 47% polymer solids, non-ionic stabilisers, and anti-foaming agents; particle size was in the range 50-200 nm, the pH value was 9.5 and specific gravity was 1.01 in each case. The essential difference was that the degree of carboxylation of SBR 1 was 1% whilst that of SBR 2 was 5%. The aqueous component of SBR 2, which included the stabilisers and anti-foaming agent but not the polymer solids, was also supplied.

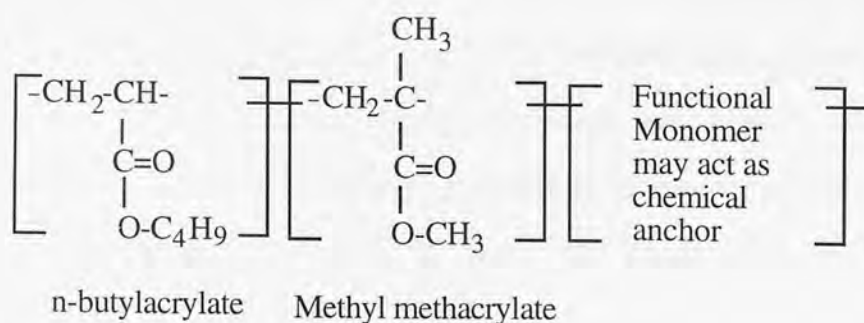
3.1.2.2 Acrylics

Acrylics may be defined as a family of resins resulting from the polymerisation of derivatives of acrylic acid and generally are copolymers of the esters of acrylic and methacrylic acids. A generic formula for acrylate ester is



in which R is H for acrylates and CH₃ for methacrylates. While those copolymers will have a certain similarity of chemical structure, the properties of each type are influenced strongly by various factors. The two most critical factors are the presence of CH₃ or H on the alpha carbon and the length of the ester side chain, R'. The acrylate polymers are believed to have more rotational freedom than the methacrylates because of having an alpha hydrogen adjacent to the carbonyl group. The substitution of a methyl (CH₃) for the hydrogen atom restricts the freedom of rotation of the polymer (steric hindrance) and thus produces harder, higher tensile strength and lower elongation polymers than the acrylate counterpart. The length of the ester side chain group also affects the properties. The longer the side chain is, the lower the tensile strength and the higher elongation the polymer has.

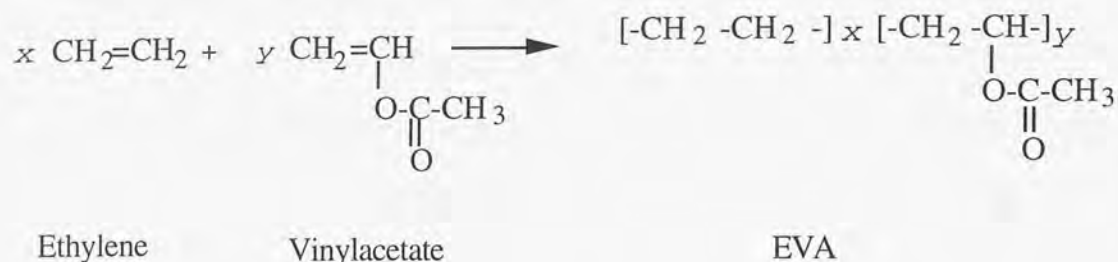
Three acrylic copolymers were used in this investigation and were all commercial products. Ac 1 and Ac 2 were milky-white emulsions and Ac 3 was a redispersible powder, but their exact compositions were not known. Ac 4 is an acrylic terpolymer (n-butyl acrylate / methyl methacrylate / functional monomer) in emulsion form. Its structure may be expressed as:



Long side chains in the structure may increase elongation, adhesion of the polymer and the stability against alkaline attack. The carboxylate group in the branch chain may interact with calcium to form "chemical anchors" (Justnes 1992).

3.1.2.3 Ethylene-Vinyl-Acetate Copolymers (EVA)

Ethylene-Vinyl-Acetate Copolymer (EVA) is a copolymer of vinylacetate and ethylene:



Like SBR, ethylene and vinylacetate can be incorporated at any ratio. The copolymerisation process must be operated under high pressure at a level depending on the incorporation ratio. The low vinylacetate copolymer (10-40 wt %) is incorporated under a pressure $\geq 103\text{MPa}$. A medium vinylacetate copolymer (45 wt%) is made at 34.5MPa . The high vinylacetate emulsion copolymers (70-90 wt%) are made in emulsion process under ethylene pressures of $2.07\text{-}5.2\text{ MPa}$.

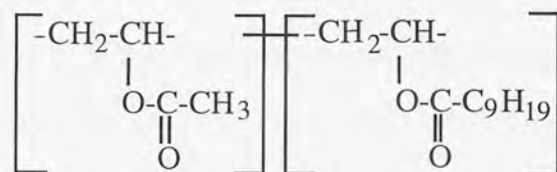
The incorporation ratio will affect the properties of the polymers, via degree of crystallinity. The crystalline phase provides rigidity and a high softening temperature, whereas the amorphous phase provides flexibility and high impact strength. As the ratio of vinylacetate increases, the crystallinity decreases and consequently the stiffness decreases. At 45 wt% of vinylacetate, crystallinity is essentially destroyed, and the copolymer is elastomeric. Above 65 wt%, the properties approach those of polyvinylacetate.

The EVAs used in the present investigation were EVA 1 in emulsion form and two water redispersible powders EVA 2 and EVA 3. Their properties are listed in Table 3.2.

3.1.2.4 Other Polymers

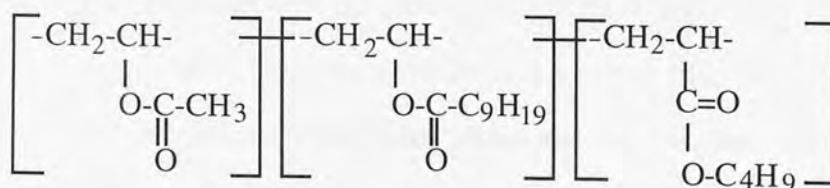
Two special polymers were also used in the study. They were vinylacetate-vinylversatate copolymer VaVe (CAS-No.9070-52-4) and vinylacetate-vinylversatate-butylacrylic terpolymer VaVeAc (67828-12-0). Versatate is a family of vinyl esters of branched carboxylic acids which usually contains 9-11 C atoms. These esters serve as comonomers for vinyl acetate to prepare emulsions for paints and adhesives, but are not widely used in the consumer market because of high price comparing with other polymers.

In these two polymers, the versatate is tert-decanoic acid, ethylene ester ($C_{12}H_{22}O_2$). Therefore their structures are respectively:



Vinylacetate

Vinylversatate



Vinylacetate

Vinylversatate

Butylacrylate

The main properties of all polymers used in this investigation are summarised in Table 3.2.

3.2 SPECIMEN PREPARATION

3.2.1 Mix Proportions and Casting

In order to study the effects of polymer additions on the properties of polymer modified cement, four polymer-cement ratios (p/c) were used. They were 0.05, 0.10, 0.15 and 0.20, being determined by weight of polymer solids to weight of cement. Two water-cement ratios (w/c) of 0.3 and 0.5 were selected. The amount of water contained in the latexes was subtracted from the mixing water. When required the addition of the defoamer was equivalent to 1% by weight of polymer solid content. The amount of the aqueous component was equivalent to that contained in the latex.

If the polymer was in the form of latex, the latex and defoamer (when it was used) were first added to the required amount of water, stirred with a glass rod and then added slowly to the cement. In the case of redispersible powder, the polymer was premixed with the cement and then mixed with water. After being mixed thoroughly for five minutes by hand, the slurry was cast into cylindrical PVC containers, 4.9cm in diameter and 7.5cm in length. The filling procedure was divided into three steps to avoid a large amount of air being trapped in the samples. For each step, the container was only filled with slurry to a depth of about one third, and subsequently compacted by a vibrator until air bubbles no longer came to the surface of the slurry. Once the filling was completed, the top layer was covered with a polythene sheet and the container tightly sealed by forcing a cap on the top. In order to prevent significant segregation and density variations before the setting of cement, the cylinders were rotated at 10rpm for 24 hours.

3.2.2 Curing Regime

The curing regime is a very important factor affecting the properties of PMC as discussed in section 2.4.5. Effects of curing are being investigated in a separate project and only two curing schemes were chosen in the present study. The majority of samples were

sealed in their containers and cured at 20°C in a curing room for the required times. It is believed that this regime maintained stable curing conditions (no water enters or leaves the system) and hence enabled reliable and repeatable results to be obtained. For a comparative study of the polymer film formation process, an alternative curing regime was used. Samples were first cured for 3 days under the above curing regime, and then demoulded and stored in a desiccator with a relative humidity of 30%, for the required times.

3.2.3 Drying of Samples

It is necessary to stop the hydration of cement at different ages in order to study microstructural development of the pastes. In general, there are three methods that can be used to stop the cement hydration. They are drying the sample in an oven at 105°C, soaking the sample with organic solvents and freezing the sample in liquid nitrogen (cryosublimation). In the present study, all samples were treated with an organic solvent, propan-2-ol. When the cylinders had been cured for the required ages, they were demoulded and broken into small pieces with a hammer and chisel. About 30g were soaked in the propan-2-ol in a flask for 2 days. After soaking, they were treated with fresh propan-2-ol in an ultrasonic water bath and dried with a hair dryer. They were then dried in an oven at 50°C for 10 hours, which accelerated the evaporation of propan-2-ol and avoided the collapse of the pore structure thought to occur at 105°C (Moukwa 1989). Finally, the dried samples were kept in a desiccator.

3.2.4 Total Solids Content of Latex

The total solid content of a latex is defined as the percentage by weight of the non-volatile component at a given temperature in an open atmosphere. The general procedure is to weigh a known quantity of latex into a flat-bottomed glass dish and allow evaporation to a constant weight at a given temperature. In the BS procedure, a 1.5-3g sample is dried at 100°C for 90 minutes + 15 minutes after turning over the dried sheet. The hot film of

dried polymer should be cooled in a desiccator before weighing. The change of weight after a further 15 minutes heating should be less than 1mg. The fractional solids content S is calculated based on the following relationship:

$$S = \frac{W}{W_0}$$

where W_0 is the initial sample weight, and W is the weight of the residue.

3.2.5 Synthetic Pore Solution

Synthetic pore solutions were prepared based on results from the analysis of pore solutions extracted from 28 day old cement paste. The concentrations of Na^+ and K^+ in pore solution were 0.1 mol/l and 0.46 mol/l respectively. According to cement chemistry (Taylor 1990), at 1 day after mixing, the SO_4^{2-} has almost totally disappeared from the solution by reaction with the C_3A , therefore no sulphate was added to the solution.

All reagents were analytical grade and the water was deionised. Firstly, 4g NaOH and 25.81g KOH were dissolved to produce a 1 litre solution, and then 2g $\text{Ca}(\text{OH})_2$ were added to saturate this solution. The pH value of the synthetic solution was 13.70 determined by titration against 0.01 mol/l nitric acid with phenolphthalein as an indicator.

3.2.6 Solution Preparation for Selective Dissolution

To separate the polymer phase from the cement phase, dissolution techniques were used. Several different solution systems have been utilised to dissolve cement, such as acetic acid/methanol (or ethanol), salicylic acid/methanol/acetone, ethylene diamine tetraacetic acid (EDTA)/Triethanolamine/NaOH and NTA/HEDTA/DCYTA complexing agents. According to Luke (1987), the system of ethylene diamine tetraacetic acid (EDTA)/Triethanolamine/NaOH gave the highest percentage of cement dissolution (about 90%). This system was therefore used in this study. The solution preparation procedure

consists of first dissolving 18.61g EDTA acid disodium salt and 10.60g Na₂CO₃ in 1000ml deionised water to get 0.05 mole/l EDTA and 0.1 mole/l Na₂CO₃ solution; then making a solution of triethanolamine-water in a proportion of 1:1; finally mixing the above two solutions with water in a proportion of 10:1:10. The pH value of the solution was adjusted to 11.6 with 1M NaOH.

3.2.7 Preparation of Polymer Films

It is not easy to prepare polymer films satisfactorily from latex, since sedimentation of ingredients may occur during the drying times, and this may lead to non-uniform vulcanisates and inhomogenities in the structure. However, in this study it seems not to have been a problem and thin sheets were used to aid the understanding of the function of the polymer phase in the diffusion properties of PMC.

The latex was poured into a petri dish and it was allowed to dry at room temperature in a dust-free atmosphere. When sufficiently dry, the film was stripped from the dish, turned over and allowed to stand for another 2 days. The thickness of the dried films was accurately measured using a micrometer. They were cut into disc shapes and stored in a desiccator ready for use.

The advantages of this method were that no additions needed to be made to facilitate the preparation of thin sheets and the period required for spontaneous setting was so short that appreciable sedimentation was unlikely to occur.

3.3 EXPERIMENTAL TECHNIQUES

3.3.1 Conduction Calorimetry

Conduction calorimetry is an easy and accurate method used to measure the hydration rate of cement. The principle of this method is that heat generated by the cement

hydration is allowed to flow through a sensitive thermopile to an aluminium heat sink. The heat sink is maintained at a constant temperature by immersing the calorimeter in a water bath, where the temperature is controlled to a high degree of accuracy ($\pm 1^\circ\text{C}$). The thermopile produces an electrical output proportional to the heat flow through it. Recording continuously the electrical output over a period with a suitable computer, the hydration process of the sample can be followed (see Fig. 3.1).

To enable the output signals to be accurate and to convert the data from mV/g of cement to mW/g of cement, the evolution curve should be calibrated for individual experiments. This can be performed, when the heat evolution from the cement hydration has reached a small stable state, by fitting a heater inside the sample holder and supplying it with a stabilised power supply.

The method of calibration, mathematical interpretation of results and the experimental procedure are given in detail in Chapter 4.

3.3.2 Mercury Intrusion Porosimetry (MIP)

Mercury Intrusion Porosimetry (MIP) was employed as one of the methods to assess the pore size distribution and the total porosity of polymer modified cement pastes. MIP is based on the fact that a liquid that does not wet a porous solid will enter its pores only under pressure. This technique consists of enclosing a sample in a glass cell, surrounding it with mercury, applying monitored increments of pressure, and measuring the volume of mercury being forced into the sample. If the pores are assumed to be cylindrical, the pressure needed to force the liquid into them is p , then the pore size can be obtained by using the Washburn equation:

$$d = - \frac{4\gamma\cos\theta}{p}$$

where d is the equivalent diameter of the intruded pores, γ is the surface tension of mercury (0.485 N/m), θ is the contact angle between mercury and the pore walls (117° was assumed).

The resulting volumes are often normalised in volumes by sample weight (cm^3/g) and the plot of normalised intrusion volume versus equivalent pore diameter gives the cumulative porosity curve.

Since MIP works at high pressure it is believed that the intrusion of mercury may destroy the original pore structure (Feldman 1984; Shi 1985), and there are additional uncertainties involved in the interpretation of the results. Nevertheless, as a means of comparing pore structure in materials of similar composition, it can provide an indication of the material's microstructure and distinguish differences in cement-based materials (Cook 1993; Day 1988).

3.3.3 Solvent Exchange Porosity and Water Absorption Porosity

Solvent exchange porosity and water absorption porosity were determined in order to get further information and assess the accuracy of MIP results.

Five replicate discs were cut from a cylinder in the same way as described later in section 3.3.13. The discs were first saturated by immersing them in distilled water for one hour; weighed in air; then placed in propan-2-ol for four weeks to allow the propan-2-ol to completely replace the water in the discs (Day 1988); then weighed again. During the exchange process, the alcohol was renewed each week. The weight reduction is due to the exchange of water for alcohol by counter-diffusion.

Let W_1 be the weight of the disc after saturation with water; W_2 the weight of the disc after the water in the disc is replaced completely with propan-2-ol and W_{dry} the weight of

the disc after drying in an oven at 105°C. As assumed, the water in the disc is completely replaced by propan-2-ol, then the volume of water V_w is equal to the volume of propan-2-ol V_p , i.e.

$$V_w = V_p$$

or

$$\frac{W_w}{\rho_w} = V_p \quad (5-1)$$

because

$$\begin{aligned} W_w &= W_1 - (W_2 - W_p) \\ &= W_1 - (W_2 - V_p \rho_p) \end{aligned} \quad (5-2)$$

Replace W_w in equation (5-1) with equation (5-2) and rearrange, gives

$$V_p = \frac{W_1 - W_2}{\rho_w - \rho_p}$$

under experimental conditions, the specific gravity of propan-2-ol, ρ_p , and water, ρ_w , are respectively 0.781 and 1.00. Therefore, the solvent exchange porosity P_p in unit of weight of disc is

$$P_p = \frac{V_p}{W_{dry}} \quad \text{or} \quad P = \frac{W_1 - W_2}{\rho_w - \rho_p} \frac{1}{W_{dry}}$$

For water absorption porosity (P_w), these discs were dried in an oven at 105°C until no further weight change occurred. After being cooled down to room temperature in a desiccator, they were weighed (W_{dry}). The difference in weight from the water-saturated condition was used to determine the water absorption porosity.

Porosities from either method were reported as volume per unit weight of dried paste (cm^3/g) in order to compare with MIP results.

3.3.4 Helium Pycnometry

As an alternative method for determining total porosity, helium pycnometry was used. This was done by Leeds University. From the helium pycnometer, the relative density (D_r) of sample is obtained. Thus, the porosity (P) of the sample is calculated by using following formula:

$$P = \left(1 - \frac{D_d}{D_r}\right)$$

where D_d is bulk (apparent) density of sample and is usually measured by mercury pycnometer (Abdelalim 1980).

3.3.5 Differential Thermal Analysis (DTA) and Thermal Gravimetric Analysis (TGA)

When a substance is subjected to thermal treatment it may undergo physical or chemical changes. For a particular substance these changes occur at characteristic temperatures. It is therefore possible to identify a substance by recording these changes as a function of temperature. In differential thermal analysis (DTA) the temperature difference between sample and reference material is recorded while in thermal gravimetric analysis (TGA) the change in mass is measured using a thermobalance.

A Stanton Redcroft 1500 Thermoanalyzer was used in this study and can simultaneously record both changes in temperature and mass and allow the sample to be heated in various atmospheres. In each run the amount of powder sample was weighed accurately (about 50mg) and the sample heated in flowing argon or air. The rate of heating was 20°C/min and the reference material was calcined alumina.

3.3.6 Scanning Electron Microscopy (SEM)

Scanning Electron Microscopy (SEM) was used to examine fracture surfaces of PMC pastes. Surfaces were examined as fractured and after etching with HNO_3 / HCl . The former allows examination of the microstructural development of the pastes, including the morphology of the cement hydrates, crystal size and pore shape. The later makes it possible to observe the existing form of polymer in the matrix.

All specimens were broken off from 90 day old cylinders and dried in the same way as described in 3.2.3. For etching samples, the specimens with flat surfaces were carefully selected. The flat surfaces were etched with a solution consisting of 1% HNO_3 + 1% HCl for 3 minutes. The specimens were rinsed with deionised water and dried with a hair dryer. Before examination by SEM they needed to be coated with a thin film of conducting material (Au).

3.3.7 Pore Solution Expression

The apparatus used to extract pore solution from concrete was first reported by Longuet (1973). This apparatus consisted of four parts , i.e. piston, die body, platen and support cylinder (see Fig. 3.2).

The sample is dropped into the bore and a PTFE seal and piston inserted. The pore presser used in the laboratory is similar to the one shown, but it is connected with a computing system so that the experimental process can be controlled automatically by a program. The operation parameters are then entered into the computer. These parameters include loading rate, maximum load, displacement of ramp and testing time. After pressing the "RUN" button, the load is increasing at the desired rate (2KN/s) until the maximum load (600KN) is attained and maintained at this level for a period of time (20 min.). The solution squeezed out flows through the fluid drain and is collected in plastic

vials. When and how much solution will be squeezed out depend on water cement ratio of samples, curing condition, age and loading rate.

Once the test is completed, all surfaces were immediately cleaned with water and acetone, wiped with soft tissue and sprayed with PTFE non-stick spray ready for the next test.

3.3.8 Analysis of Solution

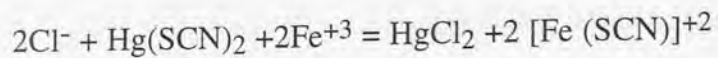
Chemical analysis of the solutions involved determination of hydroxyl (OH^-), chloride (Cl^-), sodium (Na^+) and potassium (K^+) concentrations. All analyses were carried out by standard methods.

3.3.8.1 Hydroxyl Ion

Hydroxyl (OH^-) concentration in the pore solution was determined by titration with 0.1 mol/l HNO_3 using phenolphthalein as the indicator. A 0.1 ml aliquot of sample solution was placed into a conical flask of 50ml capacity using a pipette. Two drops of phenolphthalein were added giving the solution a red colour. This was titrated with 0.1 mol/l HNO_3 until the end-point of the titration. The result is the mean value of two titrations in which their difference must be less 0.05 ml.

3.3.8.2 Chloride Ion

The mercury (II) thiocyanate method was employed for the determination of chloride ion in solution (Bassety 1978). A 0.1ml aliquot of solution was added to a 10ml test tube and filled with deionised water to the mark level, followed by 2ml of 0.25M-ammonium iron (III) sulphate $\{\text{Fe}(\text{NH}_4(\text{SO}_4)_2 \cdot 12\text{HO})\}$ in 9M-nitric acid and 2ml of a saturated solution of mercury (II) thiocyanate in ethanol, $\text{Hg}(\text{SCN})_2$. The chloride ion reacts with $\text{Hg}(\text{SCN})_2$ to liberate $(\text{SCN})^-2$ which then reacts with the Fe^{+3} to give a red-coloured compound:



The colour intensity of the solution is proportional to the original chloride ion concentration. By measuring the absorbance of the solution using a spectrophotometer at 460nm and comparing with a calibration curve, the concentration of chloride ion in the sample solution can be obtained. A series of standard sodium chloride solutions was prepared by dissolving sodium chloride in deionised water and their absorbances were measured in the same way as above.

3.3.8.3 Sodium and Potassium Ions

The determination of sodium and potassium was carried out using a flame photometer. In this technique, standard solutions of sodium and potassium were required to construct calibration curves. 2.542mg sodium chloride and 1.909mg potassium chloride were dissolved in 1000ml de-ionised water to make 1000 ppm of stock solution. This solution was diluted to give five working standard solutions containing 1, 2, 4, 6, 8 ppm of sodium and potassium ions. The reading for each concentration was first taken by aspirating standard solutions under a sodium filter or potassium filter. Thus calibration curves for sodium and potassium were prepared by plotting the readings against the concentrations. The concentrations of sodium and potassium ions in sample solutions were then evaluated from the calibration curves. If the concentration of the sample solution is too high then the solution must be diluted quantitatively before the absorption measurements.

3.3.9 Total Chloride Ion

The determinations of total chloride ion concentration in cement paste followed the following procedure. Powder samples were dried in an oven at 105°C about 5 hours. About 0.5g sample were added into a conical flask and 20ml of HNO₃ were added in it. The flask was then warmed at about 80°C for 20 minutes. The solution was filtered into a

100ml flask, which was subsequently filled with deionised water to the mark level. The concentration of chloride ions in the solution was measured by the way mentioned in 3.3.8.2. The results were expressed in m mol/g dry paste.

3.3.10 Selective Dissolution of Cement

The principle of selective dissolution is based on the fact that a solution will dissolve some components leaving other components undissolved. For PMC pastes the solution of EDTA/Triethanolamine/NaOH will preferentially dissolve the unhydrated cement and the hydration products leaving only polymer undissolved. About 1g dried powder sample was put in 100 ml EDTA/Triethanolamine/NaOH at room temperature for 3 days and stirred occasionally. The whole solution was transferred into a soxhlet extractor and filtered off under vacuum onto a filter paper and rinsed with fresh EDTA/Triethanolamine/NaOH for 1 hour. The undissolved polymer was placed in 50ml EDTA/Triethanolamine/NaOH and shaken in a ultrasonic water bath for 3 min. After further filtration, it was dried in air at room temperature and stored in a desiccator.

3.3.11 Infrared Spectroscopy (IR)

Molecules absorb infrared radiation resulting in molecular motions, particularly stretching and vibration of atomic bonds. These same types of molecular motions occur even when other atoms or functional groups are involved in the vibrational transitions. However, depending on the types of atom and their environments in the molecule, each transition will have a specific energy associated with it. Each of these vibrational modes will give rise to the absorption of infrared radiation in a specific region of the infrared spectrum. This forms the basis for qualitative analysis and structural determinations by infrared spectroscopy.

3.3.11.1 Sampling Techniques

The type of sampling technique employed depends on the phase of the material to be analysed; solid, solution or gas. The simplest method for solid samples is to press powders into the form of a disk. This technique is based on the fact that the powdered alkali halides (usually potassium bromide KBr) can be pressed into transparent disks under pressure. A few milligrams of sample are mixed well with approximately 300mg of KBr. The mixture is uniformly sprinkled into a die, a vacuum is applied to the die for 30 seconds with a pressure of 2 tonnes and then 10 tonnes pressure is applied for an additional 3 minutes while maintaining the vacuum. After the pressure and vacuum are released, the disk is removed and mounted in the spectrometer.

For solid phase polymeric materials, a free film needs to be made. The technique is to dissolve the polymer in a suitable solvent and cast it onto a metal or glass sheet. The thickness of the film can be controlled by the concentration of the solution. The dried film can then be mounted directly in the spectrometer.

For a liquid sample, the film can be formed by compressing a drop or two of the liquid between plates (sodium chloride). This technique is simple and rapid but is suitable only for non-volatile and non-aqueous liquids. In the case of latex, there is a large amount of water in it, therefore the film was formed in the way described in 3.2.7.

3.3.11.2 Interpretation

After obtaining the infrared spectrum of an unknown material, it is important to know how to interpret the spectrum and to identify the material. In qualitative analysis, there are three interpretation techniques: direct comparison, negative and positive interpretation. The direct comparison method involves comparison of the entire picture with the spectrum of known materials. If the spectra are the same, or very similar, it is reasonable to assume that the materials are nearly identical.

In the negative method, only the characteristic bands of any known functional group are compared. If these bands are absent from a spectrum, then it is said this group is not present in detectable amounts. If there is absorption present in a particular region, no information can be obtained from that region by this method and positive interpretation must then be relied upon.

Positive interpretation is to analyse each band in detail. Normally, the most intense band is first noted. Once this band is identified, confirmatory information should be obtained from the same functionality and the positions of absorption from related groups. In this technique, negative interpretation and reference spectra of known materials are also used. Some correlation charts relating band position to functionality were provided in the literature (Chicago Society for Paint Technology 1969).

3.3.12 X-Ray Diffraction

Fine powder samples of PMC pastes were analysed using a Philips X-ray Diffractometer. The X-ray diffraction pattern is plotted in a graph, with the reflecting intensity (I) as the ordinate and the Bragg reflecting angle θ increasing right to left as the abscissa. The spacing d of the reflecting planes can be obtained by using Bragg's law :

$$n\lambda = 2d \sin\theta$$

where n is the order of the reflection and λ is the wavelength of radiation ($\lambda=1.542\text{\AA}$ with Cu $K\alpha$ radiation).

With the spacing (d) and the intensity (I), the identification of the samples can be obtained by comparing with the Powder Diffraction File. An ordinary method is the Hanawalt Method. First, it is necessary to make a list of the strongest eight lines and then from the file to extract any card that contains two of these eight as the first, second, or third strongest lines; this card can then be examined more closely. If all the lines on this

card are in the observed pattern, then this phase has been identified; this is repeated for the remaining lines to identify the other phases in the sample. The Powder Diffraction File for cement-based materials is given in Appendix A.

3.3.13 Steady-State Diffusion

The experiments on chloride diffusion in hardened cement paste in the steady-state, followed the method described by Page (1981). The diffusion cell consists of two compartments and each has a capacity of about 90ml. One compartment was filled with 1 mole/l NaCl solution and 0.0325 mol/l NaOH solution. The other one was filled with 0.0325 mole/l NaOH solution only.

Each cylinder was cured for 90 days and discs with a thickness of about 3mm were cut by means of a diamond wheel. During cutting, distilled water was used as a lubricant. The surfaces of the discs were lightly ground on Grade 600 emery paper and the discs were fitted into the diffusion cells. Care was taken to select discs which were free of defects apparent on either surface and to make sure no leakage occurred before the diffusion cells were put in the water bath. The water temperature was adjusted to 7°C, 14°C, 25°C, 35°C and 45°C so that the diffusion could be determined at different temperatures. At various diffusion times, the concentration of chloride ions in the low concentration side was determined by withdrawing 100µl aliquot of the solution and analysing using the standard spectrophotometric technique. Samples were tested in this way over a period of up to 4 weeks.

The diffusion experiments in steady-state for pure polymer films were carried out using the same method, but with slight modification in fitting and sealing of the sample. Because the dried film was thin and soft, it was likely that it would not be strong enough to stand inside the diffusion cell and would easily break and leak. To prevent this, the film was put between two disc shaped PVC clamps which had a hole with a diameter of

2cm in the centre. In this way, the film was firmly held and satisfactory sealing was obtained. Fig. 3.3 shows the set-up of the cell.

3.3.14 Non Steady-State Diffusion in Hardened Paste

The experimental procedure of non-steady state diffusion was the same as that described by Sergi (1992). The samples were cured for 90 days and then demoulded. About 1cm was sliced off the cast end. The fresh surfaces were left for diffusion and the others were masked with paraffin wax.

For each polymer addition, 20 cylindrical pastes were prepared and positioned horizontally in a large sealed container. The container was filled with five litres of 1 mole/l NaCl and 0.0325 mole/l NaOH which was the same as that used in the steady state diffusion. After exposure to this solution for 100 days at a constant temperature of 20°C, 10 samples were cut into 7mm thick discs by a dry diamond coated blade from the exposed ends, while another 10 were cut at 3.5mm from the end. The purpose of this cutting method was to double analysing points along the depth of the cylinder (see Fig. 3.4). Discs were immediately sealed in polythene bags to avoid water evaporation before pressing. Eight discs from the same depth were grouped together and pressed to get pore solution. The solution was quickly analysed for OH⁻, Cl⁻ and Na⁺, K⁺ by the method described in 3.3.8. To determine total chloride contents, the cutting powders from the same depth were collected and dissolved in hot HNO₃ after drying in an oven. The clear solution was analysed for chloride.

Table 3.1
Chemical analysis of cements

Cement Type	Oxides (%)								
	CaO	SiO ₂	Al ₂ O ₃	Fe ₂ O ₃	SO ₃	MgO	Na ₂ O	K ₂ O	LOI*
OPC I	65.30	20.60	5.32	2.58	3.03	1.20	0.09	0.75	0.72
OPC II	63.50	20.20	4.90	2.65	2.93	2.60	0.19	0.95	-
Bogue Compounds (%)									
	C ₃ S		C ₂ A		C ₃ A		C ₄ AF		
OPC I	61.14		13.02		9.74		7.84		
OPC II	59.87		12.74		8.74		8.06		

* Loss on ignition

TABLE 3.2

Properties of Polymers Used in the Investigation

Polymers		Properties of polymer					Supplier-code
Code	Type	Form	Solid content (%)	pH	Particle size (μm)	Density or Specific gravity	
SBR 1	Styrene-Butadiene-Rubber Copolymer	Emulsion	47	9.5	0.05-0.2	1.01	Doverstrand-Revinex 29Y40
SBR 2	Styrene-Butadiene-Rubber Copolymer	Emulsion	47	9.5	0.05-0.2	1.01	Doverstrand-6486
Aq Comp	Aqueous Component of SBR 2						Doverstrand-6486
Ac 1	Acrylic Copolymer	Emulsion	46-47	9.5-10		1.0-1.2	Rohm Hass-Primal E330S
Ac 2	Acrylic Copolymer	Emulsion	49-51	7.0	0.2-0.5	1.08	Vinamul-Vinacryl 4001
Ac 3	Acrylic Copolymer	Powder				450-550 g/l	Wacker-Vinnapas LL512M
Ac 4	Acrylic Terpolymer (n-butyl acrylate/methyl methacrylate / functional monomer)	Emulsion	49-51	2.5-3.5	0.15-0.2	1.07	Lignotech-Borvicem A55

Continuation of Table 3.2

Polymers			Properties of polymer					Supplier-code
Code	Type	Form	Solid content (%)	pH	Particle size (μm)	Density or Specific gravity		
EVA 1	Ethylene-Vinyl Acetate Copolymer	Emulsion	54-56.5	4.0-5.0	1-3	1.07	Vinamul-10166	
EVA 2	Ethylene-Vinyl Acetate Copolymer	Powder			10-250	600-700 g/l	Vinamul-3281	
EVA 3	Ethylene-Vinyl Acetate Copolymer	Powder		4.5-5.5 (50% in water)		400-500 g/l	Elotex AG-1080	
VaVe	Vinyl acetate-Vinylversatate Copolymer	Powder		11-12.0 (50% in water)		470-570 g/l	Elotex AG-WS45	
VaVeAc	Vinyl acetate-Vinylversatate-Acrylic Terpolymer	Powder		6.0-7.0 (50% in water)		500-650 g/l	Elotex AG-511AP200	
De	Defoamer	Oily liquid				910 g/l	Hercules-1512M	



Fig 3.1 Conduction calorimeter interfaced with computer

Fig.3.2 Cross section of the conduction calorimeter system

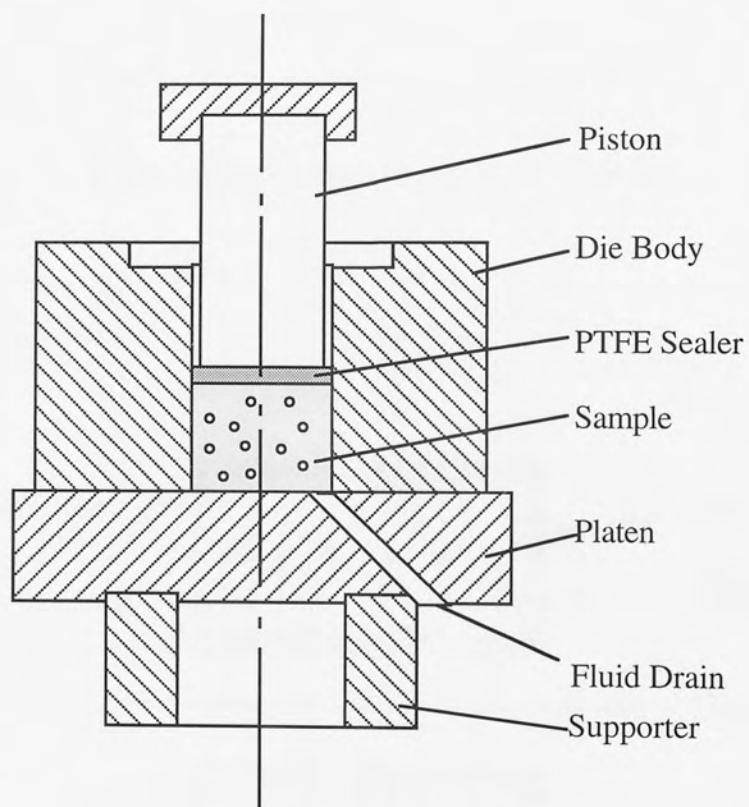


Fig.3.2 Cross section of the press used to extract pore solution

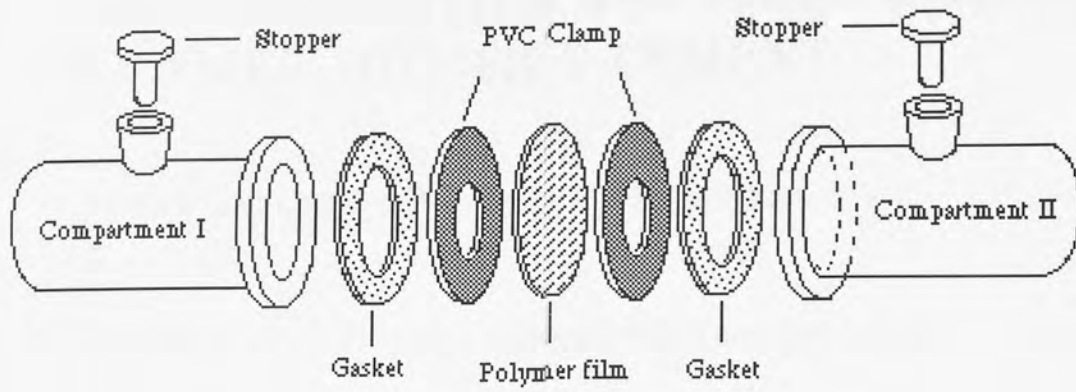


Fig.3.3 Experimental set-up of diffusion cell

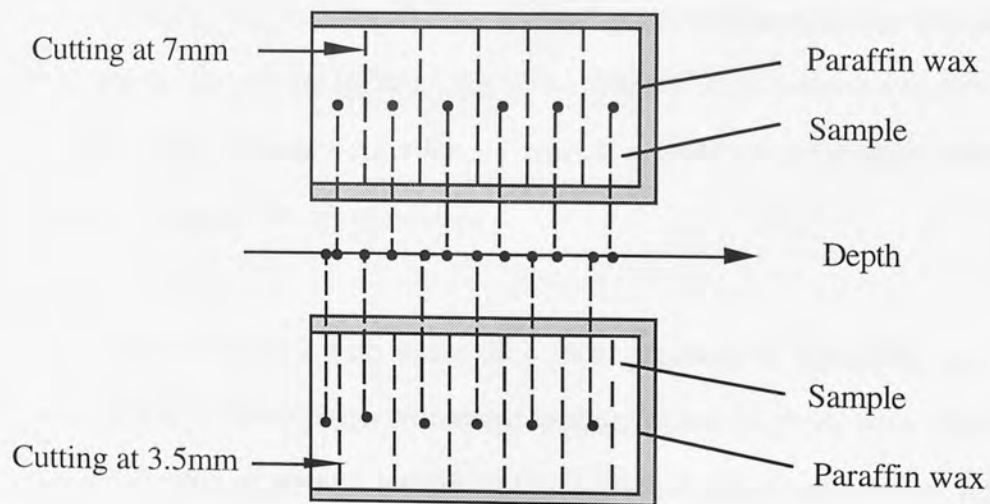


Fig. 3.4 Location of disc cutting and analysis points along the depth of the cylinder

CHAPTER 4

HYDRATION KINETICS AND MECHANISMS OF POLYMER MODIFIED CEMENT

4.1 GENERAL ASPECTS OF CEMENT CHEMISTRY

Portland cement consists of four main compounds which are listed below:

Name of Compound	Oxide Composition	Abbreviation
Tricalcium silicate	$3\text{CaO}.\text{SiO}_2$	C_3S
Dicalcium silicate	$2\text{CaO}.\text{SiO}_2$	C_2S
Tricalcium aluminate	$3\text{CaO}.\text{Al}_2\text{O}_3$	C_3A
Tetracalcium aluminoferrite	$4\text{CaO}.\text{Al}_2\text{O}_3.\text{Fe}_2\text{O}_3$	C_4AF

In commercial cement, the calcium silicates are not pure compounds, but contain small impurities of the oxides present in the clinker. The "impure" C_3S is known as alite and the "impure" C_2S as belite. In addition, a limited amount of calcium sulphate, usually in the form of gypsum, is added for set regulation.

When these compounds react with water they form products of hydration and in time produce the hardened cement paste. Numerous techniques and methods have been used to determine the hydration process of cement and the basic hydration mechanisms have been discussed in the literature (e.g. Skalny 1980, Danilov 1976, Massazza 1992). Techniques used include calorimetry, X-ray diffraction, scanning electron microscopy, analysis of pore liquid composition, quantitative measurement of the $\text{Ca}(\text{OH})_2$ and chemically combined water or the amount of unhydrated cement. Based on data obtained with these techniques, the mechanisms of hydration were proposed (Skalny 1980).

Once in contact with water, the compounds (e.g. C_3A and C_3S) immediately react. Initial hydrolysis occurs preferentially on the grain surface and the number of such sites determines how rapidly this process occurs. During this stage, Ca^{2+} and OH^- ions leach into solution and a surface layer of reaction product forms on the surface (Fig. 4.1a). This layer acts like a "passive film" and inhibits further hydration and thus initiates an induction period. Since the surface hydrate is an assembly of silicate ions, such as $H_3SiO_4^-$ and $H_4Si_2O_7^{2-}$, and has an amorphous structure, it is permeable to the diffusion of ionic species or water to and from the reaction sites.

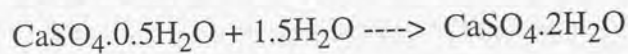
With continuous development of the surface layer and Ca^{2+} and OH^- ions passing into solution, the nuclei form by assembly of atoms in solution (Fig. 4.1b). In this stage, whereas calcium ions can diffuse through the surface layer, the silicate ions beneath the layer can not penetrate it and this increases the osmotic pressure. When the osmotic pressure is sufficient to rupture the surface layer at weak points and the ionic concentration in solution become large enough $Ca(OH)_2$ crystals and C-S-H gel are rapidly formed (Fig. 4.1c). This marks the start of the acceleratory period of hydration.

Calcium hydroxide crystals may precipitate close to the grains where ionic concentrations are the highest or form in the pores away from the grains. However, the growth of C-S-H is confined to outside the grain boundaries because of the difficulties in transporting silica. These "outer products" act as barriers to ionic transport so that further hydration slows down. Later C-S-H gels called "inner products" (Fig. 4.1d) are formed beneath the "outer products" and the hydration rate is controlled by water penetration and ionic diffusion. Further growths of the "outer products" interweave with each other to form a porous solid matrix.

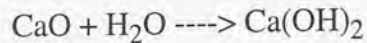
The heat evolution curve of cement hydration as determined by conduction calorimetry can be explained using this proposed hydration mechanism. Fig. 4.2 shows a typical heat evolution curve for a Portland cement. This general pattern can be divided into five stages.

In the first stage, there is a rapid evolution of heat culminating in a peak within the first few minutes. This peak is related to initial reactions (Bensted 1987):

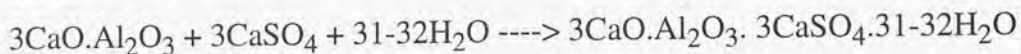
a) the rehydration of calcium sulphate hemihydrate to give the dihydrate gypsum



b) the hydration of free lime



c) the formation of ettringite



d) the heat of wetting and solution

The second stage is an induction period which is characterised by a relatively low hydration rate and usually lasts from 30 minutes to 2 hours. During this stage, the Ca^{2+} ion concentration in solution rises slowly and nuclei of Ca(OH)_2 or C-S-H form.

The third stage is called the acceleratory period. This stage contains the second major heat peak which is due to the rapid hydration of alite. A large amount of C-S-H is formed on the surface of the cement grains, while crystals of Ca(OH)_2 precipitate either on the surface or in the pores. The initial and final set of the cement takes place during this period due to the rapid development of C-S-H. A third major peak may be observed when the C_3A content of the cement is over 12%. This peak indicates the hydration of C_3A and the transition of ettringite to monosulphate ($3\text{CaO} \cdot \text{Al}_2\text{O}_3 \cdot \text{CaSO}_4 \cdot 19\text{H}_2\text{O}$).

The fourth stage is a deceleratory period and the final stage is a slow reaction period. Hydration of the cement (mainly belite) carries on slowly and is controlled by the diffusion of ionic species.

Although most of the heat curves for Portland cement systems have this general pattern, the actual rate of heat evolution varies with the compound composition of cement, the presence of cement admixtures or replacements, water/cement ratio and temperature. In

order to identify the influence of polymer latexes on cement hydration, we have characterised these curves using the following parameters:

- a) Induction time t_0 , which is taken as the intercept of the extrapolations of the horizontal portion of the induction period and the regression line of the acceleratory period as shown in Fig. 4.2.
- b) Time to reach maximum heat output t_m and the maximum rate of heat output at that time.
- c) Slope of the acceleration period which is calculated by a linear regression analysis.
- d) Total heat output over 48 hours which can be summed by integrating the curve using the Trapezoidal Rule.

4.2 PREVIOUS WORK

Compared with unmodified cement the polymer phase has a strong influence on the process of hydration, presumably as a result of physical or chemical interaction between the polymer and cement phases. A number of researchers have studied the hydration properties of these systems using various methods and most of their findings have shown that polymer retards hydration of the cement.

Using conduction calorimetry, Atkins et al (1991) studied Portland cement and 'secar71' aluminous cement with added VAl, VA, acrylic, VdC-Ac (poly-vinylidene chloride-acrylic), S-Ac and SBR latex.

The nature of the hydration of these polymer-cements is significantly different from each other. For Portland cement all polymers were found to retard the hydration rate to some extent. The conduction calorimeter traces indicated that the acrylic polymers produced the maximum effect. The SBR had a greater effect but not as much as the VA polymers. The VAl had very little effect on the heat output. The integral heat output (up to 48 h, 0.5 w/c) for unmodified OPC was 248 kJ/kg, modified with SBR was 157 kJ/kg, and modified

with acrylic was 121 kJ/kg. In case of the aluminous cement, polymer additions had minimal effects on heat evolution, but the peak was lower and broader than that of the unmodified cement.

Nakayama et al (1987) investigated the influence of polymer modification on the hydration of Portland cement, by determining the non-evaporable water (W_n). The results showed that the value of W_n varies with the time. In the first 7 h, W_n values for the VA, Ac-VA (acrylic-vinyl acetate), VdC-VC (vinylidene chloride-vinyl chloride), EVA(I) ($w/c=0.3$ $p/c=0.08$) were significantly greater than those for the control, SBR and EVA(II). At 24h, VA and EVA(I), had lower W_n values than the control, and VdC-VC had the highest W_n value. At 168h the W_n values were similar for all systems except for Vd-VC and VA, which had higher and lower values respectively.

Another set of non-evaporable water contents for the latex modified cement paste system were determined by Su et al.(1991). They found that the degree of hydration determined by non-evaporable water decreased with increasing polymer addition, especially in the early stages of hydration. For instance, after 7 days the degree of hydration for unmodified paste and of the paste modified with 15% of styrene acrylic polymer were 58% and 49% respectively.

Generally speaking, the results show that the acrylic polymers retard the hydration and setting of cement. An exception is that VpVC (vinylpropionate vinylidene chloride) tends to accelerate the hydration. This result is in agreement with Nakayama's result and Larbi (1990) explained that this polymer could break down to release Cl^- ions into the pore fluid acting as an accelerator.

Indirect estimation of the degree of hydration was made using thermal analysis and XRD (Gorur 1987), but both techniques failed to give an appreciable difference between polymer modified and unmodified pastes. Using standard laboratory procedures to

determine the non-evaporable water content, consistently lower values were observed for the polymer modified system.

Working with PMMA (polymethyl methacrylate), VA and SBR, Oye (1989) found that there was a general decrease in the degree of hydration with increasing polymer contents by determining the non-evaporable water, but the SBR did not produce any retarding effect which is in conflict with other researchers' results.

As regarding the reasons why the polymers retarded the hydration of cement, although some authors provided some explanations for their results, the mechanisms of hydration still remain a matter of debate. One opinion (Su 1991) is that the polymer phase possibly adheres onto the surfaces of hydration products and unhydrated cement grains and forms a "skin" over them. This may restrict the access of water to the cement grains and also inhibit the removal of the hydration products from the surfaces of the unhydrated core of the cement.

Another opinion argues that there is possibly a chemical interaction between polymer and cement. Based on the observation of the acrylic-cement system, Atkins (1991) believed that the acrylic polymer is partially hydrolysed by alkaline cement and the resulting carboxylate ions may "complex" the calcium ions of the unhydrated cement. As a result it is difficult for water to reach the cement grains and the overall effect is a reduction in the rate of hydration and of heat evolution from cement.

Other workers suggested that the general retarding effect on the hydration may be caused by surfactants or functional groups which are contained in the polymers. In early studies of hydration of cement with organic admixtures, Hansen (Lorprayoon 1981) suggested that the admixtures with carboxylic acid or hydroxyl groups would adsorb Ca^{2+} ions at surface. Steinor (1959) considered that any non-ionised hydroxyl group would be able to hydrogen bond with surface oxygen. The formation of insoluble hydration products retards the subsequent hydration of cement compounds by forming a barrier to water

transport, solubility and precipitation. Suzuki and Nishi (Lorprayoon 1981) also concluded that organic retarders act by forming insoluble complexes when in contact with the strongly alkaline environment of a cement, like carboxylic acid admixtures form insoluble calcium salts. This implied that complexing might be an important factor in the mechanisms of retardation.

Considering the kinetics of hydration of polymer modified cement systems, very little detailed analysis has been made. For instance numerous proprietary emulsions and redispersible powders are available. Polymer composition vary widely and all dispersions include other constituents such as surfactant, bactericide, anti-oxidant and anti-foaming agent. Little is known of how each constituent influences hydration. The work described in this chapter attempts to cover these aspects in order to have a more thorough understanding of kinetics and mechanisms of hydration since these will influence final material properties.

4.3 CALORIMETRY

4.3.1 Procedure

The rate and quantity of heat produced during hydration were measured by means of a Wexham Development JAF conduction calorimeter. Using the large sample technique (Wexham 1988), 30g of cement, the required latex and water were put in a polythene bag and mixed by kneading for two minutes. After squeezing out excess air, the bag was sealed with a rubber band and carefully formed into a sandwich shape around the aluminium disc fitted with the heater (see Fig. 4.3). 20cc of a heat conducting oil was placed into the holder as a heat conductor from the bag to the holder. Heat output was continually monitored for up to 48 hours by a computer which was interfaced with the calorimeter. Using this technique mixing is done outside the calorimeter and a period of 20 minutes is needed to allow the calorimeter to achieve a steady state temperature condition. Therefore these early readings are often unreliable.

To study the initial hydration of samples and obtain more information about the induction period of hydration, the small sample technique was used. Using this technique, 1g of cement was placed inside a small banjo shaped polythene bag by using a long glass funnel. A long fine tube was inserted into the bag. The end of the tube was slit in order to facilitate the spread of water throughout the bag when the syringe plunger was pressed home. Heat shrink sleeving was placed over the mouth of the bag to seal and prevent ingress of oil in the sample container. The sample bag and a heater for calibration were then carefully positioned inside the container. A syringe, which sucked 0.3 ml of air first followed by a further required quantity of water, was inserted through the lid of the calorimeter and connected with the tube. The 0.3 ml of air ensured that the long fine tube was completely emptied.

Since the amount of sample was only one gramme, the heat evolution was relative low. In this case, small changes in the temperature of the system may be enough to overlap the heat output of cement hydration. Sometimes, a difference of temperature between the water bath and the calorimeter will give a negative reading so that temperature control and preconditioning are very important in this experiment. In order to overcome this sensitivity to temperature and to give reliable results, the calorimeter was immersed in the water bath for about 30 min until the reading in the interface is $0.000 \pm 0.005 \text{mV}$. At that time it was believed the temperature of whole system has reached equilibrium conditions. After that, the water was injected and the heat of hydration was measured as in the large sample technique. The set-up of the experiment is shown in Fig. 4.4.

4.3.2 Theory of Calorimeter

Assuming the calorimeter is at a steady state temperature condition with a sample holder temperature of T_1 and a heat sink temperature of T_0 , then the development of a small quantity of heat dw in a short interval of time dt will raise the temperature of the sample holder by an amount T above that of the heat sink and introduce a new heat balance of the system:

$$\frac{dw}{dt} = pT + u \frac{dT}{dt} \quad (4-1)$$

The first item pT is the rate of heat loss by conduction, and the second item $u \frac{dT}{dt}$ is the absorption rate by the sample holder. The electrical output E (mV) by the thermopile is proportional to the temperature difference T , i.e. $E = gT$, therefore we get the Tian-Calvet equation:

$$\frac{dw}{dt} = k_1 E + k_2 \frac{dE}{dt} \quad (4-2)$$

where k_1 and k_2 are constants of the calorimeter

At the end of the cement hydration test when the heat evolution has reached a small steady value, a stabilising power is provided to the heater. The precise power W (mW) can be calculated from:

$$W = V \frac{C}{500} \times 1000 \quad (4-3)$$

where V and C are respectively the heater voltage and current and can be read in the interface during calibration.

Rearranging equation (4-2), gives:

$$\frac{dE}{dt} = -\frac{k_1}{k_2} E + \frac{W}{k_2}$$

which is a straight line relationship when plotting $\frac{dE}{dt}$ against E (see Fig. 4.5). If a linear regression analysis done by a computer, we get the intercept = $\frac{W}{k_2}$ and the slope = $-\frac{k_1}{k_2}$.

Since W is known, k_2 and hence k_1 can be obtained. Thus using the Tian-Calvet equation again

$$W = k_1 E + k_2 \frac{dE}{dt}$$

and we achieve a calibrated heat evolution curve in W/kg cement as shown in Fig. 4.6. Appendix B presents an example of how to calibrate the curves by using a computer.

4.4 RESULTS AND DISCUSSION

4.4.1 Styrene Butadiene Rubber-Cement System

4.4.1.1 Polymer / Cement Ratio (P/C)

Initial experiments involving triplicate runs on the same system produced conduction calorimetric curves that were virtually identical. Figure 4.7 shows the conduction calorimetric curves of SBR 1 modified OPC I at different polymer / cement ratios, a w/c ratio of 0.3 and 22°C. The unmodified OPC I curve is typical of the heat evolution pattern found for hydrating Portland cement (Bensted 1987) and can be related to the generally accepted mechanisms of cement hydration described in section 4.1. In the first few minutes there is a very rapid heat evolution attributed mainly to rehydration of calcium sulphate hemihydrate. This is followed by an induction period associated with relatively low chemical reactivity during which it is thought that needles of ettringite are formed on the surface of cement particles with nucleation of C-S-H gel and dissolution of calcium ions. Reactions then accelerate to give a major heat peak, usually attributed to the hydration of alite, increasing the thickness of the C-S-H gel interfacial layer and promoting growth of calcium hydroxide crystals. Eventually the heat evolution starts to decay and slow reaction continues over a long period of time. From these curves the induction time, the time to reach maximum heat output, maximum rate of heat output, the slope of the acceleration period and the total heat output over 48 hours were calculated and values are given in Table 4.1.

From Fig. 4.7 and comparing the values given in Table 4.1, it is evident that additions of SBR 1 result in the same general pattern of the heat evolution curve but there are some differences, especially in the length of induction period and reaction rate during the acceleration stage.

Overall, these additions act as a retarder to the cement hydration reactions. It may be seen that 5% polymer additions have a negligible effect on the length of the induction period but a very significant effect during the acceleration period, reducing the rate of alite reaction by about a half. Increases in polymer content above 5%, however, result in significant increases in the induction period with only small further reductions in the rate of alite reaction. The net result is that at lower polymer contents retardation is primarily influenced by the rate of alite reaction whilst at higher polymer contents further retardation is primarily influenced by the length of the induction period. Also, since the degree of hydration is related to total heat output it may be seen that increases in polymer content up to 10% steadily decrease the degree of hydration whilst further increases have relatively little effect.

4.4.1.2 Water / Cement Ratio (W/C)

Using the small sample technique the conduction calorimetric curves of SBR 1 modified OPC I at different polymer / cement ratios, a w/c ratio of 0.5 and 22°C were obtained (see Fig. 4.8). There is little evidence to suggest that latex additions significantly influence the very rapid heat evolution occurring during the first few minutes and therefore it can probably be assumed that the rehydration of calcium sulphate hemihydrate still occurs. However, this result does not preclude the possibility of SBR-cement grain interactions or a change in their states of flocculation. At later times an interesting phenomenon was observed when a comparison was made between w/c 0.3 and w/c 0.5. An increasing w/c did not alter the induction time but slightly reduced the acceleration rate reducing the total heat output for unmodified cement, which is in agreement with previous results (Taylor

1990). This was not the case for the modified cement systems where there was no change in acceleration rate but a significant reduction in induction time.

4.4.1.3 Alkali Content of Cement

Fig. 4.9(a-c) show the conduction calorimetric curves of SBR 1 modified OPC I and OPC II at different polymer / cement ratios, a w/c of 0.5 and 22°C. These results show that an increase in alkalinity results in a little change in the induction time for the unmodified cement but there is a small increase in the rate of the alite reaction and the degree of hydration is increased. A similar effect is found with the modified cements although this is not sufficient to counteract the retarding effect of the latex.

4.4.1.4 Modification of Polymer (Carboxylation)

Small amounts of a carboxylic acid are usually incorporated in SBR to give improved latex stability and adhesion. On raising the pH, carboxyl groups near the surface of the SBR particles ionise and this is shown schematically in Fig. 4.10(a). It has been suggested that these groups can react with calcium ions in solution, Fig. 4.10(b), or bind to calcium ions at the surface of cement grains, Fig. 4.10(c). The influence of SBR carboxylation on the conduction calorimetric curves of SBR modified OPC I at water / cement ratio 0.5 and 22°C, is shown in Figs. 4.11(a-b). Results show that increasing the carboxylation (SBR 1 contains 1% carboxylic acid, whilst SBR 2 contains 5%) has a considerable effect on retardation. The induction time is increased and the rate of alite reaction is decreased. This result suggests that the concentration of carboxyl groups is very influential in determining hydration kinetics.

4.4.1.5 Aqueous Component of Latex and Defoamer

The effect of other components in the latex on the hydration were also investigated. The equivalent amount of aqueous component to that contained in the latex was added to the

cement and the conduction calorimetric curve obtained is shown in Fig. 4.12. Similarly, the effect of defoamer on the hydration is shown in Fig. 4.13. It can be seen that the aqueous component and defoamer have little effect on the induction time but reduce the alite rate of reaction. Overall they have no influence on the degree of hydration and thus it may be concluded that their presence have little significance compared to that of the polymer solids.

4.4.1.6 Hydration Temperature

Figs. 4.14(a-c) show the conduction calorimetric curves of SBR 1 modified OPC I at hydration temperatures of 22, 29, 40 and 47°C. Table 4.2 gives the characteristic parameters. It is evident that the hydration of unmodified and modified cements was accelerated at elevated temperatures, induction periods were shortened and the second heat evolution peak became higher and sharper. For example, at 22°C the hydration rate had a maximum of 3.1 w/kg after 6 hours, while at 47°C, this value rises to 13 w / kg after 3 hours. Similarly, for a 10% SBR, the maximum rate at 47°C was 5.8 w / kg, about three times that of 2.1 w / kg at 22°C. With 20% SBR, the maximum rate at 47°C is 4 w / kg, more than two times that of 1.8 w / kg at 22°C. In the case of the unmodified cements the induction periods were shortened slightly, but the effect was much greater in the case of the modified cements so that at 47°C they were about the same. Rates of alite reaction were much greater for the unmodified cements but only slightly so for the modified cements.

4.4.2 Other Polymer-Cement Systems

4.4.2.1 Acrylic-Cement System

In order to study the influence of acrylic additions on the hydration characteristics of cement, Ac 1 in the emulsion form was selected as a representation of this kind of polymer. Acrylic-cement ratios were 10% and 20%. The water-cement ratio was 0.5 and

the hydration temperature was 22°C. Figure 4.15 shows the rate of heat liberation for hydration of acrylic-OPC I. Generally, the acrylic has the same influence as SBR on the cement hydration, i.e. retardation. An increase of addition from 10% to 20% did not produce a large change in the hydration characteristics. The induction time, the time to reach the maximum output and the heat output over 48 hours have almost the same values as those for the SBR-cement systems (see Table 4.3).

The hydration curves for Ac 1-OPC II are shown in Fig. 4.16. The higher alkali content in OPC II did seem not to help compensate for the retardation caused by the latex.

A further two acrylics, Ac 2 and Ac 3, were compared with Ac 1 at a polymer addition of 10%, and the hydration curves are shown in Fig. 4.17. These three acrylics are produced by different manufacturers. The Ac 1 and Ac 2 were in emulsion form while Ac 3 was in redispersible powder form. It can be seen that all three acrylics act as retarders of the cement hydration although to different extents. Generally, Ac 1 and Ac 3 have a similar influence on behaviour except that Ac 3 prolonged the duration of the induction period. The total heat output over 48 hours for Ac 1 and Ac 3 are respectively 127 kJ / kg and 150 kJ / kg. On the other hand, Ac 2 significantly reduced the hydration of alite and the total heat output over 48 hours is only 80 kJ / kg. These results suggested that although in a same group the properties of polymers may be quite variable, unless the composition of systems is known in detail there is no way of predicting if they will behave in a similar manner. In addition to, there is no evidence to suggest that redispersible powders are radically different to emulsions.

4.4.2.2 Ethylene-Vinylacetate Copolymers (EVA)-Cement System

Three EVA copolymers were used to investigate the influence of this kind of polymer on the cement hydration. EVA 1 and EVA 2 are produced by the same manufacturer, but EVA 1 is an emulsion latex while EVA 2 is a redispersible powder. EVA 3 is also a redispersible powder but from a different manufacturer. It has been noted that one of the

distinct differences between EVA copolymer and SBR copolymer or acrylics is their pH values. The pH values for SBR and acrylics are high, about 9.5, but the EVA pH values are about 4.5. This means that the SBR copolymers and acrylics were basic in the liquid state, and in contrast EVA copolymers are acidic. Fig. 4.18 shows the conduction calorimetric curves of the three EVA-cement systems at 10%. From Fig.4.18 and comparing the characteristic parameters in Table 4.3, it can be noted that the total heat output over 48h was about 175 kJ/kg for the EVA, which is higher than the value of 130 kJ/kg for SBR and acrylic. Thus, it seems that the EVA gave less retardation than SBR and acrylic. Furthermore two interesting facts can be noted. One is that the pH value of latex or water redispersion solution of polymer powder does not play an important role in the hydration retardation. Whether the polymers are basic or alkaline in the liquid state, they appear to impart similar effect on the cement hydration. Another fact is that whether the polymers are in emulsion or in redispersible powder their effects are similar.

4.4.2.3 Vinylversatate-Vinylacetate Copolymer (VaVe)-Cement System, Vinylacetate-Vinylversatate-acrylic Terpolymer (VaVeAc)-Cement System

The heat evolution curves of these two polymers are shown in Fig. 4.19. It can be seen that the vinylversatate-vinylacetate copolymer (VaVe) has same extent of retardation on cement hydration as other polymers. The induction time for VaVe-OPC I is 1.8 hours and the total heat output over 48 hours is 156 kJ / kg. Compared with VaVe, the vinylacetate-vinylversatate-acrylic terpolymer (VaVeAc) retarded cement hydration to a greater extent. The induction time is 2.6 hours and the time to reach maximum output is delayed to 12.6 hours, 3 hours later than other polymers. This long time retardation may be due to its special constitution, containing both acrylic and acetate groups and a large vinylversatate group. The interaction or absorption of these groups with cement phases probably formed diffusion barriers to water.

4.5 ANALYSIS OF REACTION RATES

The results of the hydration experiments showed that the conduction calorimetric curves of polymer modified cement have the same general pattern found for hydrating Portland cement. The early hydration process consists of five stages i.e. the initial reaction, induction, acceleratory, deceleratory and final slow reaction periods. Among them, the induction and acceleratory periods are the most important because the polymer phase does have a strong influence on them. It extends the duration of the induction period, influencing the nuclei formation of Ca(OH)_2 and C-S-H, and slows down the reaction rate of alite and changes morphology of the hydrates. Structural changes may be responsible for later application properties of polymer modified cement. If the kinetic parameters at various stages can be obtained, then it is useful to explain these differences in hydration mechanisms and kinetics of the polymer modified cement and ordinary Portland cement. Whilst it is generally accepted that during the period under consideration hydration of the alite phase will predominate, other reactions are proceeding concurrently. Accepting this limitation, it is thus possible to apply classical kinetic theory to determine an average reaction rate of early hydration for the system as a whole.

4.5.1 Kinetics of Induction Period

A nuclei formation theory is applied to the kinetics for this period. It is known that one of the distinct reaction characteristics during the induction period is the nuclei formation of Ca(OH)_2 and C-S-H. The author believes that it is reasonable to apply the nucleation theory to this stage to assess its kinetics. According to classical nucleation theory (Adamson 1976), the flux I , or the rate of formation of nuclei in a vapour is

$$I = Z \exp\left(\frac{-\Delta G_{\max.}}{RT}\right) \quad (4-4)$$

where Z is the gas kinetics collision frequency; $-\Delta G_{\max}$ is the free energy of formation for a cluster of water; T is absolute temperature (K); R is gas constant (8.31 J/mol/K). In the

case of nucleation from a condensed phase, such as melt or supersaturated solution, Z should be modified because the rate is related to the diffusion process. It is equal to the frequency factor kT/h times an exponential factor containing the free energy of activation for diffusion, ΔG_D .

$$Z = \frac{kT}{h} \exp\left(\frac{-\Delta G_D}{RT}\right) \quad (4-5)$$

By combining equation (4-4) and (4-5), we get

$$I = \frac{kT}{h} \exp\left(\frac{-\Delta G^*}{RT}\right)$$

or

$$\ln I = \ln \frac{kT}{h} - \frac{\Delta G^*}{RT} \quad (4-6)$$

where $\Delta G^* = \Delta G_{\max} + \Delta G_D$ is the apparent Gibbs free energy of activation for nuclei formation, h is Planck's constant (6.63×10^{-34} mol⁻¹) and k is Boltzmann's constant (1.38×10^{-23} JK⁻¹). Rewriting equation (4-6), we obtain

$$\Delta G^* = \left[\ln \frac{kT}{h} - \ln I \right] RT \quad (4-7)$$

The rate I of formation of nuclei is associated with the induction time t_i . A short induction time means that a large number of nuclei can be formed quickly, while a long induction time means that it is difficult to produce new phase nuclei. If it is assumed (Adamson 1976) that I is inversely proportional to t_i , then $\ln I$ may be replaced by $-\ln t_i$, and equation (4-7) becomes

$$\Delta G^* = \left[\ln \frac{kT}{h} + \ln t_i \right] RT \quad (4-8)$$

As described earlier, the duration of the induction period was changed greatly with different polymer addition levels. Krstulovic (1992) gave the relationship between the induction time t_i and the addition level C

$$\ln t_i = bC + \ln t_0 \quad (4-9)$$

where b and $\ln t_0$ are constants obtained by plotting $\ln t_i$ against C . Then from equations (4-8) and (4-9), the apparent Gibbs free energy of activation for new phase nuclei formation can be obtained.

Furthermore, based on transition state theory, the new phase nuclei formation rate constant k and the activated complex formation equilibrium rate K^* can be expressed respectively as :

$$k = \frac{k T}{h} \exp\left(\frac{-\Delta G^*}{RT}\right) \quad (4-10)$$

and

$$K^* = \exp\left(\frac{-\Delta G^*}{RT}\right) \quad (4-11)$$

Consequently, we can calculate k and K^* for new phase nuclei formation during the induction period.

In following calculation and analysis, we only take the SBR 1-OPC I system as an example. Figure 4.20 shows a typical relationship between the polymer addition and the induction time. A good correlation can be seen between the hydration temperatures of 22°C, 29°C and 40°C. Their coefficients of determination (r^2) are 0.937, 1.00, and 0.906 respectively. However, at 47°C the value of r^2 was only 0.75. The reason may be the retardation effect of polymer on hydration is improved during this stage with elevated temperature. In fact, an increase in SBR addition from 10% to 20% does not change the induction time. They are all 0.7 hours (see Table 4.2).

The kinetic parameters, apparent Gibbs free energy of activation ΔG^* , rate constant k and equilibrium constant K^* , were calculated according to the equations (4-8), (4-10) and (4-11) and the values are listed in Table 4.4.

It is very interesting to note that the influence of the polymer addition on ΔG^* is not significant at any given hydration temperature. However, compared with that, the influence of the hydration temperature created a much larger change in the ΔG^* at any fixed addition and this tendency decreases with increasing polymer addition. For example, the value of the ΔG^* for neat cement increased to $98.62 \text{ kJ mol}^{-1}$ from $91.25 \text{ kJ mol}^{-1}$ when the temperature rises to 47°C from 22°C , but the ΔG^* only increased to $99.52 \text{ kJ mol}^{-1}$ from $94.94 \text{ kJ mol}^{-1}$.

From the equation (4-8), it is known that ΔG^* is a function of the induction time (Int) and the hydration temperature (T). The above experimental data and analysis assumes that the temperature has a predominant effect on ΔG^* . Although an increase in polymer addition prolonged the duration of induction time, in turn increases the ΔG^* , the effect is not as large as the temperature.

Looking from the rate constant k (or the equilibrium constant K^*), two typical tendencies are observed. One is the values of k (or K^*) reduced remarkably with increasing polymer addition at any given temperature T . The second one is with rising temperature the k increased more rapidly in the polymer modified cement than in the neat cement, although their absolute values are lower (see Fig. 4.21).

Combining the above analysis and considering from the point of the transition state theory, if the ΔG^* is considered as the energy requirements for the hydration reaction of cement during induction period, i.e. the dissolution of calcium ions and the nucleation of C-S-H gel and Ca(OH)_2 , then no significant change in the ΔG^* means that the polymer phase in the reaction system does not significantly raise the initial energy barrier for hydration reaction. In other words, the polymer does not change the mechanism of

hydration reaction of cement in this stage. As long as the cement grains are in contact with water, the hydration reaction will take place as usual. The extent of the chemical reaction between polymer and cement is very small or undetectable. The potential effect of polymer on the hydration reaction is to prolong the duration of induction period and that is mainly reflected in the large reduction of the k and the K^* . This may be caused by a reduction in the number of reaction sites so that the actual amount of substance taking part in the hydration is reduced. The rate constant is inversely proportional to the induction time. The longer the induction time, the lower the rate constant and therefore the lower reaction rate.

4.5.2 Kinetics of Acceleratory Period

Various kinetic models, describing the formation of reaction products from spheres of reactant have been suggested. Two approaches will be considered here. The first involves applying a cubic law, with time-zero close to the end of the induction period, modified to take into account the probabilities of the overlap of growing phases. This approach is attributed to Avrami, Erofeev and Mampel (Harrison 1969) and results in an equation of the general form:

$$-\ln (1-\alpha)^n = k(t-t_0) \quad (4-12)$$

where α is the fraction reacted, k is the reaction rate constant, t is time, t_0 is the induction period and n is a constant.

The second approach considers an advancing reaction interface in terms of spherical geometry i.e. there is a barrier layer and reaction proceeds by parabolic diffusion. This is given by a modified version of the Jander equation (Harrison 1969) :

$$[1-(1-\alpha)^{1/3}]^n = k(t-t_0) \quad (4-13)$$

where α is the fraction reacted, t is time, t_0 is the induction period, k the reaction rate constant and n is a reaction stage coefficient. $n=1$ implies surface area control and $n=2$ implies diffusion control. In this equation further analysis shows that $k = (AD/x^2)$. Hence calculation of an absolute value of the reaction rate constant, k , is not possible since this would require a knowledge of diffusion coefficient D for all species, particle size, x , and A which includes terms to represent the exact geometry, chemical potentials of the species on both sides of the interface and the nature of the products. Thus the values of k calculated relate only to the materials and reaction conditions used in this present work.

In order to calculate values of the exponent, n , and the reaction rate constant, k , in equations (4-12) and (4-13), the degree of hydration, α , should first be obtained. It can be determined by the expression:

$$\alpha = \frac{Q(t)}{Q(f)} \quad (4-14)$$

where $Q(t)$ is the hydration heat at time t , and $Q(f)$ is the final hydration heat. If it is assumed that all hydration heat is released within 72 hours, then it is possible to substitute $Q(72)$ for $Q(f)$. Using the Trapezoidal Rule, the heat of hydration $Q(72)$ and $Q(t)$ at different times can be obtained, therefore α , relative to $Q(72)$ of unmodified cement at the various temperatures can be calculated. In this work the tail of the heat evolution curve has been extrapolated from 48 to 72 hr. It is considered that the assumptions used in this analysis will not introduce significant errors (Krstulovic 1992).

Using equation (4-12), plots of $\ln [-\ln (1-\alpha)]$ versus $\ln (t-t_0)$, allows determination of n and k . Similarly using equation (4-13) plotting $\ln [1 - (1-\alpha)^{1/3}]$ against $\ln (t-t_0)$, gives n and k . In both cases approximate linear relationships were obtained (Fig. 4.22) and Table 4.5 lists the values of n , k and r^2 using the two models.

Subsequently it was shown that the reaction rate constant was dependent on temperature in a form given by means of the Arrhenius equation:

$$k = A \exp \left(- \frac{E_a}{RT} \right) \quad (4-15)$$

where: k is the reaction rate constant, E_a is the activation energy, T is absolute temperature, R is universal gas constant and A is a constant. Plotting $\ln k$ vs $1/T$ in Fig. 4.23, values of E_a were determined with 95% confidence limits and these are shown in Table 4.6.

4.6 GENERAL DISCUSSION

The experimental evidence shows that the curves of heat evolution for all samples with or without polymer have the same general pattern. This suggests general similarities between the mechanisms of hydration of polymer modified cement and unmodified cement. On the other hand, some differences in detail, especially in the length of induction period and rate during the acceleratory periods, indicates that the presence of the polymer phase influences the hydration process of cement, and hence the hydration mechanisms and kinetics.

Possible interactions between polymer latexes and cement particles which may result in retardation include: destabilisation of the suspension so that flocculation of cement particles occurs giving a lower surface area for hydration; formation of complexes between polymer particles and calcium ions in solution, Fig. 4.10(b) reducing the formation of calcium hydroxide crystals; binding between polymer particles and surfaces of cement grains reducing the number of sites available for calcium dissolution and hydration; the formation of a sheath of polymer particles around cement grains impeding access of water molecules required for hydration.

4.6.1 Initial Reaction and Induction Period

When cement grains contact with the mixture of water and latex, an initial reaction, corresponding to the rehydration of the calcium sulphate hemihydrate and the heat of solution and wetting, takes place immediately between cement and water. The results from the small sample technique of the conduction calorimetry show similar heat evolution curves for polymer-cement system in the first few minutes (see Fig. 4.8). This suggested that the initial reaction is not significantly affected by the latex although this would not preclude some destabilisation of the cement suspension giving rise to the formation of flocs. However, such a mechanism would not be in keeping with the observation that rheology of fresh cement pastes is substantially improved by the presence of latex (Salbin 1996).

The latex prolongs the induction time i.e the time before phase growth starts. Since the results in section 4.4.1.5 have shown that the aqueous component of latex and defoamer have little influence on the cement hydration it may be assumed that this results from the presence of the polymer phase itself. It is not, however, likely that this is only due to complexing of polymer with calcium ions in the pore solution. If calcium were removed from solution in such a manner, there would be a driving force for more to dissolve but the opposite is generally found. Wagner 1978, Chandra 1987, Larbi 1990 have shown that the amount of calcium hydroxide produced is reduced in polymer modified cements. This may be due to binding of calcium ions in solution although there is no evidence for this. Therefore, another reason for the increased induction time may be that the polymer particles adhere on the surface of cement grains and block calcium dissolution sites.

From the kinetic analysis of the induction period, it can be seen there is no significant change on the apparent Gibbs free energy of activation (G^*) for new phase nuclei formation, but the rate constant has a large reduction with increasing the polymer addition. This may imply that during the induction period, in the presence of polymer the hydration reaction could take place usually as long as the cement is contact with water.

However, the reaction rate greatly slows down since the polymer particles adhere on the surface of unhydrated cement or hydration products. As a result, the calcium could not dissolve in the same quantity in the presence of polymers.

Generally speaking, the induction time increases as the polymer addition increases, but shortens as the temperature rises. It seems that the type and the form of polymers do not impart a large change to the induction time. At a polymer level of 10%, the induction time is in the range of 1.5~2 hours, except in the case of the terpolymer VaVeAc ($t_0=2.6$ hours). At 20% polymer, the induction time is in the range 2.5~3 hours. The influence of carboxylation is remarkable. In SBR latex, when carboxylic acid increases from 1% to 5%, the induction time increases from 1.5 to 3.5 hours at 10% polymer and from 3 to 4.5 hours at 20%.

4.6.2 Acceleratory Period

Growth rate of phases during the acceleration stage were influenced by the polymer content, surfactant, and degree of carboxylation and also by the alkalinity of the cement. An increase in polymer addition reduces the maximum rate of heat output and delayed the time to reach the maximum rate. Further increase of polymer (over 10%) are not so significant but still reduce the rate. In this stage, a large number of hydrates are produced and water is rapidly consumed so that the polymer concentration in the solution increases greatly. It is possible, in this case, that some polymer particles coalesce into large ones. They probably stick to the surface of cement and this tendency will be emphasised when the surfactant or carboxylic acid increases. The growth of C-S-H and Ca(OH)_2 is confined to less space and ionic transport controlled by diffusion process is restricted.

Very good coefficients of determination were obtained for the analyses when using both the Avrami and Jander models and comparable values of reaction rate constants and activation energies were obtained. For the acceleratory period, the rate constants increase with increase in hydration temperature, but decrease with increasing polymer level. The

increase in rate constant is possibly due to increase in collision frequency of molecular movement. The decrease in rate constant is because the polymer reduces effective collision of ions for combining into hydrates and raising the temperature might favour increased adsorption of polymer.

The value of the exponent n is seen to vary slightly with temperature in both models, possibly caused by experimental uncertainty. In Jander's model, the value of n , as a resistant coefficient, may related to the number of occupied sites by polymer. A low n implied the reaction which had a less dense reacted layer and a high n implied the reaction which had a denser reacted layer. For unmodified cement, the n was approximate equal to 2.00, the hydration reaction was considered to be controlled by diffusion of ions through reacted layer. For polymer-cement, we also considered the reaction was controlled by the diffusion. However, the polymer increased the n from 2.00 of unmodified cement to 2.63 of SBR 20%-cement, revealing the diffusion layer was thickened as it adsorbed or coagulated polymer.

The activation energy for hydration of the unmodified cement was calculated to be ~ 35 kJ / mol which is similar to values obtained in other work $\sim 38-50$ kJ / mol (e.g. Krstulovic 1992, Wu 1983). The value obtained for modified cement containing 10% polymer was ~ 32 kJ/mol and within experimental error it was same as that obtained for the unmodified cement. This suggests that the rate controlling step, diffusion of ions through a reacted layer, is unaltered on addition of 10% polymer. That the actual rate is reduced suggests that polymer is occupying some of the diffusion sites.

In the case of the modified cement containing 20% polymer, the activation energy was ~ 9 kJ / mol, and this is well below the other figures. This suggests that a different mechanism is now controlling the rate of hydration. It is interesting to note that this activation energy is similar to that found for the self diffusion of water, ~ 13 kJ / mol. It is thus possible that the reaction is now controlled by movement of water to hydration sites. That the actual rate is low may be because the configuration of polymer particles is

such that they provide a more tortuous path, e.g. through a sheath formed by the polymer around the cement particles.

4.6.3 Deceleratory Period

After the acceleratory period, the reaction was decelerated because supersaturation and hydration condition were getting worse. At this time polymer partly exists in pore solution, and partly agglomerated into large particle, i.e. so called 'film', which surrounds or cross links with hydrates and unhydrated cement particles. This environment makes further hydration and crystal growth more difficult. The heat evolution over this stage was lower than unmodified cement. At later period, hydration continues slowly and polymer will form film gradually as water is completely removed by hydration and/or evaporation.

The final structure of the hardened polymer modified cement paste generally consists of hydrates, unhydrated cement, polymer solid and capillaries. The polymer phase to a great extent exists in its mixture form with hydrates or unhydrated cement or both of them rather than in pure film (see section 5.3).

4.7 CONCLUSIONS

(1) The addition of polymers acted as a retarder to cement hydration in that it increased the induction period and time to maximum heat output whilst reducing the total heat outputs observed in conduction calorimetry. Quite low concentrations of polymers had a significant effect during the acceleration period. Higher concentrations had a greater influence on the induction period.

(2) Increasing the water / cement ratio for polymer modified cement significantly reduced the induction time but had little effect on the acceleration rate. This finding was contrary to that obtained for unmodified cement.

(3) Increasing the alkalinity of the cement had little effect on the induction time but increased the acceleration rate resulting in an increase in the degree of hydration. The presence of polymer did not appear to influence these effects.

(4) Increased concentration of carboxyl groups in the polymer significantly increased retardation. It is thought that this was a result of increased binding between the carboxyl groups and hydration sites on the surface of the cement grains.

(5) The aqueous component had little effect on the induction period but reduced the acceleration rate compared to that of the unmodified cement. Overall it had no influence on the degree of hydration and thus it may be concluded that other components of the latex have little significance compared to that of the polymer solids.

(6) Increased temperature reduced the induction period, the time to reach maximum heat output, and increased the maximum heat output. It was found that a nuclei formation theory could be applied for the kinetic analysis of the induction period, and that the Avrami or Jander models could be used to calculate reaction rate constants of the acceleratory period. Values of the apparent Gibbs free energy of activation may suggest that the hydration mechanism of PMC during the induction period is similar to that of Portland cement. Whilst values of activation energy for acceleratory period suggested that at higher concentrations of polymer (>10%) the mechanism for cement hydration changed from control by diffusion of ions through growing interaction layers, to control by the diffusion of water to interaction sites.

TABLE 4.1

Characteristic Parameters for Heat Evolution of SBR Modified Cement Pastes, at 22°C

Polymer-Cement system	W/C	Polymer addition (%)	Induction time (h)	Time to reach maximum output (h)	Maximum rate of heat output (w/kg)	Slope of acceleration period (w/kg/h)	Heat output over 48h (kJ/kg)
SBR 1 - OPC I	0.3	0	0.5	6.0	3.7	0.65	216
		5	0.6	7.0	2.3	0.32	161
		10	2.0	8.0	2.0	0.28	124
		15	4.0	10.5	2.0	0.26	125
		20	5.5	13.0	1.8	0.22	124
OPC I	0.5	0	0.7	6.5	3.1	0.53	201
		10	1.5	8.0	2.1	0.30	130
		20	3.0	10.0	1.8	0.25	116
SBR 1 - OPC II	0.5	0	1.0	6.0	3.7	0.71	235
		10	0.5	6.5	2.3	0.42	157
		20	3.0	9.5	2.3	0.34	152
SBR 2 - OPC I	0.5	10	3.5	12.5	1.2	0.13	105
		20	4.5	15.0	1.1	0.08	92
Aq Comp - OPC I	0.5	10	0.5	7.5	2.8	0.42	202
		20	0.5	8.0	2.9	0.39	208

TABLE 4.2

Characteristic Parameters for Heat Evolution of SBR I Modified Cement Pastes
at w/c=0.5 and Different Temperatures

Hydration temperature °C	Addition of polymer (%)	Induction time (h)	Time to reach maximum output (h)	Maximum rate of heat output (w/kg)	Slope of acceleration period (w/kg/h)	Heat output over 48h (kJ/kg)
22	0	0.7	6.5	3.1	0.53	201
	10	1.5	8.0	2.1	0.30	130
	20	3.0	10	1.8	0.25	116
29	0	0.5	7.0	4.4	0.68	262
	10	0.7	8.0	2.6	0.37	170
	20	2.3	10	2.4	0.28	154
40	0	0.5	4.0	8.9	2.44	302
	10	0.7	6.0	3.8	0.71	186
	20	1.7	8.5	3.2	0.52	174
47	0	0.5	2.5	12.8	5.32	329
	10	0.7	5.5	5.8	1.66	218
	20	0.7	6.5	4.1	0.66	209

TABLE 4.3

Characteristic Parameters for Heat Evolution of Other Types
of Polymer Modified Cement Pastes, at 22°C and W/C=0.5

Polymer-Cement system	Polymer addition (%)	Induction time (h)	Time to reach maximum output (h)	Maximum rate of heat output (w/kg)	Slope of acceleration period (w/kg/h)	Heat output over 48h (kJ/kg)
Ac 1	0	0.7	6.5	3.1	0.53	201
-	10	1.5	7.5	2.0	0.42	127
OPC I	20	2.5	10.0	1.8	0.34	121
Ac 1	0	1.0	6.0	3.7	0.71	235
-	10	1.5	8.0	2.4	0.37	175
OPC II	20	2.5	8.5	2.2	0.32	161
Ac 2-OPC I	10	1.5	9.5	0.9	0.13	80
Ac 3-OPC I	10	1.8	9.2	1.9	0.41	150
EVA 1-OPC I	10	2	9.5	2.2	0.34	175
EVA 2-OPC I	10	1.5	8.4	2.1	0.34	172
EVA 3-OPC I	10	2	9.1	2.5	0.34	171
VaVe-OPC I	10	1.8	9.2	2.0	0.28	156
VaVeAc-OPC I	10	2.6	12.5	1.5	0.17	146

TABLE 4.4

Kinetic parameters of the induction period for new phase nuclei
formation for SBR 1 modified OPC I, w/c=0.5

Hydration Temperature °C	SBR 0%			SBR 10%			SBR 20%		
	ΔG^* kJ/mol	K^* $\times 10^{17}$	k $\times 10^4/s$	ΔG^* kJ/mol	K^* $\times 10^{17}$	k $\times 10^4/s$	ΔG^* kJ/mol	K^* $\times 10^{17}$	k $\times 10^4/s$
22	91.25	6.36	3.94	93.24	3.06	1.90	94.94	1.48	0.91
29	92.42	10.1	6.43	94.33	4.74	3.01	95.44	2.99	1.90
40	96.01	9.31	6.12	97.60	5.06	3.32	99.19	2.75	1.81
47	98.62	7.83	5.26	99.07	6.61	4.44	99.52	5.58	3.74

TABLE 4.5

Constant, n and Reaction Rate Constant, k (s^{-1}), for SBR 1 modified OPC I,
w/c=0.5, and different temperatures.

Temperature (°C)	Polymer Addition (%)	Jander Model			Avrami Model		
		n	k ($\times 10^5$)	r^2	n	k ($\times 10^5$)	r^2
22	0	2.08	1.36	0.994	0.66	1.33	0.992
	10	2.63	0.78	0.976	0.60	0.76	0.974
	20	2.63	0.72	0.989	0.85	0.78	0.988
29	0	2.00	1.45	0.995	0.63	1.73	0.993
	10	2.00	0.92	0.990	0.65	0.98	0.988
	20	2.70	0.81	0.965	0.87	0.87	0.962
40	0	1.67	3.10	0.996	0.54	3.25	0.995
	10	1.82	1.27	0.992	0.59	1.42	0.991
	20	2.17	0.90	0.978	0.71	0.95	0.976
47	0	2.04	3.78	0.997	0.66	3.81	0.997
	10	1.75	2.06	0.993	0.56	2.33	0.992
	20	2.38	0.99	0.988	0.77	1.03	0.986

r^2 -- the coefficient of determination

TABLE 4.6

Activation Energy for the hydration of SBR 1 modified OPC I

SBR Addition (%)	Jander Model		Avrami et.al. Model	
	Ea (kJ/mol)	r ²	Ea (kJ/mol)	r ²
0	35.6 ± 4.8	0.941	34.8 ± 1.8	0.985
10	29.1 ± 4.1	0.936	33.7 ± 2.5	0.964
20	9.8 ± 0.5	0.996	8.3 ± 0.4	0.990

r² -- the coefficient of determination

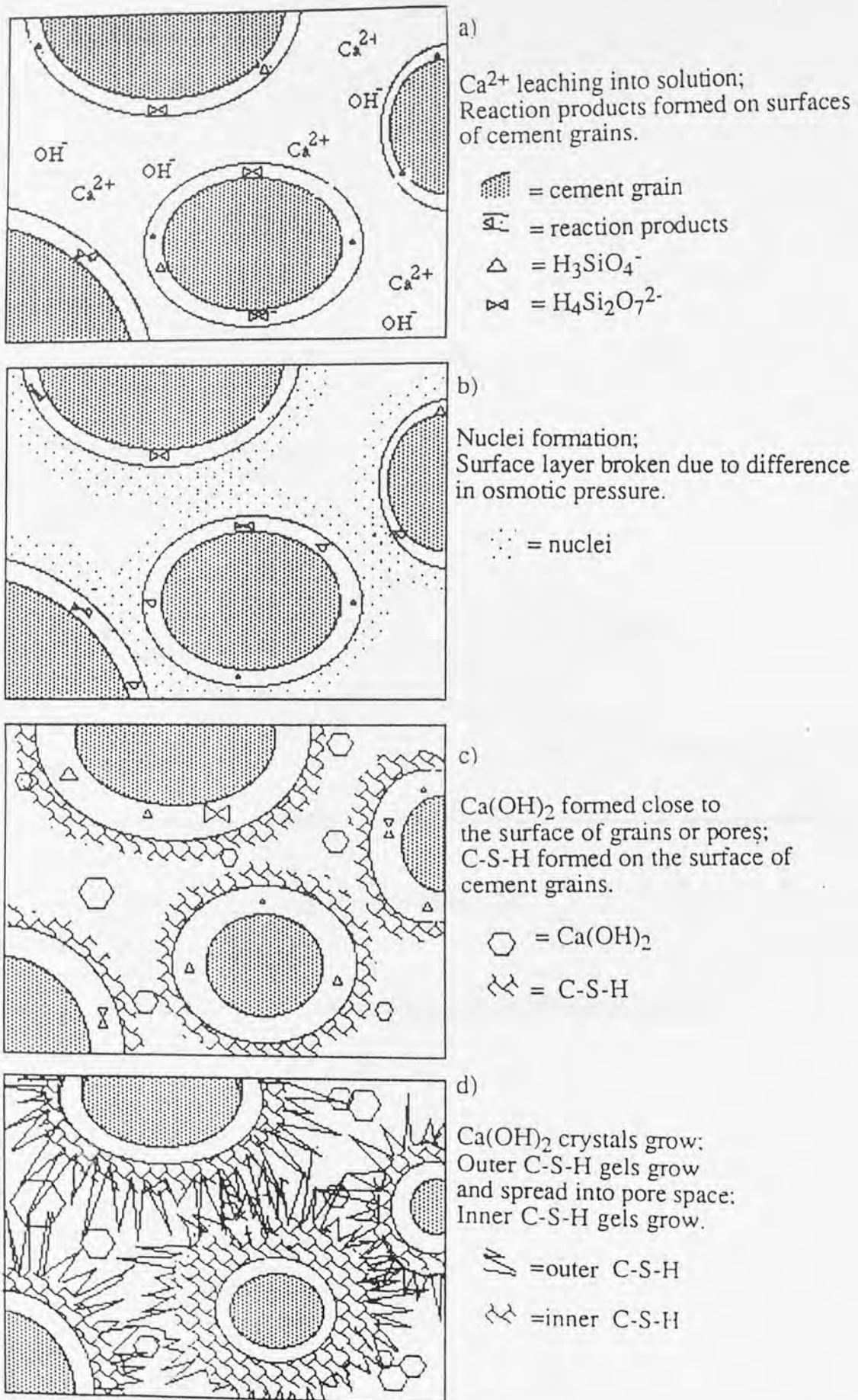


Fig. 4.1 Mechanisms of Portland cement hydration

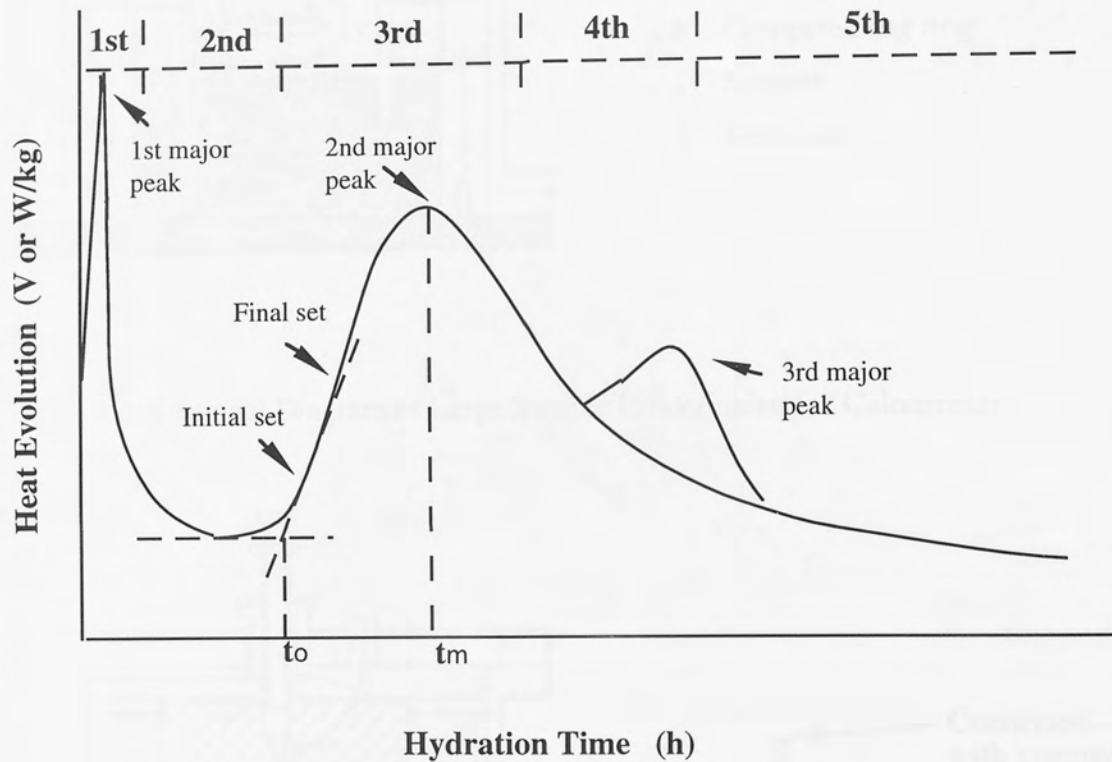
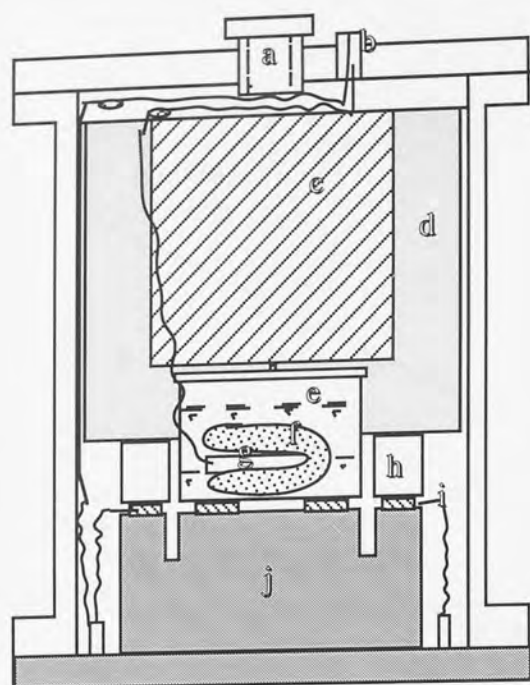


Fig 4.2 Typical heat evolution curve for Portland cement



- a Syringe entry
- b Cable gland
- c Polystyrene insulator (inner)
- d Polystyrene insulator (outer)
- e Large sample can
- f Sample in polythene bag
- g Heater
- h Compensating ring
- i Sensors
- j Heat sink

Fig. 4.3 Sectional Diagram of Large Sample Holder assembled Calorimeter

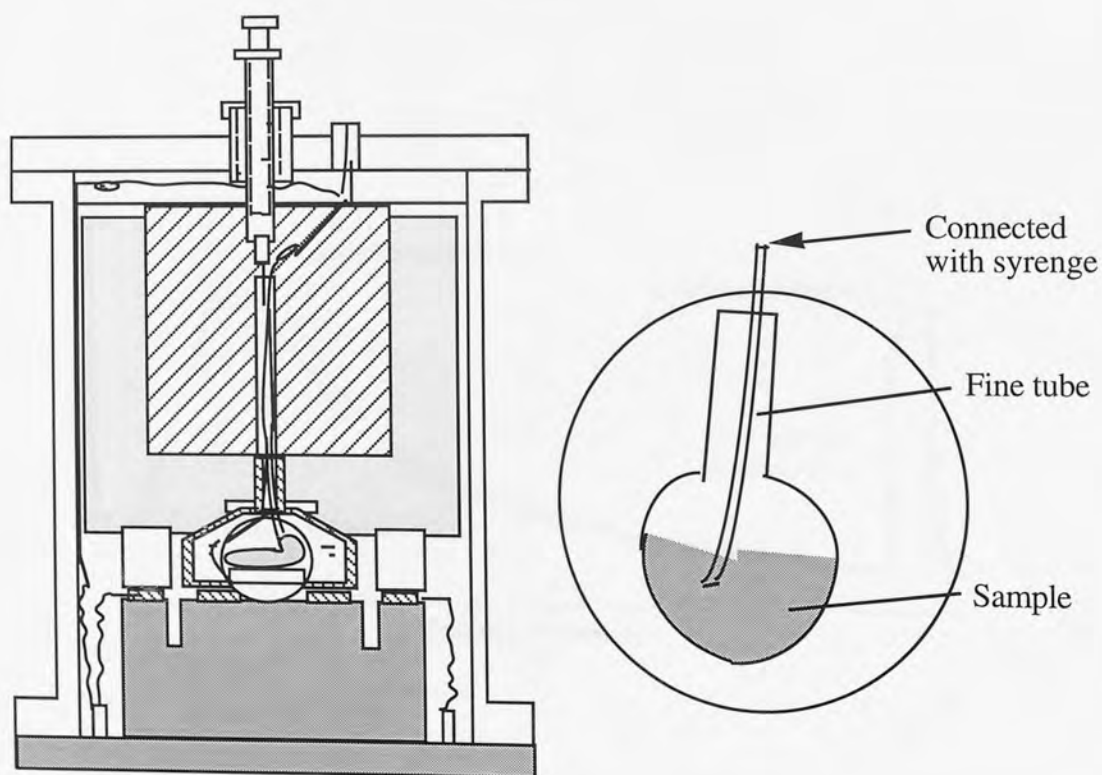


Fig. 4.4 Sectional Diagram of Small Sample Holder assembled Calorimeter

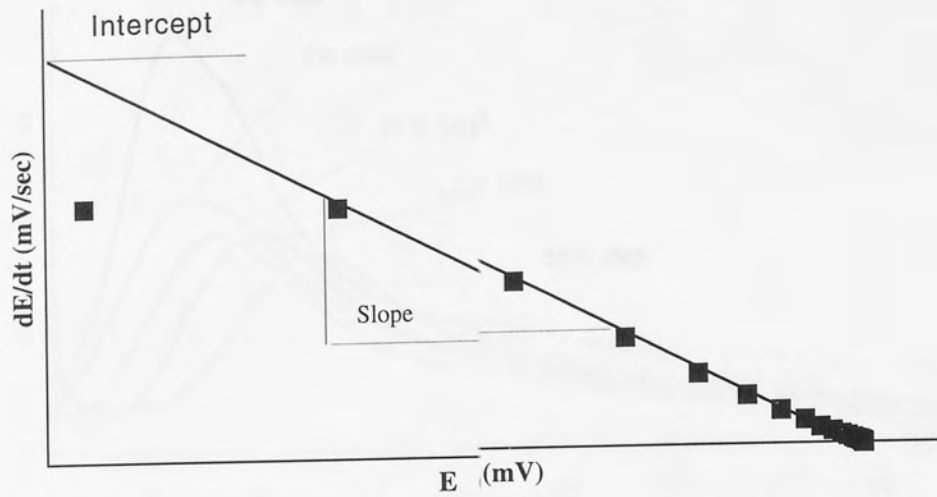


Fig.4.5 Typical graph of dE/dt versus E

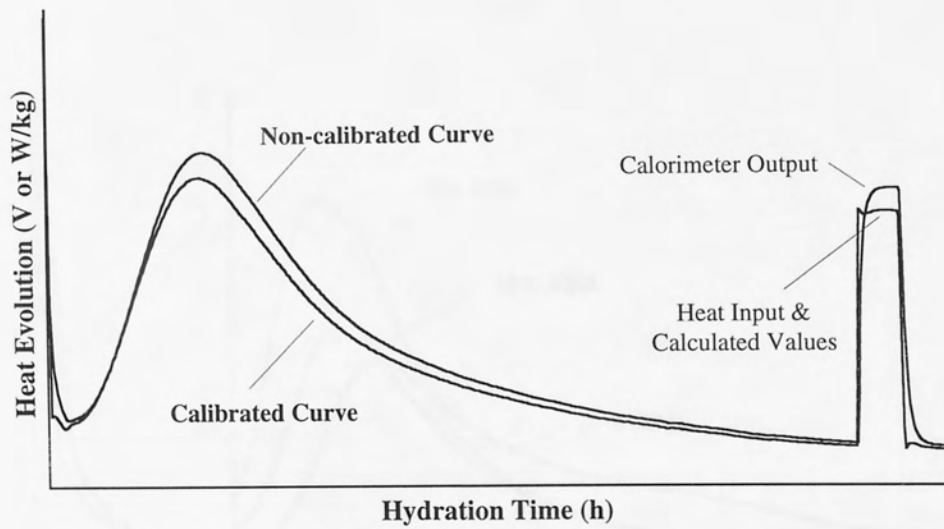


Fig.4.6 Calibration of heat evolution curve

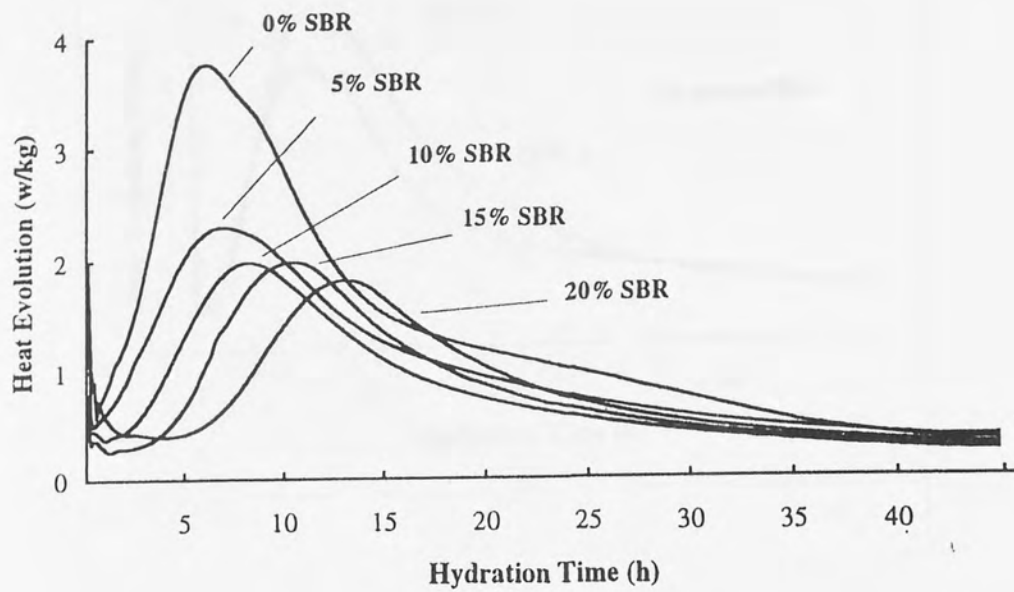


Fig.4.7 Heat evolution curves of SBR 1 modified OPC I at $w/c=0.3$ and 22°C

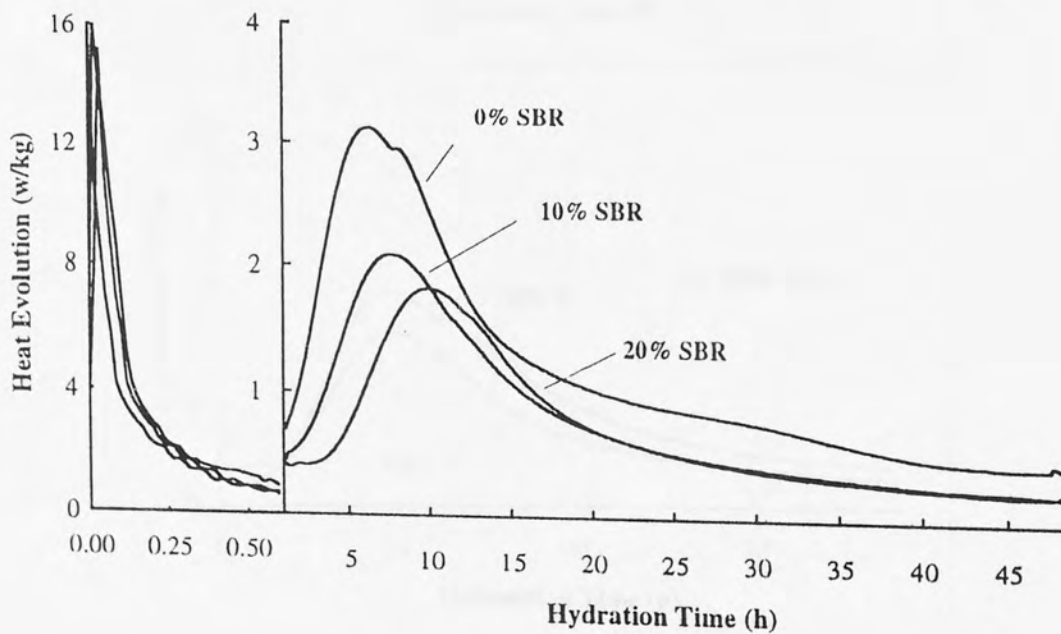


Fig.4.8 Heat evolution curves of SBR 1 modified OPC I at $w/c=0.5$ and 22°C

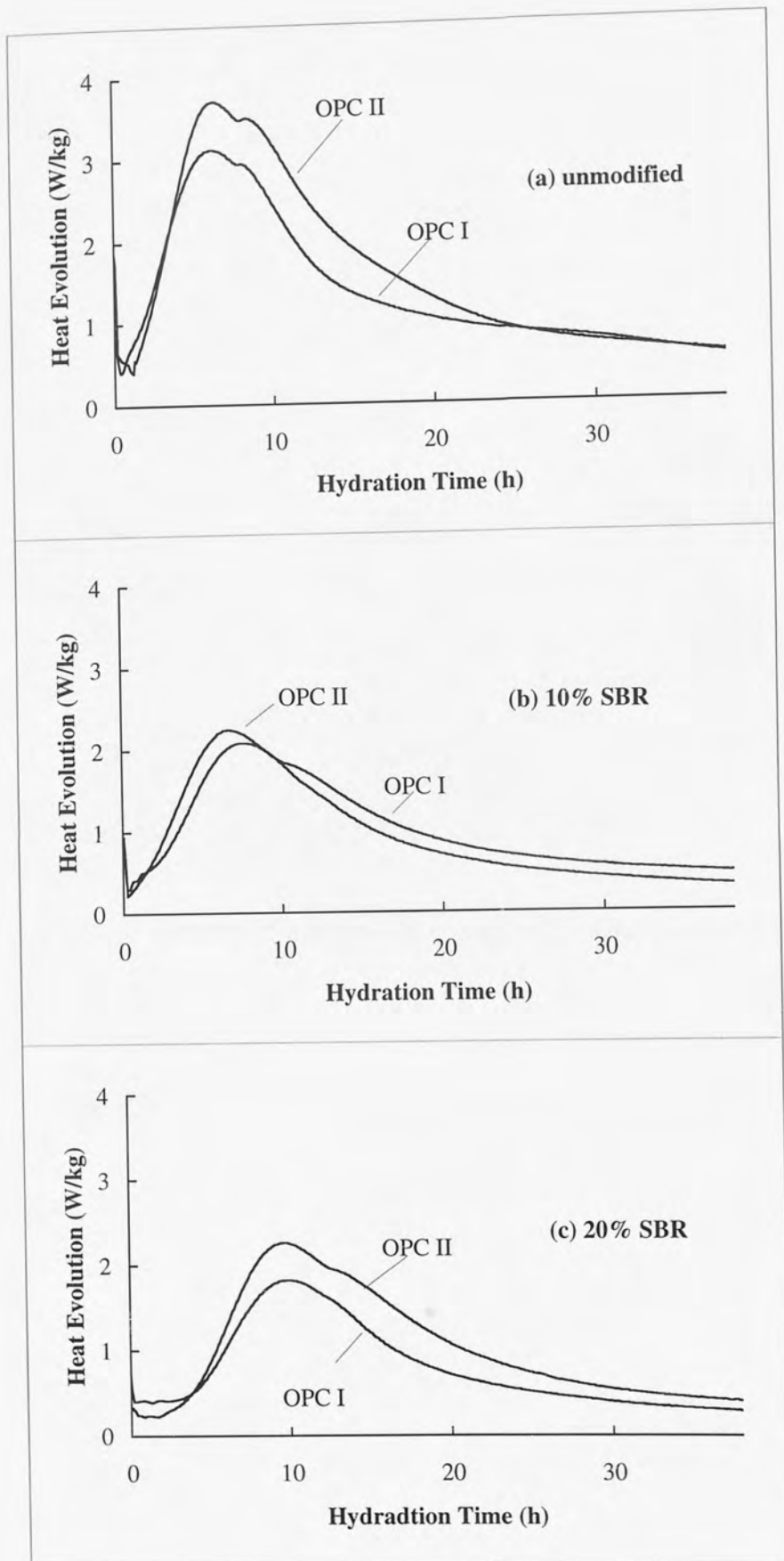


Fig. 4.9 Influence of alkali content of cement on heat evolution curves for SBR 1-cement system at $w/c=0.5$ and 22°C

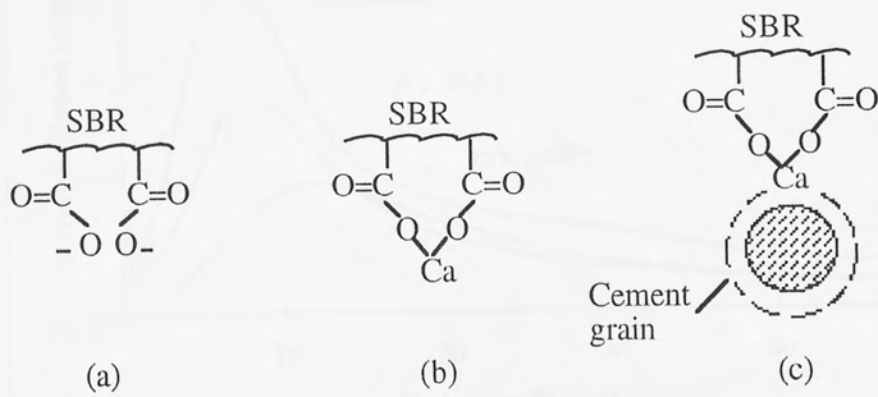


Fig.4.10 Scheme of polymer adsorbing or bonding to cement grains

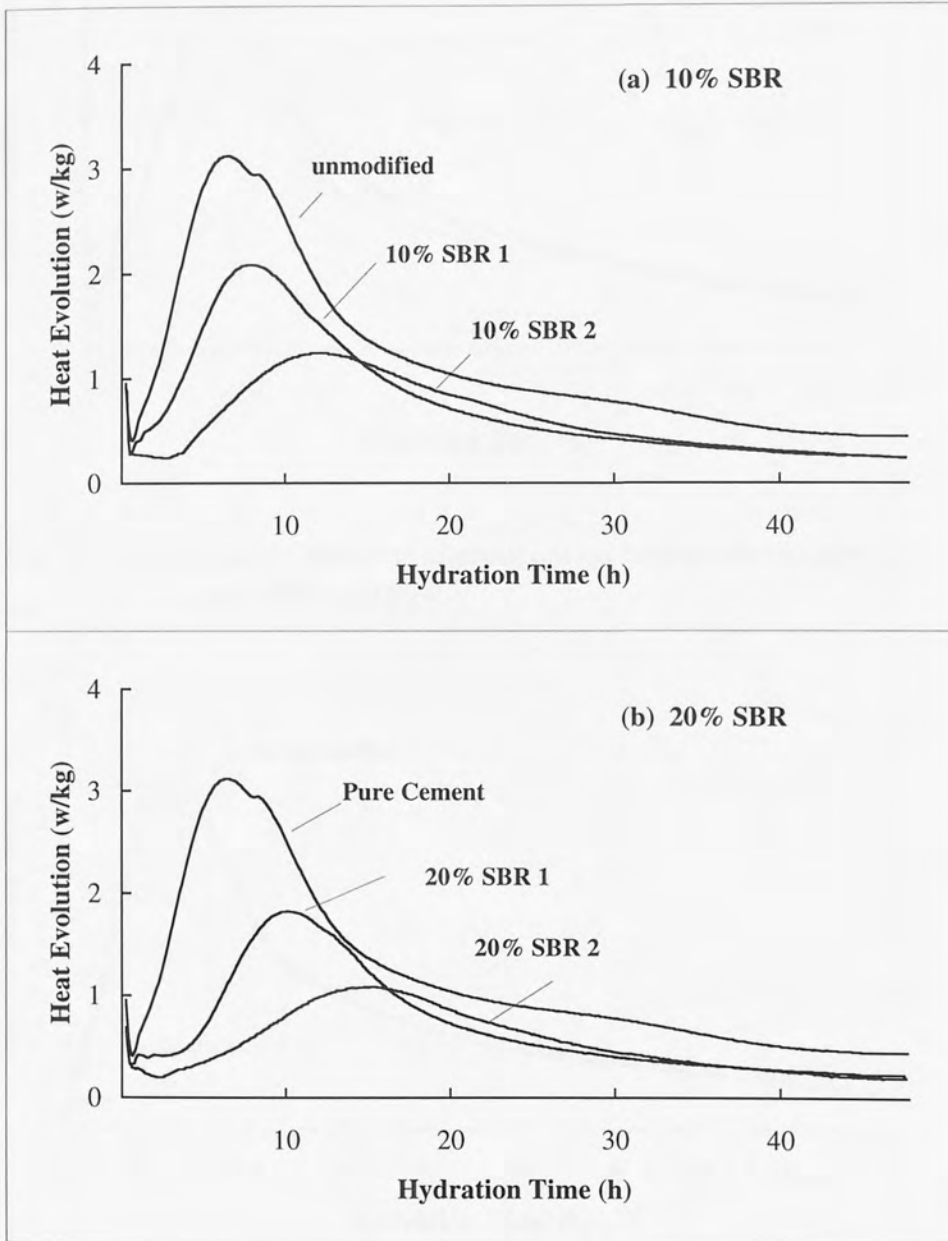


Fig. 4.11 Influence of carboxyl groups on heat evolution curves at $w/c=0.5$ and 22°C

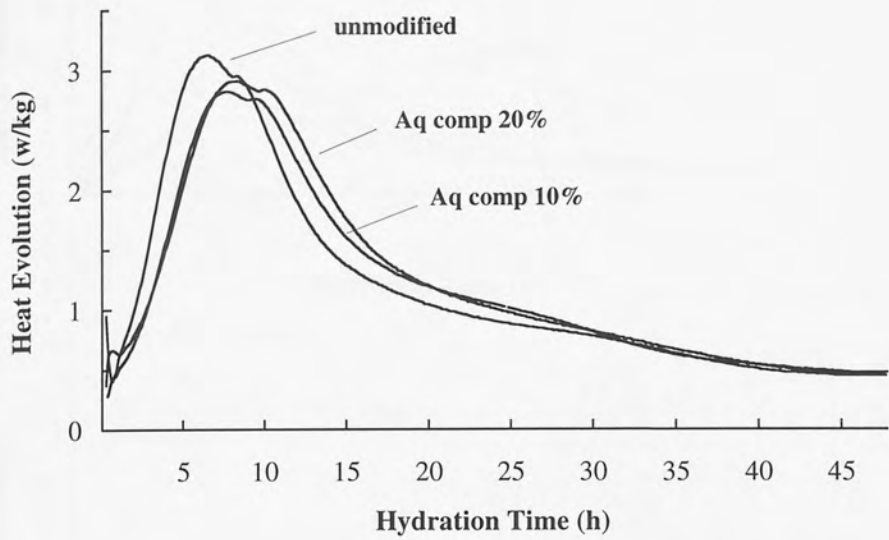


Fig. 4.12 Influence of aqueous component on heat evolution curves at $w/c=0.5$ and 22°C

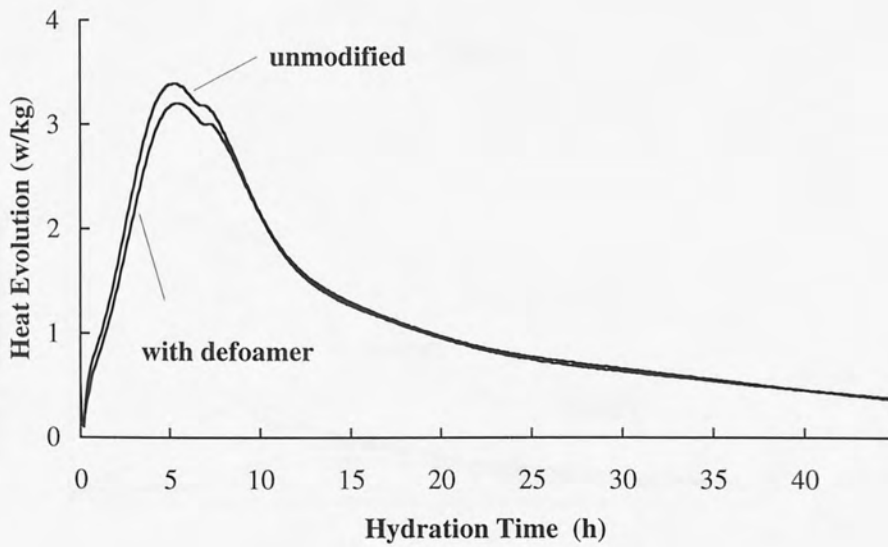


Fig. 4.13 Influence of defoamer on heat evolution curves at $w/c=0.5$ and 22°C

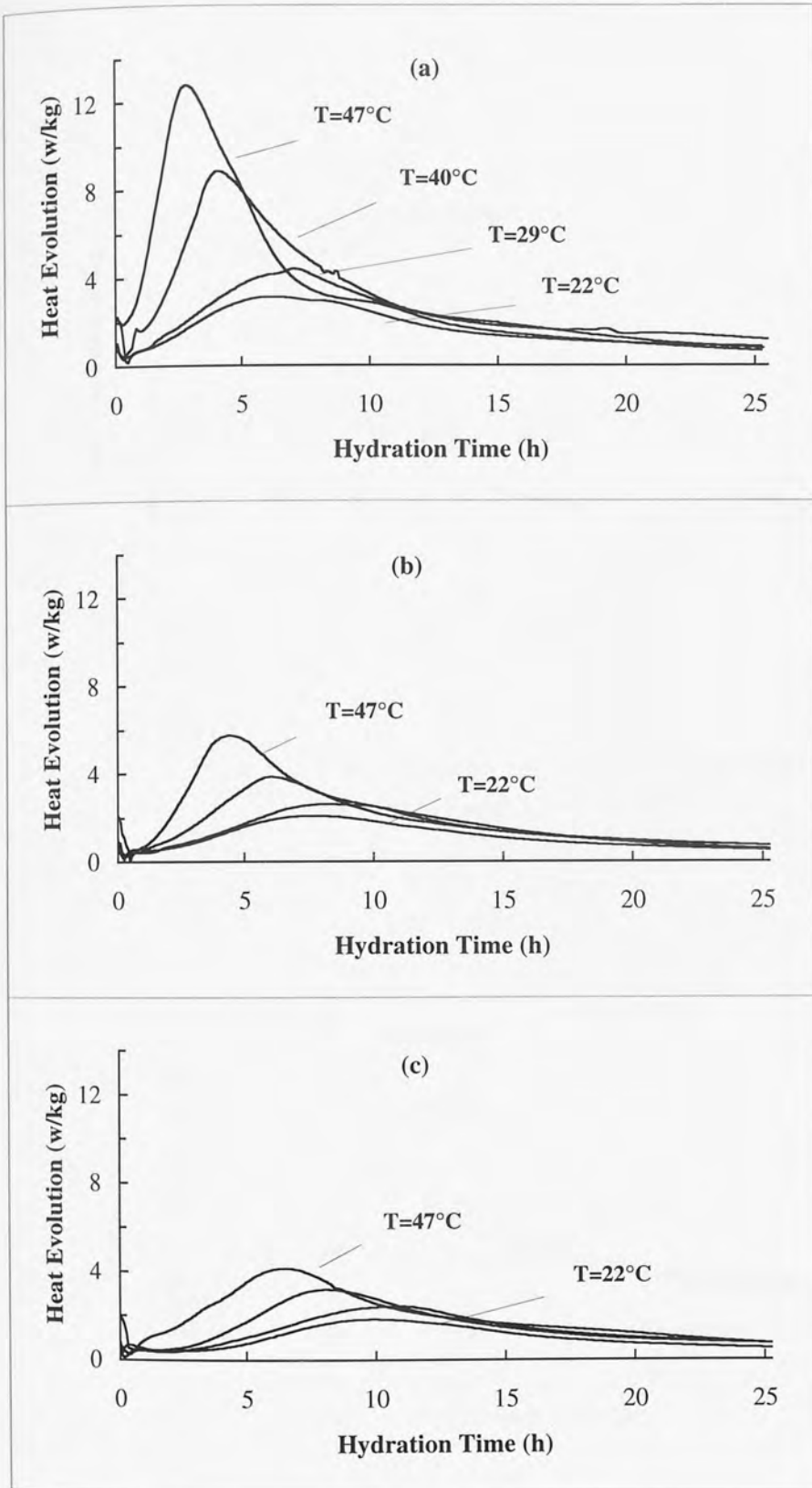


Fig. 4.14 Heat evolution curves of SBR 1 modified OPC I at different hydration temperature
 (a) Unmodified; (b) 10% SBR; (c) 20% SBR

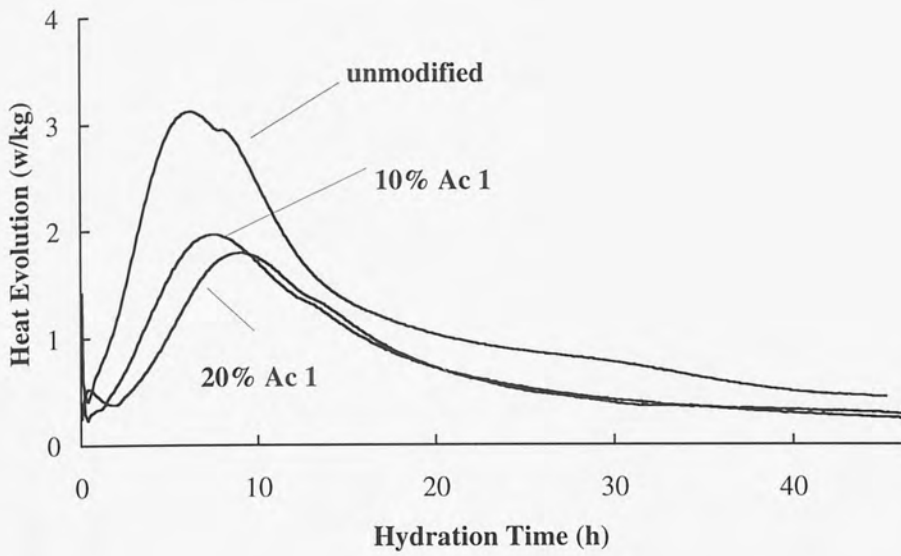


Fig.4.15 Heat evolution curve of Ac 1 modified OPC I at $w/c=0.5$ and 22°C

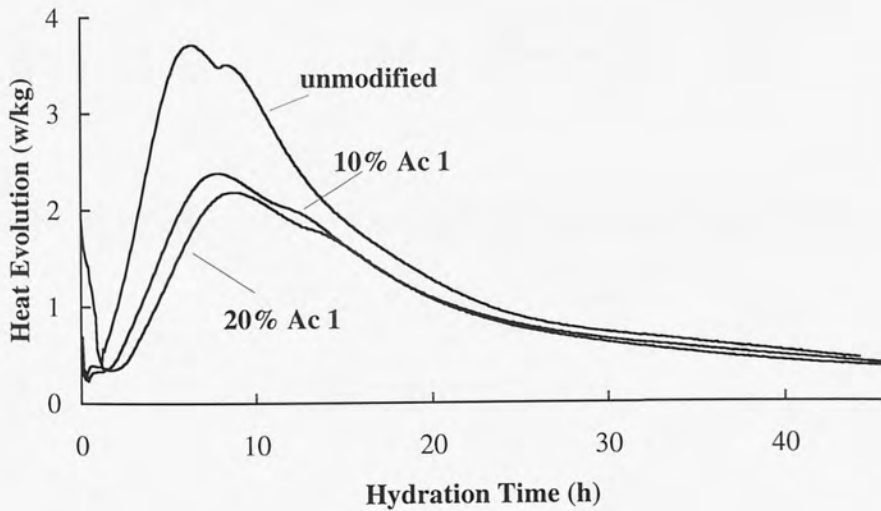


Fig.4.16 Heat evolution curve of Ac 1 modified OPC II at $w/c=0.5$ and 22°C

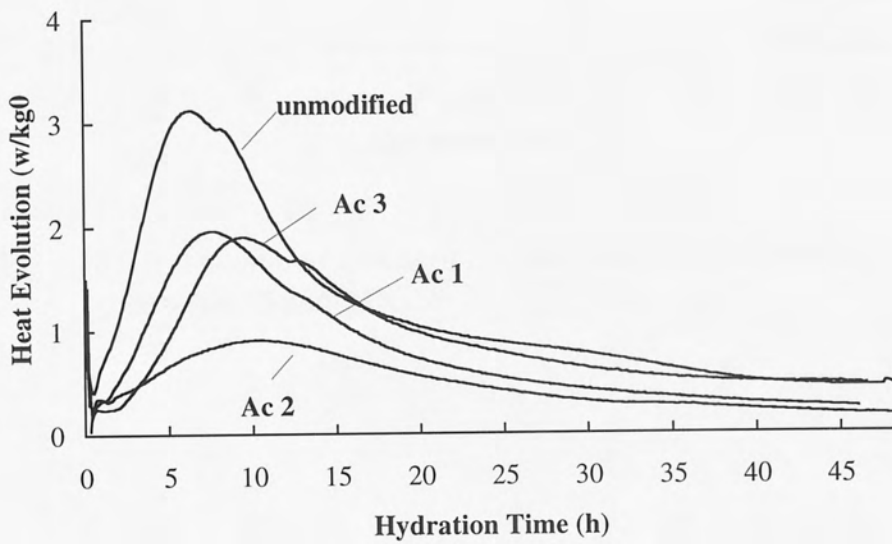


Fig. 4.17 Heat evolution curves of acrylic-OPC I at $w/c=0.5$ and 22°C

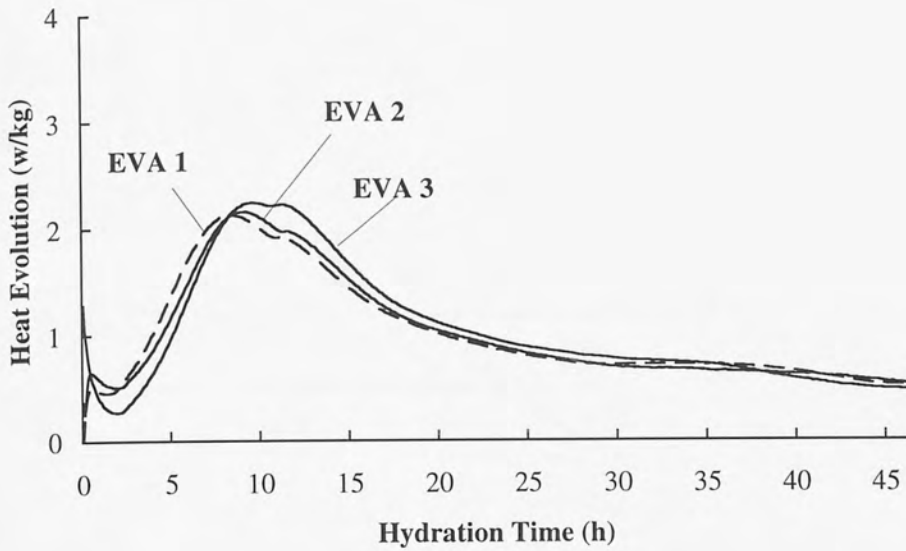


Fig.4.18 Heat evolution curves of ethylene-vinylacetate-OPC I at $w/c=0.5$ and 22°C

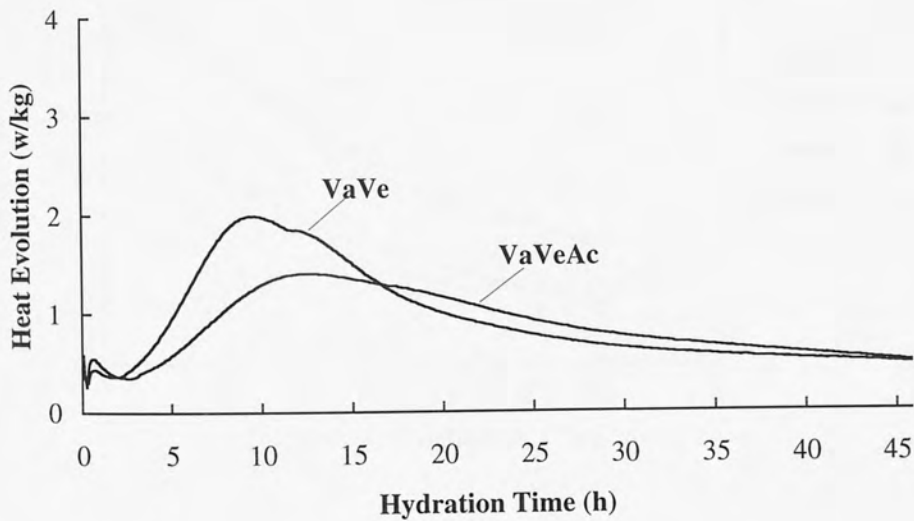


Fig.4.19 Heat evolution curves of vinylversatate-vinylacetate-OPC I and vinylacetate-vinylversatate-acrylic-OPC I at $w/c=0.5$ and 22°C

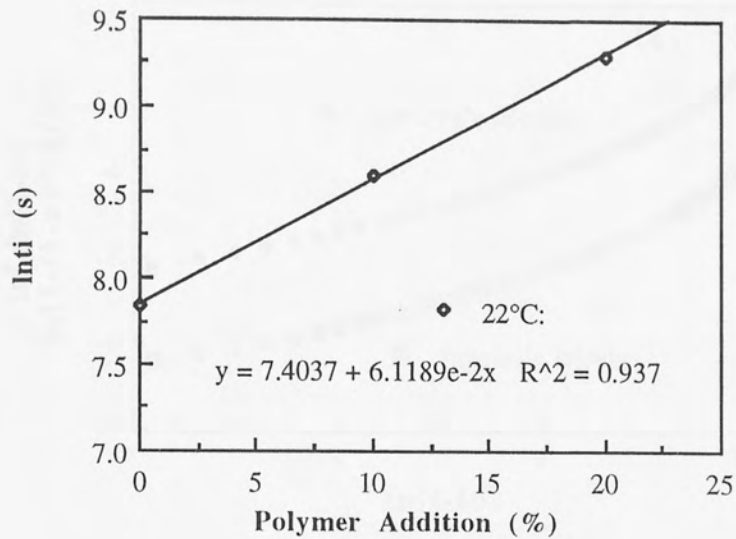


Fig. 4.20 A typical relationship between induction time and polymer addition for SBR 1 modified OPC I at w/c ratio 0.5

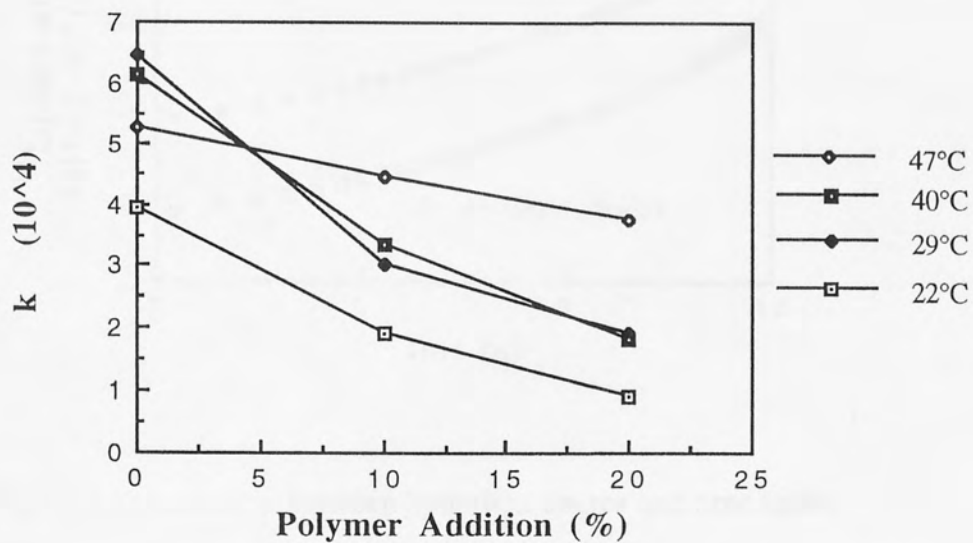


Fig.4.21 Influence of polymer addition and hydration temperature on the rate constant (k)

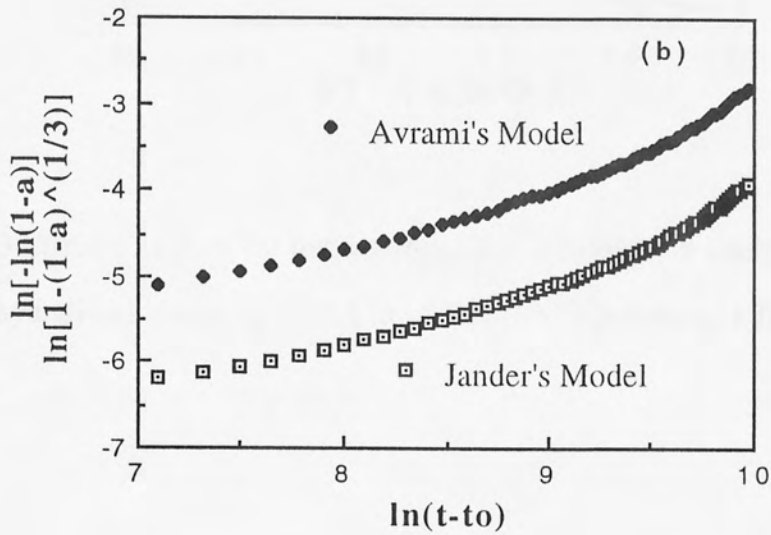
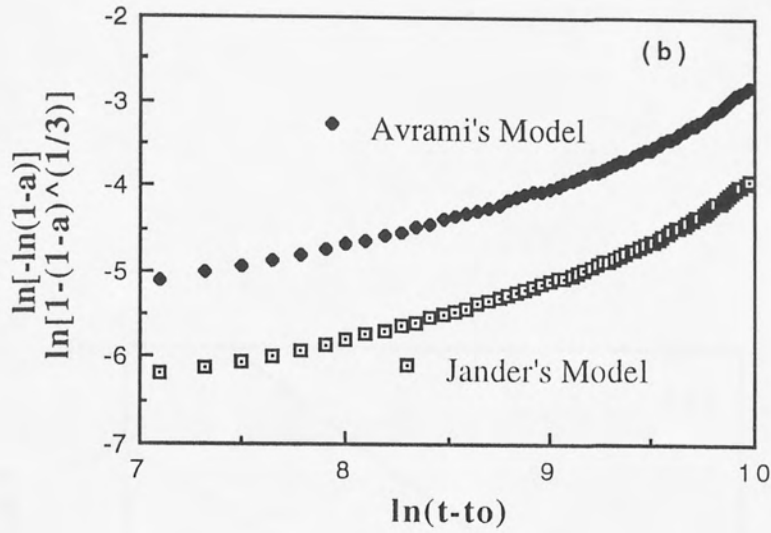


Fig. 4.22 Relationship between hydration degree and time under Jander's model and Avrami's model at w/c ratio 0.5 and 22°C
 (a) OPC I, (b) 20% SBR 1-OPC I

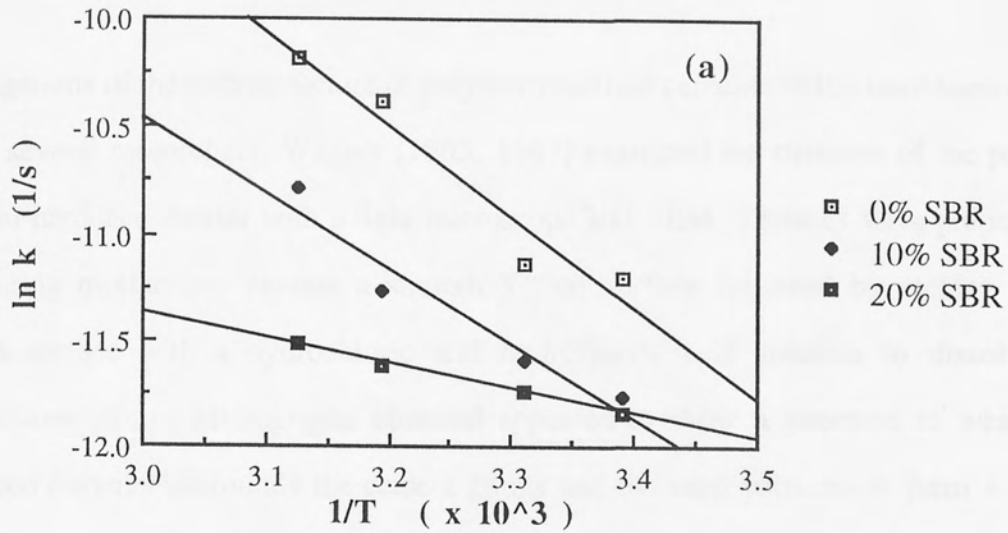


Fig. 4.23 Arrhenius plots for the determination of activation energy for the hydration kinetics of SBR 1 modified OPC I (values of k from Jander Model)

CHAPTER 5

MICROSTRUCTURAL DEVELOPMENT OF POLYMER MODIFIED CEMENT

5.1 PREVIOUS WORK

Investigations of the microstructure of polymer modified cement (PMC) have been carried out by several researchers. Wagner (1965, 1967) examined the structure of the polymer phase in hardened mortar with a light microscope and SEM. Surfaces were prepared by first curing mortar cast against a smooth Teflon surface followed by etching of the smooth surface with a hydrochloric and hydrofluoric acid solution to dissolve the cementitious phase. Micrographs obtained appeared to show a structure in which the coalesced polymer surrounds the cement grains and the sand particles to form a coarse network.

Isenburg (1974) also examined this network on the fracture surface of styrene butadiene copolymer modified mortar. In the electron micrographs, some continuous microfibrils were observed which appeared to bridge both sides of microcracks in the hardened mortar. For a fracture surface of unmodified mortar, the microcracks were clearly seen at the interface between the cement paste and nonshrinking materials such as sand. From this point of view, they postulated that the continuous film may contribute to the higher tensile strength of the PMC by resisting propagation of cracks.

Grosskurth (1987) observed similar polymer films which linked the walls of pores in styrene acrylic-cement paste.

In order to study the distribution of polymer in the cement matrix, Lewis et al.(1990) observed fracture surfaces and polished sections of acrylic-cement pastes by a bromine "tagging" method. Because the polymer consists of carbon and hydrogen atoms, the

presence of the polymer latex can not be detected directly by conventional energy dispersive X-ray analysis. However, when a reagent containing heavier elements such as bromine is added to the polymer, it is capable of detecting the polymer phase because the reagent can bond to the carbon-carbon double bonds. The concentration and location of the bromine in the surface indicates the density and location of the polymer in the matrix. A non-uniform distribution of the polymer was found, the polymer concentration being high at the interface of aggregate and cement and low in the rest of the cement matrix.

When studying the morphology of cement hydrates, Marusin (1987) made a simple comparison between conventional concrete and PMC. She observed that the hydration products were well developed in a conventional concrete with a w/c ratio of 0.44. The C-S-H gel possessed essentially a fibrous character, whilst the development of this type of structure in the PMC only occurred in limited areas. A micrograph showed a pocket filled with fibrous C-S-H gel and a small number of ettringite needles and partially developed silicate crystals. The fibres of C-S-H gel were found to be much smaller than those found in the conventional concrete.

The pore structure has been investigated by several researchers and the essential method used to measure the pore size distribution was mercury intrusion porosimetry (MIP). Ohama et al. (1987, 1991) determined the pore size distribution of polyacrylic ester-modified mortar and styrene butyl acrylate-modified mortar with various w/c ratios from 0.57 to 0.78. They reported that the polymer dispersions reduced the pore volume of large radii pores of 0.2 μm or more, and increased the smaller radii of 75 nm or less. The total pore volume tended to decrease with an increase in the polymer addition. Nishi et al. (1990) reported similar results.

On the other hand, Grosskurth (1987) found that with increasing polymer contents (S-Ac) the specific pore volume was extended. Oye (1989) showed that all pore size distribution curves of mortars modified with PMMA lay above the curve of the control sample. This indicated that the total porosity of modified mortar was higher than that of

unmodified mortar. Oye assumed that this effect may be caused by the high mercury pressure. Mercury may force its way through the polymer plugs and consequently increase the pore volume.

Using SEM Marusin (1987) and Sandrolini (1992) showed that PMC contained a relatively small amount of discontinuous pores which were not uniformly distributed. The pores were generally spherical although several pores were found to be oval shaped. In comparison, an unmodified sample contained a relatively large number of almost spherical pores which were often surrounded by a number of fine pores.

Another feature of the microstructure of PMC is the microcracks existing in the matrix. Kuhlmann (1991) discussed how microcracks occurred in latex-modified concrete overlays and how to avoid them. He pointed out that polymer modified concrete, like any concrete, is liable to produce microcracks as a result of external and internal sources. The typical internal sources are plastic and drying shrinkages and the external sources include structural movement, thermal expansion and tearing while finishing.

Soroushian et al. (1991) presented a more detailed report about the influence of latex modification on microcracks and their propagation under compression in concrete materials. The sliced SBR-concrete specimens were stained with a black ink and ground with silicon carbide on rotating laps over a sequence of grit sizes. These specimen preparation steps helped distinguish the microcracks under the microscope. The cracks at the prepared faces of the slice were visible as black lines. The results showed that the microcrack intensities in the PMC were much lower than that in a plain concrete. For example, the microcrack intensity at a transverse section in the plain concrete was 0.29 cm / cm², but only about 0.03 cm / cm² in PMC. The microcracks in plain concrete appeared predominantly at the interfaces between coarse aggregate and cement paste, but in PMC the microcrack intensities at the aggregate-paste interfaces tended to be reduced, indicating improvements in bonding between the cementitious paste and aggregates. Furthermore, when concretes were subjected to loading and microcrack propagation

under compression was observed, it was found that the microcrack intensity tended to be reduced at lower stress levels with latex modified cement. This reduction may result from the restraint of microcrack propagation by polymer films bridging across the cracks.

5.2 PORE CHARACTERISTICS OF PMC

5.2.1 Methods of Pore Structure Determination and Problems

Hardened cement mortar and concrete may be classified as porous materials. The presence of pores not only affects their mechanical properties, but also the permeability of gases e.g. water vapour and CO₂, and diffusion of ions e.g. chloride, and hence the durability of the concrete. The size of the pores, the total porosity and their geometry are factors of prime importance in determining the properties of such materials and suitability for practical applications. The determination of pore structure is therefore often a vital step in the evaluation of these materials and in the quality control of products, and is of both scientific and economic significance.

A large number of methods are available for pore structural analysis, such as mercury intrusion porosimetry (MIP), water absorption, solvent exchange, adsorption isotherms of water or N₂ and helium pycnometry, but none of these give a true volume measurement since each of the methods are based on a number of underlying assumptions. For some methods, the validity of these assumptions has been questioned. Since different principles are involved, the different methods may yield different information for a given material being examined.

Among the various methods, MIP is a favourite with researchers in construction materials. In the present study, we also used this method to measure porosity and pore size distribution, but bearing in mind the following factors which may affect the MIP results.

The extent and manner of drying is of considerable importance. It is said that direct oven-drying of sample at 105°C tends to collapse the delicate microstructure and removes some chemically bound water as well as the so-called capillary and interlayer waters (Buenfeld 1986). All samples were therefore dried by a solvent replacement method whereby they were immersed in propan-2-ol for 2 days and dried with a hair drier after treatment in a ultrasonic bath. It has been claimed that all the pore water can be removed and because of the lower surface tension, less damage should occur as the liquid evaporates.

On the other hand, some researchers reported that organic liquids may be strongly retained by cement hydrates (Taylor, 1987). In order to avoid this effect, our samples were kept in an oven at 50°C for 10 hours after drying with propan-2-ol, which accelerated the evaporation of the organic liquid without collapsing the pore structure. To ensure propan-2-ol does not dissolve the polymer film in the samples, one piece of SBR1 and Ac 1 film were immersed in the propan-2-ol for two weeks. No discernable dissolution was observed. Thus, all samples were actually dried by a combination method of solvent replacement and oven-drying. It is believed that this combination takes advantage of both solvent replacement and oven-drying but overcomes their weak points.

Figs. 5.1a and 5.1b show a comparison between propan-2-ol replacement drying, propan-2-ol+oven drying (50°C) and oven drying (105°C) with an unmodified cement paste aged 7 days. At a water cement ratio of 0.3 (Fig. 5.1a), there is no difference in the pore structure when propan-2-ol replacement drying and propan-2-ol+oven drying are used. A small difference in the pore structure can be seen at w/c 0.5 (Fig. 5.1b). The porosity determined by propan-2-ol replacement method is slightly lower than by the propan-2-ol+oven drying method. This may be caused by retention of propan-2-ol, which is expected to be removable either by drying at 50°C or by keeping the sample in a desiccator for a long period of time to allow the organic liquid to evaporate. The oven-drying at 105°C produced a large change in the pore structure (see Fig. 5.1b). The total porosity increased from 0.18 to 0.25 cm³/g. This large change is probably caused by the loss of interlayer or chemically bound water.

Besides the drying method, one should be aware of the influences caused by the mercury porosimetry technique itself. As described in 3.3.2, mercury porosimetry is based on the fact that the mercury does not wet a porous solid and will enter its pores only under pressure. In addition, it is assumed that the pores are cylindrical and the pore size may be calculated by the Washburn equation. Therefore, the MIP result may be affected by applied pressure, contact angle, surface tension and pore shape. Cook et al. (1993) investigated these influences and presented some assumptions and corrections relevant to its application to cement-based materials. According to this study, the volume changes including sample compression, mercury compression and porosimeter chamber expansion do not affect the pore size distribution, but affect the total porosity. The changes of contact angle and pore shape factor have no effect on the total porosity but do have an influence on the threshold diameter by shifting the pore size distribution curve horizontally. Gane et al. (1995) attempted to make some corrections by a software package known as Pore-Cor, but this only considered the factor of volume change.

These considerations mentioned above are of significance when we intend to measure the true value of porosity. But the study is still in the stage of theoretical consideration and the findings have not yet been put into practical application for mercury porosimetry. Fortunately, in most cases, the pore structure characteristics are often compared between similar materials. Thus, provided that the experimental conditions are kept consistent, the MIP results are still useful when comparing different pore structures.

For polymer modified cement, the determination of pore structure by MIP may be complicated further by the addition of polymer. One problem is that the polymers adsorb on the surfaces of hydration products, which change the surface property of pore walls, and in turn, the contact angle between mercury and pore walls. Another problem is that the polymer may change the compressibility of samples. PMC may be more compressible than unmodified cement paste.

The problems above are complicated and need special investigation. In the present study, it is believed that when using MIP it is still possible to compare relatively the pore characteristics between samples. Because the contact angle θ only shifts the pore size distribution curve, it does not affect the relative comparison. For the second problem, it is assumed that the compressivity change of the samples is very small and the influence is negligible. Consequently, MIP is used as the main method to determine the pore structure of samples although some results are compared to those determined by solvent exchange porosity, water absorption porosity and helium pycnometer porosity.

5.2.2 Results and Discussion

5.2.2.1 Mercury Intrusion Porosity

Influence of Polymer Addition

The total porosity measured by MIP for polymer modified cement pastes is listed in Table 5.1. Figs. 5.2(a-d) show the pore size distribution curves for SBR 1-OPC I pastes at a w/c of 0.3. Figs. 5.3(a-c) show the pore size distribution curves for SBR 1-OPC I pastes at a w/c of 0.5 and Figs. 5.4(a-b) show the pore size distribution curves for Ac 1-OPC I pastes at a w/c of 0.5.

From the figures, it can be seen that all curves have a similar shape in that the cumulative intrusion volume does not increase at the larger pore sizes (about 1-100 μm), but in the smaller pore size range, the shape of the curves suddenly changes and the cumulative intrusion volume rapidly increases. This characteristic pore size corresponds to the pore size through which mercury penetrates the bulk of the sample and is called the threshold or critical pore size (Cook 1993).

Addition of latex to cement generally resulted in an increased threshold pore size and greater total porosity. This tendency was intensified with increasing polymer addition. Figs. 5.2(a-d) show the pore size distribution curves for SBR 1-cement pastes cured for

3, 7, 28 and 90 days. The curves in Figs. 5.2(a-b) have a slight overlap above a pore diameter of $1\mu\text{m}$, but below this size the curves begin to separate due to the change of threshold pore size. The threshold pore size is about $0.04\mu\text{m}$ for 3 and 7 day old unmodified cement paste, but addition of 5% SBR 1 enlarge this size to $0.2\mu\text{m}$ and at addition of 15% SBR 1 to $0.7\mu\text{m}$. The intrusion volume of mercury at the threshold pore diameter also rapidly increased with increasing SBR 1. At 10% SBR 1 and 15% SBR 1, the curves raise rapidly so that their cumulative intrusion volumes at a pore size of $0.7\mu\text{m}$ reach respectively 0.12 and $0.15\text{ cm}^3/\text{g}$ paste compared to $0.01\text{ cm}^3/\text{g}$ paste for unmodified cement paste. Therefore, SBR 1 increases significantly the size of threshold pore and the volume of this pore size in young cement pastes.

Similar results have been obtained for SBR 1-OPC I pastes with $w/c=0.5$ (see Fig. 5.3a). For 7 day old pastes, polymer again increased the threshold pore size and the pore volume at this size. This tendency continues in 28 day old pastes (see Fig. 5.3b).

Figs. 5.4a and 5.4b show the pore size distribution curves of acrylic-cement pastes with $w/c=0.5$. Acrylic performance is similar to that of SBR although there are some differences in the shape of the curves.

Change of Pore Structure with Time

The results described above show that at short curing times polymer modified cements had a much coarser pore structure than unmodified cements. However, it is interesting to note that this tendency decreased at longer curing times. When plotting pore size distribution curves against different curing ages (see Figs. 5.5-5.6), the changing process of pore structure with time is clearly observed. For polymer modified cement pastes, it can be seen that at 3 days the curve (Figs. 5.5b and 5.6b) is quite different to that at 90 days and there is a big gap between them. As curing age increases, however, these differences rapidly diminish. At 90 days, the curves are so close to the curve of unmodified cement paste that they almost overlap (see Figs. 5.2d, 5.3c and 5.4b). In contrast, the change of pore structure in unmodified cement paste with time is much less

(see Fig. 5.5a and 5.6a). Even the curve of 3 day old paste is very close to the curve of 90 day old paste.

These observations revealed that the development of microstructure in polymer modified cement paste is delayed by the presence of polymer. In the early stages, the microstructure is developed slowly resulting in a higher porosity of the paste, but for longer curing time the microstructure developed so that the porosity of the paste declined and the pore structure became similar to the structure of the unmodified cement paste at 90 days.

These results match the results obtained from the hydration experiments using isothermal conduction calorimetry. As discussed in Chapter 4, the polymer retarded the hydration of cement. Hence, the hydrates such as $\text{Ca}(\text{OH})_2$ crystals and C-S-H gel are produced at a lower rate, resulting in a slow development of structure and a porous matrix. The analysis of pore solution also provided similar results (see 6.2.2). The concentration of OH^- ions extracted from modified pastes aged 7 days was much lower than that of unmodified paste, but after 14 days the concentration of OH^- rapidly increased, indicating a low hydration reaction in early stage. During hydration, products rapidly form and spread into the pore space leading to a more compact matrix. At the same time, the polymer particles coalesce into the polymer film and fill some pores. As a result, the microstructure of paste is rapidly refined and the porosity decreases. Compared with unmodified cement paste, the pore structure of polymer modified cement matrix is more tortuous which may contribute to improvement of diffusion property although its total porosity is similar or even slight coarser.

Influence of Surfactant and Carboxylate

Apart from the effect of the polymer solid phase on the development of the microstructure of polymer modified cement paste, the aqueous component contained in the latex, including surfactant may also have an effect on its structural development. Figs 5.7a and

5.7b compare the MIP results for pastes containing 10 or 20% SBR 1, SBR 2 and the aqueous component of SBR 2.

It can be seen that the SBR 2-OPC I has a greater porosity $0.23 \text{ cm}^3/\text{g}$ than SBR 1-OPC I $0.18 \text{ cm}^3/\text{g}$ at a polymer addition of 20%. Since SBR 2 contains 5% carboxylate while SBR 1 only 1%, the increment of porosity could be caused by an increase in carboxylate. On the other hand, it can be seen that the aqueous component-OPC I paste has almost the same pore size distribution as the unmodified cement paste. This indicated that the aqueous component in the latex does not in itself affect the pore structure. Consequently, one conclusion that can be drawn here is that the carboxylate affects the pore structure by changing the properties of the polymer solid phase, in particular the surface properties. This is in agreement with the results of hydration where the aqueous component had little influence on hydration (see Fig. 4.12), whereas the percentage of carboxylation had a significant effect (see Fig. 4.11).

5.2.2.2 Solvent Exchange Porosity and Water Absorption Porosity

Being aware that MIP is subject to several uncertainties due to the factors discussed earlier, solvent exchange and water absorption methods were also used to determine the porosity of the samples to assess the validity of the MIP results and ensure their correct interpretation.

Several organic solvents can be used in the exchange procedure, such as ethanol, methanol and propanol. Some researchers (Day 1981) have reported that some organic solvents, such as methanol may react with calcium hydroxide during exchange and proposed that it is better to use propanol in this method. Therefore, propan-2-ol was selected and the detailed experimental process was described in section 3.3.3. The solvent exchange porosity and water absorption porosity for SBR 1-OPC I system with $w/c=0.5$ are listed in Table 5.2.

5.2.2.3 Porosity from Helium Pycnometry

Total porosity for SBR 1-OPC I system and Ac 1-OPC I system were measured by a Helium Pycnometer. The results are summarised in Table 5.3.

5.2.2.4 Comparison of Porosity Results Obtained by the Various Techniques

As seen from Table 5.2, the values of total porosity for five replicate discs cut from a cylinder are very close, which indicates that the methods of water absorption and solvent exchange are of good reproducibility.

In order to compare the three methods with MIP, the porosity of SBR 1-OPC I samples with a water cement ratio 0.5 are summarised in Table 5.4 and plots of the porosity determined by water absorption, solvent exchange and helium pycnometry against the MIP porosity are shown in Fig. 5.8. This figure does not regard paste type, period of cure and polymer addition, it therefore shows a one-to-one corresponding relationship between results obtained by water absorption or solvent exchange or helium pycnometry and by MIP. In Fig. 5.8, all data points of water absorption, solvent exchange and helium pycnometry porosity lie above a line of equality, indicating that the porosity obtained by these three methods is higher than by MIP. The difference mainly arises from the missing of pore sizes below $0.004\mu\text{m}$ within the measuring range of MIP or the failure of mercury to enter or vacate interlayer spaces (Taylor 1990).

Furthermore, it is noted that the results obtained by solvent exchange are consistently lower than those obtained by water absorption. This is a common occurrence reported in the literature (Day 1988; Feldman 1983) and is usually attributed to the inability of alcohol to enter the interlayer spaces.

Although differences exist between these methods, the general changes with curing time and polymer addition are the same. Fig. 5.9 clearly shows this tendency. The total porosity of paste obtained by any of these four methods increases with increasing polymer addition and decreases with curing time extension. Therefore, MIP is still a valuable tool to get information on pore structure and correlation between the pore volume and permeability or strength. Of course, caution should be taken when interpreting the pore size distribution because of the weak points of this method. For example, it was noted that the pastes aged 90 days with 10% polymer or less had a lower cumulative intrusion volume in the pore size 0.05-1 μ m range although the cumulative intrusion volume at pore size 0.004 μ m is higher than for pure cement paste. In Figs.5.2d, 5.3c, and 5.4b, this phenomenon could be seen for different polymers. This result may suggest that with suitable addition (say 10%), the polymer decreased the large pore volume in the range of 0.05-0.1 μ m and increases the small pore volume of 0.05 μ m and less. However, since the difference is not very significant, the conclusion that the polymer improved the pore size distribution needs to be confirmed.

5.3 MORPHOLOGY OF CEMENT HYDRATES AND POLYMER FILM WITHIN HARDENED MATRIX

As well as pore structure characteristics, another important microstructural feature is the morphology of the hydration products and the distribution and form of polymer in the hardened matrix. Since the latexes normally used in polymer modified cement are able to form films at the working temperature, it is commonly accepted that latex particles coalesce around each cement grain and aggregate particle to form an interpenetrating network throughout the structure. This postulation has been supported by some SEM observations by Wagner (1967) and Isenburg (1974). However, they did not analyse these areas which were supposed to be polymer films and afterwards virtually no another researcher has observed similar polymer films in the hardened matrix. Therefore, the distribution and morphology of polymer in the polymer modified cement still needs further investigation.

In order to do that, we examined fracture surfaces and etched fracture surfaces of polymer modified cement pastes by using SEM. Other techniques including SEM/EDXA, optical microscopy, microhardness and bromine or osmium tagging were also used in a parallel research investigation (Salbin 1996).

5.3.1 SEM Observation of Fracture Surfaces

SEM examination of the fracture surfaces of polymer modified cement pastes are shown in Figs. 5.10-13. The pastes had 20% polymer addition and a water cement ratio 0.5 and were cured for 90 days. Fig. 5.10 is the SEM of unmodified cement paste. It shows well defined hydrates, with some C-S-H gel and the Ca(OH)_2 crystals in the layer form, some C-S-H gel in the fibre form. It seems that they spread into the pore space, but do not completely fill the space and leave large voids.

The SEM image of polymer modified cement shows a quite different morphology. In general, the morphology of the fracture surface has more fibrillar outgrowths, or more reticular networks. Fig. 5.11 shows the gross structure of SBR-cement paste. The C-S-H gel in this structure is finer and more acicular. It seems that some polymer adheres or deposits on the surfaces of the C-S-H gel. Needles of C-S-H appear to spread out from a cluster of hydrates and interweave together forming a crossing network. The SEM of acrylic cement paste (Figs. 5.12) displays a fishing-net or honeycomb structure.

An additional observation of interest in these figures is the morphology and dimension of Ca(OH)_2 crystals. A group of fine Ca(OH)_2 crystal are observed in the SBR 2-cement paste (see Fig.5.13). The Ca(OH)_2 crystals in the pastes are in the form of plates, not tightly packed. The size of Ca(OH)_2 crystals is much smaller than that in unmodified paste. These fine Ca(OH)_2 crystals are concentrated in limited areas. This may suggest that the presence of polymer confines the ionic diffusion so that the Ca(OH)_2 crystallised locally to form fine crystals.

The void in the structure seems to be smaller, but no polymer film appears to be bridging the walls of the pores although many polymer bands or C-S-H gel spread into the pore space.

5.3.2 SEM Observation of Etched Fracture Surfaces

Figs. 5.14-15 show the SEM of etched fracture surfaces of unmodified and polymer modified cement pastes. The fracture surface of the sample was etched in a solution of HCl+HNO₃ which is considered to dissolve the cementitious phase. Therefore, it should be possible to observe the morphology of the polymer film in the matrix by SEM.

A typical SEM micrograph of unmodified cement paste (Figs. 5.14) shows uniform etching of the surface. The Ca(OH)₂ crystals and C-S-H gel observed in the fracture surface have been "damaged" by acid attack.

On the etched surface of a polymer modified cement paste Fig. 5.15, the structure of polymer films are clearly displayed. The white rings correspond to the coalesced polymer network, while the grey areas inside the rings correspond to positions originally occupied by the cementitious phase. Later energy dispersion X-ray analysis (EDXA) (Salbin 1996) showed these rings were rich in the carbon. This observation suggests that most of polymers exist in the mixture form with hydrates. These mixtures form rings and connect each other and form a network in the hardened matrix.

5.3.3 Flocculation of Polymer Particles during Hydration

During hydration it is thought polymer particles flocculate and then coalesce. Obviously, it would be useful to know when and to what extent the flocculation and coalescence take place for understanding the development of microstructure and estimating of the strength of polymer modified cement, particularly during early ages. However, there is no information about these aspects in published papers.

In the present work, we used the pore solution extraction technique to study the flocculation of polymer particles, although this technique could not provide information about coalescence of particles. Pore solutions were extracted from cement pastes and then analysed to determine its polymer content. Because samples had different curing ages and different latex additions, the polymer contents in the pore solution indicate the disappearing rate of polymer particles from pore solutions and thus in principle, reflect the process of latex flocculation during hardening. A high polymer content could imply a low flocculation rate.

5.3.3.1 Method of determining polymer contents in pore solution

The polymer contents in the pore solution were determined by measuring the absorption using visible spectrophotometry (section 3.2.4) and comparing the values with a calibration curve produced using a series of standard solutions. The standard incorporated synthetic pore solution to simulate the environment in which the polymer particles exist in the cement paste. The standard solutions were made of synthetic pore solution and different concentrations of polymer. The wavelength of visible light used was 450nm, determined by scanning a standard solution over a range of wavelength. Maximum absorbance was produced at 450nm and the calibration curve is shown in Fig. 5.16.

5.3.3.2 Polymer Contents in Cement Pastes

Acrylic-cement pastes were used in this experiment. Acrylic addition was 20% of the weight of cement and water cement ratio was 0.5. Two curing schemes were used. One was the so-called "wet" curing, in which the sample was kept in the plastic pot until required time. The other scheme was the so-called "wet-dry" curing, in which the sample was first sealed in the plastic pot for 3 days and then demoulded and kept in a desiccator. The relative humidity in the desiccator was controlled to 30% by a saturated solution of $MgCl_2$.

After the samples were cured individually for 3, 7, 14 and 28 days in sealed containers, they were pressed to get pore solution and the polymer contents in the pore solutions determined. Tables 5.5 gives the results.

Under the "wet" curing condition, the pore solutions for 3 and 7 day old pastes were white milky colour. The polymer content in the solution was at 12.2%. With curing age increasing, the pore solution became clearer. After 14 days, the pore solution still contained 4.7% polymer and after 28 days the pore solution became clear without polymer particles.

Under the "wet-dry" curing condition, the polymer contents in the pore solution of pastes were much lower when compared to the "wet" curing condition. There was only 1.3% polymer in the pore solution of 7 day old cement paste. No solution could be extracted from the pastes cured for 14 days and 28 days.

The change of polymer content in the pore solution with time show a clear picture about the flocculation process of polymer particles in the paste. The decrease of polymer content in the pore solution with time indicated that the polymer flocculation is gradually taking place accompanying the cement hydration and this process is strongly affected by several factors, including curing condition, polymer concentration (solid polymer/water), water and solid phase ratio (w/s), polymer and solid phase ratio (p/s) and polymer type. As we know, in cement paste with a water cement ratio 0.5, the initial polymer concentration in fresh mixture was 40%. After 3 days, in the "wet" curing condition, the polymer concentration was 12.2%, only 28% of the initial concentration. This meant that about 70% polymer solid, disregarding hydrated water, had been flocculated or absorbed by the cement phase. After 7 days, about 90% polymer had been flocculated. A 100% flocculation of polymer solid may be completed after 28 days. In the early stage (say before 3 days), cement rapidly hydrates and a large amount of water was consumed. As a result, most of the polymer particles flocculated and in the meantime were absorbed by the cement phase so that they were not pressed out. In the later stage, the flocculation of

polymer mainly depended on the rate of water consumed by cement hydration. In the "wet-dry" condition, the process was accelerated as the rapid evaporation of water. At 7 days, about 97% of polymer had been flocculated.

5.4 Conclusions

1) The total porosity and pore size distribution of PMC were measured by MIP and the results of the total porosity were compared with values obtained by solvent exchange, water absorption and helium pycnometry. Results showed that the different techniques resulted in different values, but the trends with curing time and polymer addition were the same. This suggests that MIP is still a useful tool for comparing the influence of polymer phase on pore structure of PMC.

2) Addition of polymer to cement changes the pore structure of hardened cement paste. Compared with unmodified cements (constant w/c), it may increase porosity of young paste and the tendency increases with increasing polymer content. However, with an increase of curing time, PMC exhibited similar or slightly coarser pore structure.

3) Increased carboxylate content of latex particles may increase porosity of PMC, but the aqueous component of the latex does not seem to affect the pore structure.

4) The flocculation of polymer particles within the matrix depends on the mix design, curing conditions and the type of polymer. Generally, most of the polymer particles may have been flocculated in the first 3 days and after 7 days all polymer disappeared from the pore solution.

5) SEM examination of the fracture surfaces of PMC showed different morphology of cement hydrates to unmodified cement. Whilst SEM examination of etched fracture surfaces of PMC indicated that polymer was in a ring form. The rings may be a mixture of polymer and hydrates and they form a network in the hardened matrix.

TABLE 5.1

Porosity Measured by Mercury Intrusion Porosimetry
for Various Polymer-Cement Systems

Type of Polymer -cement Paste	Water Cement Ratio	Curing Age (days)	Cumulative Intrusion Volume (cm ³ / g paste)				
			Polymer Addition (percentage of cement by weight)				
			0	5	10	15	20
SBR 1 -OPC I	0.3	3	0.12	0.15	0.18	0.18	-
		7	0.11	0.13	0.16	0.17	-
		28	0.10	0.11	0.11	0.11	-
		90	0.10	0.11	0.12	0.12	-
	0.5	7	0.18	-	0.24	-	0.32
		28	0.17	-	0.20	-	0.20
90		0.17	-	0.18	-	0.18	
SBR 2 -OPC I	0.5	90	0.17	-	0.19	-	0.23
Aq Comp -OPC I	0.5	90	0.17	-	0.16	-	0.17
Ac 1-OPC I	0.5	7	0.18	-			
		28	0.17	-	0.22	-	0.24
		90	0.17	-	0.18	-	0.18

TABLE 5.2

Porosities Measured by Solvent Exchange and Water Absorption Methods

for SBR 1-cement system with w/c=0.5

(Unit: cm³/g paste)

Curing Age (Days)	Water Absorption			Propan-2-ol Exchange		
	SBR 1 Addition (%)			SBR 1 Addition (%)		
	0	10	20	0	10	20
7	0.28	0.35	0.36	0.25	0.31	0.32
	0.27	0.36	0.36	0.25	0.30	0.32
	0.28	0.35	0.36	0.25	0.29	0.33
	0.28	0.35	0.36	0.25	0.31	0.32
	0.27	0.36	0.35	0.25	0.31	0.32
Ave.	0.28	0.35	0.36	0.25	0.31	0.32
28	0.27	0.28	0.29	0.24	0.23	0.26
	0.27	0.28	0.29	0.24	0.22	0.26
	0.27	0.28	0.28	0.24	0.22	0.25
	0.27	0.28	0.27	0.24	0.22	0.25
	0.27	0.27	0.28	0.24	0.226	0.24
Ave.	0.27	0.28	0.28	0.24	0.22	0.25
90	0.25	0.26	0.26	0.22	0.21	0.22
	0.26	0.25	0.27	0.21	0.18	0.22
	0.26	0.26	0.27	0.22	0.18	0.22
	0.26	0.26	0.27	0.23	0.19	0.24
	0.26	0.26	0.26	0.23	0.19	0.23
Ave.	0.25	0.26	0.26	0.22	0.19	0.23

TABLE 5.3

Porosities Measured by Helium Pycnometer for SBR1-OPC I and Ac 1-OPC I systems

(Unit: cm³/g paste)

Sample	Curing age (days)	D _d (g/cm ³)	D _r (g/cm ³)	P (%)	P (cm ³ /g paste)
OPC I	7	1.50	2.34	0.36	0.24
10% SBR 1	7	1.33	2.15	0.38	0.28
20% SBR 1	7	1.25	2.33	0.46	0.37
10% Ac 1	7	1.32	2.45	0.46	0.35
20% Ac 1	7	1.24	2.30	0.45	0.36
OPC I	28	1.47	2.25	0.35	0.24
10% SBR 1	28	1.41	2.08	0.32	0.23
20% SBR 1	28	1.41	2.22	0.37	0.26
10% Ac 1	28	1.41	2.26	0.38	0.27
20% Ac 1	28	1.35	2.19	0.38	0.28

TABLE 5.4

Porosities Measured by MIP, Solvent Exchange, Water Absorption
and Helium Pycnometry for SBR1-OPC I system, with w/c=0.5

(Unit: cm³/g paste)

Measure Methods	7 day curing	28 day curing	90 day curing
Unmodified OPC I			
MIP	0.18	0.17	0.17
Solvent Exchange	0.25	0.24	0.22
Water Absorption	0.28	0.27	0.25
Helium Pycnometry	0.24	0.24	-
10% SBR 1			
MIP	0.24	0.20	0.18
Solvent Exchange	0.31	0.22	0.19
Water Absorption	0.35	0.28	0.26
Helium Pycnometry	0.28	0.23	-
20% SBR 1			
MIP	0.32	0.20	0.18
Solvent Exchange	0.32	0.25	0.23
Water Absorption	0.36	0.28	0.26
Helium Pycnometry	0.37	0.26	-

TABLE 5.5

Polymer Contents in the Pore Solution of Acrylic -Cement Paste

Samples	3W	7W	14W	28W	7W-D	14W-D	28W-D
ABS Reading	1.843*	0.976	1.193	0.001	0.366	no solution	
Concentration of Polymer (%)	12.19	3.83	4.73	~0.00	1.31		
W---"wet " curing; W-D---"wet-dry" curing;							
* --- pore solution is diluted (51 times), other diluted (31 times).							

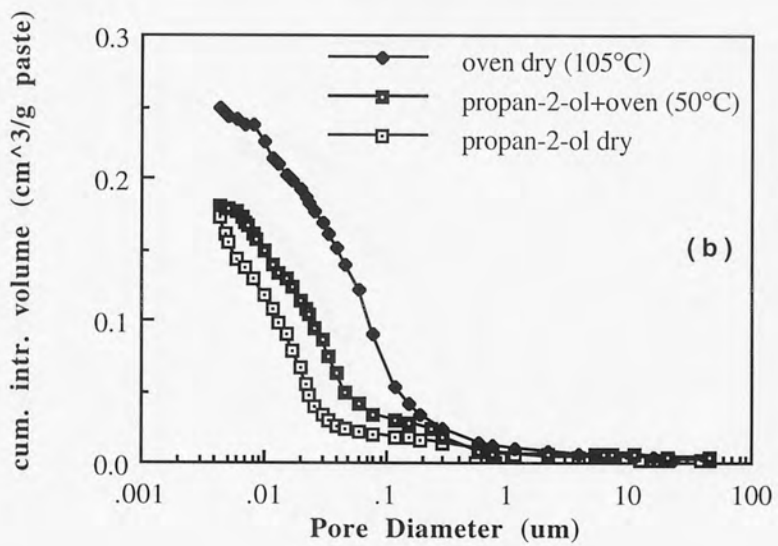
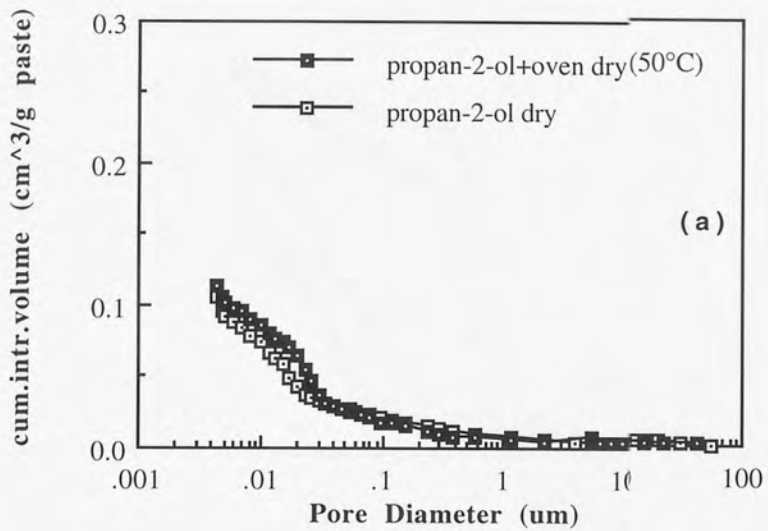


Fig. 5.1 Influence of different drying methods on MIP results of unmodified cement pastes aged 7 days (a) with $w/c=0.3$, (b) with $w/c=0.5$

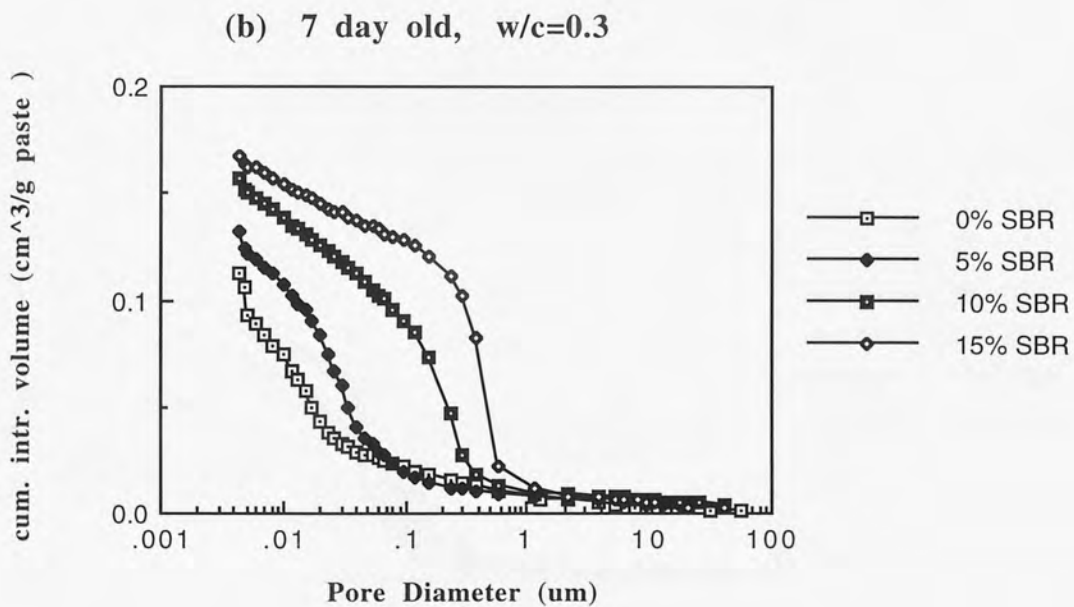
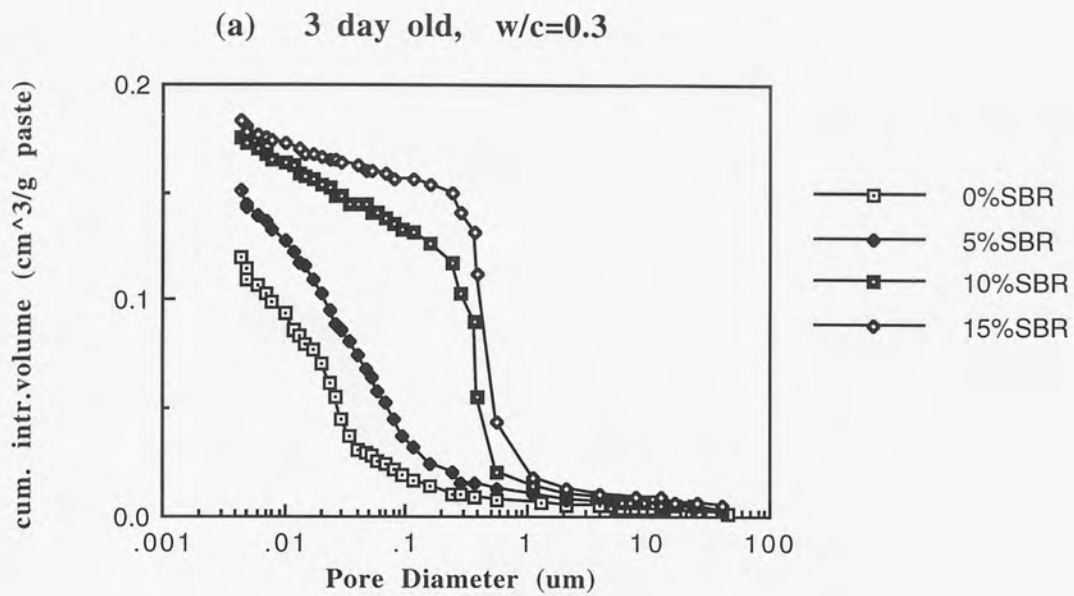
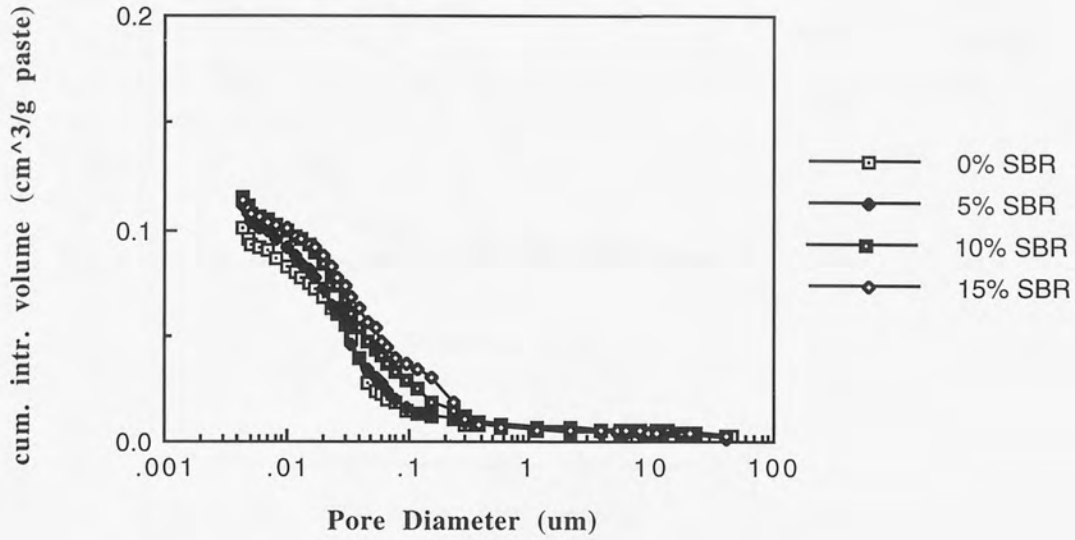


Fig.5.2 Pore size distribution for SBR 1-OPC I pastes at $w/c=0.3$

(c) 28 day old, w/c=0.3



(d) 90 day old, w/c=0.3

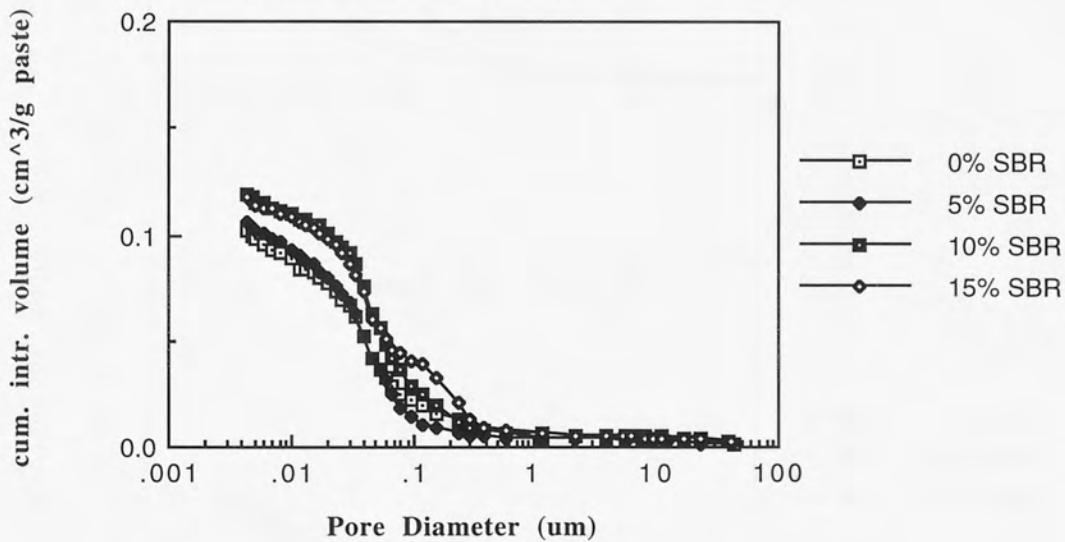


Fig.5.2 Pore size distribution for SBR 1-OPC I pastes at w/c=0.3

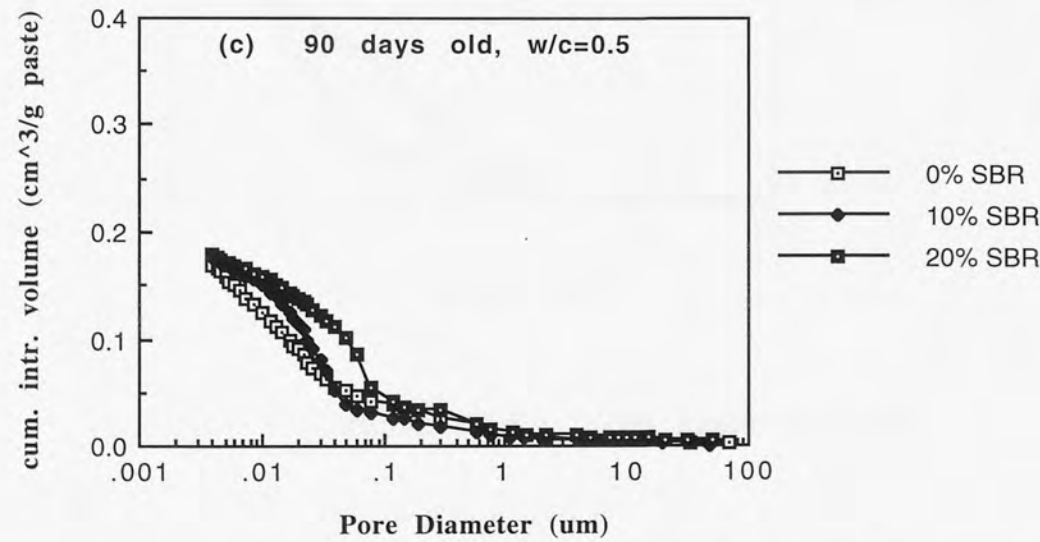
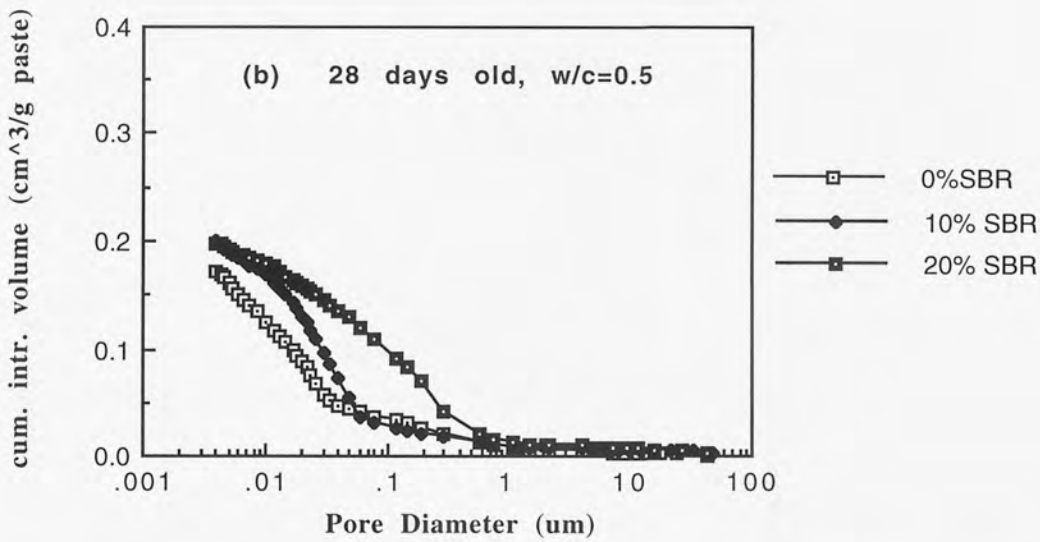
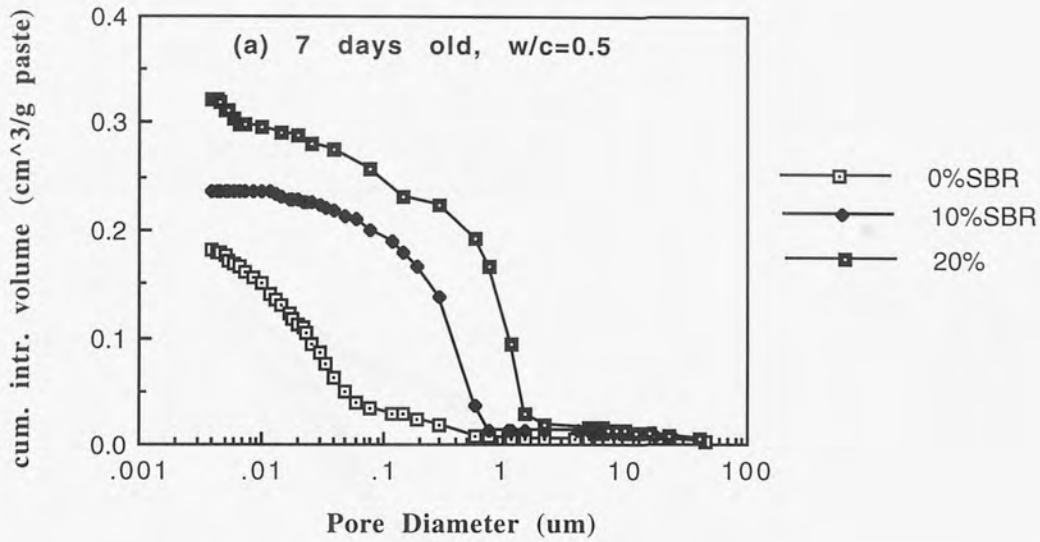


Fig.5.3 Pore size distribution for SBR 1-OPC I at w/c=0.5

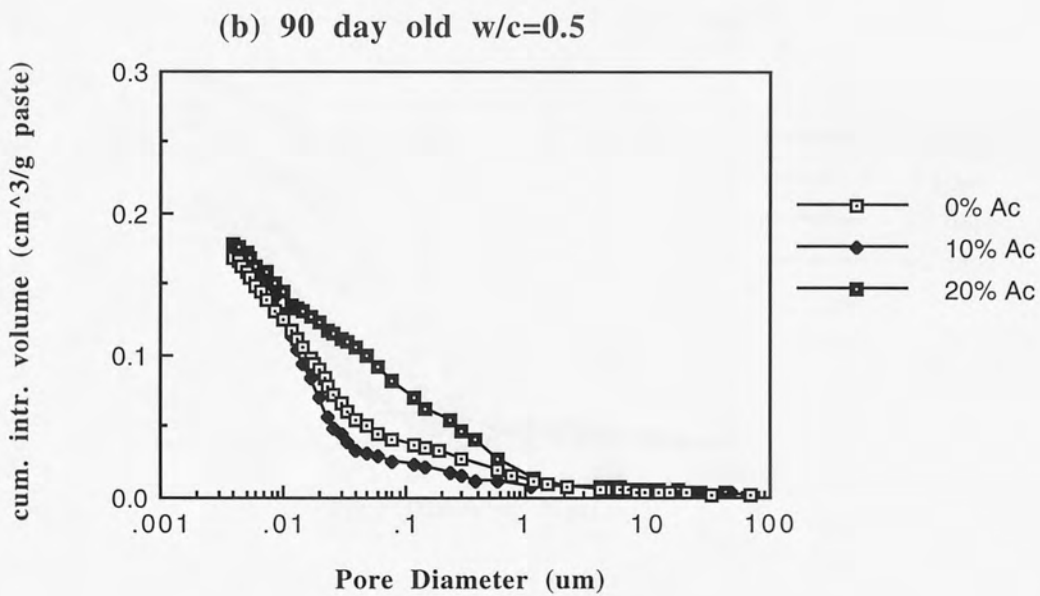
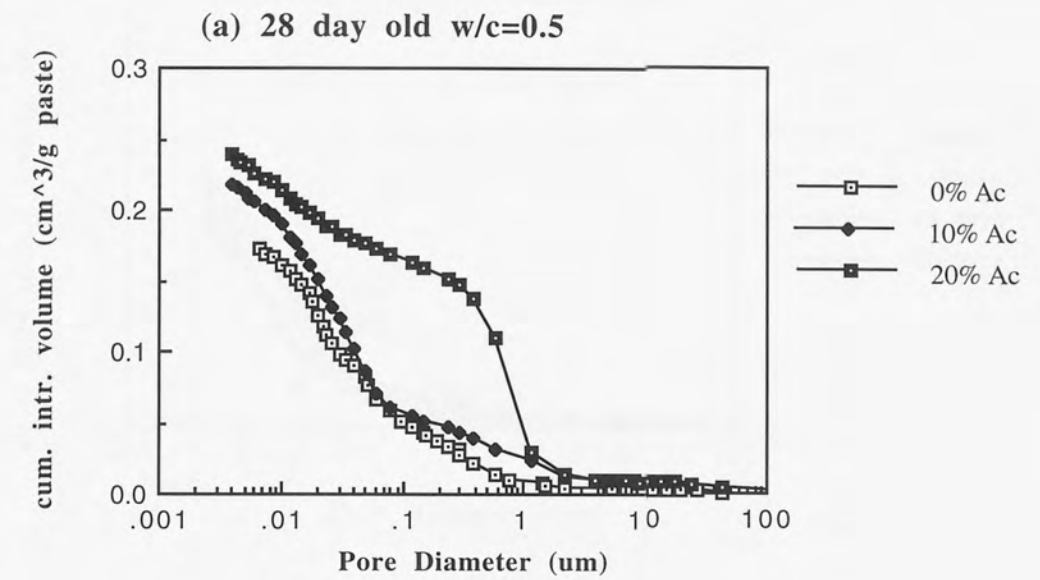
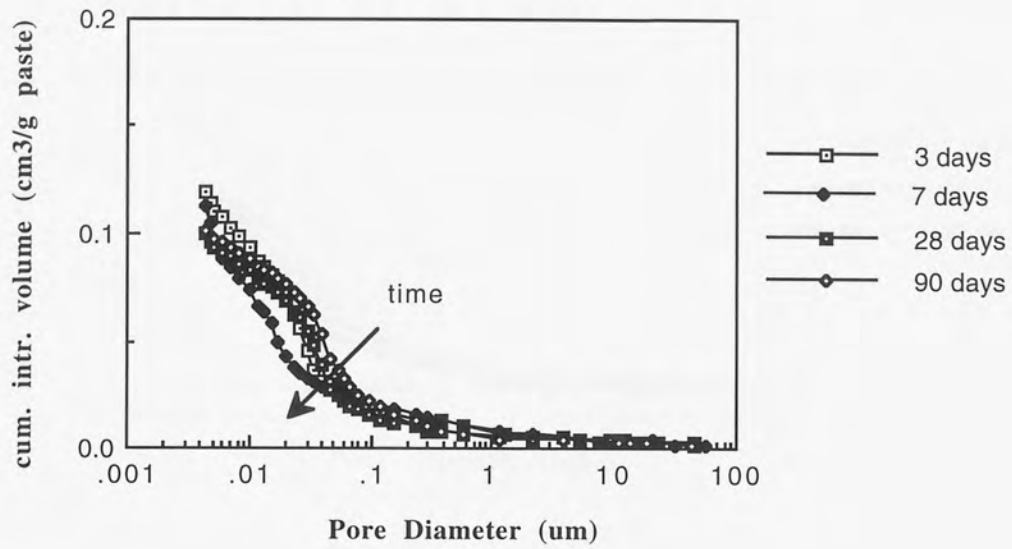


Fig.5.4 Pore size distribution for Ac 1-OPC I pastes at w/c=0.5

(a) unmodified OPC I paste, w/c=0.3



(b) 10% SBR, w/c=0.3

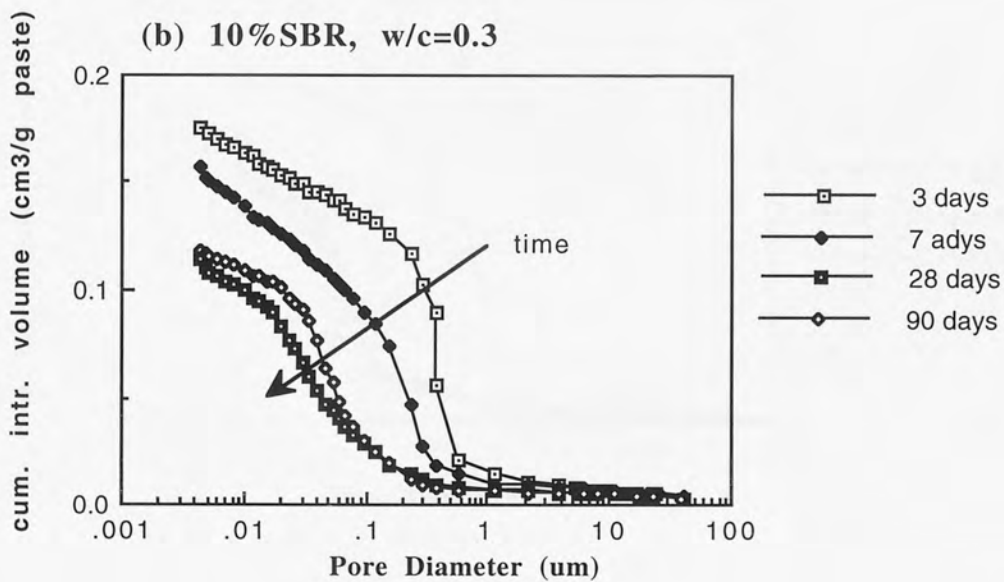


Fig. 5.5 Change in Pore Structure for SBR 1-OPC I Paste at w/c=0.3

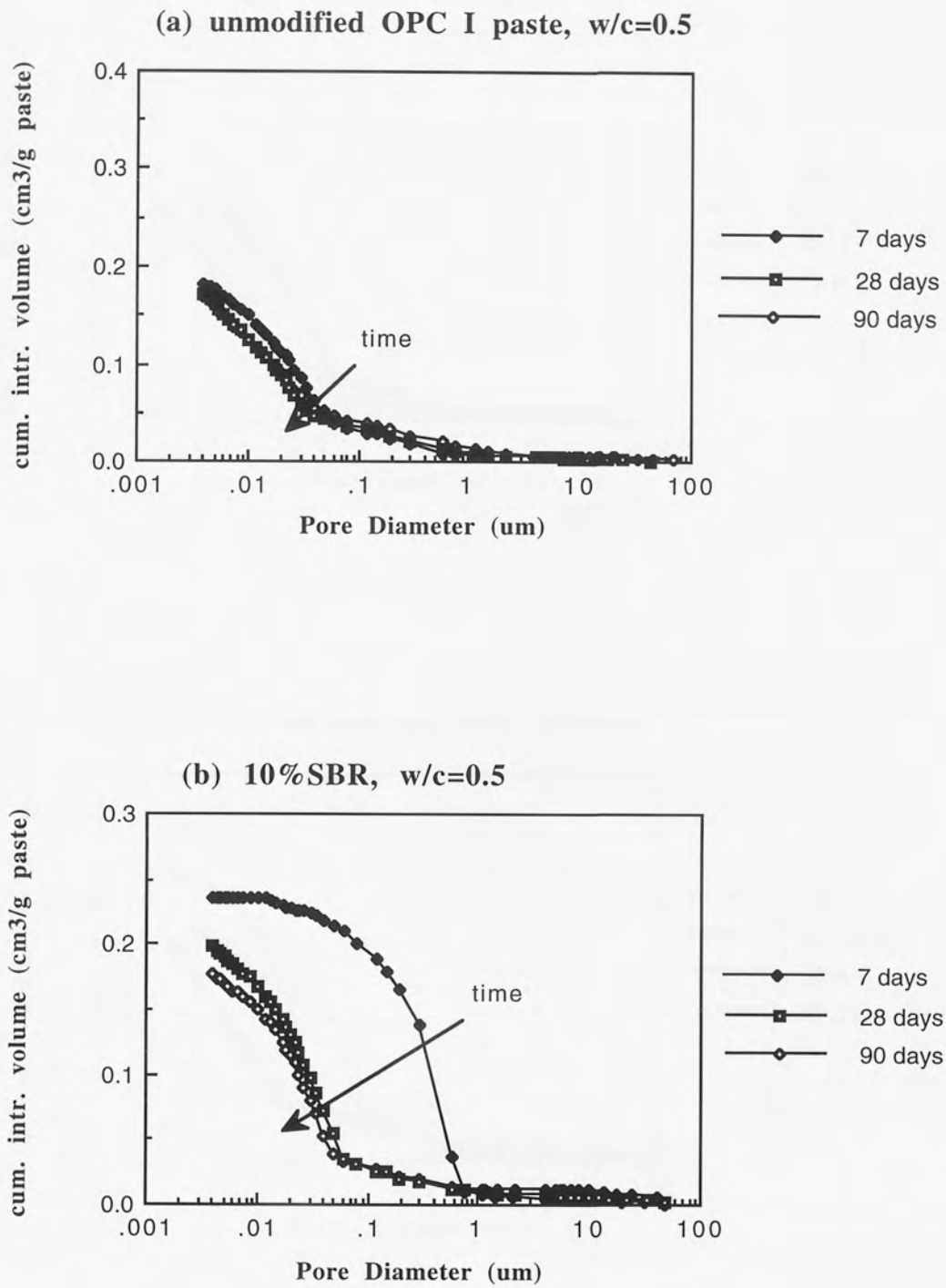


Fig. 5.6 Change in Pore Structure for SBR 1-OPC I Paste at $w/c=0.5$

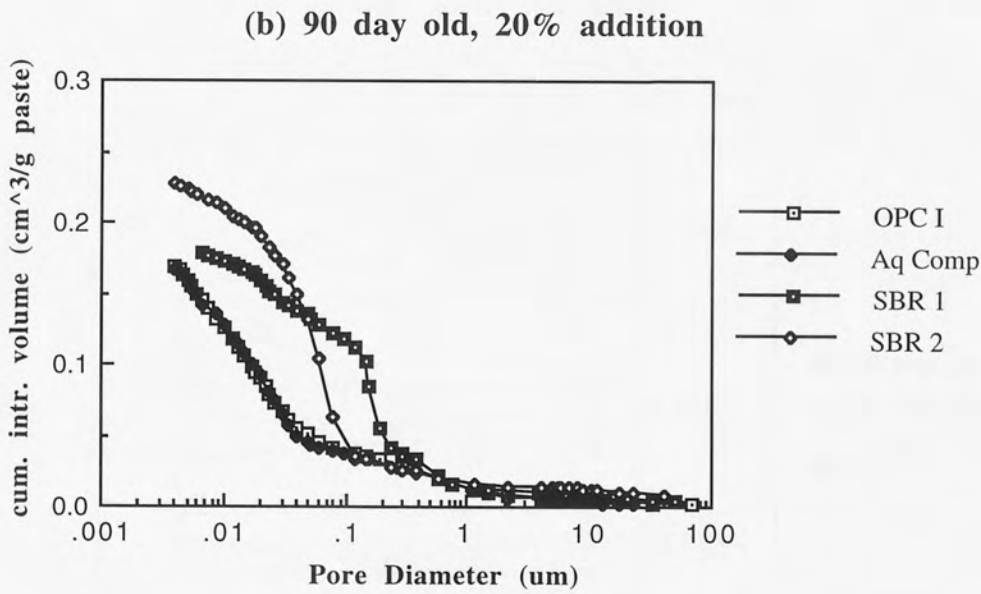
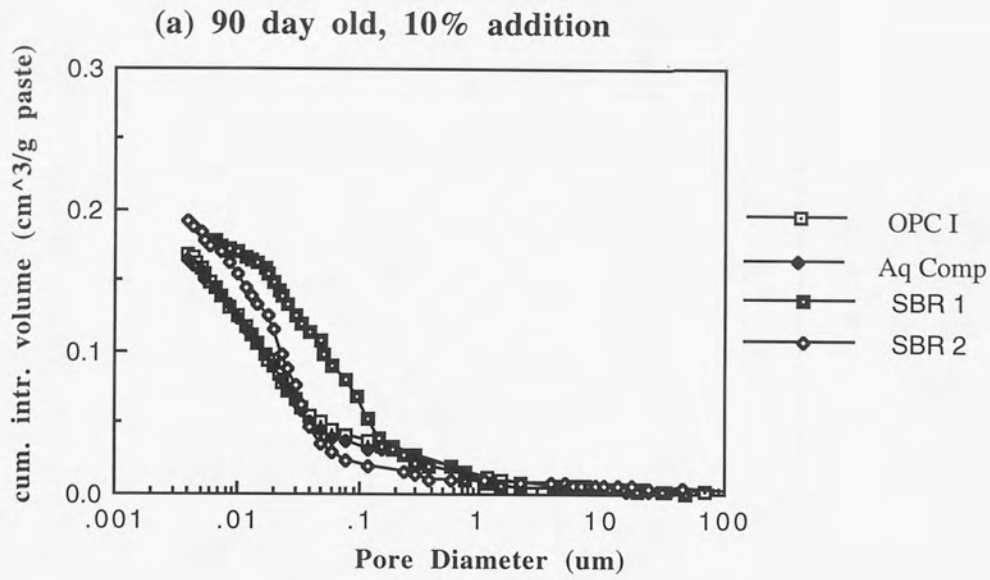


Fig.5.7 Influence of Surfactant and Carboxylate Content on Pore Structure, at $w/c=0.5$

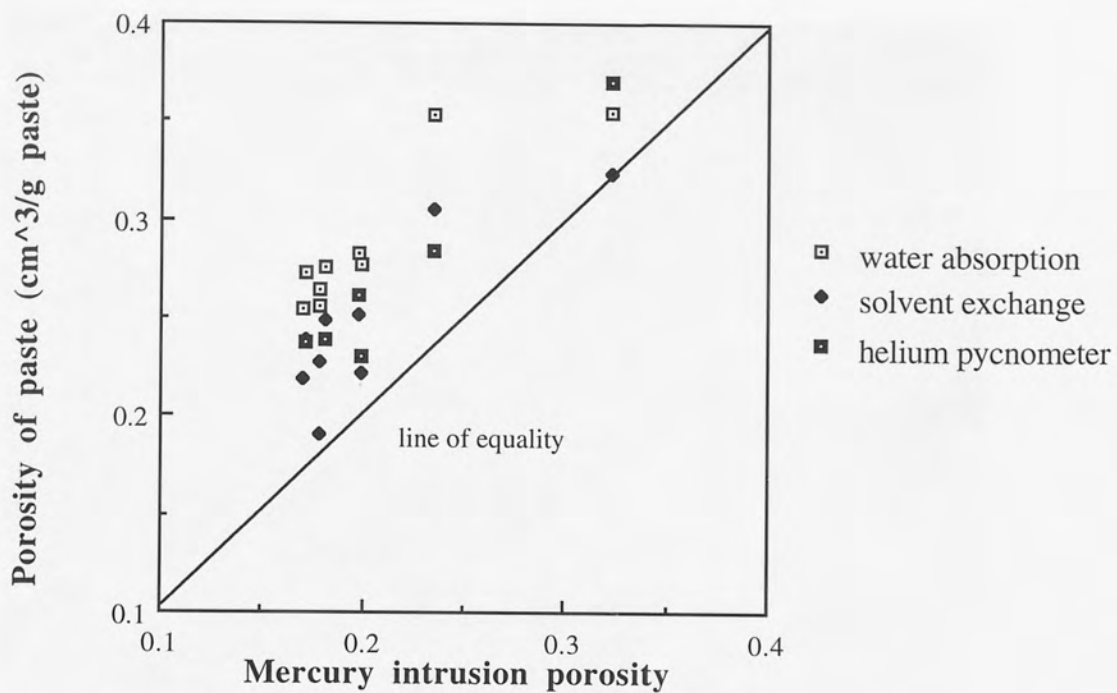


Fig 5.8 Relationship between porosities measured by water absorption, solvent exchange, helium pycnometer and MIP

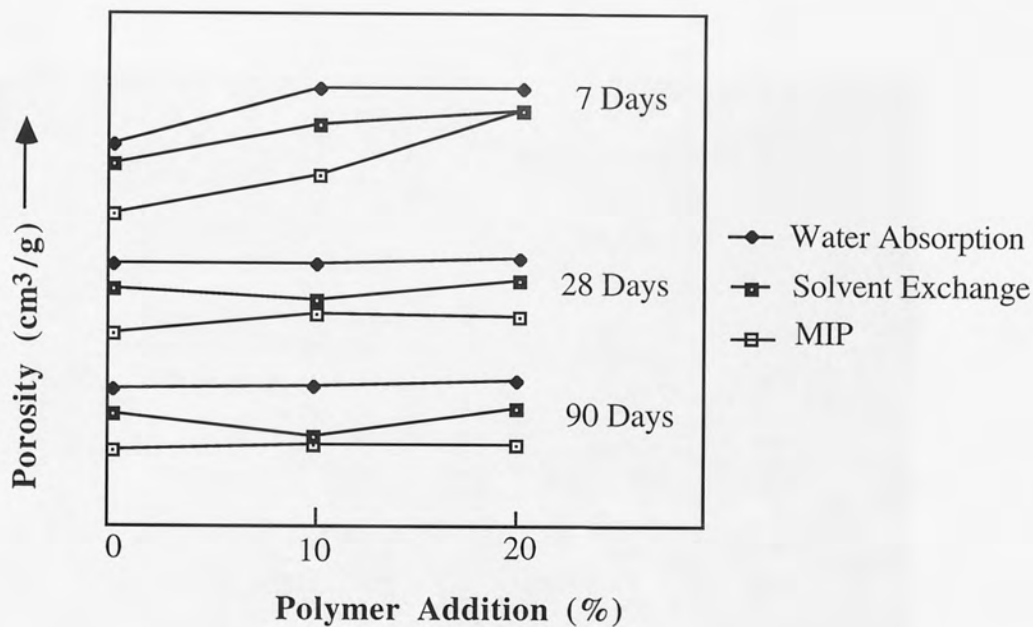


Fig 5.9 A comparison of porosities measured by water absorption, solvent exchange and MIP



Fig.5.10 SEM picture of fracture surface of OPC I paste, 90 days with w/c=0.5

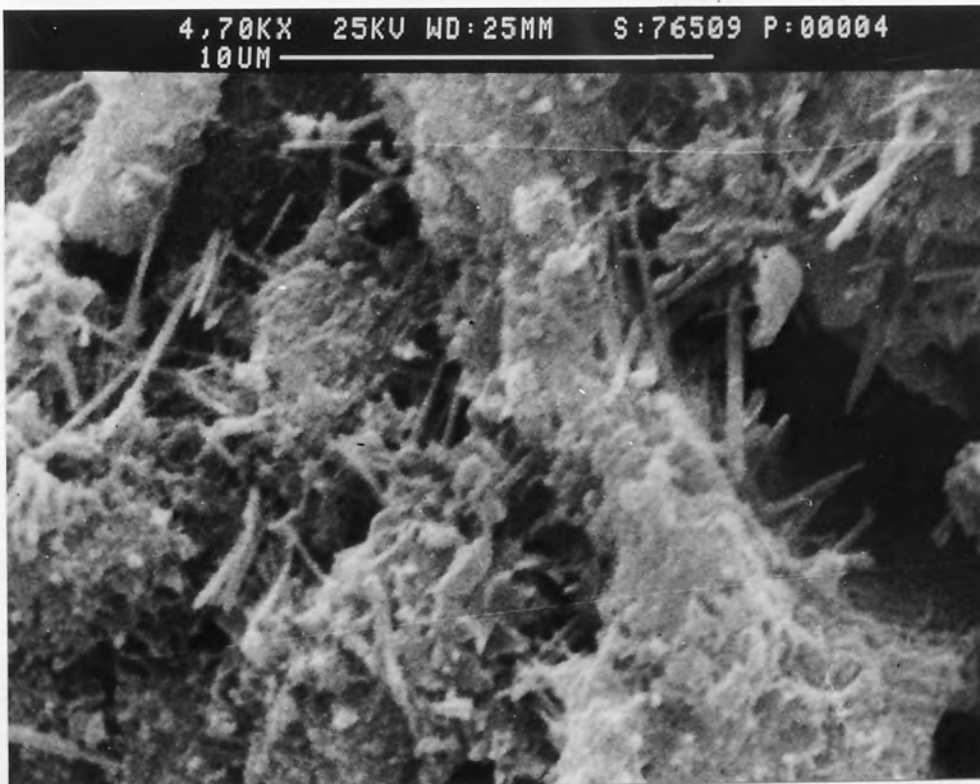


Fig.5.11 SEM picture of fracture surface of SBR 1-OPC I paste, 90 days with w/c=0.5

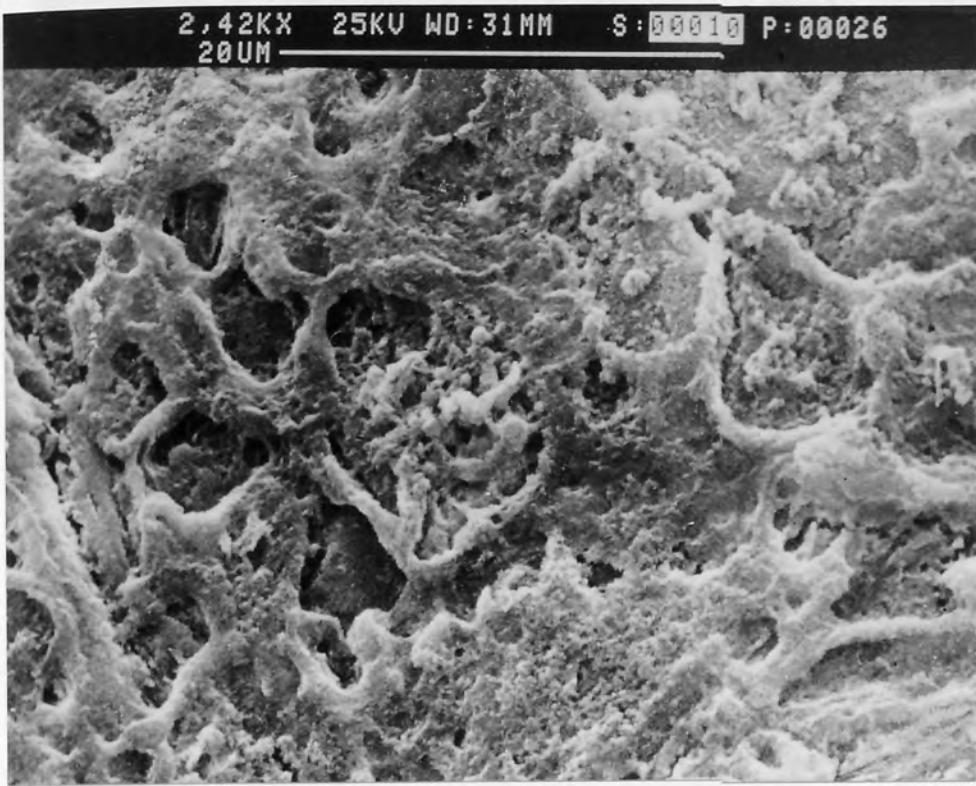


Fig.5.12 SEM picture of fracture surface of Ac 1-OPC I paste, 90 days with w/c=0.5

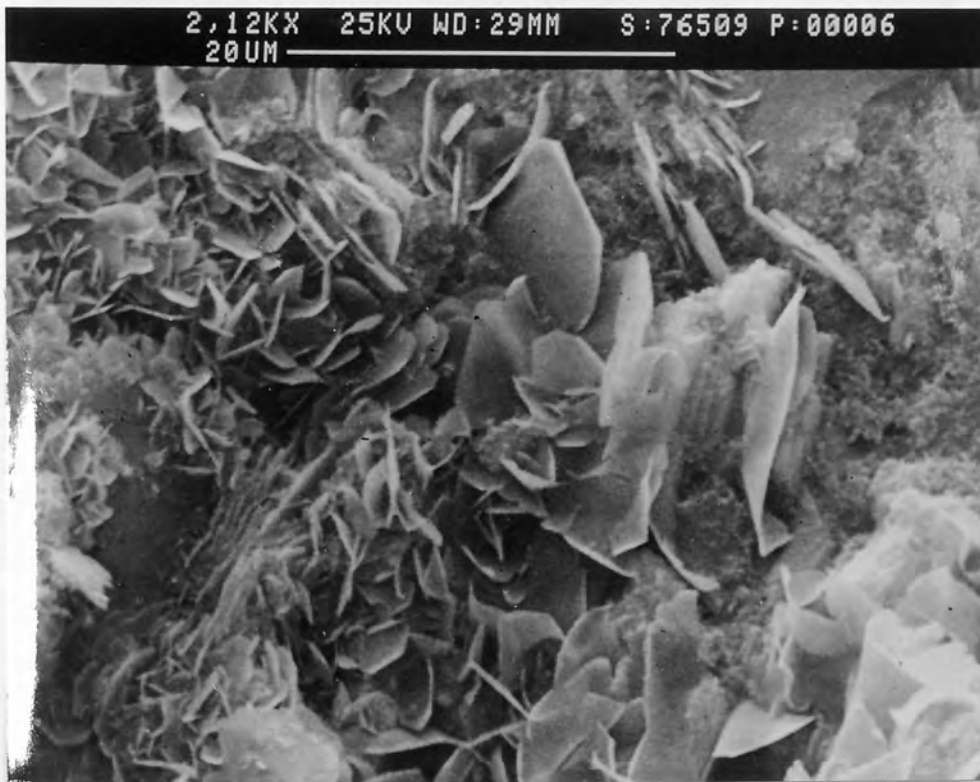


Fig.5.13 SEM picture of fracture surface of SBR 2-OPC I paste, 90 days with w/c=0.5



Fig.5.14 SEM picture of etched fracture surface of OPC I paste, 90 days with w/c=0.5



Fig.5.15 SEM picture of etched fracture surface of SBR 1-OPC I paste, 90 days with w/c=0.5

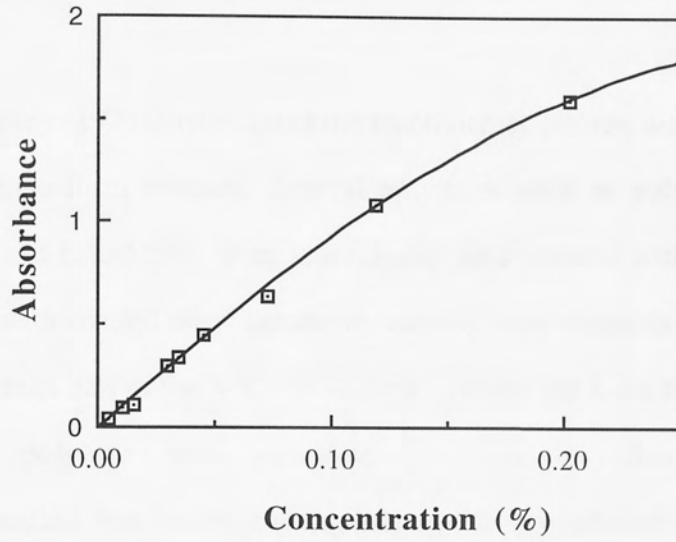
STUDY OF POLYMER-CEMENT
INTERACTIONS

Fig.5.16 Calibration Curve of Polymer Content in Solution

CHAPTER 6

STUDY OF POLYMER-CEMENT INTERACTIONS

6.1 PREVIOUS WORK

Wagner & Grenley (1978) investigated the reactivity of latexes with cement by extracting the polymer phase from mortars. Several polymers such as polyethylene, polystyrene, VdC-VC-EAc and EAc-MMA were individually incorporated with sand and cement and then extracted with methyl ethyl ketone at various time intervals up to 24 hours. They found that less than half of the VdC-VC-EAc was extracted from the mortar, even though this starting polymer was completely soluble in this solvent. Extensive dehydrohalogenation was noted, and significant and progressive changes in the infrared spectra of the polymer relative to the starting material were observed.

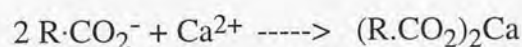
In a similar manner, the EAc-MMA copolymer latex was found to be completely converted from a methyl ethyl ketone-soluble to an insoluble form. Calcium ion was found to be contained in the polymeric residue to the extent of 0.013g calcium per 1g polymer. When the polymeric residue was immersed in 1 mole HCl for a period of 3 hours, calcium ions were displaced and the solubility in methyl ethyl ketone was regained. It was believed that saponification of the vinyl acrylate portion of the polymer might be occurring in the alkaline environment and an "ionomer" type bonding of the carboxylate groups thus was obtained, this effecting cross linking of the polymer.

In a further study, four additional latexes were mixed with Ca(OH)_2 slurry for several days and it was found that a styrene latex and an ethylene-vinyl chloride copolymer latex showed no insolubilization; a SBR latex showed partial insolubilization; a CR latex showed nearly complete insolubilization.

Using a similar method, Shaw (1989) extracted polymer from a polyvinylidene dichloride copolymer-cement paste with tetrahydrofuran. IR spectroscopy for extracted polymer showed an additional absorption band at 1610cm^{-1} and this absorption peak was intensified with increasing polymer/cement ratio. He suggested that interaction between polymer and cement had occurred. The nature of reaction may be associated with liberation of Cl^- ions and consumption of OH^- ions.

Instead of extracting polymer from pastes, Chandra and Flodin (1987) studied the interaction of polymer with calcium hydroxide by adding polymer into saturated solutions of $\text{Ca}(\text{OH})_2$. In each of five glass cylinders, 5g $\text{Ca}(\text{OH})_2$ was mixed with 20ml of water. To them was added 5, 10, 15, 20 and 25ml, respectively, of an acrylic polymer dispersion. It was observed that large aggregates of calcium hydroxide crystals and polymer particles grow and then settle leaving a transparent supernatant liquid. The supernatant liquid was transparent till the polymer addition exceeded 25ml of polymer. When more polymer was added the liquid became milky and there was no further increase of the precipitate.

Analysing the precipitate by X-ray diffraction, it was found that the $\text{Ca}(\text{OH})_2$ peak at $2\theta = 38.4^\circ$ diminished with increasing polymer and finally turned into a broad shoulder. From these phenomena, they suggested that divalent calcium ions interact and make complexes with the carboxylate groups of the polymer:



The $\text{Ca}(\text{OH})_2$ in the precipitates was not in its original crystal form but possibly in the form of amorphous or very small crystals which did not give discrete reflections.

In a parallel experiment, they mixed tricalcium silicate with water and polymer. The mixture was analysed by X-ray diffraction and SEM. When C_3S was hydrated with polymer latex no distinct crystals could be seen as in the case of calcium hydroxide. X-ray

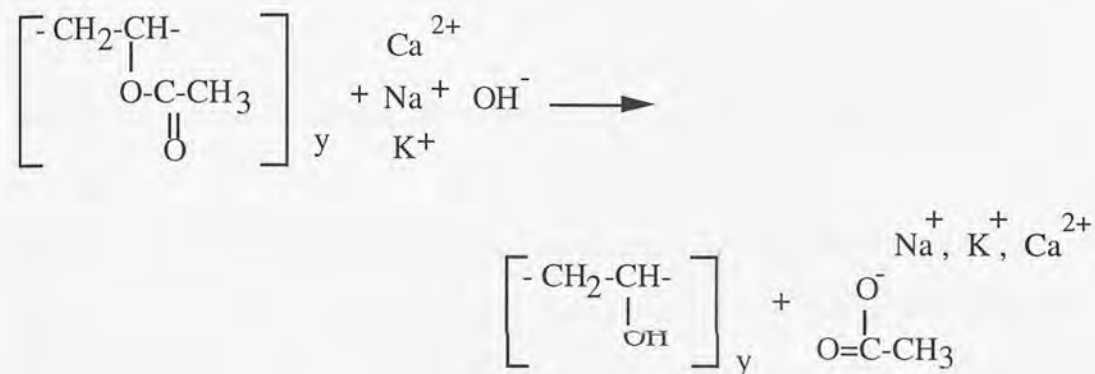
diffraction analysis also showed a decrease in the height of the Ca(OH)_2 reflections and a higher background. This meant that the Ca(OH)_2 formed during hydration had interacted with polymer in the same way as in the case of Ca(OH)_2 .

Thermal analysis (DTA/TGA) techniques have been used by many researchers to seek evidence of possible interactions. Gebauer and Coughlin (1971) found that in a PMMA impregnated cement the endothermic dehydration peaks for calcium hydroxide decomposition were reduced remarkably compared with pure cement paste. It was inferred that an interaction occurred between the MMA/PMMA and hydrated cement.

Auskern (1972) made a careful study of PMMA impregnated cement and a MMA- Ca(OH)_2 mixture. It was reported that during polymerisation of methyl methacrylate in contact with calcium hydroxide, a product with an endothermic decomposition peak at about 430°C was formed and the product was probably the calcium salt of methacrylic acid.

In 1976, Cook et al premixed cement with six polymers including acrylonitrile, styrene, MMA, VA, polyester-styrene and isoprene. Polymerisation of the monomer was achieved by thermal catalysis or irradiation. The thermal analysis showed the type of treatment did not influence the DTA curve and the thermograms of premix polymer-cement pastes were very similar to the control mix. The only difference was the peak temperature and size of the endotherm which corresponds to the dehydration of calcium hydroxide. Polystyrene and polyisoprene had no effect on the size of the Ca(OH)_2 dehydration peak; polyacrylonitrile and PMMA slightly reduced the size of this peak, while VA and polyester greatly reduced the size of the peak. For polystyrene, a mixture of the polystyrene and pure cement paste gave an endothermic peak corresponding to the decomposition of polystyrene, but the peak was not observed in the premixed prepared material. On the basis of those differences, they believed that the polymers reacted with the hydrating cement.

It is possible to obtain some information about chemical reactions which have occurred between polymer and cement by IR spectroscopy analysis. Atkins et al (1991) investigated several polymer-cement systems using this technique. The results showed that all peaks present in the VdC-Ac film were present in the VdC-Ac-cement sample. The SBR and VA did not affect the IR spectrum of the pastes. The spectrum of VA showed a large carbonyl group absorption, but in the VA-cement sample, no carbonyl peak was present and a new peak existed at 1560cm^{-1} which corresponds to a carboxylate group. This indicated that the polymer had been hydrolysed and that the ester linkage had broken to form polyvinyl alcohol and acetate ion $\text{CH}_3\text{C}^-\text{OO}$:



In the spectrum of polyacrylic cement, the carboxylate peak was found to get larger as hydration progressed. Further investigative work on the acrylic- $\text{Ca}(\text{OH})_2$ system revealed that the ester linkage of the acrylic group was broken leaving negatively charged carboxylate groups, which probably complexed with calcium ions.

IR analysis (Shaw 1989) confirmed that MMA reacted with cements to form methacrylates, primarily calcium methacrylates, but PMMA did not react with cements.

By extracting the pore solution from polymer-modified cement pastes, Larbi and Bijen studied the interaction of polymer with the cement hydrates during hydration. The chemical analyses of the pore solution demonstrate that the calcium ion content in pastes modified with S-Ac, VdC and S-Ac+coupling agent are lower than in the pure cement paste. It is believed that the calcium ions reacted with the small amount of carboxylic group of the polymer. For VdC-Ac modified paste, the chloride ion concentration of the

pore solution increased with the polymer dosage and this showed the possibility that VdC-Ac was broken down and chloride released into the pore solution.

From the previous research work, it is evident that there are discrepancies on the possibility and nature of interactions between polymer and cement.

6.2 RESULTS AND DISCUSSION

6.2.1 Differential Thermal Analysis (DTA) and Thermal Gravimetric Analysis (TGA)

6.2.1.1 Characterisation of Unmodified Cement Pastes

Figs. 6.1 shows a typical thermogram for a cement paste. The experiment was run in a flow of argon. Five endothermic peaks are exhibited at 140, 200, 290, 500 and 750°C. From previous work (see Fig.6.2), it is possible to show that the peak at 140°C corresponds to dehydration of calcium silicate hydrate; the strong peak at 200°C and the small shoulder at 290°C are due to dehydration of monosulphate calcium sulpho aluminate ($3\text{CaO} \cdot \text{Al}_2\text{O}_3 \cdot \text{CaSO}_4 \cdot 12\text{H}_2\text{O}$); the large endotherm at 500°C represents the dehydration of calcium hydroxide and the very weak peak at 750°C is due to decomposition of calcium carbonate (Ramachandran 1969).

The TGA curves show several steps of weight loss during heating. In the first stage, i.e. before 500°C, the TGA curve gradually declined indicating that water in the C-S-H gel was being gradually lost. In the second stage (between 450 and 520°C), the TGA curve drops quickly corresponding to rapid dehydration of $\text{Ca}(\text{OH})_2$.

6.2.1.2 Characterisation of Polymers

Differential thermal analysis is a sensitive method for the observations of all changes which occur when a polymer sample is heated and which are accompanied by absorption or evolution of heat. Fig.6.3 is a schematic representation of a thermogram for a polymer (Korshak 1971). Such curves yield very accurate values of melting and vitrification points, and also of the temperature corresponding to the crystallisation, oxidation and decomposition of polymer.

In this study, calcined alumina (same as the reference material used for DTA/TGA) and latex was first mixed and then dried. Here, it is supposed that the calcined alumina is an inert component and there is no chemical reaction between the calcined alumina and polymer when the mixture is subjected to the thermal analysis.

The DTA and TGA curves of SBR 1 and Ac 1 prepared by this treatment are presented in Fig.6.4. In a flow of argon (Fig.6.4a), the DTA curve of SBR 1 begins with a large endotherm at around 100°C. TGA shows no significant weight loss through this temperature zone suggesting a melting transition. At a higher temperature (440°C) another endothermic peak is displayed and is accompanied by a large weight loss (11%), suggesting the decomposition of SBR 1.

The DTA thermogram of SBR 1 in air (Fig.6.4b) is much more complicated because of oxidation of polymer. Besides one endotherm in the vicinity of 100°C, there are four exothermic peaks at 226°, 365°, 409° and 561°C. These peaks probably correlate with the oxidation of different parts in of the SBR chain.

Compared with SBR 1, the thermogram of Ac 1 in air (Fig.6.4c) is quite different. The DTA curve displays a broad and large endotherm in the temperature region up to 230°C, which is similar to SBR. However, immediately above 230°C, one exotherm appears at

306°C and is followed by another sharp exothermic peak at 447°C. In this region, the TGA curve drops sharply about 16% of weight loss.

6.2.1.3 Characteristics of Polymer Modified Cement Paste and Physical Mixes

Figs 6.5-6.8 show the thermograms of polymer modified cement pastes and physical mixtures of polymer and hydrated cement. Physical mixtures of Portland cement and polymer were made by the following method. The hydrated cement (90 day old) was ground into powder and sieved through a 300µm sieve. The hydrated cement powder was then mixed with the calcined alumina which had coated polymer on the surfaces in a proportion equivalent to 20% polymer addition.

In a flow of argon, the DTA curves of SBR 1-OPC I (Fig. 6.5a) do not show any significant difference compared with pure cement. The only difference is that SBR 1-OPC I has a small plateau in the temperature range of 340 to 460°C. This effect may have arisen from the overlap of endothermic peak of SBR in this temperature range (Fig.6.4a). The physical mixture also has a similar DTA curve as others. On the other hand, the TGA curve of SBR 1-OPC indicated higher weight loss, especially in the temperature range of 300° to 500°C (Fig. 6.5b), which corresponds to the decomposition of SBR.

In an air environment, the thermograms of polymer modified cement are dominated by the oxidation of polymer. The endothermic peak of $\text{Ca}(\text{OH})_2$ around 500°C is masked by heat evolution during oxidation of the polymer (Fig. 6.6).

SBR 1-OPC I (Fig. 6.6a) exhibits three exothermic peaks at 264°, 362° and 504°C, respectively compared to Fig.6.4b. SBR 2-OPC I (Fig. 6.6b) which exhibits two peaks. This may be correspondent to a change in polymer property caused by the increased carboxylate concentration.

The DTA curves of Ac 1-OPC I show a sharp endothermic peak (Fig. 6.7a). Because the acrylic completed its decomposition at a low temperature (about 400°C), the exothermic peak does not completely mask the Ca(OH)₂ peak so that the polymer oxidation peak is split into two. The alkali content of the cement does not seem to influence the DTA curves (Fig. 6.7b).

6.2.1.4 Discussion on the Results of Thermal Analysis

Polymer Addition and Curing Age

As seen from Fig.6.5 an increment of polymer from 10% to 20% does not significantly change the pattern of the DTA curves but a slight decrease in the intensity of Ca(OH)₂ is noted. This effect could have arisen from the dilution effect of polymer, or overlap of polymer oxidation peak and Ca(OH)₂ dehydration or possible reaction between Ca(OH)₂ and polymer. Weight loss is increased with increasing polymer which is obviously reflected in the TGA curve.

Fig.6.8 shows the thermograms of 10%SBR-cement pastes with different curing ages. For 7 day old pastes, the unmodified cement paste has a general pattern of DTA curve (Fig.6.5). For 7 day old 10%SBR-cement paste (see dotted line), the endothermic peak of monosulphate at 200°C is absent, only a sharp peak at about 100°C is observed. However, after 28 days, this peak appears again. Furthermore, the intensity of Ca(OH)₂ decomposition peak is much smaller than the unmodified cement. For example, the areas under the Ca(OH)₂ decomposition peak are 106 μV sec/mg for 7 day pure paste and 52 μV sec/mg for 7 day 10%SBR paste, respectively. These differences may be due to the retardation of cement hydration by polymer in the early stages as discussed in Chapter 4. The absence of a monosulphate peak probably suggests that the hydration of C₃A is confined to a greater extent so that the formation of ettringite and the conversion to monosulphate is slow. With longer curing ages, the cement hydration continues and more hydrates are produced so that the DTA curves revert to their original pattern.

Qualitative Identification and Quantitative Analysis of PMC

It is evident that the different types of polymers have their own characteristic DTA curves in air and these characteristics are still present in the DTA curves of the polymer modified cement pastes. For instance, SBR has four exothermic peaks in DTA curves and these peaks can be traced in the SBR-cement pastes. Similarly, the acrylic is characterised by a small endothermic peak at about 305°C and a large exothermic peak around 447°C. In the acrylic-cement pastes, these two peaks are seen although the large exothermic peak is split into a large sharp peak and small peak by overlap of the endothermic peak of $\text{Ca}(\text{OH})_2$.

Therefore, this technique does offer the possibility for identifying the type of polymer used in samples where this is in doubt, e.g. in assessing the failure of a patch material of unknown origin. Quantitative analysis could be obtained by estimating the area under each peak or by thermal gravimetric analysis (TGA). The TGA curve (e.g. Fig. 6.5b) showed that weight losses of modified cements compared to unmodified cements are roughly proportional to polymer content. For instance, pure cement has 14% weight loss when heating in a flow of argon. However, 10%SBR-cement has 19% weight loss and the weight loss of 20%SBR-cement is 22% (Fig. 6.5b). Further work in this aspect should be carried out to get an accuracy of assessment.

6.2.2 Pore Solution Extraction and Analysis of PMC

The hydration of Portland cement may be looked on as a process involving a sequence of chemical reactions between the suspended solid cement components and water. On setting, the continuous fluid is converted to a discontinuous pore solution because of the formation of hydration products, e.g. C-S-H gel. Further hydration takes place by continued reaction of the cement components with this pore solution. Therefore, studies of the pore solution composition can reveal the interactions which may happen among the system components during the hydration processes.

In this study, four polymer-cement systems: SBR 1-OPC I; SBR 1-OPC II; Ac 1-OPC I and Ac 1-OPC II were investigated. The pore solution expression device used in this work has been described in section 3.3.3.

6.2.2.1 SBR 1-OPC I and SBR 1-OPC II Systems

The concentration of Na^+ , K^+ and OH^- in pore solutions extracted from SBR 1-OPC I and SBR 1-OPC II system are summarised in Table 6.1 and plotted in Figs 6.9-6.10.

It is evident from these two figures that the $[\text{Na}^+]$ is about 0.1 mol/l and is constant for the times investigated. There is some evidence to suggest that the concentration increases slightly with increase in polymer addition. The $[\text{K}^+]$ is higher and seems to increase to a maximum at 14 days, thereafter decreasing slightly. It is evident that the concentration of K^+ decreases with increase in SBR.

The slight increase in $[\text{Na}^+]$ with increasing polymer content is probably a result of the polymers containing Na^+ , since NaOH is added to the emulsion to adjust the pH and sodium lauryl sulphate, or sodium dodecyl mercaptan and sodium persulphate are added in as surfactant (0.1%) or initiator. The concentration of Na^+ in the SBR 1 latex tested using a flame photometer is 1471ppm, i.e. 0.06 mol/l latex. No K^+ was detected in SBR 1 by this method.

The combined $[\text{Na}^++\text{K}^+]$ changes with time and polymer addition are reflected by those found individually. The values are higher than those for $[\text{OH}^-]$ suggesting the presence of other anions not analysed e.g. sulphate. Addition of polymers reduces the $[\text{OH}^-]$, particularly at times shorter than 14 days. This implies that SBR retards the cement hydration, especially in the early period of hydration.

Figs. 6.10 shows pore solution analysis for SBR 1-OPC II pastes. Since OPC II contains a higher alkali content than OPC I, its pore solution contains higher $[\text{Na}^+]$ and $[\text{K}^+]$. For

example, the concentration of $[\text{Na}^++\text{K}^+]$ in the pore solution of pure OPC II paste cured 28 days is 0.62 mol/l, but 0.59 mol/l for pure OPC I paste. When polymers are added into this cement, the $[\text{Na}^+]$ in pore solution was slightly increased with SBR 1 addition because SBR 1 brought Na^+ into the system. The $[\text{K}^+]$ and $[\text{OH}^-]$ were slightly decreased with the SBR 1 addition and with time. Compared to SBR 1-OPC I, SBR 1-OPC II contains a higher concentration of OH^- in the early stage. This suggests that SBR 1-OPC II has a higher hydration rate which is in agreement with the results obtained using conduction calorimetry in section 4.4.13.

6.2.2.2 Ac 1-OPC I and Ac 1-OPC II Systems

Pore solutions extracted from Ac 1-OPC I and Ac 1-OPC II were also analysed. The results are given in Table 6.2 and plotted in Fig. 6.11-6.12. Similarly, the $[\text{Na}^+]$ in the pore solution reached about 0.1 mol/l after 14 days and kept constant after that time. The increase of the $[\text{Na}^+]$ with polymer increase also arose from acrylic latex which contains about 0.078 mol/l latex. The $[\text{K}^+]$ reduced with polymer increase and the time. At early ages, the $[\text{OH}^-]$ in Ac 1-OPC I showed a large reduction, but not so in Ac 1-OPC II.

6.2.3 Infrared Spectroscopy Analysis

Some polymers used in the experiments were analysed using infrared spectroscopy. Some polymers were analysed in their original powder forms; some polymers have been extracted from the cement pastes by selective dissolution described in 3.3.3; while some polymers have been immersed in a synthetic pore solution for 120 days and were then filtered and washed with deionized water. The important functional groups for these polymers have been assigned.

6.2.3.1 SBR 1-OPC I System

Infrared absorption spectra of the SBR 1-OPC I system are shown in Fig. 6.13. Curve 1 is the infrared spectrum of hydrated cement. It showed characteristic absorptions at 3620, 3420, 1650, 1485, 1430, 1120 and 970 cm^{-1} . The sharp band at 3620 cm^{-1} and the broad bands at 3420 and 1650 cm^{-1} are likely to be due to stretching and bending modes of water molecules. The twin bands at 1485 and 1430 cm^{-1} may be associated with the presence of carbonate (Harchard 1980). The bands at 1120 and 970 cm^{-1} may be correspondent to silicates and aluminates.

Curve 2 shows an infrared spectrum of pure SBR 1. The intense bands between 3200 and 3000 cm^{-1} are due to the C-H stretching of aromatic or olefinic protons. The absorption bands between 3000 and 2800 cm^{-1} are due to the C-H stretching of CH_3 , CH_2 , or CH. The low intensity bands in the region from 2000-1668 cm^{-1} are due to overtones and combination frequencies of aromatic hydrogen vibrations. The bands at 1500, 1450 and 700 cm^{-1} correspond to the aromatic ring, including the vibration of C=C and the out-of-plane bending of five adjacent hydrogens on the aromatic ring.

Curve 3 is the infrared spectrum of SBR 1-OPC I paste. The introduction of the SBR 1 polymer into a cement paste seems does not really affect the infrared spectrum of the paste. It can be seen that the spectrum has same pattern as the curve (1). This means that the cement phase in the sample dominates absorption. Some new bands appeared at 3200-3000 cm^{-1} and 760 cm^{-1} . The original twin bands at 1485 and 1430 cm^{-1} became sharper. Those differences should be associated with the absorption of SBR 1. It seems that the spectrum of hydrated cement simply overlapped the spectrum of SBR 1.

6.2.3.2 Acrylic-OPC I Systems

Fig.6.14 and Fig.6.15 show the infrared spectra of Ac 1-OPC I and Ac 3-OPC I systems, respectively. Generally, Ac 1 and Ac 3 have similar spectrums. The band at 3600-

3400cm^{-1} is due to O-H stretching and the band at 3000cm^{-1} is due to C-H stretching. The intense band at 1740cm^{-1} is associated with C=O stretching of O=C-O and the band at 1470cm^{-1} is methylene and methyl bending.

In looking through the spectra of Ac 1 immersed in synthetic pore solution (curve 2) or extracted from the paste (curve 3), it can be noted that there is a new absorption band at 1560cm^{-1} compared with curve 1. This band is due to carboxyl salt. It suggested that the carboxyl acid group in polymer may react with metallic ions e.g. Ca^{2+} ions. However, this band was not pronounced in the spectra of Ac 3 immersed in synthetic pore solution and extracted from the paste. The spectrum of VaVeAc (Fig. 6.16) also showed some evidence for this band.

6.2.3.3 Ethylene Vinyl Acetate-OPC I Systems

Fig. 6.17 and Fig. 6.18 showed the infrared spectra of EVA 1-OPC I and EVA 3-OPC I systems. Like the acrylics, EVA 1 and EVA 3 show absorptions at $3600\text{-}3400\text{cm}^{-1}$, 3000cm^{-1} , 1740cm^{-1} and 1470cm^{-1} . The band at 1370cm^{-1} is intensified CH_3 bending of O=C- CH_3 . Comparing pure EVA 1 with EVA 1 immersed in pore synthetic pore solution, it was found that there is a small new band at 1560cm^{-1} . Similar absorptions were observed in the spectrum of EVA 3 extracted from the paste. Again, these absorptions suggest the formation of a carboxyl salt.

6.2.4 X-Ray Diffraction Analysis

X-ray diffraction patterns of hydrated cement pastes with SBR 1 and without SBR 1 are shown in Figs.6.19-6.20. In unmodified cement paste, main hydration products are well identified. They are $\text{Ca}(\text{OH})_2$, ettringite and monosulphate. Unhydrated $\beta\text{-C}_2\text{S}$ is also revealed.

The X-ray diffraction pattern of SBR 1-OPC I paste is the same as that for the unmodified cement paste. No new peak is formed and the presence of SBR 1 is not revealed since it is amorphous.

6.2.5 Discussion on the Possibility of Chemical Reaction

The experimental results obtained by several analytical methods in this Chapter did not give conclusive evidence for chemical reactions occurring between polymer and cement. Thermal analysis (DTA/TGA) did not show any change which could be attributed to reaction. Some early researches have put forward reservations regarding this technique. Ramachandran and Sereda (1973 and 1977) believed that the thermal analysis technique probably failed to identify the reaction because the amount of reacted products is too small and a masking effect may exist. In their studies, the DTA investigation was carried out in N_2 and air. The thermograms of cement pastes modified with MMA and PMMA exhibited some new effects including a decrease in the intensity of the $Ca(OH)_2$ peak and new peaks. However, they believed that these new effects did not imply an interaction between PMMA and the hydrated cement phase during impregnation. The decreased intensity of the $Ca(OH)_2$ may be a result of cement dilution by the polymer leading to smaller amounts of $Ca(OH)_2$, or the masking effect of an exothermic effect occurring at about the temperature of decomposition of the $Ca(OH)_2$. New peaks may be caused by complex reaction which occurred between the hydrated cement and the decomposition products of PMMA during heating in the DTA furnace. The DTA results obtained by Gorur (1987) and Shaw (1989) also have not shown any evidence for chemical reaction between the polymers (polyester-styrene, MMA/PMMA) and cement. Shaw held the same opinion as Ramachandran and thought that the usefulness of DTA is limited due to the masking effects.

In the present study, a similar conclusion may be drawn. First, in the flow of argon, DTA curves showed the same peaks for all samples with or without polymer. A lower intensity of dehydration peak of $Ca(OH)_2$ was noted, but it is still arguable and not certain because

the lower intensity of Ca(OH)_2 peak may be caused by dilution of polymer or by chemical reaction. A physical mixture of SBR 1 and hydrated cement paste gave similar DTA traces to the corresponding SBR 1 modified cement. This confirms that there is no significant chemical reaction between polymer and hydrating cement phase. However, this observation does not preclude the possibility of surface interactions. As discussed in Chapter 4, the polymers retarded the cement hydration and may trap Ca^{2+} ions resulting in a decrease of Ca(OH)_2 .

Furthermore, in the air environment, exothermic peaks of polymer almost masked the endotherms from the decomposition of C-S-H gel and calcium hydroxide. For example, in Fig.6.10, the decomposition peaks of SBR at 504°C completely overlapped the dehydration peak of Ca(OH)_2 . In Fig.6.11, the decomposition of acrylic at 430°C was split into two peaks due to the overlap of Ca(OH)_2 . At the same time, the intensity of Ca(OH)_2 was greatly reduced due to this effect. Therefore, in this case it is impossible to characterise the degree of hydration or quantity of calcium hydroxide and identify new phase formation in these modified cement pastes.

The analysis of pore solutions extracted from polymer modified pastes showed a reduction in concentration of ions compared to unmodified paste in the early stages, which may be the result of hydration retardation. The reasons for the concentration reduction of K^+ with time have not been fully elucidated, but it may be saponification of polymers in the high alkali environment.

Infrared spectroscopy analysis of various polymer-cement systems indicated that chemical reaction between polymer and cement may occur depending on different type of polymers. No evidence shows that chemical reactions happen between SBR 1 and cement. The spectra of extracted or immersed Ac 1, EVA 1 and EVA 3 exhibited a new absorption band at 1560cm^{-1} , which is for carboxylic acid and carboxyl salt. This suggested possible reaction occurred between carboxylate group in polymer chains with calcium ions. However, infrared spectra of other polymers including Ac 3 and VaVeAc

did not give evidences for this reaction. It is possible that the amount of reaction products are so small that it is not detectable.

Samples with or without SBR polymer have the same X-ray diffraction patterns. No new peak was detected and no original peak had disappeared. Since X-ray diffraction only detects the substances with a crystalline structure, no change in the pattern does not preclude the possibility of the formation of amorphous reaction products.

6.3 CONCLUSIONS

1) DTA and TGA could provide useful information to help to identify the type of polymers used in a PMC when the source of materials is unknown. However, these techniques are not suitable for studying any chemical reactions between polymer and cement.

2) The pore solution chemistry indicated that the concentrations of OH^- , Na^+ , K^+ in the pore solution of PMC are reduced in the early stage, which suggested that latex particles occupy cement dissolution sites and retard hydration. There was no evidence to show chemical reactions occurring between polymer and cement.

3) Infrared spectroscopy suggested that chemical reaction between polymer and cement may occur but depended on the type of polymer. Ac 1, or EVA 1, or EVA 3 may react with constituents of the cement to form a calcium salt of carboxylic acid. However, there was no evidence of this in the case of other polymers.

TABLE 6.1

Chemical Analysis of Pore Solution for SBR 1-OPC I and OPC II at w/c=0.5

Curing Age (Day)	Polymer Addition (%)	SBR 1-OPC I System			SBR 1-OPC II System		
		OH ⁻ (mole/l)	Na ⁺ (mole/l)	K ⁺ (mole/l)	OH ⁻ (mole/l)	Na ⁺ (mole/l)	K ⁺ (mole/l)
7	0	0.511	0.065	0.438	0.608	0.123	0.451
	5	0.495	0.110	0.425			
	10	0.304	0.113	0.378	0.563	0.141	0.435
	15	0.273	0.136	0.341			
	20				0.528	0.155	0.401
14	0	0.514	0.072	0.460	0.631	0.117	0.484
	5	0.500	0.085	0.448			
	10	0.461	0.097	0.421	0.579	0.132	0.390
	15	0.460	0.117	0.384			
	20				0.570	0.157	0.401
28	0	0.520	0.113	0.474	0.614	0.115	0.506
	5	0.486	0.136	0.435			
	10	0.456	0.132	0.420	0.578	0.132	0.429
	15	0.437	0.127	0.433			
	20				0.585	0.160	0.401
60	0	0.533	0.096	0.462			
	5	0.534	0.135	0.421			
	10	0.484	0.107	0.384			
	15	0.505	0.130	0.366			
90	0				0.635	0.125	0.489
	10				0.485	0.121	0.329
	20				0.452	0.128	0.339
120	0	0.535	0.068	0.448			
	5	0.527	0.087	0.430			
	10	0.483	0.097	0.414			
	15	0.441	-	-			

* the contents of Na⁺ and K⁺ in the SBR 1 latex was 0.060 mol/l latex and 0.000 respectively determined by flame photometer.

TABLE 6.2

Chemical Analysis of Pore Solution for Ac 1-OPC I and OPC II at w/c=0.5

Curing Age (Day)	Polymer Addition (%)	Ac 1-OPC I System			Ac 1-OPC II System		
		OH ⁻ (mole/l)	Na ⁺ (mole/l)	K ⁺ (mole/l)	OH ⁻ (mole/l)	Na ⁺ (mole/l)	K ⁺ (mole/l)
7	0	0.511	0.065	0.438	0.608	0.123	0.451
	10	0.312	0.066	0.273	0.594	0.162	0.429
	20	0.263	0.086	0.268	0.558	0.176	0.395
14	0	0.514	0.072	0.460	0.631	0.117	0.484
	10	0.493	0.102	0.422	0.579	0.149	0.423
	20	0.460	0.128	0.372	0.600	0.179	0.401
28	0	0.520	0.113	0.474	0.614	0.115	0.506
	10	0.501	0.102	0.422	0.611	0.151	0.479
	20	0.497	0.135	0.397	0.589	0.179	0.423
90	0				0.635	0.125	0.489
	10	0.545	0.104	0.424	0.567	0.144	0.453
	20	0.544	0.139	0.377	0.517	0.153	0.363

* the contents of Na⁺ and K⁺ in the Ac 1 latex was 0.078mol/l latex and 0.000 respectively determined by flame photometer.

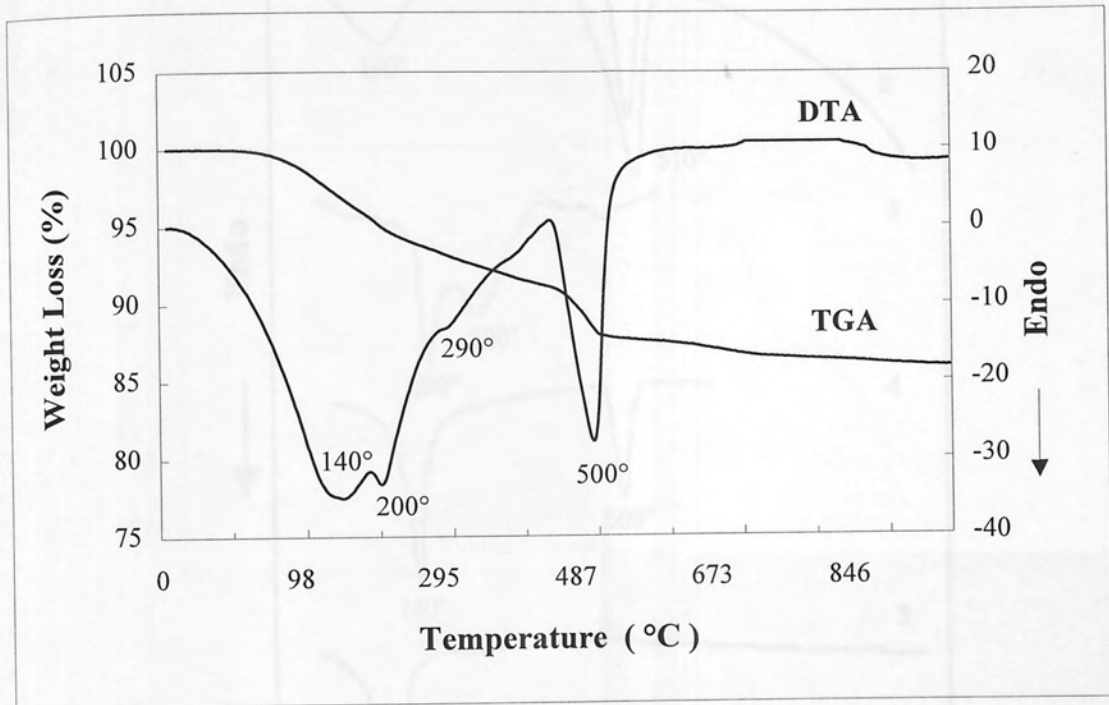


Fig . 6.1 A typical thermogram of cement paste

- Fig 6.2 DTA curves of cement-based compounds
1. Calcium hydroxide $\text{Ca}(\text{OH})_2$
 2. neat C_3S paste, hydrated 100 days (Ghosh 1983)
 3. C_3A + 5% gypsum, hydrated 60 min. (Ghosh 1983)
 4. C_4AF + lime + gypsum, hydrated 60 days (Ghosh 1983)
 5. Firingite (Taylor 1990)
 6. Monosulphate (Taylor 1990)

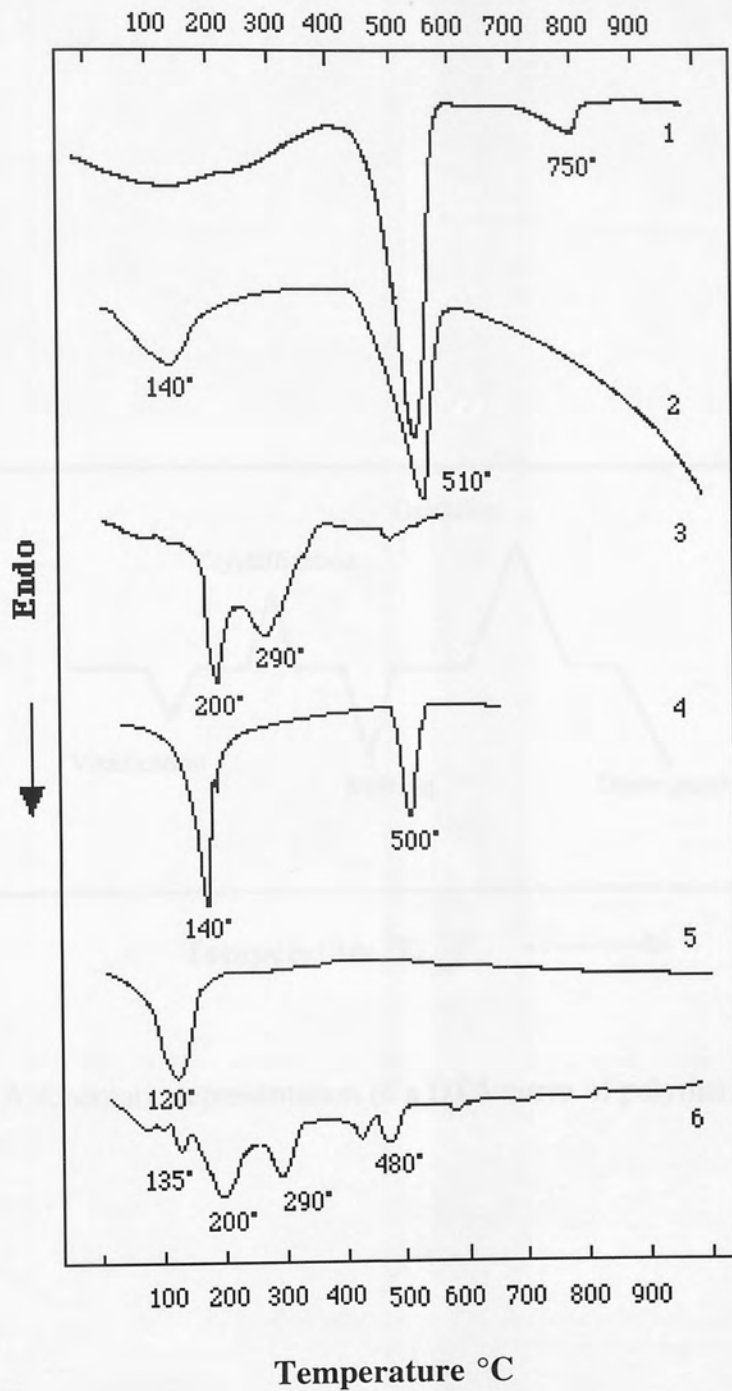


Fig.6.2 DTA curves of cement-based compounds

1. Calcium hydroxide $\text{Ca}(\text{OH})_2$
2. neat C_3S paste, hydrated 100 days (Ghosh 1983)
3. C_3A + 5% gypsum, hydrated 60 min. (Ghosh 1983)
4. C_4AF + lime + gypsum, Hydrated 60 days (Ghosh 1983)
5. Ettringite (Taylor 1990)
6. Monosulphate (Taylor 1990)

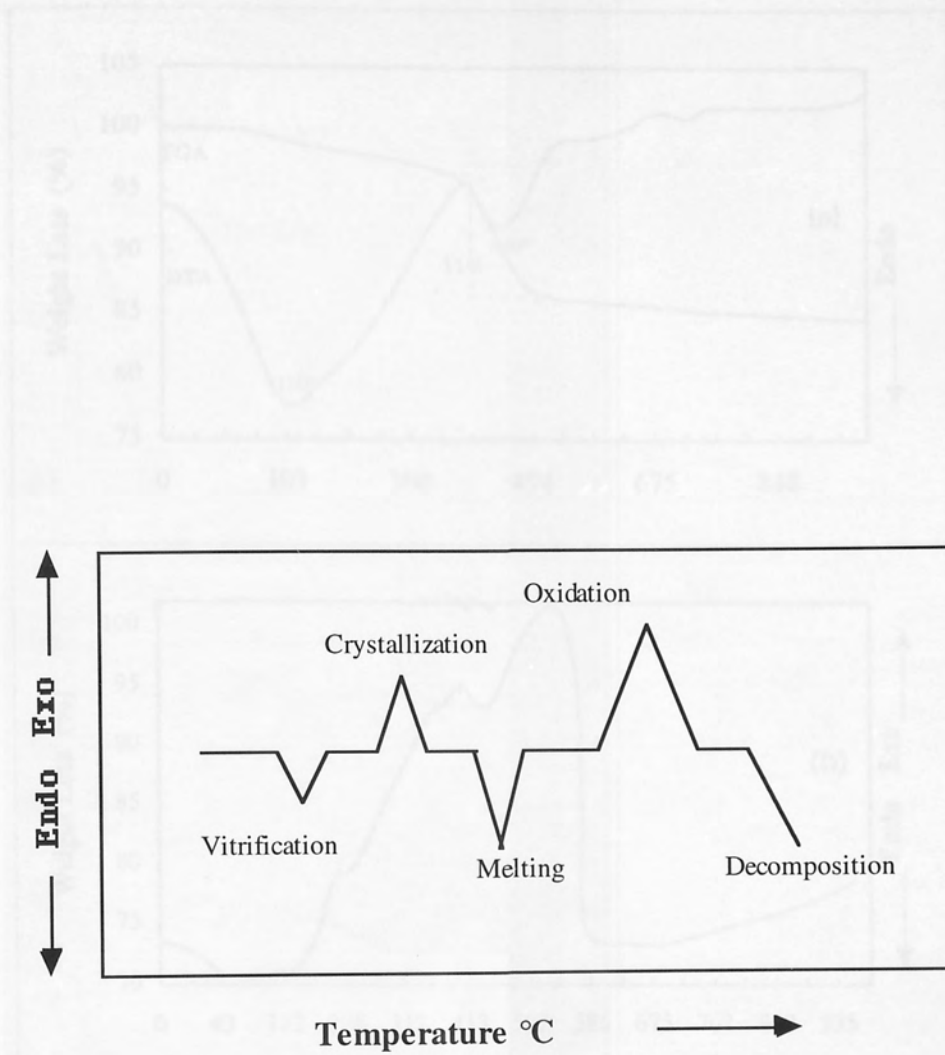


Fig. 6.3 A schematic representation of a DTA curve of polymer

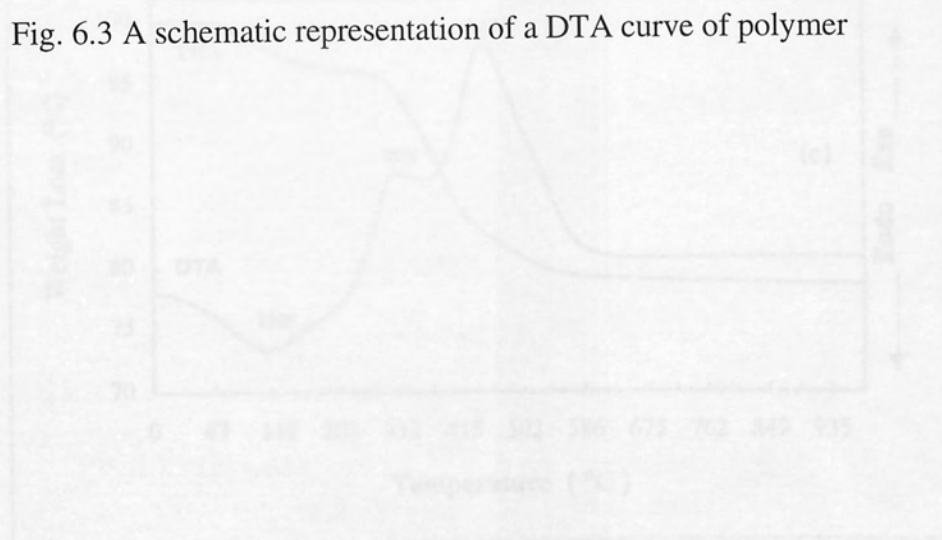


Fig. 5.4 Thermograms of polymers
 (a) SBR 1 in argon; (b) SBR 1 in air; (c) Ac 1 in air

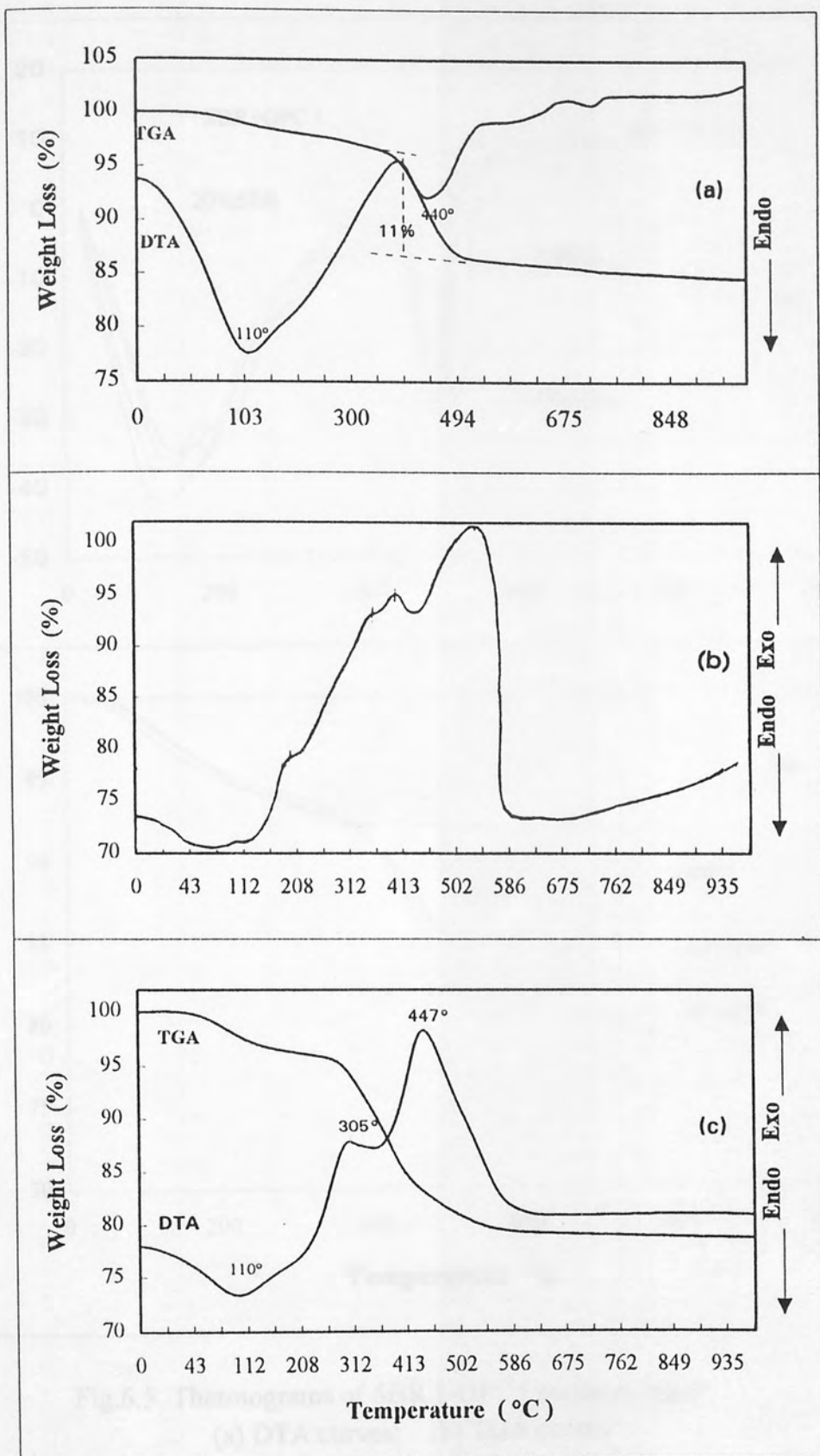


Fig.6.4 Thermograms of polymers
 (a) SBR 1 in argon; (b) SBR 1 in air; (c) Ac 1 in air

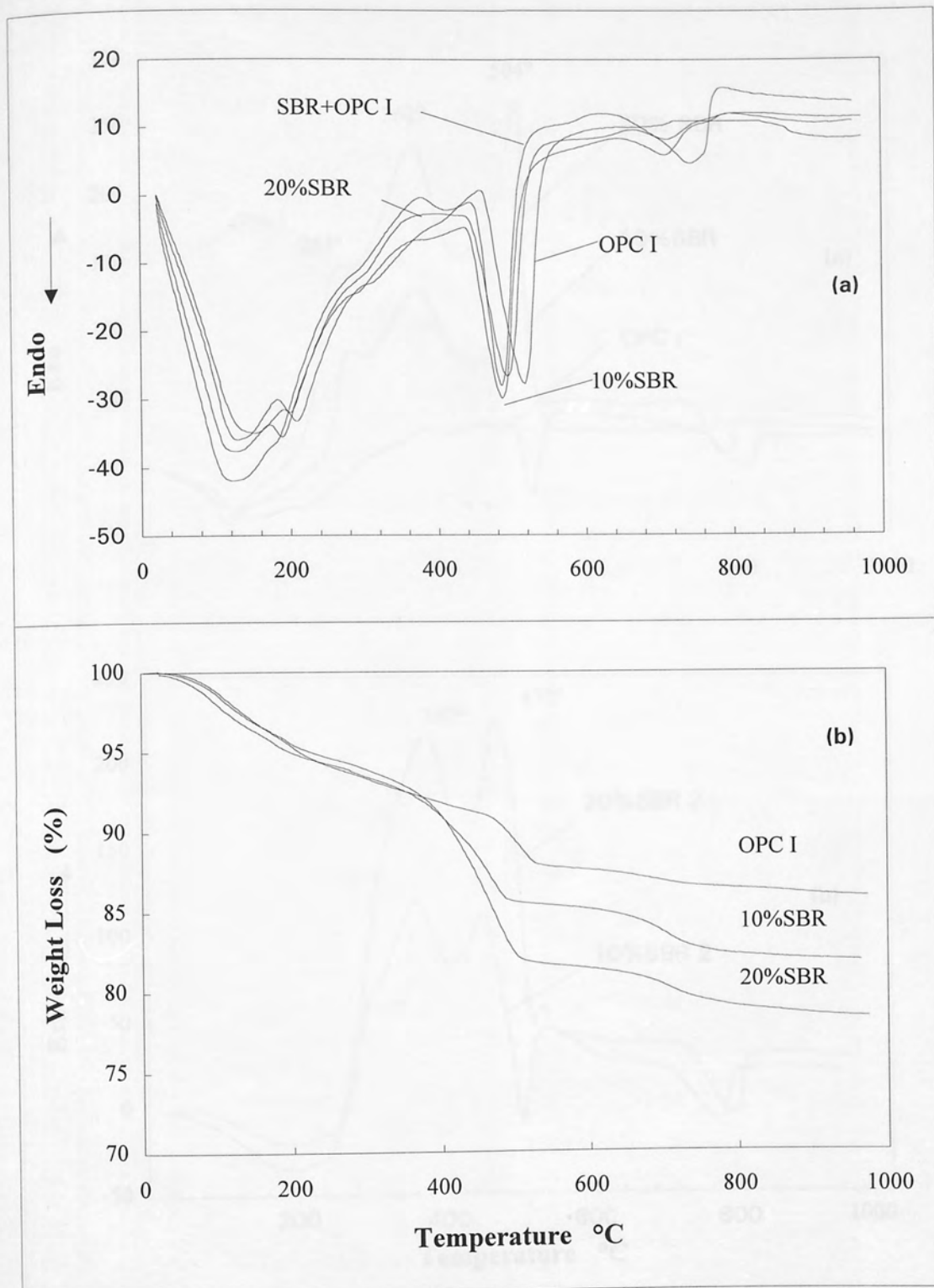


Fig.6.5 Thermograms of SBR 1-OPC I pastes in argon
 (a) DTA curves; (b) TGA curves

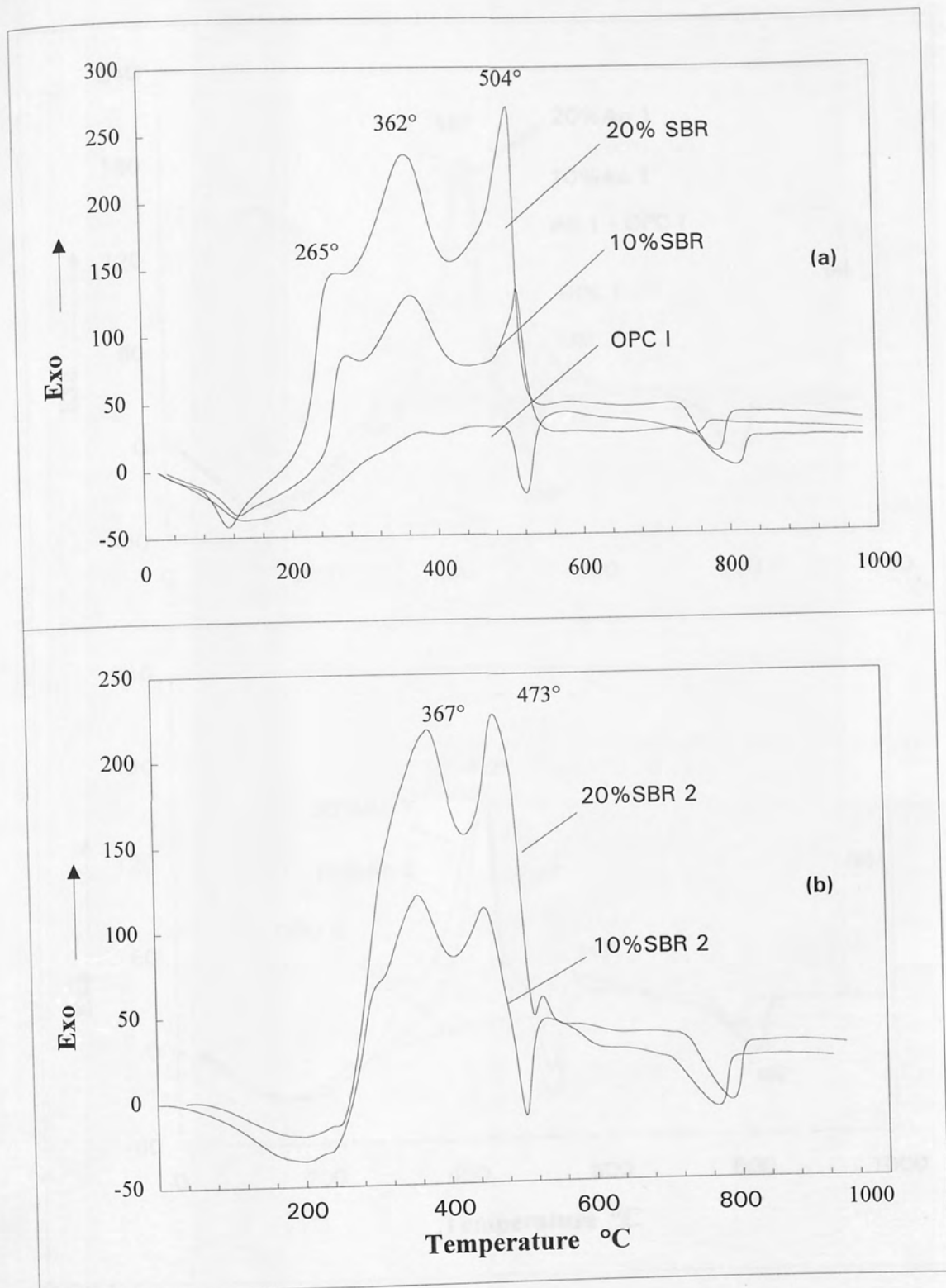


Fig. 6.6 Thermograms of SBR-OPC I pastes in air
 (a) SBR 1-OPC I; (b) SBR 2-OPC I

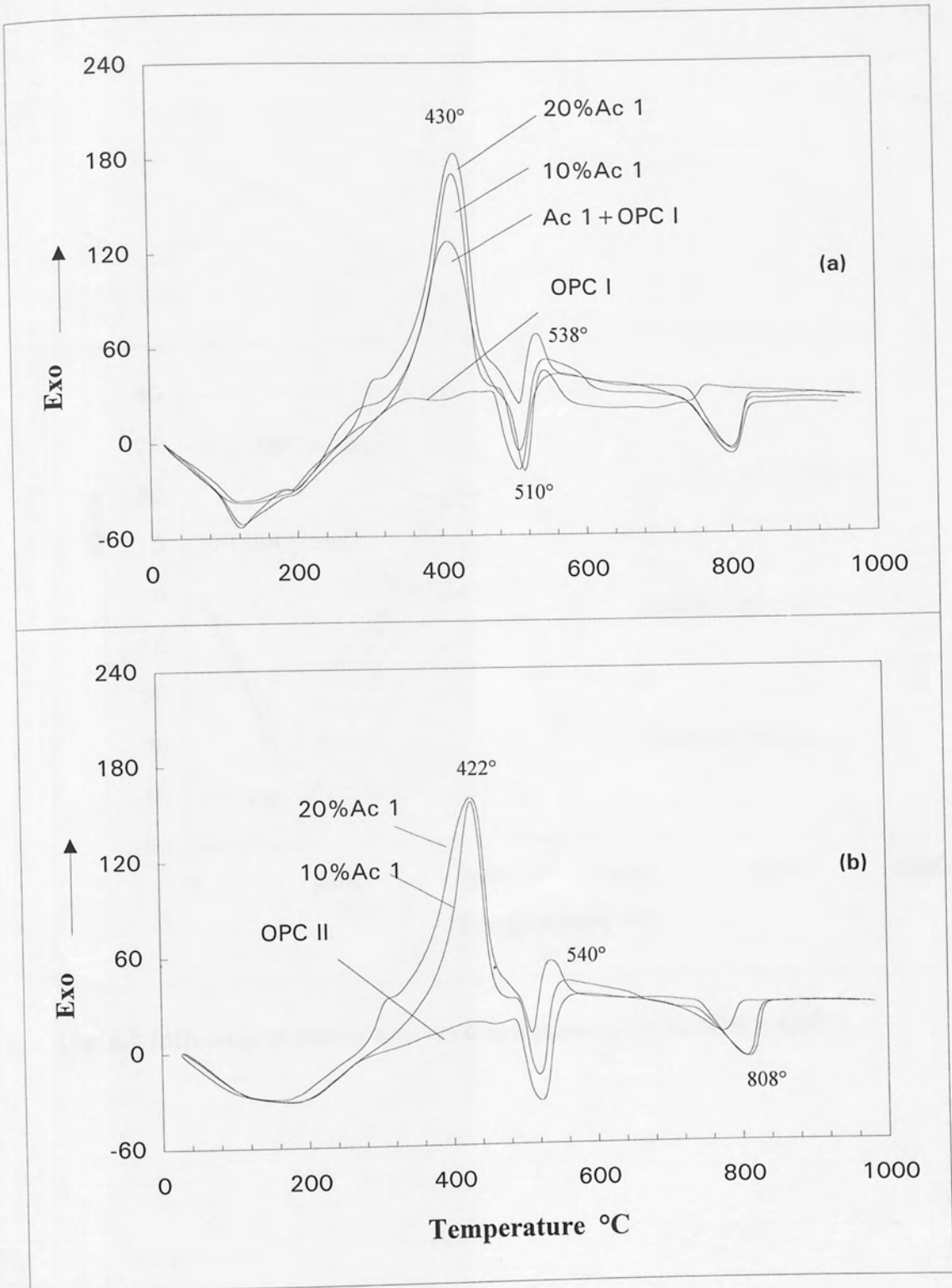


Fig.6.7 Thermograms of Ac 1-OPC pastes in air
 (a) Ac 1-OPC I; (b) Ac 1-OPC II

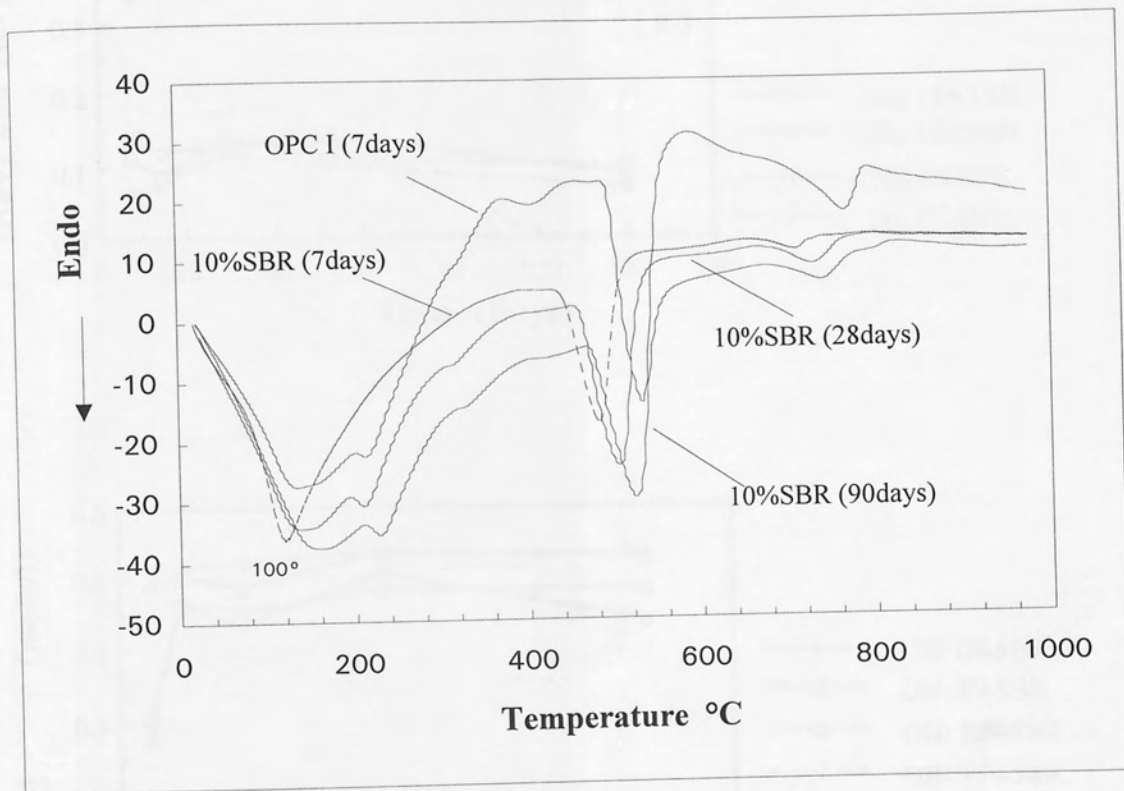


Fig. 6.8 Influence of curing time on themograms of 10% SBR 1-OPC I

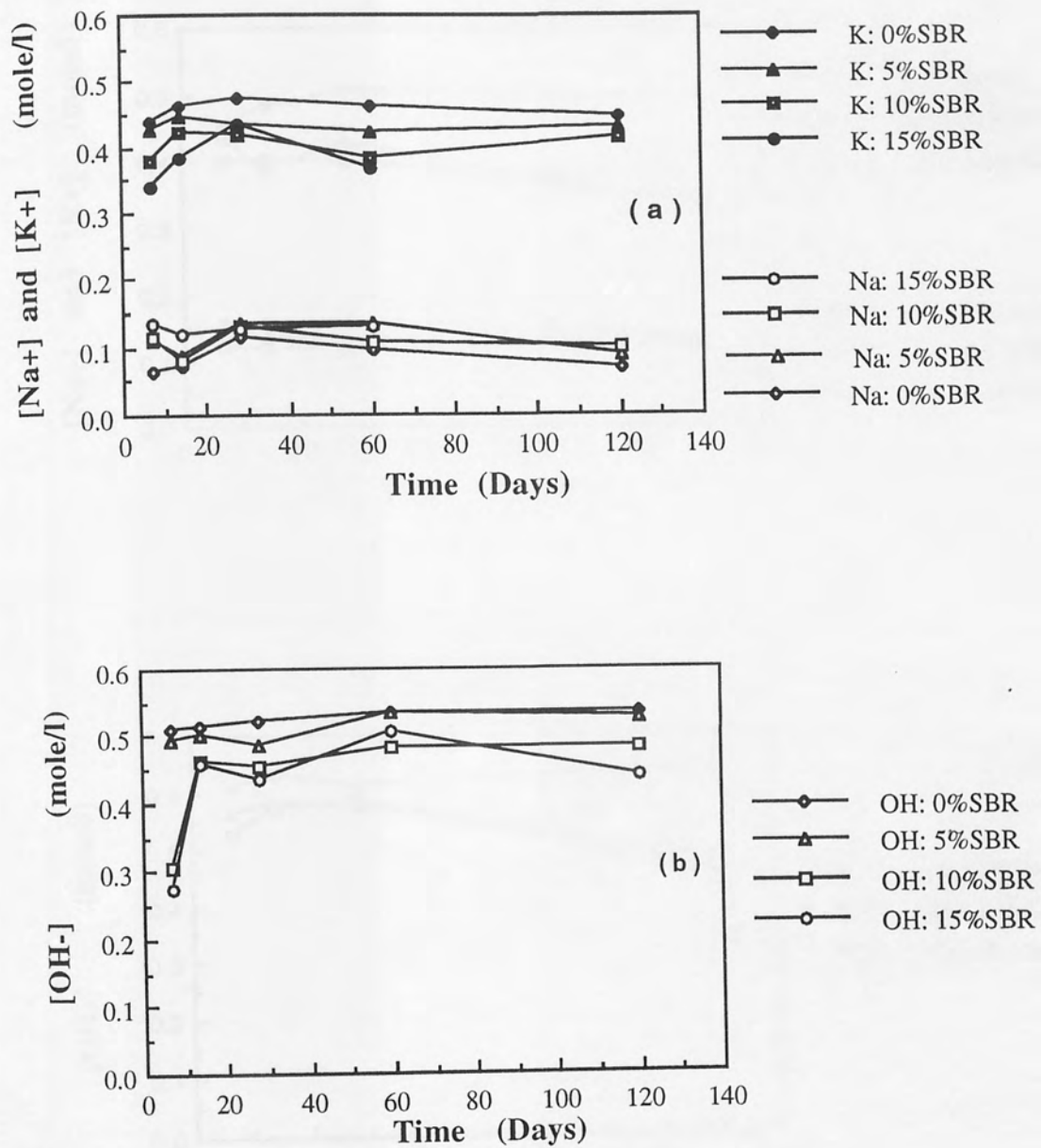


Fig.6.9 Pore Solution Analysis for SBR 1-OPC I system (w/c=0.5)

(a) concentration of K^+ and Na^+ , (b) concentration of OH^-

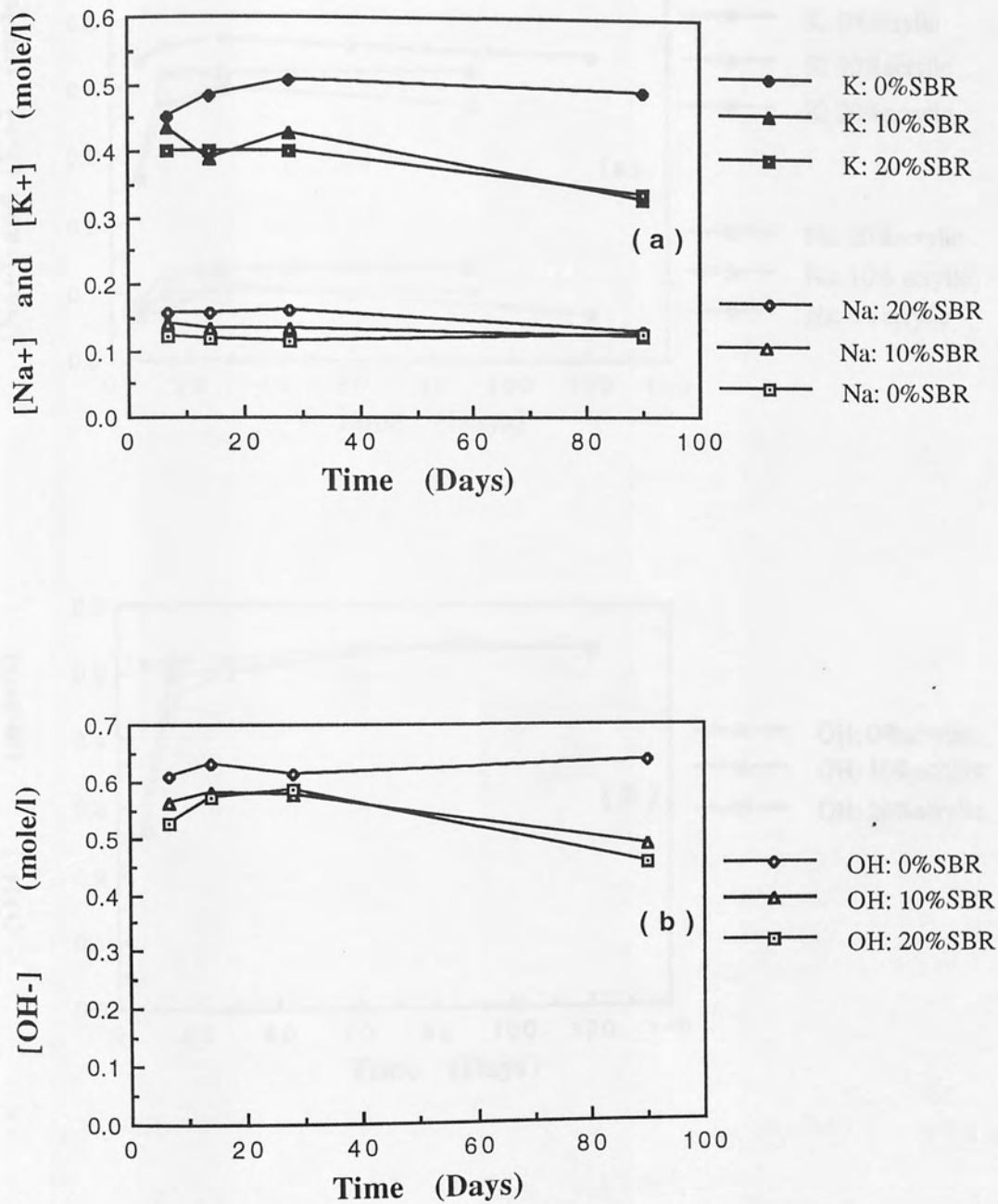


Fig.6.10 Pore solution analysis for SBR 1-OPC II system (w/c=0.5)

(a) concentration of K^+ and Na^+ , (b) concentration of OH^-

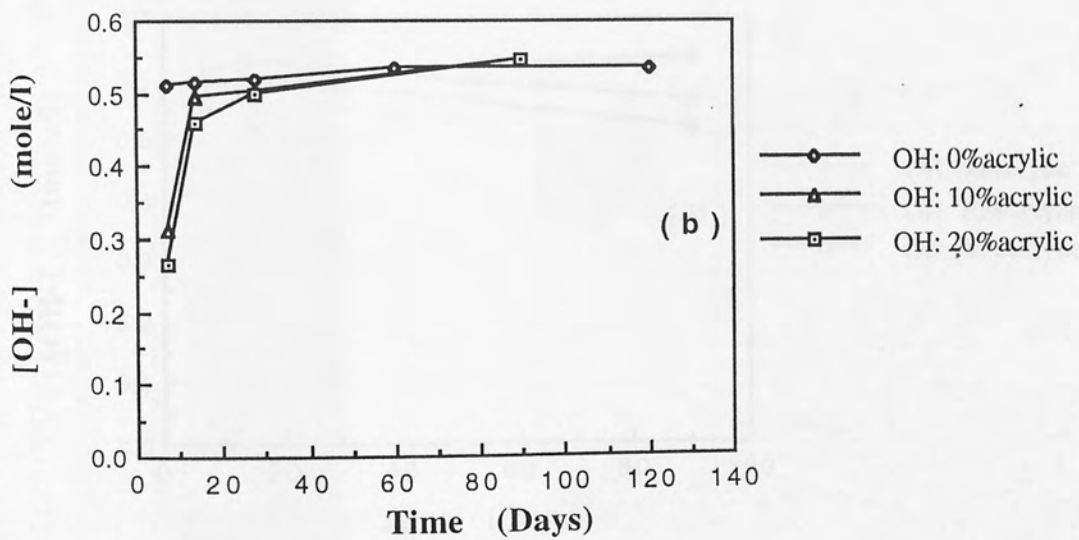
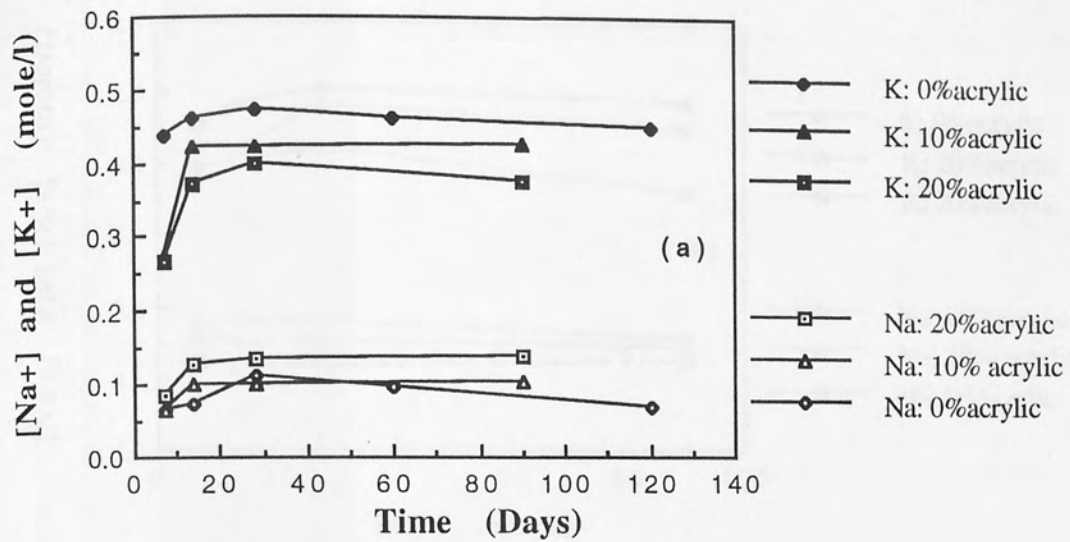


Fig.6.11 Pore solution analysis for Ac 1-OPC I system ($w/c=0.5$)

(a) concentration of K^+ and Na^+ , (b) concentration of OH^-

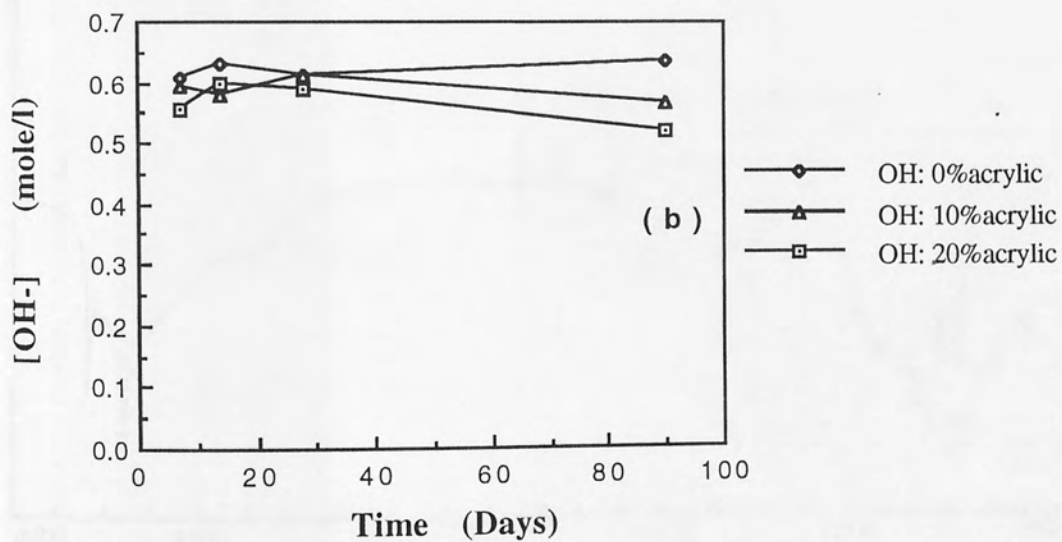
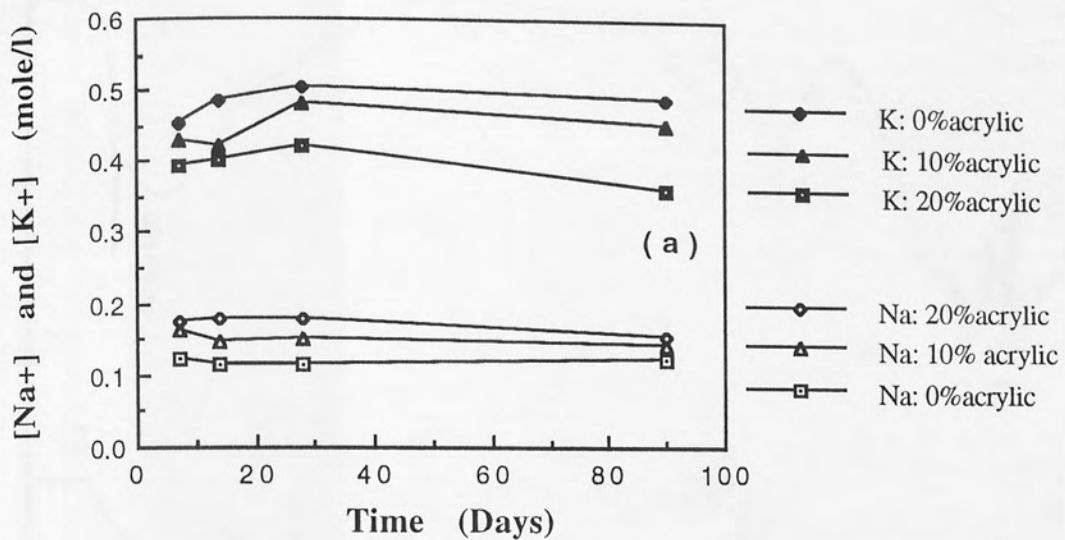


Fig.6.12 Pore solution analysis for Ac 1-OPC II system (w/c=0.5)

(a) concentration of K^+ and Na^+ , (b) concentration of OH^-

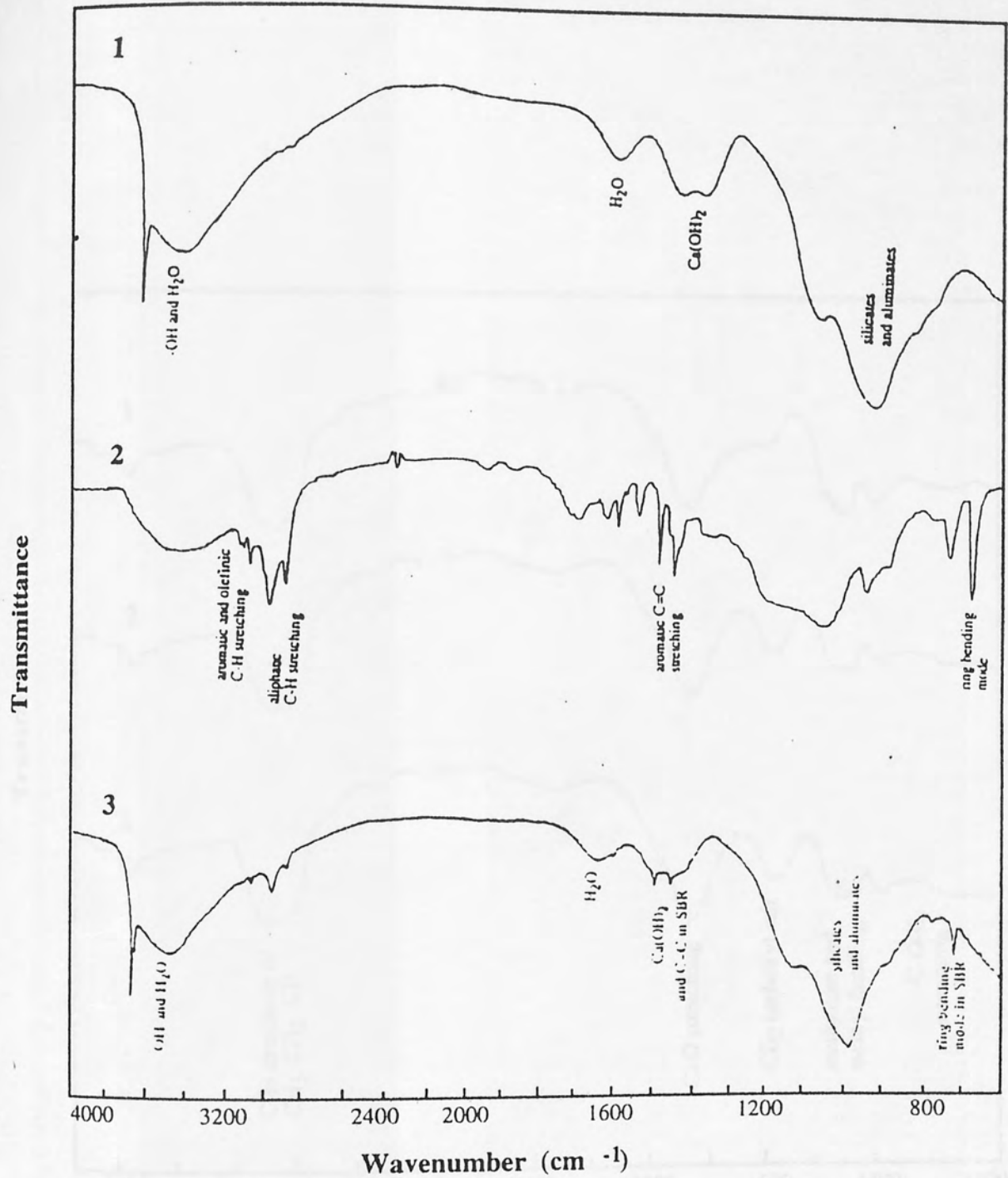


Fig. 6.13 Infrared spectra of SBR 1-OPC I system
 Curve 1. hydrated cement (90 days w/c=0.5)
 Curve 2. SBR 1
 Curve 3. SBR 1-OPC I paste (90 days w/c=0.5)

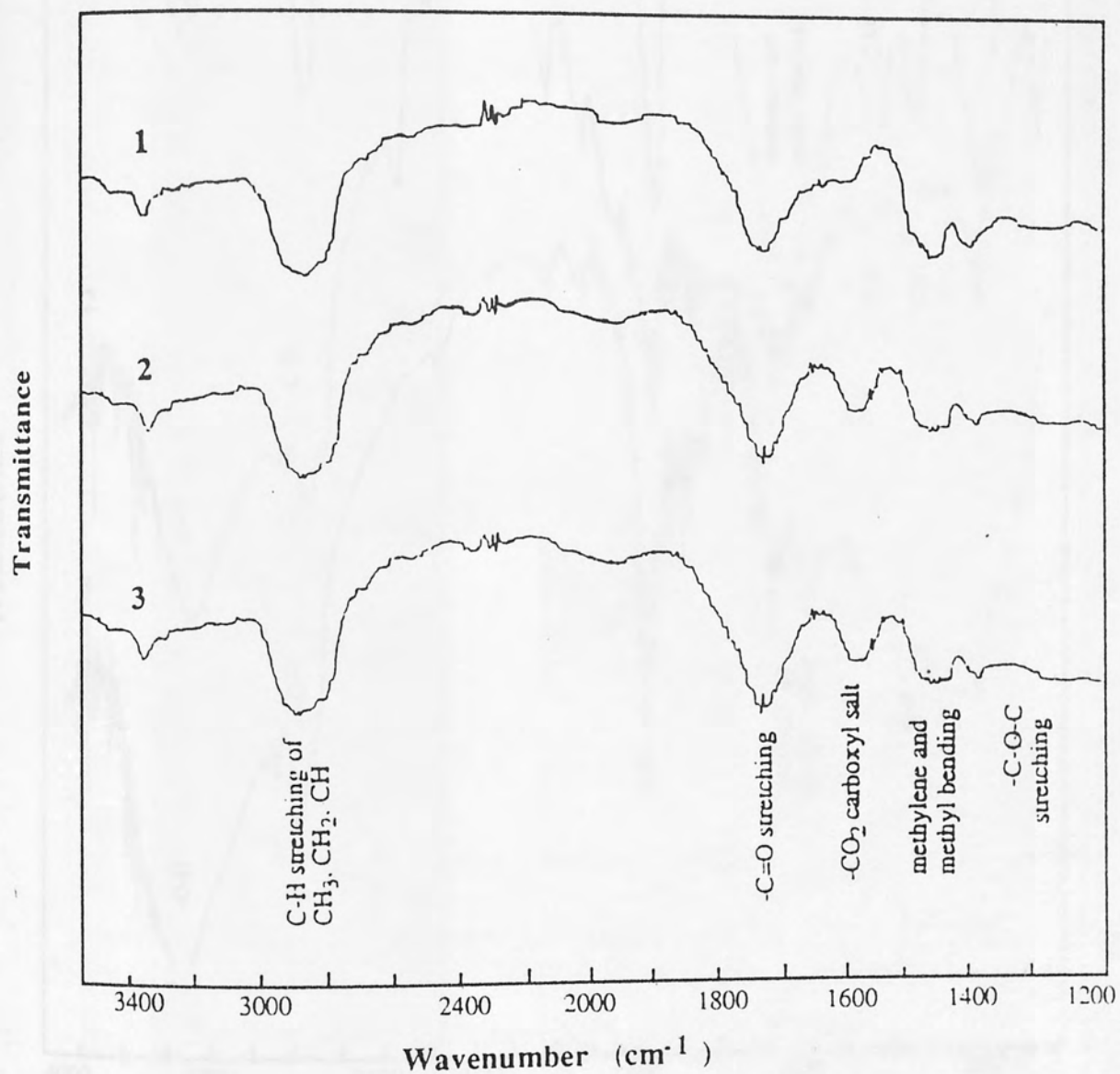


Fig. 6.14 Infrared spectra of Ac 1-OPC I system

Curve 1. Ac 1

Curve 2. Ac 1 immersed in synthetic pore solution

Curve 3. Ac 1 extracted from Ac 1-OPC I paste

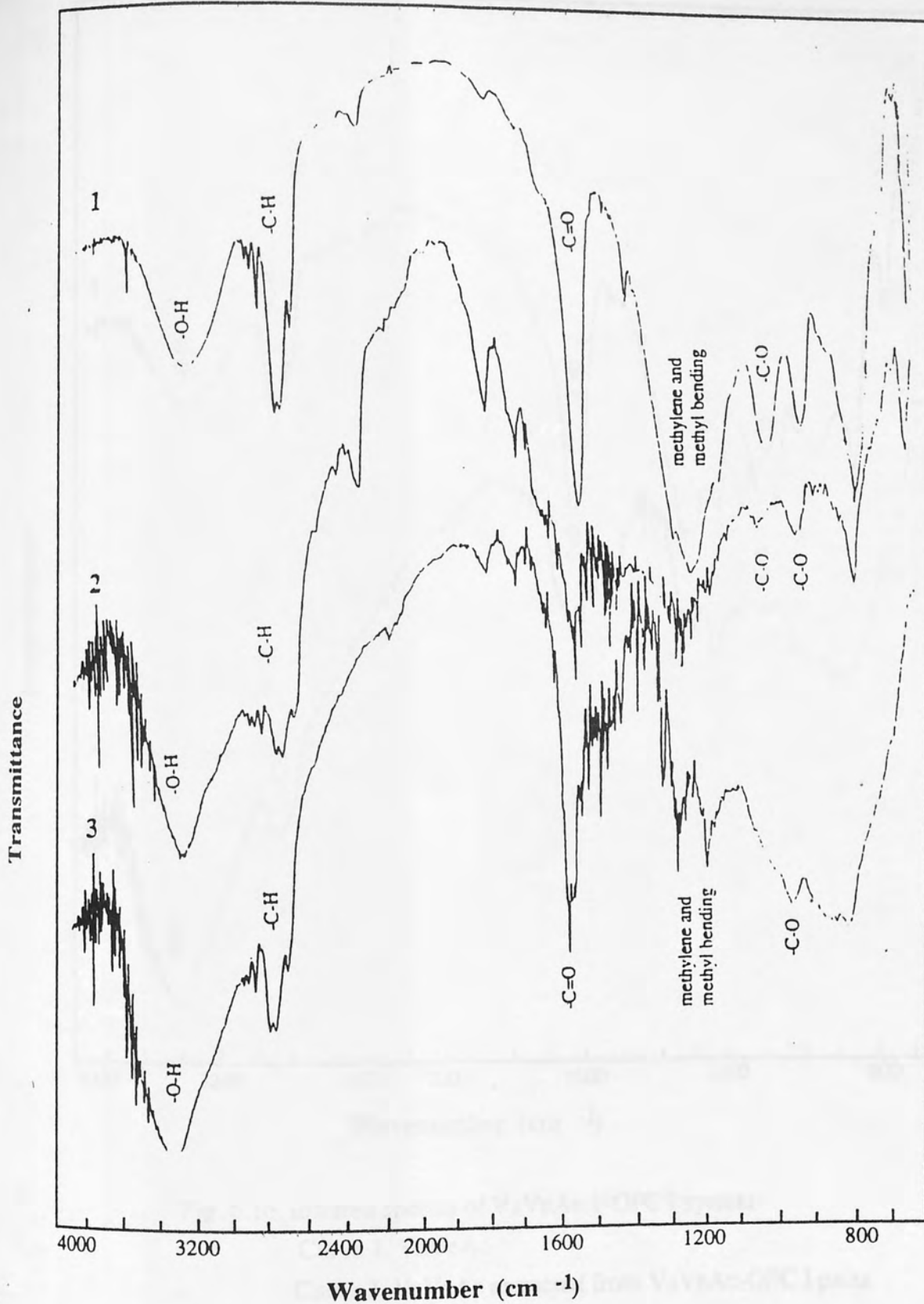


Fig. 6.15 Infrared spectra of Ac 3-OPC I system

Curve 1. Ac 3

Curve 2. Ac 3 immersed in synthetic pore solution

Curve 3. Ac 3 extracted from Ac 1-OPC I paste

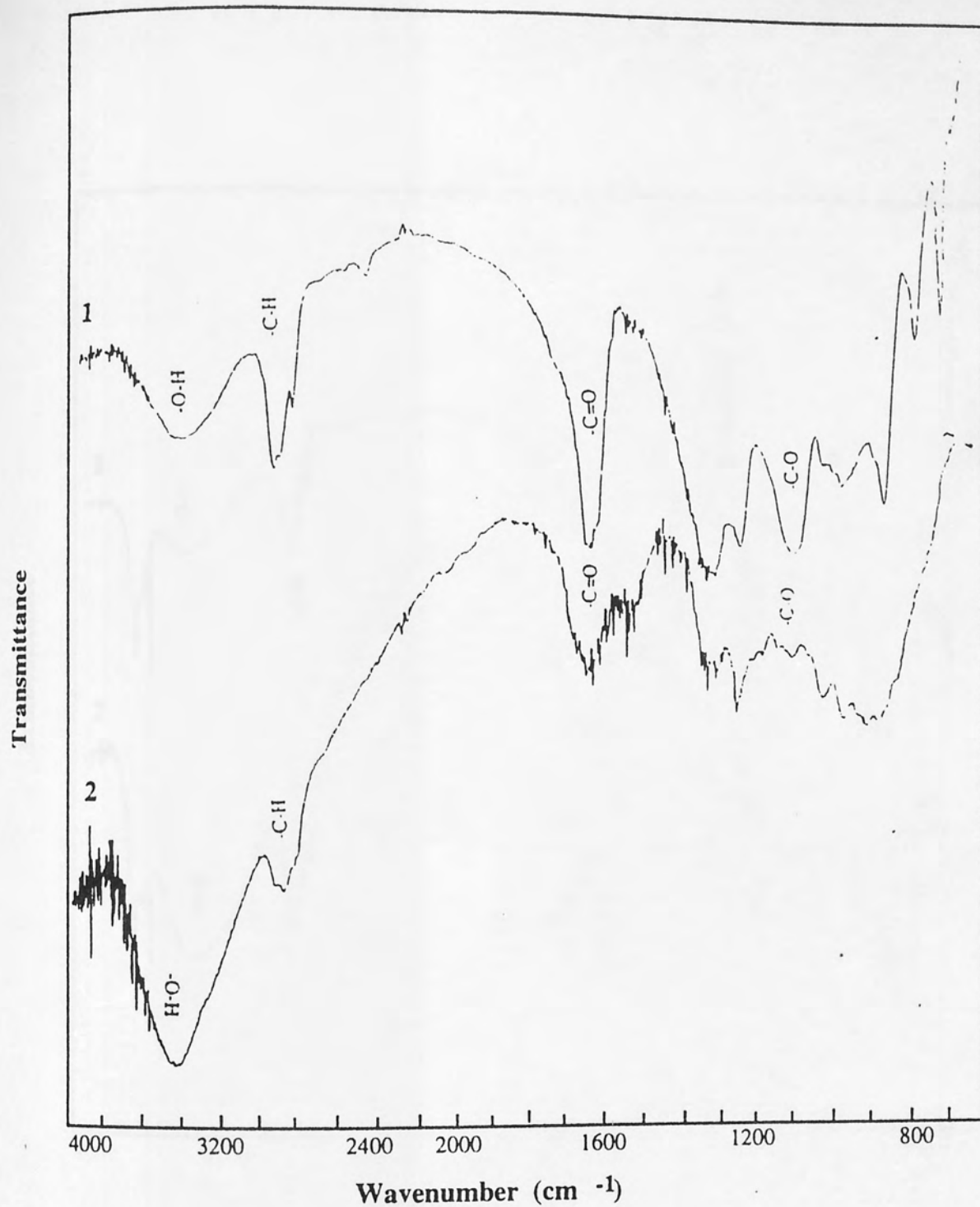


Fig. 6.16 Infrared spectra of VaVeAc 1-OPC I system

Curve 1. VaVeAc

Curve 2. VaVeAc extracted from VaVeAc-OPC I paste

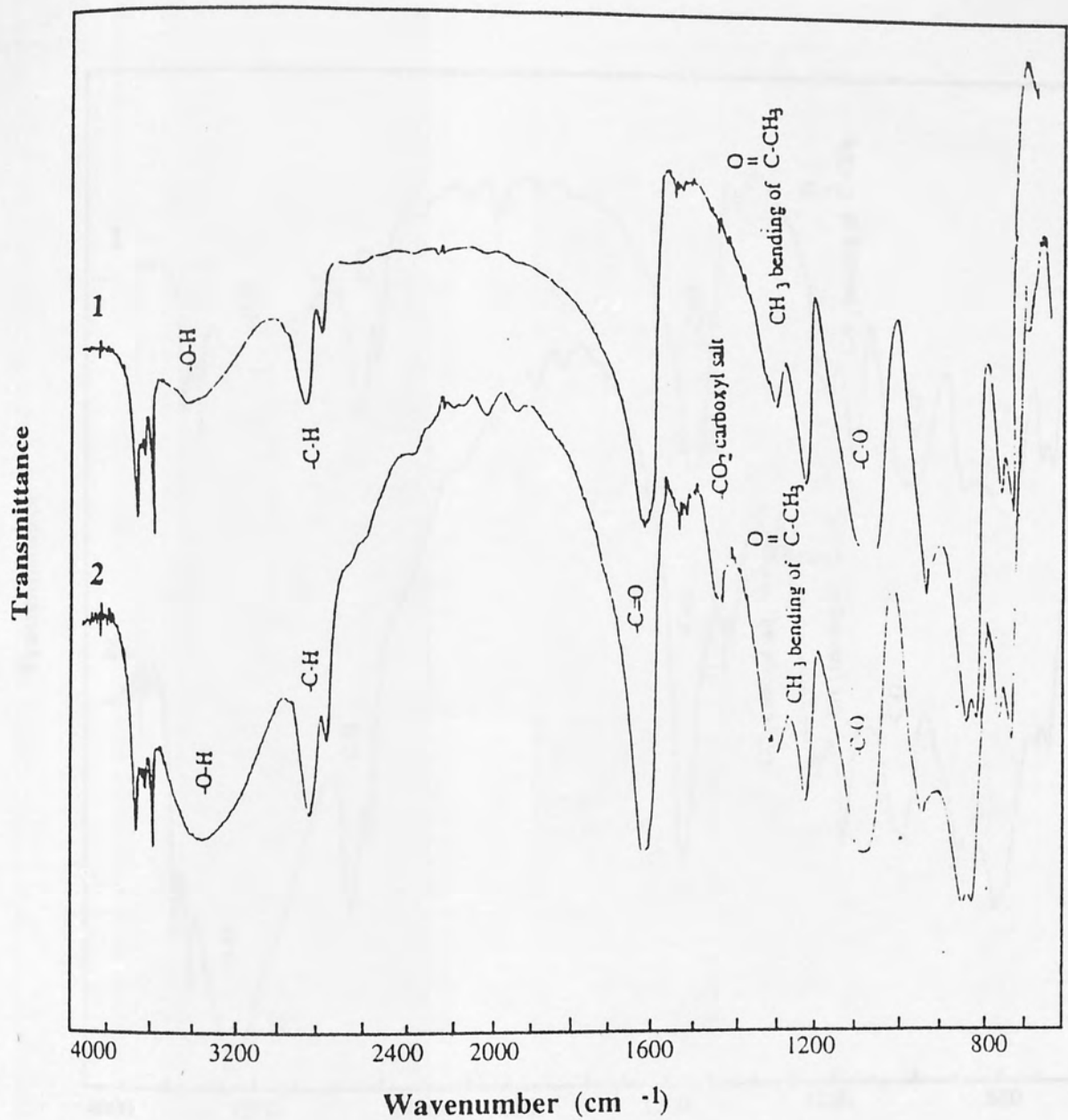


Fig. 6.17 Infrared spectra of EVA 1-OPC I system

Curve 1. EVA 1

Curve 2. EVA 1 immersed in synthetic pore solution

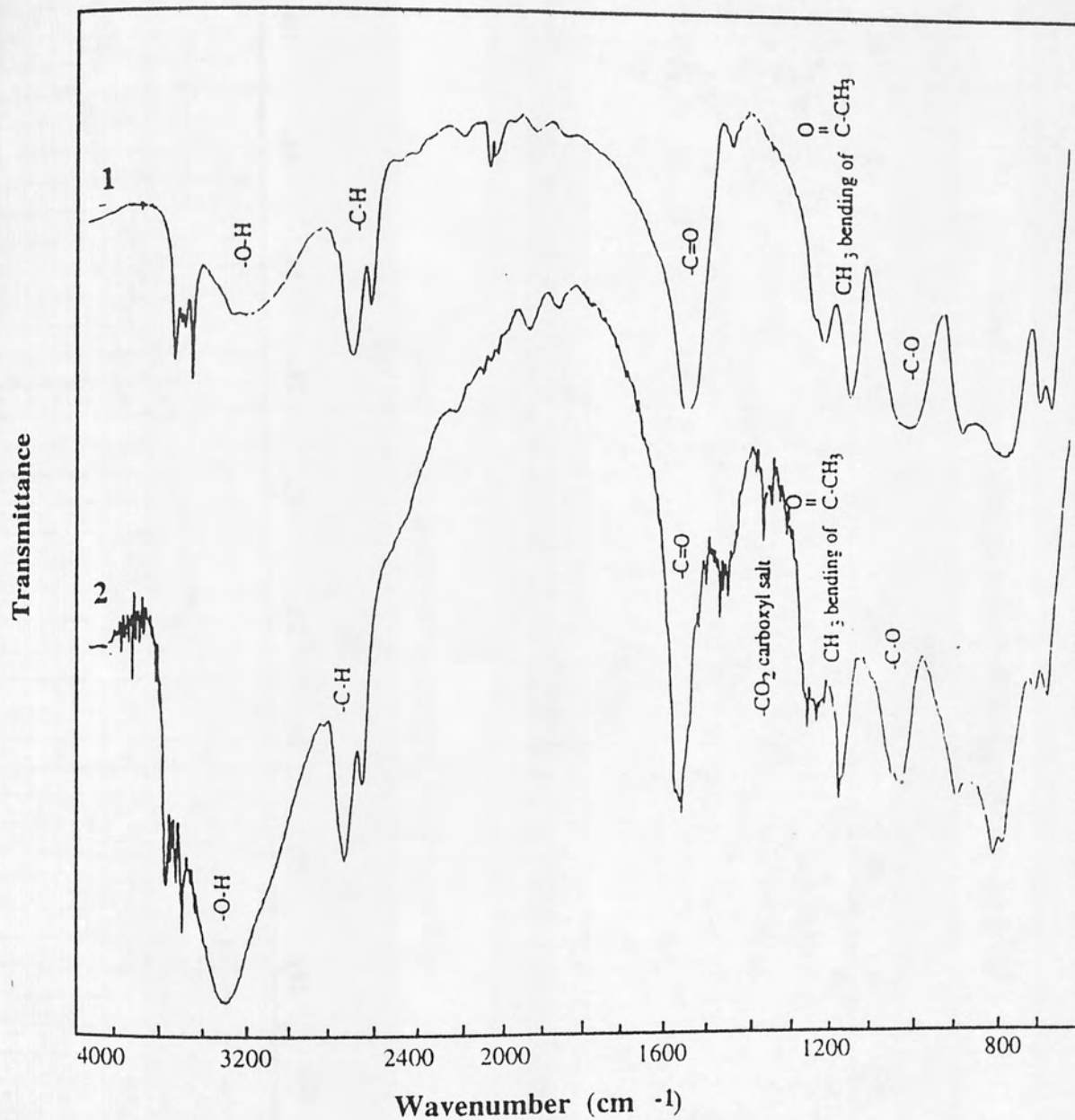


Fig. 6.18 Infrared spectra of EVA 3-OPC I system

Curve 1. EVA 3

Curve 2. EVA 3 extracted from EVA 3-OPC I paste

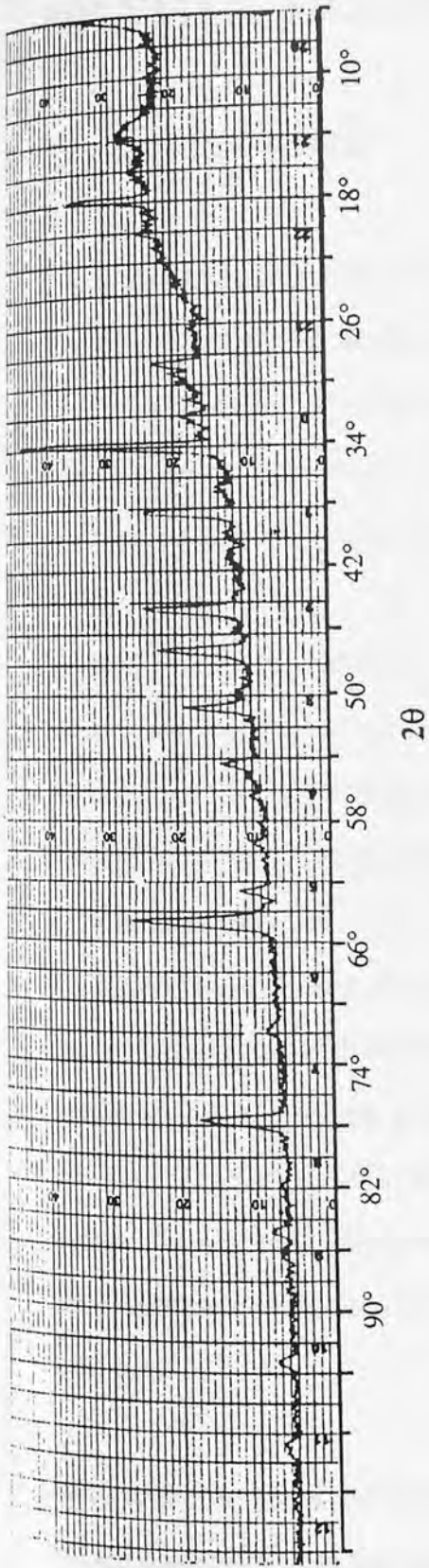


Fig.6.19 X-ray diffraction pattern of OPC I paste

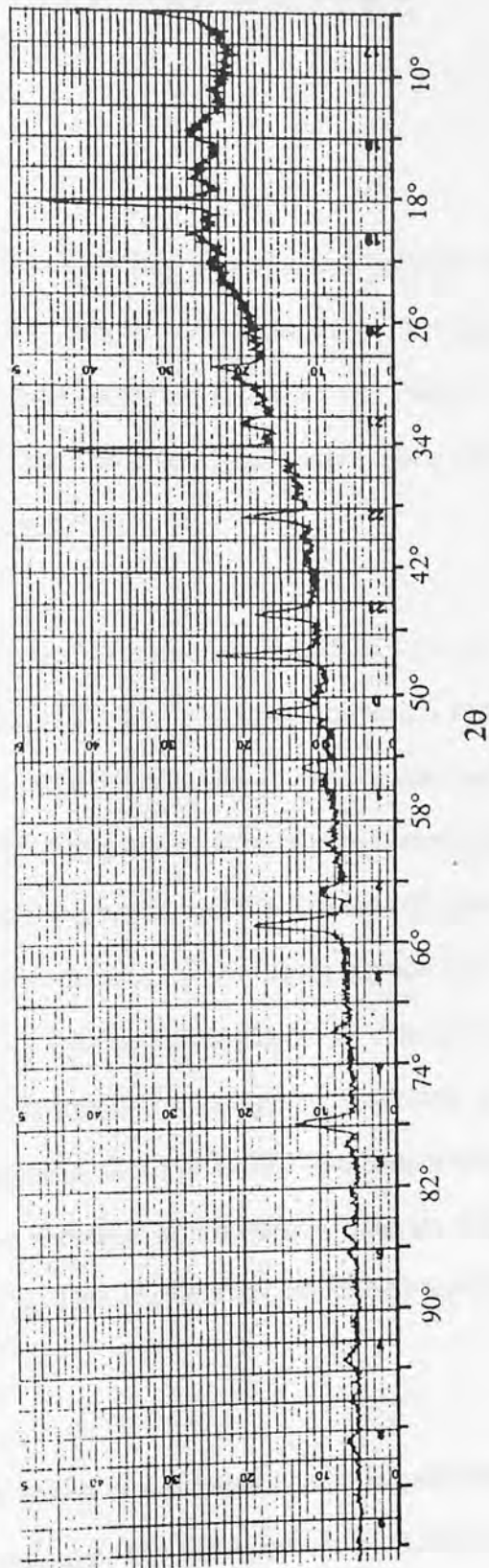


Fig.6.20 X-ray diffraction pattern of SBR 1-OPC I paste

DIFFUSION OF CHLORIDE IONS IN POLYMER MODIFIED CEMENT PASTES

7.1 PREVIOUS WORK

One of the major criteria for evaluating the engineering properties of polymer modified cement is its long term durability, which is largely dependent upon its resistance to penetration by water and ionic species such as chlorides, sulphates and carbon dioxide. There are several tests which measure this such as chloride diffusion, water absorption, water vapour transmission and carbonation resistance.

The main experimental methods and techniques to measure the resistance to chloride ion diffusion may be divided into two categories, i.e. free and forced diffusion tests. In the free diffusion test, two testing procedures are available. One is to set a disc sample in a diffusion cell with two compartments and let chloride ions from a high concentration side penetrate through the disc into a low concentration side, and the diffusion of chloride ions is monitored by analysing the chloride ion content in the low concentration side. This is called the steady state diffusion technique and allows calculation of an effective diffusion coefficient. Another testing procedure is to immerse a sample in a solution containing chlorides, and after a specific time the sample is sliced or drilled to different depths. The chloride ion content is measured using an indicator or a chemical analysis method and thus a concentration profile can be obtained. This is called the non-steady state diffusion technique.

In the forced diffusion test the sample is placed in a solution containing chlorides and a voltage is applied across the sample and solution. The diffusion of the chloride ions into the sample is monitored using the same chemical methods as used in the free diffusion test or by measuring the electrical current flowing through the sample.

Previous studies reported that the presence of polymer could reduce chloride ion diffusion in polymer modified cement. Al-Qaser et al (1990) studied the diffusion of various ions from sea water into polymer modified cement pastes by steady-state test, using a diffusion cell developed by Page et al (1981). The results showed that polymer latex reduced the diffusion of all the various ions and the rate of diffusion depended on the type of polymer, concentration of polymer and type of cement. The diffusion of chloride through polymer modified SRPC (sulphate resisting Portland cement) discs was reduced compared to unmodified cement. The sulphate content in the modified SRPC disc was much lower than in the unmodified SRPC disc. The diffusion of sodium, potassium, calcium and magnesium ions were also reduced to some extent in the presence of polymer.

Marusin (1987) and Lavelle (1988) carried out non-steady state experiments. They used a wet-dry curing regime to cure their samples before immersing them in salt water solutions. In Marusin's experiments, concrete cubes were cured for 21 days in plastic bags and then placed in the curing room for 14 days of air drying. The concrete cubes were immersed in a 15 per cent sodium chloride water solution for 21 days. Powder samples were obtained by drilling to different depths to determine the chloride ion concentration profile. The results showed a lower rate of chloride diffusion in latex modified concrete than conventional concrete.

Lavelle (1988) cured the concrete samples at 95 per cent relative humidity for 1 day following 6 day immersion in water. The measurements were carried out by ponding the latex cement surface with 3 per cent sodium chloride solution for 60 days. The samples were then sectioned and analysed for chloride as a function of depth. Good resistance to chloride ion penetration was observed in acrylic modified concrete.

In the same test, Marusin also measured water transmission of concrete. After being immersed in a 15 per cent sodium chloride solution for 21 days, the samples were removed from the solution and exposed to air in a curing room for other 21 days to

observe the water transmission characteristics. Unmodified concrete with w/c ratio of 0.4 was able to expel about 65 per cent of absorbed water by vapour transmission. Acrylic latex-modified concrete lost all the absorbed water and SBR latex modified concrete lost 66 per cent of its absorbed water when allowed to dry.

Ohama's (ACI 548.3 R-91) results of water absorption tests of mortar modified with styrene butadiene latex also indicated a significant reduction of water absorption, compared to an unmodified mortar, and an increasing improvement in this property as latex content increases. Water vapour transmission tests showed similar effects.

It has been reported that polymer modified concretes have excellent carbonation resistance ability compared to unmodified concretes. Ohama (1984) investigated the polymer modified concretes exposed to carbon dioxide gas and carbon dioxide in solution (NaHCO_3), under a pressure of 0.1 to 0.6 MPa for a period of up to 6 months. After the exposure the carbonation depth was measured with phenolphthalein solution. The results indicated that with both types of exposure, carbonation was significantly reduced by the addition of latex to the concrete.

Walters (1990) exposed specimens to 0.10MPa of carbon dioxide gas for 72 hours and then split them. The carbonation depth was measured with phenolphthalein solution and showed that SBR and S-Ac modified mortars had a low carbonation depth (1 mm), but butyl-methyl methacrylate and polyvinyl acetate modified mortars had higher carbonation depths (7 and 5 mm).

Several authors attribute the reduction of water permeability or ionic diffusion to the refinement of pore structure. Ohama (1991) reported that polymer dispersions reduced the pore volume of the large pore sizes and increased that of the small pore sizes. Nishi (1990) found that the total porosity of hardened cement paste decreased with latex addition. It was believed that the polymer latex may form a water-proof film and fill the capillary pores resulting in a lower porosity cement matrix. However, this opinion is in

conflict with results reported by other researchers.

Oye (1989) obtained a higher porosity in PMMA/PBA modified cement than an unmodified cement and this tendency increased when the polymer addition increased. A carbonation test gave contrasting results compared to Ohama's. The test samples were subjected to 3% carbon dioxide in air at 50-70% relative humidity and a temperature of 20°C. Since the carbon dioxide content was 100 times greater than the content in natural air and the moisture conditions were optimum for the carbonation reaction to take place, carbonation was strongly accelerated. The general impression is that polymer modified mortars do not appear to reduce the rate of carbonation.

Using forced diffusion test, Justnes et al (1987) measured chloride ingress through cylinders of polymer modified mortars. The chloride source was natural sea-water and a constant voltage of 5 volt was applied between the embedded steel and a steel sheet immersed in the sea-water. The results showed some disagreement with previous work. Even though three commercial latexes (vinyl acetate/vinyl chloride/ethylene; vinyl acetate/versate ester; SBR) increased the penetration time for chlorides at $w/c=0.5$, they did not lead to an improvement at $w/c=0.4$. In addition, it was reported (Justnes 1992) that acrylic latex performed much better than SBR. This improvement increased with increasing acrylic addition up to a level of 15%, but a decreasing efficiency was observed with increasing SBR which was not in agreement with Ohama's results.

Kuhlmann (1981) summarised the performance of latex-modified concrete overlays in the United States. The data and conclusions collected from 184 bridge decks, aged two months to 13 years, were not uniform. In some cases the latex-modified overlay prevented or minimised the penetration of chlorides, but in others it was reported that chloride ions permeated down through the latex-modified overlay and there was considerable variation in chloride content from one structure to another.

Based on the above observations, it can be seen that factors governing the ionic diffusion

through a polymer modified cement matrix are not fully understood. The diffusion characteristics are very variable and depend on type of polymer, its addition, curing regime and testing methods. Any improvement in diffusion properties is not simply related to reduction of porosity. Therefore, a more systematic investigation on the diffusion characteristics of polymer modified cements to clarify some of the discrepancies and scatter in the reported data is desirable. The work carried out in this chapter investigated the effect of various polymer systems on chloride diffusion under the steady-state and non-steady state diffusion conditions. Parameters such as polymer type and addition level, aqueous component of latex, defoamer, water cement ratio and temperature were studied. Combining the results described in previous chapters for the pore structure, thermal analysis (DTA/TGA), infrared spectroscopy (IR) and pore solution extraction techniques, it was hoped to find a relation between the diffusion rate and cement matrix characteristics. It was hoped to remove some of the uncertainties of the earlier results and to get a more sound understanding on the kinetics and mechanisms of chloride diffusion in polymer modified cement.

7.2 MATHEMATICAL MODELLING OF DIFFUSION PROCESS

7.2.1 Steady-State Diffusion

Using the experimental conditions described in section 3.3.13, a disc is fixed in a diffusion cell and chloride ions diffuse from compartment I to compartment II passing through the disc. It is assumed that the surfaces of the disc, $x = 0$, $x = L$, are maintained at constant chloride concentrations C_1 , C_2 respectively and the concentration remains constant at all points through the disc. The chloride diffusion through the disc is then in steady state after a time t and the diffusion process follows Fick's First Law (Crank 1975, Page et al 1981):

$$J = -D \frac{dc}{dx} \quad \text{or} \quad J = -D \frac{C_1 - C_2}{L} \quad (7-1)$$

where J is the diffusion flux (mole/cm²·s), D is the effective diffusion coefficient D (cm²/s), dc/dx is the concentration gradient, L is the thickness of the disc (cm).

From a consideration of the kinetics of transport of ions

$$J = -\frac{V}{A} \frac{dC_2}{dt} \quad (7-2)$$

where A is the cross-sectional area (cm²), V is the volume of solution in compartment II (cm³). From the equation (7-1) and (7-2), we get

$$\frac{V}{A} \frac{dC_2}{dt} = D \frac{C_1 - C_2}{L} \quad (7-3)$$

Rearranging and integrating equation (7-3)

$$\int_{t_0}^t \frac{DA}{VL} dt = \int_0^{C_2} \frac{1}{C_1 - C_2} dC_2$$

$$\frac{DA}{VL} (t - t_0) = \ln\left(1 - \frac{C_2}{C_1}\right)$$

when $C_1 \gg C_2$

$$\frac{DA}{VL} (t - t_0) = -\frac{C_2}{C_1}$$

so

$$C_2 = \frac{DAC_1}{VL} (t - t_0) \quad (7-4)$$

7.2.2 Non-Steady State Diffusion

If diffusion under the experimental conditions described in section 3.3.14 is considered as a problem of diffusion into a semi-infinite medium, with a constant boundary

concentration C_0 and an initial constant concentration C_i throughout the cylinder (for Cl^- , $C_i = 0$), then the ionic diffusion process through the cylinder would obey Fick's second law (Crank 1975)

$$\frac{\partial C}{\partial t} = D \frac{\partial^2 C}{\partial x^2} \quad (7-5)$$

A required solution of equation (7-5), satisfying the boundary condition:

$$C = C_0, \quad x = 0, \quad t > 0.$$

and the initial condition:

$$C = 0, \quad x > 0, \quad t = 0.$$

is

$$C = C_0 \operatorname{erfc} \frac{x}{2\sqrt{Dt}} \quad (7-6)$$

where $\operatorname{erfc}(z) = 1 - \operatorname{erf}(z)$ and $\operatorname{erf}(z)$ is the error function

$$\operatorname{erf}(z) = \frac{2}{\sqrt{\pi}} \int_0^z \exp(-x^2) dx$$

In the special case ignoring ionic bonding during the diffusion (Sergi 1992), then the equation (7-5) would be in the following form

$$\frac{\partial C}{\partial t} = D^* \frac{\partial^2 C}{\partial x^2} \quad (7-7)$$

where D^* is the apparent diffusivity of various ions.

7.3 DIFFUSION PROPERTIES OF SBR-CEMENT PASTES

7.3.1 Results and Discussions of Steady State Diffusion

7.3.1.1 SBR 1-OPC I Pastes

Fig. 7.1 shows typical results for the change in chloride concentration change in compartment II of the diffusion cell with the diffusion time. There is an induction period which allows diffusant to reach equilibrium in the pore liquid of the solid disc. After that time, the concentration of chloride ions increases linearly with time. Plotting C_2 against time t and using the equation (7-4) and the diffusion coefficient D can be obtained from the slope of the straight line, i.e. slope = DAC_1/VL .

Table 7.1 lists the effective diffusion coefficients of chloride for SBR 1-OPC I systems at different water cement ratios and diffusion temperatures. From the average values of diffusion coefficients for four discs, we can see that:

i) Addition of SBR reduced the diffusivity of chloride ions. The diffusion coefficients were about half the value of unmodified cement paste for both water-cement ratios of 0.3 and 0.5. A 10% addition of polymer seems to give a better improvement than a 20% addition. In fact, increasing polymer content from 10% to 20% in some cases resulted in the diffusion coefficient increasing slightly although they were still lower than that for the unmodified paste. This improvement may relate to the change of pore structure and pore surface property. As discussed in section 5.2.2, polymer modified cement matrix may have a more tortuous diffusion paths which result in a low diffusion rate. Furthermore, polymer adsorbed on pore surfaces may change diffusion behaviour.

ii) The water cement ratio played an important part in diffusion for both modified and unmodified pastes. A reduction in water cement ratio from 0.5 to 0.3 decreased the diffusion coefficient 4 times at 25°C. Thus if the polymer can decrease the demand for

water and still give the required workability, then the diffusion properties of PMC will be improved. For example, the diffusion coefficient of 10%SBR 1-OPC I paste with $w/c=0.3$ at 25°C was less than one eighth of that for unmodified paste with $w/c=0.5$, and the workability of the former was as good as for the later (Salbin 1996). From this point of view, the effect is significant.

iii) The change in temperature drastically affects the diffusion coefficient in all samples, especially for polymer modified cements at $w/c=0.5$. With rising temperature and SBR 1 level, the diffusion coefficient increases significantly. For example, when temperature rose from 25°C to 35°C , the diffusion coefficient for 10% SBR 1-OPC I ($w/c=0.5$) increased from 42.8 to $87.0 \times 10^{-9} \text{ cm}^2/\text{sec}$. From 35°C to 45°C , the diffusion coefficient for 20% SBR 1-OPC I increased from 61.0 to $338 \times 10^{-9} \text{ cm}^2/\text{sec}$. The reasons for this are not clear.

If it is assumed that the diffusion process obeys the Arrhenius equation:

$$D = A \exp \left(- \frac{E_a}{RT} \right)$$

where A is pre-exponential constant, E_a is activation energy, R is universal gas constant and T is absolute temperature, we can obtain the activation energy E_a for SBR 1-OPC I system at $w/c=0.3$ and 0.5 by plotting $\ln D$ against $1/T$ (see Fig.7.2 and 7.3). It was found that there were generally good linear relationships between $\ln D$ and $1/T$ (excluding the value at 45°C for 20% addition). At a w/c of 0.3, the value of activation energy with 95% confidence limit for unmodified cement is $36.9 \pm 1.7 \text{ kJ/mole}$, $34.6 \pm 3.6 \text{ kJ/mole}$ for 10%SBR 1-OPC I and $33.5 \pm 2.8 \text{ kJ/mole}$ for 20%SBR 1-OPC I, respectively. At a w/c of 0.5, these values are 34.4 ± 2.5 , 46.4 ± 2.0 and $41.8 \pm 5.6 \text{ kJ/mole}$. Within experimental error, it seems that the activation energy for chloride ions was not changed significantly with polymer presence, suggesting that the polymer has only a minor effect on the diffusion mechanism.

7.3.1.2 SBR 2-OPC I Pastes

The steady-state diffusion test for SBR 2-OPC I was only carried out at 25°C and a w/c of 0.5. The effective diffusion coefficients were 68.9×10^{-9} cm²/sec for 10% SBR 2-OPC I and 43.5×10^{-9} cm²/sec for 20% SBR 2-OPC I. These values were slightly greater than for SBR 1-OPC I system but still less than unmodified cement. It is known that the main difference between SBR 1 and SBR 2 is the degree of carboxylation, 1% in SBR 1 and 5% in SBR 2. Thus, this difference in the diffusion characteristic should come from the effect of carboxylate. As described in section 4.4.1.4 and 5.2.2.1, the concentration of carboxyl groups retarded cement hydration and increased porosity. Therefore, excessive carboxylate in the latex appears to not improve the diffusion property of polymer modified cement.

7.3.1.3 Aqueous Component-OPC I Pastes

In order to understand the effect of surfactants on the chloride ion diffusion, similar diffusion tests were carried out for cement modified with the aqueous component of the latex, i.e. no polymer particles were present. The effective diffusion coefficient for pastes with 10% and 20% aqueous component were 141×10^{-9} cm²/sec and 138×10^{-9} cm²/sec respectively. These values are much higher than the 101×10^{-9} cm²/sec for unmodified cement paste and nearly three times that of SBR 2-OPC I. This indicated that surfactants in the latex increased the rate of chloride diffusion. It is interesting to note, however, that the aqueous component had only a little effect on hydration kinetics and pore structure. The reason for such high diffusion rate may be that surfactant molecules adsorb on pore surfaces, change pore surface characteristics, or occupy the chloride binding sites in cement. In fact, it should be noted that the existing form of surfactants in latex is different from that in the aqueous component only. In the latex, surfactants are usually bound to the surface of the latex solid, whilst in the aqueous component they are free in the liquid. This may be one of reasons for significant difference between SBR 2 and the aqueous component.

7.3.2 Results and Discussions of Non-steady State Diffusion Tests

7.3.2.1 Ionic Concentration Profile and Apparent Diffusivity D^*

The non-steady state diffusion test is useful since it is closer to a practical ionic diffusion process where the concentration of diffusion ions at all points of a cylinder are not constant and vary with diffusion depth. This test was carried out with the SBR 1-OPC I system at a water cement ratio of 0.5. All samples were cured in plastic cylinders for 90 days and then subjected to chloride ion diffusion by immersing in a salt solution for 100 days. After that, the cylinders were sliced and the pore solutions were extracted and analysed for various ions (see section 3.3.8 for details). Table 7.2 gives the ionic concentration profiles of OH^- , Cl^- , Na^+ and K^+ . Figs. 7.4-7.6 show the change of concentration with the diffusion depth.

In general, ionic diffusion has following tendencies:

- i) The Cl^- concentration in the extracted pore solution is very high at the surface, but decreases rapidly as the depth increases and reaches zero at a depth of 60mm. Accompanying the Cl^- diffusion, Na^+ also penetrates into the paste. After a depth of 30mm, the Na^+ concentration keeps nearly constant level which corresponds to the original Na^+ concentration in cement.
- ii) The OH^- concentration is low at the surface, but increases with depth and reaches a constant level at a depth of 30mm. The profile of K^+ has similar pattern as the OH^- , which suggests that the K^+ leached out from the inside of paste.
- iii) The ion profiles of 10%SBR 1-OPC I are similar to that of unmodified cement. However, the Cl^- concentration was lower and the K^+ concentration was higher. These differences suggest that addition of SBR minimised the Cl^- penetration and the K^+ leaching as a result of diffusion property improvement.

iv) Compared with 10%SBR 1-OPC I, the ion profiles of 20%SBR 1-OPC I are quite different. Although the Cl^- concentration had a large drop within depth of 0-20mm, it still very high at a depth of 60mm. This indicated that the rate of ion diffusion in this paste was higher than 10%SBR 1-OPC I.

Using the equation (7-7) and the computing method provided by Sergi et al (1992) apparent diffusivity D^* of various ions can be calculated. For unmodified cement, the D^* values of Cl^- , OH^- , Na^+ , and K^+ are 7.4, 19.1, 4.9 and 4.8×10^{-7} cm^2/sec , respectively. For 10%SBR 1-OPC I cement, these values are 4.7, 8.4, 2.9 and 5.8×10^{-7} cm^2/sec , which are lower than that for unmodified paste. This suggests that the ionic diffusion in the SBR modified pastes is slower. The D^* values of various ions for 20%SBR 1-OPC I cement were not calculated because the ion profile did not match the calculation conditions. In addition to, it should noted that the computing method for calculating D^* ignored ionic binding, therefore the apparent diffusivity D^* calculated by this method only provided a relative comparison.

7.3.2.2 Free and Bound Chloride Ions

The chloride ions, no matter whether added during mixing or later transported into concrete, may exist bound with the solid hydration products of cement or in the aqueous pore solution phase. The former is called bound chloride and the later is called free chloride. Since only free chloride ions in the pore solution can move towards steel bars in concrete and possibly destroy the passive film on the surface of the steel bars and initiate corrosion, the chloride binding capacity of concrete is one important factor when considering chloride induced corrosion.

According to the results of steady and non-steady state diffusion, it is evident that to some extent the SBR can improve diffusion properties of the cement paste. A natural question that can be asked is "Does the polymer influence the chloride binding capacity of cement?". So far there is no published paper contributing to this question. Here we hope to give

a guidance to this by analysis of free and bound chloride ion concentrations. Of course, it should be remembered that the conclusions drawn from here only apply to the present experimental material, i.e. SBR 1-OPC I system since different materials, particularly polymer latex, may perform in different ways.

In the above non-steady state diffusion tests, we have obtained chloride concentration profiles in the pore solution for SBR 1-cement pastes. For the same samples, the total chloride ion content was also measured by the method described in section 3.10. Furthermore, to measure evaporated water of pastes, a set of corresponding discs was dried in the oven at 105°C until no further weight loss occurred. As expected, the results showed the content of evaporable water along a cylinder was nearly constant and the average content of evaporable water was 0.27, 0.26 and 0.24 for unmodified paste, 10%SBR 1-OPC I and 20%SBR 1-OPC I, respectively.

With the results of the chloride concentration in the pore solution, the content of evaporable water and the total chloride, the free and the bound chloride ionic profiles can be calculated. Table 7.3 gives their values expressed in terms of concentration per unit weight of sample.

As seen from Table 7.3 and Fig.7.7 the total Chloride ion content in paste was reduced by the addition of SBR. Within a diffusion depth of 20mm, the total chloride ionic content in SBR 1-OPC I pastes was lower than in unmodified cement paste. For instance, at depth 13mm, the total chloride in 10%SBR 1-OPC I is 0.113 and 0.124 in 20%SBR 1-OPC I but 0.242 (mM/g paste) in unmodified cement paste.

Fig.7.8 shows a relationship between bound chloride and the chloride concentration in pore solution. A steady increase in the portion of bound can be seen in all samples when the chloride concentration in pore solution increases. But the polymer reduced this tendency, i.e. reduced the portion of bound chloride, particularly for 20%SBR 1-OPC I paste.

The early studies in the mechanism of chloride ions binding to hydration products have pointed out that the chloride binding capacity is strongly dependent on the chemical components of cement, especially the content of C_3A (Lambert et al 1985) and the content of C-S-H in concrete (Tang et al 1989), but independent of the water cement ratio (Tritthart 1989). In other words, the chloride can be bound to the hydration products in concrete either by chemical binding or by adsorption. This means that the surface area of hydration product C-S-H gel will influence greatly the amount of bound chloride ions. From the study of hydration kinetics of polymer modified cement (see Chapter 4), it was known that SBR reduced the cement hydration rate by binding to cement grains. Similarly, in hardened SBR-cement pastes, the polymer solid or film may adsorb on the surface of hydrates, which occupies some chloride binding sites and possibly causes a reduction of bound chloride ions.

7.3.2.3 Estimate of Service Life

The practical significance of the lower diffusion rate in polymer-cement paste could be assessed by comparing the required induction time for pitting corrosion of embedded rebars at a cover depth (or layer thickness). Based on the mathematical modelling of the non-steady state diffusion process, the diffusion process obeys Fick's second law and a required solution is given by equation (7-6), i.e. the total chloride concentration C can be expressed as a function of x/\sqrt{t} . Plotting C against x/\sqrt{t} , we get two curves in Fig. 7.9. If we assume that the total chloride concentration in the paste is 0.1 for the threshold value which initiates pitting corrosion, then we got two expressions $x = 5.6\sqrt{t}$ and $x = 3.1\sqrt{t}$ for unmodified cement and 10%SBR 1-OPC I paste, respectively. Hence the relationship between the cover depth and the induction time can then established (see Fig.7.10), and consequently the induction time at a cover depth can be predicted. For instance, when the cover depth is 5cm, the induction time is 0.8 years for unmodified cement and 2.6 years for 10%SBR-OPC I. This demonstrates that SBR can delay the induction time for pitting corrosion by about 2 years which may contribute to a longer service life for polymer modified concrete.

7.4 DIFFUSION PROPERTIES OF OTHER POLYMER-CEMENT SYSTEMS

Using the steady state diffusion technique, the effective diffusion coefficients of chloride ions were obtained for other polymer-cement systems. The w/c ratio of pastes varied from 0.3 to 0.5 and the temperature was 25°C. The average diffusion coefficients for four discs are summarised in Table 7.4.

7.4.1 Acrylic-Cement Pastes

It is seen from Table 7.4 that the diffusion characteristics were similar for all acrylics, except Ac 2. Ac 1 and Ac 3 decreased the chloride diffusion slightly through the pastes compared to the unmodified cement paste. An increase of polymer from 10% to 20% did not significantly decrease the chloride diffusion further. The w/c ratio has a great influence on the diffusion property. The diffusion coefficient for paste with w/c=0.3 is only one quarter of that for w/c=0.5. Ac 1-OPC II paste showed similar behaviour.

Ac 4 had a little higher diffusion coefficient than unmodified cement, but Ac 2 considerably increased the rate of chloride diffusion, nearly seven times that of other acrylics. The reason for this effect is probably due to the considerable retardation of cement hydration. As shown in Chapter 4, Ac 2-OPC I only released half the hydration heat of other polymer-OPC I systems during the first 48 hours. This remarkable retardation in hydration resulted in a poor structure development and high porosity. The porosity of Ac 2-OPC I (w/c=0.3, 90 days) measured by MIP was 0.177 cm³/g (see Fig. 7.11), which was much higher than unmodified cement paste (0.10cm³/g) and 10% SBR 1 -OPC I (0.12cm³/g). This total porosity is even higher than the porosity of 3 day old SBR 1-OPC I paste (0.175cm³/g). Thus high porosity resulted in a high rate of diffusion of chloride.

Compared to SBR 1, no significant differences in behaviour were noted between SBR 1

and Ac 1, Ac 3 and Ac 4.

7.4.2 VaVeAc, VaVe, and EVA-OPC I Systems

The pastes modified with VaVeAc, VaVe and EVA had similar diffusion resistances. Unlike SBR and some acrylics, it seems that those polymers slightly increased the rate of chloride diffusion compared to unmodified cement

7.4.3 Influence of Defoamer on Diffusion Property

Because of the surfactants used in the manufacturer of latex, excessive amounts of air can be entrained when latex is mixed into a Portland cement system. In order to avoid this a defoamer is usually incorporated in the latex. For some latexes such as SBR, the defoamer has been incorporated in the latex by manufacturer. For some latexes such as acrylics, the defoamer was directly added to the mixture of latex and cements by user during mixing.

Here, the influence of the defoamer on the diffusion property of Ac 1-OPC I and EVA 2-OPC I pastes have been studied. An oily liquid defoamer was used in this experiment. This defoamer is based on hydrocarbon oil and is capable of controlling foam over wide temperatures and pH variations. The amount of defoamer is 1% and 2% of polymer solid content and was added to the latex and stirred uniformly before mixing with cement. The diffusion test is same as previous process.

From Table 7.4, it can be seen that the diffusion coefficients for pastes with 1% defoamer were nearly same as pastes without defoamer. For example, the diffusion coefficient for 10%Ac 1-OPC I with 1% defoamer is 20.8×10^{-9} cm²/sec, and 20.7×10^{-9} cm²/sec for without defoamer. 10%EVA 2-OPC I has a diffusion coefficient of 31.4×10^{-9} cm²/sec with 1% defoamer and 27.0×10^{-9} cm²/sec without defoamer. However, a 2% defoamer decreased the diffusion coefficient. 10%Ac 1-OPC I with 2% defoamer has half diffusion

coefficient of 1% defoamer.

The reduction of the diffusion coefficient with 2% defoamer may be caused by changes of pore surface property or porosity decrease. However, a parallel test of this project (Salbin 1996) showed that the defoamer (1%) had little effect on the porosity of cement paste. For 10% EVA 2-OPC I paste, the total porosity is $0.08\text{cm}^3/\text{g}$ with 1% defoamer and $0.09\text{cm}^3/\text{g}$ without defoamer. MIP showed that both pastes had almost same pore size distribution. Therefore, one reason is probably due to the changes of pore surface characteristics.

7.4.4 Chloride Diffusion through Pure Polymer Films

In order to understand the behaviour of polymer films on diffusion characteristics of PMC, the diffusion test under steady-state was carried out for pure SBR 1 and Ac 1 films. Preparation of polymer films and experimental set up have been described in sections 3.2.7 and 3.3.12, respectively. The mean diffusion coefficient from two sets experimental results was $86.5 \times 10^{-9} \text{ cm}^2/\text{sec}$ for the SBR film and $113 \times 10^{-9} \text{ cm}^2/\text{sec}$ for the acrylic film. The values have the same order of magnitude as cement pastes under present experimental conditions. From this point of view, the influence of polymer on diffusion property of PMC is the effect of interaction between cement and latex, including changes in pore structure or surface characteristics of pores or possible chemical reaction, not its own diffusion property.

7.5 CONCLUSIONS

1) The chloride ion diffusion characteristics of polymer modified cements have been investigated using steady and non-steady state techniques. Compared with unmodified cement at a given w/c, a suitable polymer addition (10%) reduces effective diffusivity by about 50%. Further additions have little effect.

2) Water cement ratio plays an important part in reducing the rate of chloride ion diffusion. Polymer latexes improve workability and result in the ability to use a lower w/c for the desired workability, thus greatly improving the resistance to chloride ion penetration.

3) The type of polymer affects the diffusion properties of polymer modified cement. SBR, acrylics and EVA have very similar effect. The presence of a reactive component in the polymer chain (Ac 4) and long side chains (VaVe and VaVeAc) have little effect on diffusion characteristics. In contrast the polymer (Ac 2) which significantly retards cement hydration greatly increases the diffusivity of chloride ions.

4) Surfactants and carboxyl groups in the polymer affect diffusion property of PMC. However, whether polymers are added as a latex or redispersible powder does not have effect on this aspect.

5) Increasing temperature increases the diffusivity of chloride ions in the SBR 1-OPC I system as could be expected. The values of activation energies calculated from Arrhenius plots showed little difference at a w/c of 0.3 and a slight increase at a w/c of 0.5 compared to unmodified cements. These observations suggest that the polymer has only a minor effect on the diffusion mechanism.

6) According to the results of the diffusion experiment using pure SBR 1 and Ac 1 films, it is noted that the diffusion coefficients are nearly the same for those for the cement paste and demonstrates that the polymer films themselves do not provide increased resistance to chloride ion penetration.

7) Using the non-steady state technique, diffusion profiles of free and total chloride, hydroxyl, sodium and potassium ions were determined in SBR 1-OPC I system. The results confirm that SBR modified cements reduce penetration of chloride ions. Further data suggests that when the p/c is over 10% the cement loses its capacity to bind

chlorides.

TABLE 7.1

Quality Diffusivity of Chloride Ion for SBR (40°C) (page)

Temperature (°C)	$D \times 10^6$ (cm ² /sec)					
	WA-002 SBR (%)			WA-003 SBR (%)		
	0	10	20	0	10	20
7	1	3.4	5.1	14.6	21.3	32.1
	12	14.5	3.7	18.9	11.5	14.8
	8.1	4.5	6.5	21.1	11.5	14.1
	12.1	10.7	11.7	22.1	10.2	7.4
	Avg. 7.2	8.3	7.3	22.1	13.6	18.8
14	20	17.0	17.0	50.1	24.3	19.3
	17.5	17.0	2.9	34.1	16.3	21.3
	11.7	17.0	12.1	24.1	14.4	19.3
	14.0	21.1	13.4	50.7	10.7	25.6
	Avg. 14.7	18.7	11.1	46.3	18.7	28.3
25	17.1	12.6	12.6	98.4	37.1	35.1
	15.0	11.7	11.7	98.7	17.3	37.3
	28.1	16.7	16.7	102	41.5	36.1
	14.3	8.6	8.6	107	42.6	42.1
	Avg. 21.3	11.3	17.6	101	42.6	39.2
35	30.0	19.8	21.1	114	72.2	35.4
	31.0	12.2	21.7	152	32.3	50.1
	26.7	21.0	24.1	136	44.7	62.6
	41.6	23.4	28.1	142	10.1	66.3
	Avg. 33.7	17.1	24.6	133	47.6	61.0
40	37.1	22.0	32.0	190	14.1	27.1
	39.0	25.0	34.1	200	12.0	26.1
	44.3	28.1	31.3	211	12.0	26.1
	37.3	30.1	30.0	227	14.0	30.5
	Avg. 37.7	26.4	34.2	216	17.2	33.6

TABLE 7.1

Effective diffusivity of chloride ion for SBR 1-OPC I paste

Temperature (°C)	D X 10 ⁹ (cm ² /sec)					
	W/C=0.3			W/C=0.5		
	SBR (%)			SBR (%)		
	0	10	20	0	10	20
7	7.5	3.4	5.3	34.6	21.2	12.8
	7.8	4.3	5.7	38.9	11.5	14.8
	8.1	4.5	6.5	33.1	11.5	8.1
	13.3	5.0	11.7	42.1	10.2	7.4
	Ave.9.2	4.3	7.3	37.2	13.6	10.8
14	10.6	5.1	8.6	58.5	24.3	19.3
	10.5	6.5	9.8	34.1	16.3	21.3
	11.9	12.0	12.5	44.5	14.4	35.8
	13.0	11.3	13.6	50.7	19.7	35.8
	Ave.11.5	8.7	11.1	46.9	18.7	28.1
25	20.8	14.2	15.6	98.4	37.4	35.1
	18.7	11.3	14.7	98.7	37.5	37.3
	23.1	10.8	10.7	103	41.8	39.2
	24.9	13.2	9.4	103	42.6	41.5
	-	-	-	-	46.1	42.9
Ave.21.9	12.3	12.6	101	42.8	39.2	
35	26.8	19.8	22.3	116	72.5	55.6
	31.3	22.2	23.7	137	82.5	59.3
	35.2	21.0	24.2	136	85.1	62.6
	40.6	25.4	28.2	111	110	63.5
	Ave.33.5	22.1	24.6	125	87.0	61.0
45	52.9	22.9	32.9	190	116	273
	55.6	25.0	34.2	204	126	281
	65.8	28.9	34.3	211	138	391
	66.4	29.7	36.6	257	148	405
	Ave.60.2	26.6	34.3	216	132	338

TABLE 7.2

Ionic concentration profiles for SBR 1-cement pastes with a w/c ratio of 0.5

Type of paste	Depth (cm)	C_{OH^-} (mole/l)	C_{Cl^-} (mole/l)	C_{Na^+} (mole/l)	C_{K^+} (mole/l)
Pure-Cement Paste	0.18	0.087	0.890	0.822	0.067
	0.45	0.096	0.879	0.805	0.090
	1.00	0.164	0.504	0.467	0.218
	1.35	0.188	0.464	0.431	0.232
	1.90	0.204	0.342	0.404	0.249
	2.25	0.303	0.300	0.248	0.301
	2.80	0.330	0.200	0.234	0.280
	3.15	0.392	0.126	0.182	0.307
	3.70	0.400	0.084	0.172	0.316
	4.05	0.403	0.079	0.170	0.330
	4.60	0.420	0.063	0.168	0.330
	4.95	0.431	0.047	0.154	0.339
	5.50	0.434	0.037	0.131	0.339
	5.85	0.446	0.010	0.127	0.342
	6.30	0.449	0.005	0.126	0.354
SBR10 - Cement Paste	0.18	0.082	0.798	0.752	0.075
	0.45	0.084	0.775	0.714	0.098
	1.00	0.168	0.492	0.468	0.226
	1.35	0.183	0.379	0.352	0.183
	1.90	0.352	0.226	0.237	0.257
	2.25	0.358	0.153	0.220	0.311
	2.80	0.415	0.095	0.196	0.335
	3.15	0.452	0.068	0.181	0.359
	3.70	0.420	0.063	0.184	0.348
	4.05	0.467	0.058	0.169	0.361
	4.60	0.461	0.063	0.151	0.363
	4.95	0.475	0.032	0.143	0.363
	5.50	0.462	0.030	0.130	0.355
	5.85	0.467	0.010	0.138	0.338
	6.30	0.474	0.000	0.149	0.340
SBR20%-Cement Paste	0.18			0.792	0.086
	0.45	0.095	0.879		
	1.00			0.375	0.234
	1.35	0.167	0.492		
	1.90			0.255	0.253
	2.25	0.290	0.258		
	2.80			0.244	0.282
	3.15	0.305	0.204		
	3.70			0.240	0.274
	4.05	0.35	0.171		
	4.60				
	4.95				
	5.50			0.229	0.300
	5.85	0.431	0.132		
	6.30				

TABLE 7.3

Total, Free and Bound Chloride Concentration Profile of SBR 1-OPCI Paste in Non-Steady-State Diffusion

Depth (mm)	Unmodified OPC I			10% SBR 1-OPCI			20% SBR 1-OPCI		
	Total Cl ⁻ mM/g paste	Free Cl ⁻ mM/g paste	Bound Cl ⁻ mM/g paste	Total Cl ⁻ mM/g paste	Free Cl ⁻ mM/g paste	Bound Cl ⁻ mM/g paste	Total Cl ⁻ mM/g paste	Free Cl ⁻ mM/g paste	Bound Cl ⁻ mM/g paste
1.75	0.530	0.259	0.271	0.557	0.220	0.337			
3.50	0.437	0.246	0.191	0.416	0.196	0.220	0.266	0.231	0.035
9.00	0.319	0.138	0.181	0.205	0.120	0.085			
12.5	0.242	0.127	0.115	0.113	0.092	0.021	0.124	0.117	0.007
18.0	0.185	0.094	0.091	0.088	0.068	0.020			
21.5	0.140	0.082	0.058	0.072	0.046	0.026	0.065	0.061	0.004
27.0	0.091	0.055	0.036	0.051	0.024	0.027			
30.5	0.075	0.035	0.040	0.042	0.017	0.025	0.053	0.047	0.006
36.0	0.072	0.023	0.049	0.042	0.016	0.026			
39.5	0.052	0.022	0.028	0.022	0.015	0.007	0.045	0.037	0.008
45.0	0.051	0.017	0.034	0.020	0.016	0.004			
48.5	0.039	0.013	0.026	0.018	0.008	0.010	0.033	0.031	0.001
54.0	0.040	0.010	0.030	0.008	0.008	0.000			
57.5	0.035	0.003	0.032	0.000	0.003	0.000			
63.0	0.032	0.001	0.031						

TABLE 7.4

Effective Diffusivity for all Polymer-cement Pastes

System	Effective Diffusivity, D (x 10 ⁹ cm ² /sec) 25°C		
	0.3	0.35	05
OPC I	21.9	35.9	101.0
OPC II			63.2
10%SBR 1-OPC I	12.3		42.8
20%SBR 1-OPC I	12.6		39.2
10%SBR 2-OPC I			68.1
20%SBR 2-OPC I			43.5
10% Aq comp-OPC I			141.0
20% Aq comp-OPC I			138.0
10%Ac 1-OPC I 1% Defoamer	20.8		71.2
20%Ac 1-OPC I 1% Defoamer	15.6		65.2
10%Ac 1-OPC II 1% Defoamer			25.6
20%Ac 1-OPC II 1% Defoamer			27.7
10%Ac 1-OPC I 0% Defoamer	20.7		
10%Ac 1-OPC I 1% Defoamer	20.8		
10%Ac 1-OPC I 2% Defoamer	10.4		
10% Ac 2-OPC I 1% Defoamer	148.0		
10% Ac 3-OPC I 1% Defoamer			52.6
10%Ac 4-OPC I 1% Defoamer	28.0		
10%VaVeAc-OPC I 1% Defoamer			76.1
10%VaVe-OPC I 1% Defoamer	28.8		
10% EVA 1-OPC I 1% Defoamer	27.7	38.5	
10% EVA 3-OPC I 1% Defoamer		34.5	
10% EVA 2-OPC I 1% Defoamer		27.0	
10% EVA 2-OPC I 0% Defoamer		31.4	

note: the results of EVA 2 and EVA 3 from a parallel project (Salbin 1996)

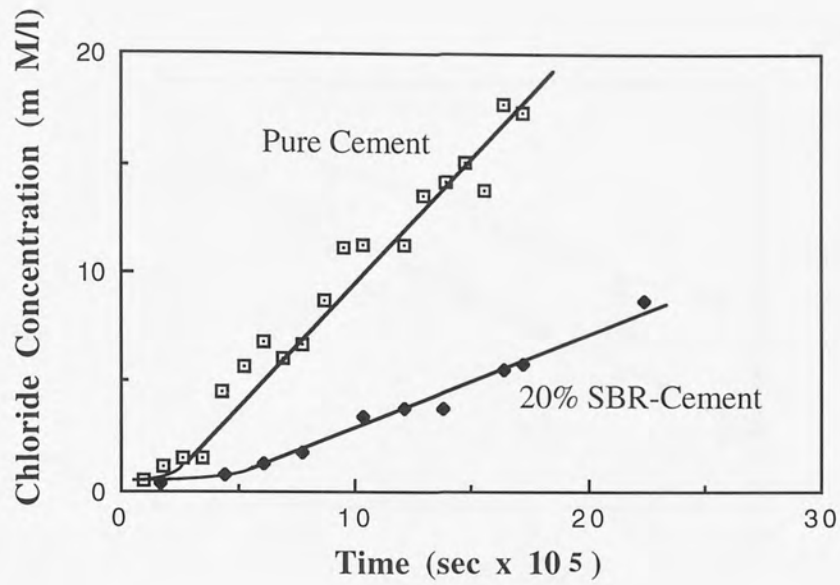


Fig.7.1 Chloride diffusion through pure cement paste and SBR 1-cement at $w/c=0.3$ and 25°C

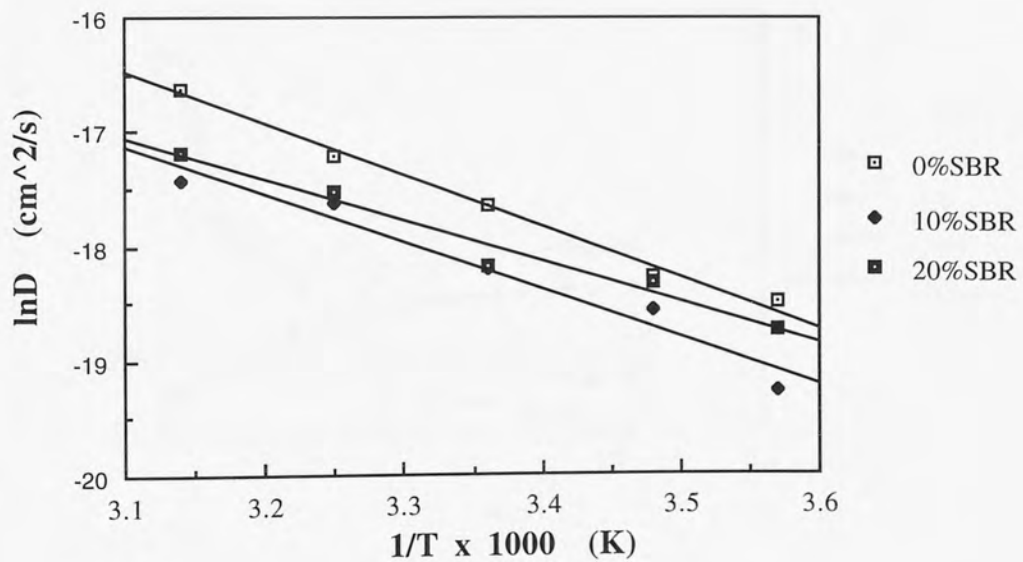


Fig.7.2 Arrhenius plots for SBR 1-OPC I system with $w/c=0.3$

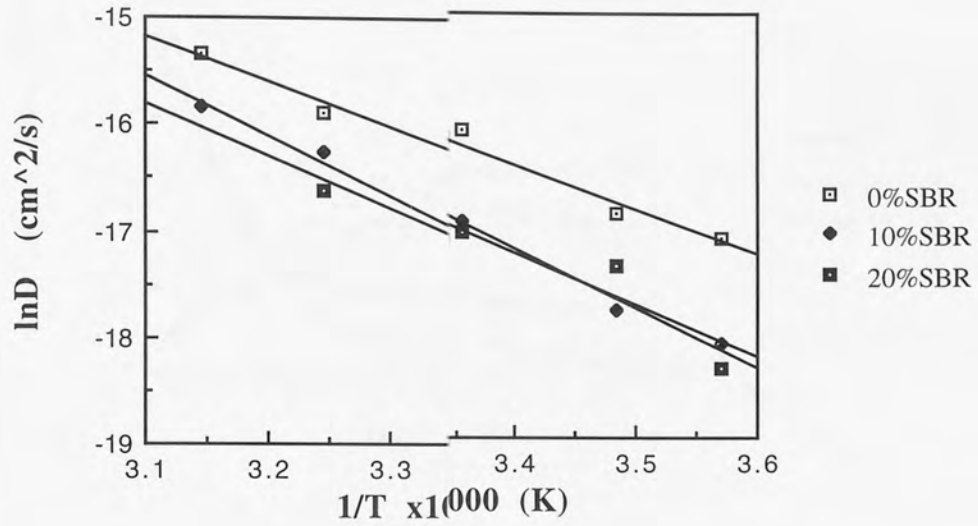


Fig.7.3 Arrhenius plots for SBR 1-OPC I system with w/c=0.5

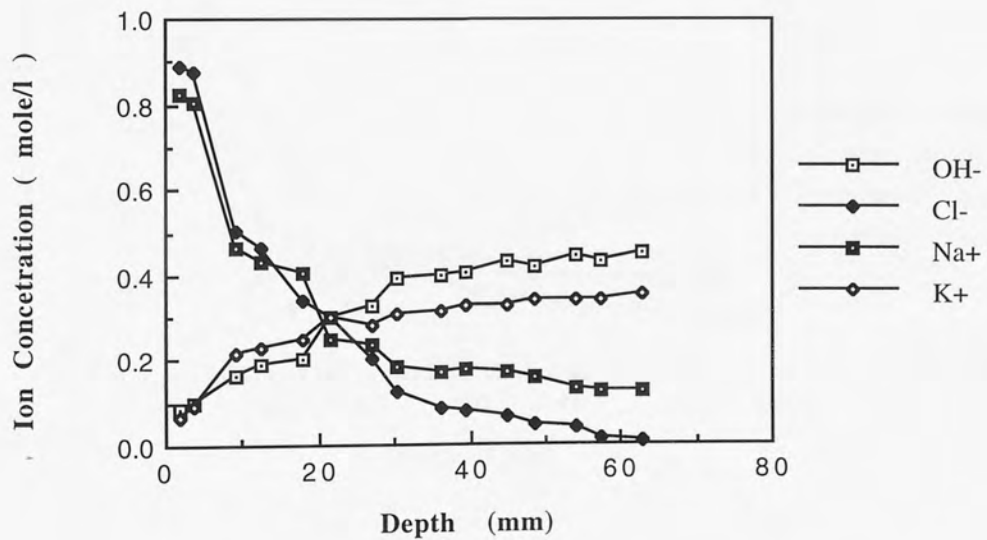


Fig. 7.4 Ionic concentration profile of pure cement with w/c=0.5

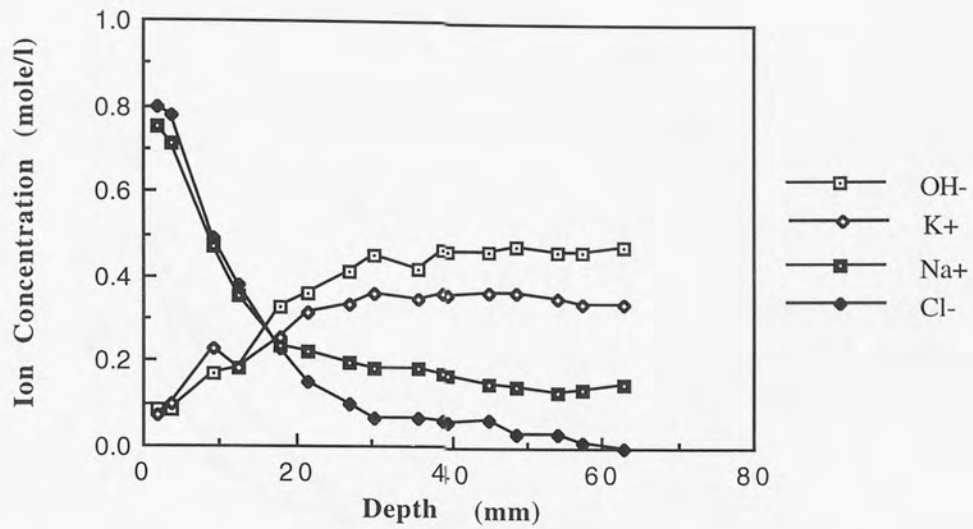


Fig. 7.5 Ionic concentration profile of 10% SBR 1- cement with w/c=0.5

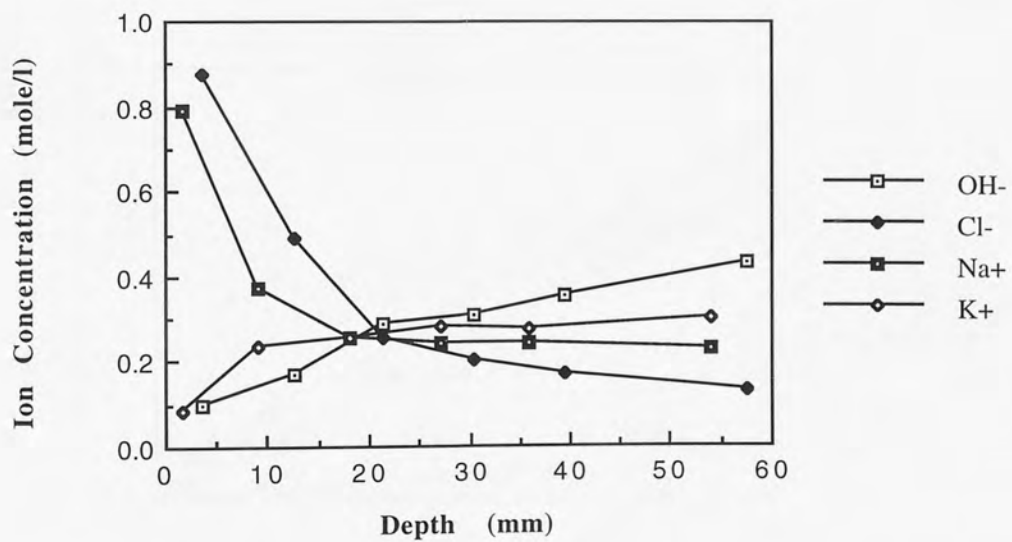


Fig. 7.6 Ionic concentration profile of 20% SBR 1- cement with w/c=0.5 at 20°C

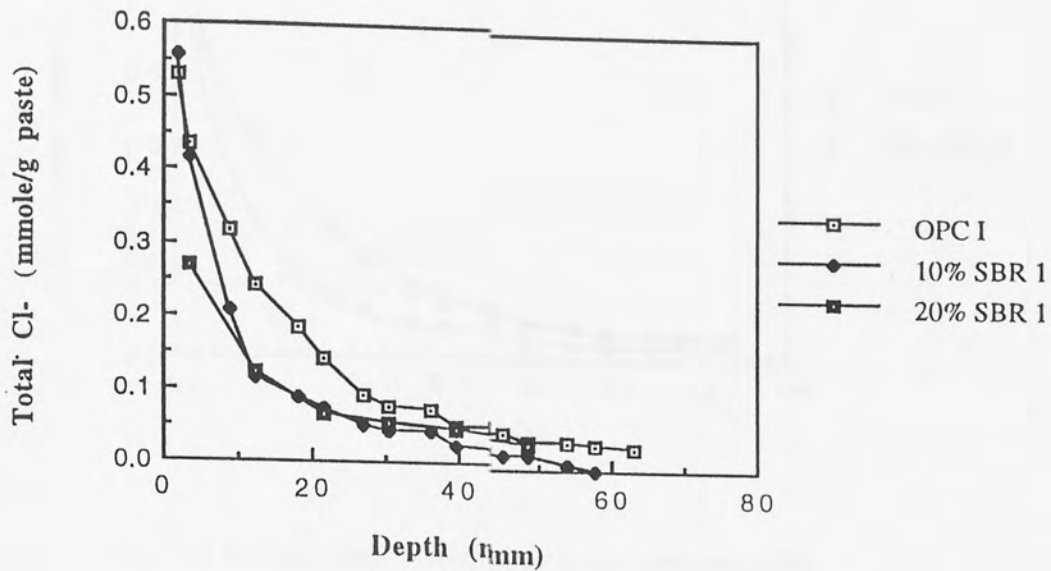


Fig. 7.7 Total Chloride concentration profile in SBR 1-OPC I paste

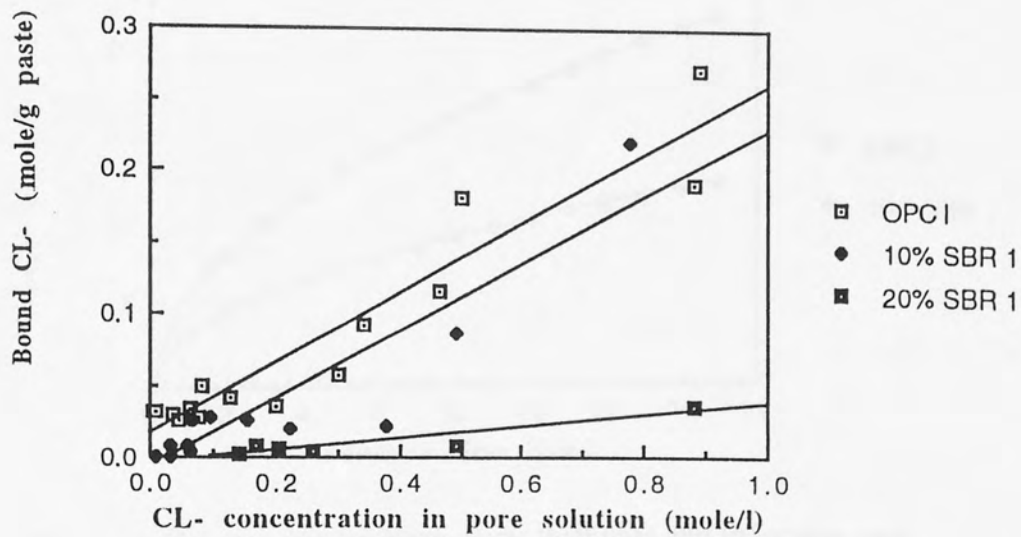


Fig. 7.8 Relationship between bound chloride and chloride concentration in pore solution

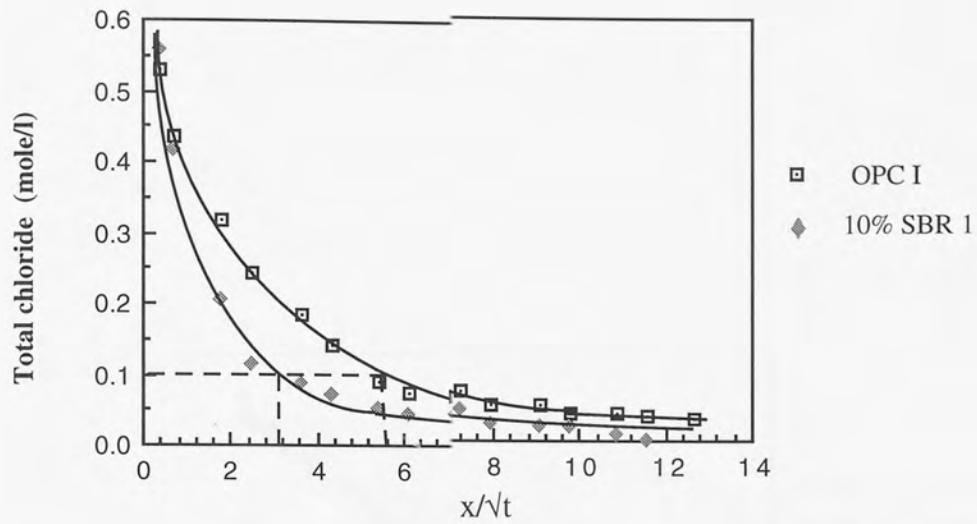


Fig. 7.9 Relationship between total chloride and x/\sqrt{t}

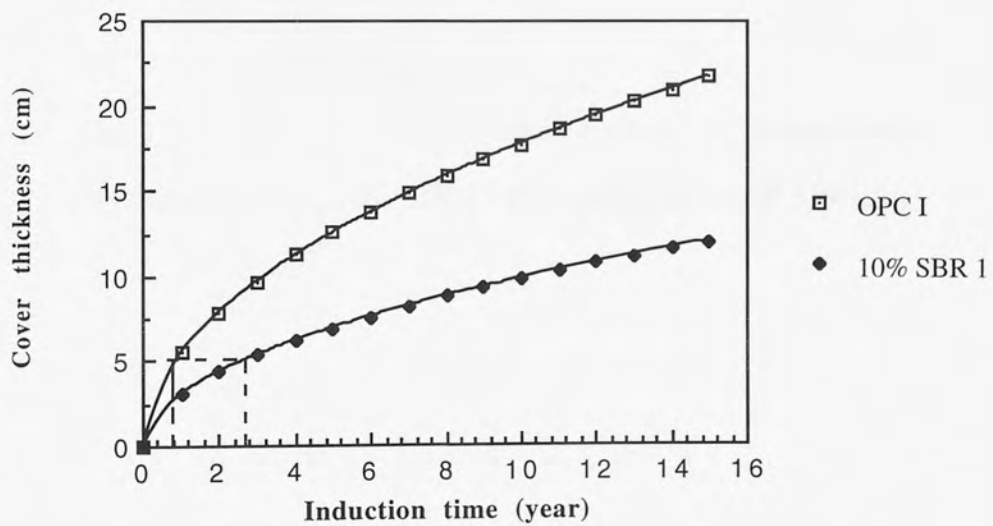


Fig. 7.10 Relationship between cover thickness and induction time

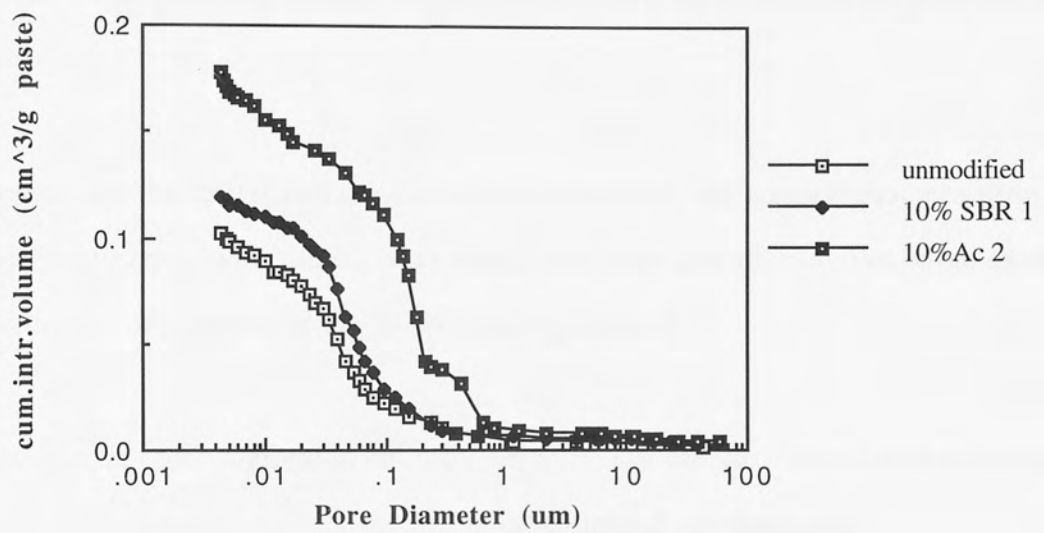


Fig. 7.11 Pore size distribution for 10%Ac 2-OPC I compared to unmodified and 10%SBR 1-OPC I paste, at w/c=0.3, 90 days

CHAPTER 8

GENERAL DISCUSSION, CONCLUSION AND FURTHER WORK

The aim of this study was to identify the fundamental nature of the interactions between hydrating cement phases and polymer particles in a PMC, and the role of these interactions in determining composite properties such as resistance to chloride ion diffusion.

Investigations on the hydration kinetics and microstructure, including characterisation of cement hydration products, the polymer phases and pore size distribution, were carried out and a model of microstructural development proposed.

The resistance of these systems to chloride ion diffusion was determined and an attempt was made to relate results to the model of microstructural development.

Most of the work was carried out using SBR latexes although supplementary experiments utilised acrylics, ethylene vinyl acetates and versatates. All of these systems are available commercially.

8.1 HYDRATION KINETICS OF PMC

Hydration experiments for all the polymer-cement systems were carried out using conduction calorimetry. By connecting a computer to the calorimeter, all experimental data were automatically recorded at desirable time intervals. This ensured that heat output was accurately calibrated and avoided the experimental errors caused by analysing data from a chart recorder output as in previous work (Shaw 1989).

The general conclusion obtained was that all the polymers used in this work retarded

cement hydration. Firstly, they prolonged the induction period by suppressing the nucleation of cement hydration products and secondly they restrained the growth of these phases during the acceleration period, the overall effect being a reduction in total heat output. The extent of retardation depended on the p/c so that with e.g. SBR, quite low concentrations had a significant effect during the acceleration period whilst higher concentrations had a greater influence on the induction period.

Retardation was reduced when the w/c ratio or the alkalinity of cement was increased, whilst the aqueous component of the latex had little effect. Significantly increased concentration of carboxyl groups in the SBR polymer increased retardation. It is thought that this results from an increased binding between the carboxyl groups of the polymer and hydration sites on the surface of the cement grains.

Generally the retardation of cement hydration in PMC may be caused by possible interactions between the polymer phase and cement particles. These interactions may be physical and/or chemical, the latter being from carboxyl groups as mentioned above. Adsorption of polymer particles onto cement grain surfaces reduce the number of sites available for calcium dissolution and C-S-H gel formation. The layer of polymer particles around the cement grains form a barrier to water and ionic diffusion.

Increased temperature reduced the induction period, reduced the time to reach maximum heat output, and increased the maximum heat output. Using this data the hydration kinetic parameters for the acceleration period were calculated using both the Avrami and Jander hydration models. Values of activation energy suggested that at higher concentrations of polymer (>10%) the mechanism for cement hydration changed from control by diffusion of ions through growing interactive layer to control by diffusion of water to interactive sites.

An attempt was made to calculate the hydration kinetic parameters for the induction period by the application of classical nucleation theory and the assumed relationship

between the induction time and polymer addition given by Krstulovic (1992). Gibbs free energy of activation did not significantly change with different polymer additions but the rate constant decreased with increasing polymer. This suggested that the polymer may not change the initial energy barrier for hydration but reduced the nucleation rate.

Results from pore solution expression and analysis showed that virtually all of the polymer disappeared from the pore solution during the first three days of curing. It is unlikely that they coalesced into larger polymer particles (which would be easily observed in the SEM) and thus it may be concluded that the polymer particles have adsorbed onto the surface of cement grains during the early stages of hydration. This results in retardation of hydration as observed during the isothermal calorimetry experiments. Furthermore the concentration of hydroxyl ions was initially very low compared to those found in unmodified cements correspond to slower dissolution rates of alkali.

8.2 MICROSTRUCTURE OF PMC

Engineering properties of PMC such as strength and resistance to penetration of e.g. chloride ions depend on microstructure. In this work, pore size distribution and the total porosity of samples were measured by mercury intrusion porosimetry (MIP). In view of the possible limitations of this technique, other methods such as solvent exchange, water absorption and helium pycnometry were also used. Results showed that the different techniques gave different values for total porosity. However, they also showed the same tendencies, i.e. the total porosity of PMC depended on the type of polymer and the curing regime. It was concluded that MIP was a useful technique for comparing the influence of various parameters on pore size distribution.

The microstructure of PMC developed slowly at early ages owing to the retardation of cement hydration. In the first few days, this retardation resulted in a large total porosity

and a pore size distribution with a large fraction of coarse pores. After 28 days for pastes with a w/c ratio of 0.3, these differences had been largely eliminated. However, for a w/c ratio of 0.5, after 28 days the influence of the polymer was still evident. After 90 days, the total porosity rapidly reduced so that the PMC had about the same total porosity or a little coarser pore structure compared to unmodified cement. (Note: if retardation is excessive, as e.g. with Ac 2, then the total porosity can be 2x that of the unmodified cement.)

The addition of the aqueous component of latex on its own, had no effect on the pore structure. A higher carboxylation concentration in the latex particles resulted in a larger total porosity. These results are in keeping with the retardation effects described in the calorimetry studies.

The distribution of the polymer in a hardened cement paste was investigated by several techniques but is still not fully understood. Scanning electron microscopy (SEM) was used to examine the morphology of fracture and etched fracture surfaces. The SEM image showed that PMC has a fishing-net or honeycomb type of structure. On the etched fracture surface, some rings were clearly observed. It was thought that these rings were the coalesced polymer networks which were left after the cementitious phase was dissolved away by acid. These rings are believed to be polymer intimately combined with C-S-H gel. No distinct polymer film which e.g. bridged both sides of the microcracks has been observed.

Comparison of infrared spectra of SBR modified and unmodified cements were very similar, showing no evidence for a chemical reaction. In the case of Ac 1, EVA 1 and EVA 3 polymer modified cements a small new absorption band at 1560cm^{-1} , suggested the formation of a calcium salt of carboxylic acid.

8.3 A MODEL FOR MICROSTRUCTURE DEVELOPMENT OF PMC

In an early SEM study on polymer modified cement, Isenburg (1974) observed the presence of a distinct polymer film and used this evidence for a hypothesis for reinforcement of Portland cement by polymer latex. Subsequently, Ohama (1987) presented a simple three-step model showing how such a film may arise. The first step is the normal cement hydration process; the second and the third steps are related to the flocculation of the polymer particles onto cement grains and film formation due to the consumption of water. This model considered the cement hydration and the coalescence of the polymer particles as two separate processes and did not consider the influence of polymers on the hydration process itself. Furthermore, attempts to reproduce samples showing a distinct polymer film have not been fruitful either in the present work or other laboratories.

The stages of microstructure development are considered in more detail below and in Fig. 8.1.

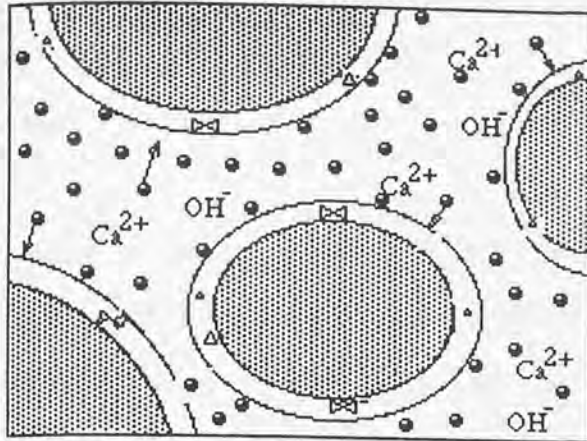
The first stage is the initial hydration reaction of cement and flocculation of polymer particles to the surface of the cement grains. On immediately mixing the cement with a latex, the initial reactions of cement take place as usual because these reactions happen quickly and a relatively large amount of water is available. Meanwhile, some of the polymer particles are moving towards the cement grains and are bound on the surface of the grains by e.g. Van der Waals' forces.

The second stage includes the induction period of the cement hydration and interactions between polymer and cement. During this stage, more polymer particles are bound onto the surface of the cement grains and some of them may combine with calcium ions, via carboxyl groups, to form complexes. These particles form a barrier layer of polymer, which reduces the number of reaction sites and blocks calcium dissolution. In addition any calcium ions which do dissolve may be bound with free polymer in the pore

solution although we have no evidence of this. As a result of the barrier layer and binding of calcium ions in solution, nuclei formation of C-S-H gel and Ca(OH)_2 respectively, are very slow. The hydration of cement at this stage is thus retarded, resulting in a long induction time.

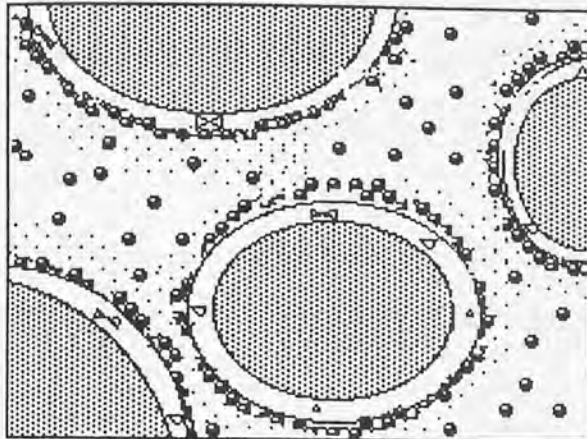
In the third stage, the hydration of cement enters the acceleratory period when hydration of C_3S to give C-S-H gel proceeds rapidly. In addition, with a difference of osmotic pressure, the growth of the "outer" C-S-H gel may produce enough stress to break the barrier layer of polymer leading to a faster hydration reaction. However, the new surfaces of C-S-H gel adsorb more polymer particles from the solution. The growth of Ca(OH)_2 crystals is confined in a small space due to the adsorption of polymer, resulting in small sized Ca(OH)_2 crystals. By this stage a multilayer of polymer particles may surround the cement grains (see Appendix C) followed by coalescence into a film like structure.

Further growth of the C-S-H gel and Ca(OH)_2 crystals occurs in the pore spaces between cement grains so that the porosity is reduced. This growth and that from adjacent particles result in the formation of polymer C-S-H gel rings. These rings connect with each other and form a network structure in the hardened cement paste. SEM clearly shows this ring type structure when an acid etches the surface of a paste.

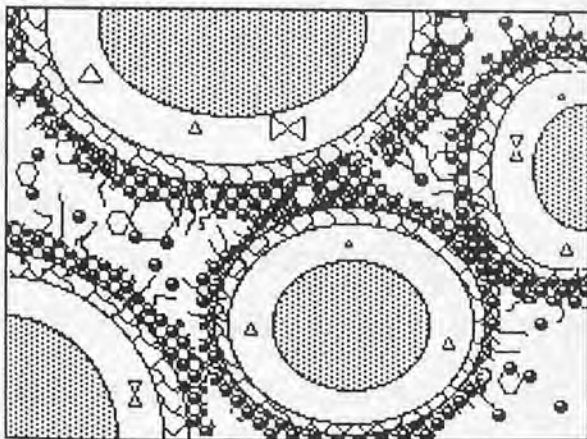


(a)
Initial hydration of cement,
 Ca^{2+} and OH^- leaching into solution;
Polymer particles moving towards
cement grains and adhering on the
surfaces of the cement grains.

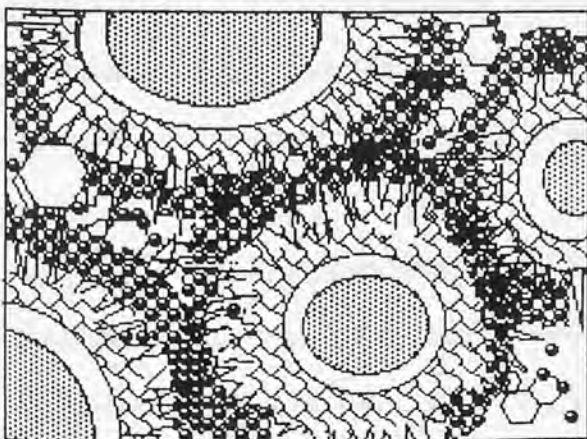
• = polymer particles



(b)
Induction period of cement hydration,
surface hydration layer formation;
Monolayer of polymer particles formed on
surface of cement grains;
Complexes may be formed between Ca^{2+} and
polymer.



(c)
Acceleratory period of cement hydration,
growth of $\text{Ca}(\text{OH})_2$, C-S-H gels and
"outer" C-S-H formation;
Multilayer of polymer particles formed on
surface of cement grains;
Some polymer particles coalesce into larger size
particles or polymer film.



(d)
Hydration of cement continues slowly;
C-S-H gels interweave;
Polymer particles films formation
and join together and merge with C-S-H
gels and $\text{Ca}(\text{OH})_2$ to produce polymer rich
rings.

Fig.8.1 Microstructural developing model of polymer modified cement

8.4 INFLUENCE ON ENGINEERING PROPERTIES

8.4.1 Strength

Using the model described in the previous section it may be considered that the interfacial nature of C-S-H gel and Ca(OH)_2 contact points have changed. The polymers on the surface of C-S-H gel or Ca(OH)_2 crystals probably act as a "bonding agent", which increases the connection between hydrates. It may then be assumed that the increase in tensile/flexural strength of PMC is due to this improvement in the connection of interfaces between hydration products.

Such a process could have two effects - (i) blunting of crack tips thus reducing stress concentrations, and (ii) bridging the faces of cracks thus making their propagation more difficult.

8.4.2 Diffusion

Influence of Polymer Type

Using the steady state method a range of polymer types were investigated. Compared with the unmodified cement at a given w/c, values of D were reduced to about a half with SBR, to about three quarters with all but one of the Acrylics and are about the same with EVA and vinyl versatate. In the case these acrylics and EVAs, values of D are reduced slightly by increasing additions of defoamer. The form in which the polymers are added, emulsions or redispersible powders, does not affect the diffusion properties.

In the case of one polymer addition, Ac 2, the value of D was about seven times larger than that of the unmodified cement. This was attributed to its considerable retardation effect which in turn resulted in a greater total porosity and coarser pore size distribution, see Fig. 7.11.

Influence of w/c

As expected the water cement ratio was an important factor governing the rate of diffusion of chloride ions in both modified and unmodified pastes. Thus a reduction in w/c from 0.5 to 0.3 resulted in a decrease in effective diffusivities by about four to five times.

It is known that the polymer acts as a plasticiser in that the w/c may be reduced whilst the workability is still maintained (Salbin 1996). It thus may be more appropriate to compare the modified and unmodified systems at constant workability rather than constant w/c. For example, the effective diffusion coefficient for the 10% SBR 1 modified paste at 25°C with a w/c of 0.3, was less than one eighth of that for the unmodified paste with a w/c of 0.5, a significant improvement, and the workability of the former was as good as that for the later (Salbin 1996). Such improvements may then be interpreted in terms of the porosity of the pastes, where reductions in w/c from 0.5 to 0.3 result in a lower total porosity and finer pore structure for both unmodified and modified pastes.

Influence of p/c

At a given w/c and temperature the addition of 10% SBR 1 reduced the diffusivity of chloride ions to about one half the value found for the equivalent unmodified cement paste. Increasing the addition of SBR 1 to 20% does not significantly further reduce the diffusion coefficient, being about the same as, or in some cases greater than, that for the 10% addition, see Table 5.2. This is in keeping with observations of changes in porosity that for a given w/c the p/c has little effect, see Fig. 5.3. These results suggest that there is little merit in additions of polymer as high as 20% although this value represents the upper limit used in practice (on cost grounds).

Influence of Temperature

For SBR 1 at a given w/c and p/c the chloride diffusivity generally increased systematically with increasing temperature. Values of activation energy calculated from

Arrhenius plots showed little difference at a w/c of 0.3 and a slight increase at w/c 0.5 compared to the unmodified cement. These observations suggest that the polymer has little effect on the diffusion mechanism.

The Polymer Film

Since it is often assumed that the polymer phase exists as a distinct film binding the hydration products it was decided to determine their diffusion characteristics. The mean diffusion coefficient from two sets of experimental results was 86.5 (SBR 1) and 113.5 (Ac 1) $\times 10^{-9}$ cm²/sec. The values have the same order of magnitude as unmodified cement pastes under present experimental conditions. Infra-red spectra of the films before and after diffusion were similar, demonstrating that there is no binding between chloride ions and the polymers. These results would suggest that the polymer film in itself would not offer a more resistant barrier to diffusion. However, it was noted that during these experiments the polymer films was able to swell and therefore diffusivity values given above are probably overestimated. In the present model the polymer is intimately combined with C-S-H gel. They are not likely to be same as the pure polymer film and may be more resistant to swelling.

SBR 2 modified pastes

Owing to limited amount of the special SBR 2 available the diffusion test was only carried out at 25°C and a w/c of 0.5. The effective diffusion coefficients were 68.9×10^{-9} cm²/sec for 10% SBR 2 and 43.5×10^{-9} cm²/sec for 20% SBR 2. These values were slightly greater than those found when using SBR 1 but still less than for unmodified cement. Since the main difference between SBR 1 and SBR 2 was the degree of carboxylation, differences in the diffusion characteristics should come from the effect of carboxylate. It was shown that the concentration of carboxyl groups retarded cement hydration and increased porosity. Therefore, an excess of carboxylate in the latex appears to not improve the diffusion property of polymer modified cement.

Aqueous Component modified Pastes

In order to understand the influence of other latex components, principally free surfactant, on the chloride ion diffusion, similar diffusion tests were carried out for cement modified with the aqueous component of the latex, i.e. no polymer particles were present. The values were higher than the values for unmodified cement paste and nearly three times that of the modified pastes. It is interesting to note, however, that the aqueous component had little effect on hydration kinetics and the porosity is not changed, Fig. . The reason for the increased diffusion rate could be that surfactant molecules adsorb on pore surfaces changing their characteristics, or occupy the chloride binding sites. In fact, it should be noted that the existing form of surfactants in latex is different from that in the aqueous component only. In the latex, surfactants are usually bound to the surface of the latex solid, whilst in the aqueous component they are free in the liquid and this may be one of reasons for significant difference between polymer modified and the aqueous component.

Non-steady state technique

Using the non-steady state technique, diffusion profiles of free and total chloride ions were determined. The results confirm that SBR modified cements reduce penetration of chloride ions. Data suggests that the binding capacity of cements is reduced by the presence of polymer and this is particularly so at p/c of >10%. These results are in agreement with the model whereby polymer particles are bound to hydrate surfaces thus obstructing chloride ion binding sites.

8.5 CONCLUSIONS

1) All latexes used in this study acted as retarders for cement hydration, but the extent of retardation depended on the type and addition of polymer. The polymer solids are more important than the aqueous component of the latex. At higher additions of polymer the mechanism for cement hydration is changed.

2) Pore solution analysis shows polymer particles remove from solution within 3 days and concentration of OH^- , Na^+ and K^+ in PMC are reduced. These observations are probably a result of polymer-cement surface interactions since there was no evidence of chemical reactions/degradation of the polymer.

3) Samples of well cured polymer modified cements exhibited coarser pore structures compared with unmodified cements at early ages, but both have similar pore structures in later ages (after 90 days).

4) SEM images show that a non-uniform distribution of the polymers exists in a network formation. The network consists of an intimate mixture of polymer combined with cement hydrates and binds the bulk of the other cement hydrates. No evidence was found for the formation of a separate and distinct polymer film phase.

5) Some evidence of reactions between Ac 1, EVA 1 and EVA 3 polymer and cement was provided by IR.

6) In general at constant w/c, PMC shows a small reduction in the effective diffusivity of chloride ions compared to unmodified cements. Larger reductions in diffusivity may be obtained when using a lower w/c as a result of the improved workability. Latexes which excessively retard cement hydration result in cement matrices with poor resistance to diffusion. There is some evidence to suggest that high addition of polymer reduce the chloride binding capacity of the cement.

7) Thermoanalytical investigations have shown that DTA/TGA techniques are not suitable for determining degree of hydration or the calcium hydroxide content of a PMC. These techniques could, however, play a very useful role in identifying the type of polymer and the quantity used in samples where this is in doubt, e.g. when assessing failure of a material the source of which is unknown.

8.6 FURTHER WORK

This project has studied several aspects of the characteristic properties of polymer modified cement, but there are still some areas or questions raised in this study which have not been researched in detail within the timescale available. For further work, two areas are recommended when the conditions make the researches possible.

One area is to identify the polymer used in the polymer modified cement by thermal analysis techniques and pyrolysis. With increasing application of polymers in practical engineering, it is necessary to identify what type and how much of polymer being used in the samples where this is in doubt or the original materials are unknown. The results of Differential Thermal Analysis (DTA) and Thermal Gravity Analysis (TGA) in Chapter 6 has shown that the thermoanalytical techniques could be a potentially valuable method for this purpose. However, it needs to look at a wider range of polymers to develop and perfect this method for practical application.

The work should include establishing a set of standard curves of DTA and TGA for various polymers and polymer modified cement samples; obtaining a series of calibration curves with a given polymer content and establishing the relationship between polymer level and peak height, peak wide, area under peaks or weight loss. Obviously, the establishment of standard curves is for qualitative analysis, i.e. assessing type of polymer, while the calibration is for quantity analysis. Pyrolysis could be helpful for this research.

Another area is to study oxygen diffusion characteristic of polymer modified cement, which should help further understanding about chloride diffusion mechanism through the polymer modified cement pastes.

In the microstructure study (Chapter 5) and the diffusion characteristic study (Chapter 7), the results have revealed that for mature cement pastes with or without polymer,

they have nearly same porosity, but their diffusion rates of chloride ions are different. We assume that the reason for this is that the polymer changed the surface property of pore walls or pore structure of pastes. The further experiments over aqueous component of latex (free polymer solid) indicated that the aqueous component did neither influence cement hydration, nor porosity and pore structure, but significantly affect chloride ionic diffusion rate. This suggests that the change of diffusion characteristic might cause by the change of surface property of pore walls. However, the function of polymer in the cement paste is different from that of aqueous component because the polymer solid phase may change both pore structure and surface property of pore walls. Oxygen is a neutral molecule without dipolar character, it is not expected to encounter electrostatic surface interactions which may influence the transport of chloride ions in the paste (Ngala 1995). In this case, the oxygen diffusion technique should provide us further information to understand the mechanism which the polymer influences the chloride diffusion through the polymer modified cement paste.

Other areas may concern are that diffusional characteristics of polymer modified cement at high temperature environment and the role of carboxylation and surfactant in latex in determining diffusional mechanisms of polymer modified cement since only limited work have been done in this study.

REFERENCES

- Abdelalim, A. M. K.** (1980) "Mechanical Characteristics of fresh and hardened aluminous cement pastes" PhD thesis, Department of Construction and Environmental Health, Aston University, Birmingham.
- ACI 548.3R-91** (1991), "State-of-the Art Report on Polymer-Modified Concrete", Reported by Committee 548, American Concrete Institute Journal Sept. 1989 pp. 813.
- Adamson, A. W.** (1976), *Physical Chemistry of Surfaces*, A Wiley-Interscience Publication, John Wiley & Sons, London, pp. 372.
- Aimin, X. & Chandra, S.** (1988), *The International Journal of Cement Composite and Lightweight Concrete*, **10** (1), pp. 49-52.
- Al-Qaser, A.N.F., Griffiths, D. L., & Mangabhai, R. J.** (1990), "Diffusion of various ions from sea water into polymer modified cement paste", in Page, C. L., Treadaway, K. W. S., & Baufotl, P. B.(eds), *Corrosion of Reinforcement in Concrete* Elsevier-App. Sci. pp. 246-257.
- Aminabhavi, T. M.** (1982-83), "Use of polymers in concrete technology", *JMS-REV. Macromol, CHEM. PHYS. C22* (1), pp. 1-55.
- Atkins, K. M., Edmonds, R. N. & Majumdar, A. J.** (1991), "The hydration of portland and aluminums cements with added polymer dispersions", *Journal of Materials Science*, **26**, pp. 2372-2378.
- Atkinson, A. & Nickerson, A. K.**(1984), "The diffusion of ions through water-saturated cement", *Journal of Materials Science*, **19**, pp. 3068-3078.
- Auskern, A., Prach, T. & Horn, W.** (1972), "Thermal analysis of polymer filled hardened cement paste", Informal Report, Brookhaven National Laboratory Associated Universities, Inc. Upton, L. I., New York.
- Bares, R. & Czarnecki, L.** (1987), "Concrete polymer composites in RILEM activity-current status and prospects" *The 5th International Congress of Polymers in Concrete*, Brighton, pp. 417-422.

Bassety, J., Denney, R. C., Jeffery, G. H. & Mendham, J. (1978), *Vogel's Textbook of Quantitative Inorganic Analysis*, Longman Scientific & Technical, pp. 753.

Bhargava, J. K. (1981), *Applications of Polymer Concrete*, American Concrete Institute, Publication, SP-69, pp. 205-218.

Buenfeld, N. (1986), "Discussion on 'Permeability of normal and lightweight mortars' contributed by Nyame, B. K." *Magazine of Concrete Research*, **38** (134) pp. 51-52.

Bensted J. (1987), "Some applications of conduction calorimetry to cement hydration" *Advances in Cement Research*, **1**, pp. 35-44.

Burge, T. A. (1987), "Evaluation of polymers for improving cement mortars" *The 5th International Congress of Polymers in Concrete*, Brighton, pp. 293-300.

Chandra, S. & Flodin, P. (1987), "Interaction of polymer with calcium hydroxide and calcium trisilicate", SP119-14 Ottawa Conference pp. 263-268.

Chicago Society for Paint Technology (1969) *Infrared Spectroscopy : Its Use in the Coatings Industry*. Philadelphia, chapter IV, pp. 20.

Clear, K. C & Chollar, B. H (1978), "Styrene butadiene latex modifier for bridge deck overlay concrete", FHWA-RD-78-35.

Concrete Society (1994), "Polymers in concrete" A technical Report No.39 of The Concrete Society's Technical Development Centre, prepared by a Working Party of its Materials Group.

Cook, R.A. & Hover, K. C. (1993), "Mercury porosity of cement-based materials and associated correction factors", *ACI Materials Journal March-April*, pp. 152-161.

Crank, J. (1975), *The Mathematics of Diffusion* (2nd edition), Clarendon Press, Oxford.

Crank, J. & Park, G. S. (1968), *Diffusion in Polymer* Academic Press, London.

Danilov, V.V. (1976), "On hydration mechanisms in cement pastes", *The 6th International Congress on the Chemistry of Cement*, (1974), Moscow, **II** Book 1, pp. 73.

Day, R. L. (1981) "Reactions between methanol and Portland cement paste" *Cement and Concrete Research* , **11** pp. 341-349.

Day, R. L. & Marsh, B. K. (1988), " Measurement of porosity in blended cement pastes", *Cement and Concrete Research* , **18** pp. 63-73

Dennis, R. (1984), "Latex in the construction industry", *Chemistry and Industry*, pp. 505-511.

Dennis, R (1988), "Polymer dispersion or latexes", in Hewlett, P.C.(ed), *Cement Admixtures Uses and Application*, (2nd edition), Longman Scientific and Technical, Chapter 9, pp. 130-143.

Diab, H., Dor, L.B., Wirguin, C.H. & Bonen, D. (1985), "The porosity and compressive strength of polymer-cement", *Cement and Concrete Research* , **15**(6), pp. 1061-1066.

Emberson, N. K. & Mays, G. C. (1990) "Significance of property mismatch in the patch repair of structural concrete, Part 1: Property of repair system" *Magazine of Concrete Research* , **42**(152), pp 147-160.

Evbomwan, N.F.O. (1987) "A state of the art report on the strength and durability properties of polymer modified mortars and concrete", *The 5th International Congress of Polymers in Concrete*, Brighton, pp. 52-59.

Evbomwan, N.F.O. & Hughes, B. P. (1992), "Drying shrinkage of a polymer modified mortar containing microsilica with or without fibres", *The 7th International Congress of Polymers in Concrete*, Moscow, pp. 108-115.

Feldman, D. (1989), *Polymeric Building Materials*, Elsevier Applied Science London New York

Feldman, R.F. (1983) "Fly ash, silica fume, slag and other mineral by-products in concrete" American Concrete Institute, Publication SP-79, 1, pp. 415-433.

Feldman, R.F. (1984) "Pore structure damage in blend cement pastes caused by mercury intrusion" *Journal of American Ceramic Society*, **67**, pp. 30-33.

Gane, P. A. C., Kettle, J. P., Matthewa, G. P. & Ridgway, C. J. (1995), "Void space structure of compressible polymer spheres and consolidated calcium

carbonate paper-coating formulations", A Draft provided by University of Plymouth and English China Clays International R&D.

Gebauer, J. & Coughlin, R. W. (1971), "Preparation, properties and corrosion resistance of composites of cement mortar and organic polymers", *Cement and Concrete Research*, **1**, pp. 187-210.

Ghosh, S. N. (1983), *Advances in Cement Technology*, Pergamon Press, pp. 673-710.

Gierloff, M. (1982), "Resin Dispersion modified concrete under traffic simulation" *The 3th International Congress of Polymers in Concrete*, Koriyama, **1**, pp. 291-310

Gorur, K. V. & Wittman, F. H. (1987), "Hydration of a cement in a polymer system", *The 5th International Congress of Polymers in Concrete*, Brighton, pp. 199-203.

Grosskurth, K. P. & Konietzko, A. (1987), " Structure and mechanical behaviour of polymer modified cement concrete" *The 5th International Congress of Polymers in Concrete*, Brighton, pp. 171-174.

Hackel, E., Beng, P. & Horler, S. (1987), *The 5th International Congress of Polymers in Concrete*, Brighton, pp. 305-308.

Harchard, K.S. & Chandra, V.K. (1980), "Infrared and mossbaure study of two indian cements", *Cement and Concrete Research*, **10** pp. 243-252.

Harrion L. G. (1969), "Theory of Solid Phase Kinetics", in Bamford, C.H.B. & C F H Tipper, C.F.H.(eds), *Comprehensive Chemistry Kinetics*, **2**, Elsevier, London, pp 377-462.

Isenburg, J. E. & Vanderhoff, J. W. (1974), "Hypothesis for reinforcement of portland cement by polymer latexes", *Journal of American Ceramic Society*, **57**(6) pp. 242.

Justnes, H. & Oye, B. A. (1987), "Protection concrete against chloride ingress by latex additions", *The 6th International Congress of Polymers in Concrete*, Shanghai, pp. 261-267.

Justnes, H., Cantens, J. & Polet, J. (1992), "Chloride penetration in mortars modified with different acrylic latexes", *The 7th International Congress of Polymers in Concrete*, Moscow, pp. 125-129

Korshak, V. V. (1971), *Heat-Resistant Polymers*, Israel Program for Scientific Translations.

Krstulovic R. & Krolo P. (1992), "Determination of kinetic parameters in cement hydration", *Proceeding of 9th International Congress on the chemistry of Cement*, New Delhi, 4, pp. 31.

Kuhlmann, L. A. (1981), "Performance history of latex-modified concrete overlays" *Applications of Polymer Concrete*, SP-69, American Concrete Institute, Baltimore, Md. pp 123-144.

Kuhlmann, L. A. (1987), "Application of styrene-butadiene latex modified concrete" *Concrete International* , pp. 48-53.

Kuhlmann, L. A. (1988), "Using styrene/butadiene latex in concrete overlays" *Transportation Research Board*, Session 195.

Kuhlmann, L.A. (1991), "Cracks in latex-modified concrete overlays--How they get there, How serious they are, and What to do about them", *Transportation Research Record*, N1301 pp. 17-21.

Lambert, P. Page, C. L. & Short, N. R. (1985), "Pore solution chemistry of the hydrate system tricalcium silicate/sodium chloride/water", *Cement and Concrete Research*, 15 pp. 675-680.

Larbi, J. A. & Bijen, J. M. (1990), "Interaction of polymers with Portland cement during hydration: A study of the chemistry of the pore solution of polymer modified cement systems", *Cement and concrete Research* , 20, pp. 139-147.

Lavelle, J. A.(1988), "Acrylic latex-modified portland cement", *ACI Materials Journal*, pp. 41-48.

Lewis, W. J. & Lewis, G. (1990), "The influence of polymer latex modifiers on the properties of concrete", *Composites*, 21, No.6 pp. 487-494.

Longuet, P., Burglen, L & Zelwer, A. (1973), "The liquid phase of hydrated cement", *Review of Materials Constructure*, No. 676 pp. 35-41.

Lorprayoon, V. & Rossington, D. R. (1981), "Early Hydration of Cement constituents with organic admixtures", *Cement and Concrete Research*, pp. 267.

Luke, K & Glasser, F. P. (1987), "Selective dissolution of hydrated blast furnace slag cements", *Cement and concrete Research*, **17**, pp. 273-282.

Mark, H. F., Bikales, N. M., Overberger, C. G. & Menges, G. (1987), *Encyclopedia of Polymer Science and Engineering*, A wiley-interscience publication John Wiley and Sons. **5**, pp. 36-67. **16**, pp. 67-77.

Mark, H. F., Bikales, N. M., Overberger, C. G. & Menges, G. (1987) *Encyclopedia of Polymer Science and Engineering*, A wiley-interscience publication John Wiley and Sons. **8**, pp. 662.

Marusin, S. L. (1987), "Microstructure, pore characteristics and chloride ion penetration in conventional concrete and concretes containing polymer emulsions" *Paper SP 99-8, ACI Special Publication SP99*, American Concrete Institute, Detroit, pp. 135-150.

Massazza, F. & Daimon, M. (1992), "chemistry of hydration of cements and cementitious systems", *The 9th International Symposium on the Chemistry of Cement*, New delhi, **IV**, pp. 383-446.

Moukwa, M. & Aiticin, P. C. (1989), "The effect of drying on cement pastes pore structure as determined by mercury porosimetry", *Cement and Concrete Research*, **18**, pp. 745.

Nagaraj, T. S., Iyengar, K. T. S. R. & Rao, B.K. (1988), "Super-plasticized natural rubber latex modified concrete", *Cement and Concrete Research*, **18**, pp.138-144.

NaKayama, M. & Beaudoin, J. J. (1987), "Bond strength development between latex-modified-cement paste and steel", *Cement and Concrete Research*, **17**, pp. 562-572.

Ngala, V. T. (1995) "*Pore structure and Diffusion properties of hardened cement pastes*" PhD thesis, Aston University, Birmingham.

Nishi, T. K. O., Matsuda, M., Chino, K. & Kikuchi, M. (1990), "Porosity and ion diffusivity of latex-modified cement", *Materials Research Society Symposium Proceeding*, **176**, pp. 109-114.

Ohama, Y. (1973), "Study on properties and mix proportioning of polymer modified mortars for buildings", *Report of the Building Research Institute*, No. 65, Tokyo, Japan, Building Research Institute.

Ohama, Y. & Kan, S. (1982), "Effects of Specimen size on strength and drying shrinkage of polymer modified concrete", *The international Journal of Cement Composites and Lightweight Concrete*, **4**, No.4

Ohama, Y. (1984), "Polymer modified mortars and concrete", Chapter 7, *Concrete Admixtures Handbook: Properties, Science, and Technology*, Noyes Publication, Park Ridge, pp. 337-429.

Ohama, Y. (1987), "Principle of latex modification and some typical properties of latex-modified mortars and concrete", *ACI Materials Journal*, **84**, No. 6 pp. 511-518.

Ohama, Y., Demura, K., Hamatsu, M. & Kakegawa, M. (1991), "Properties of polymer-modified mortars using styrene-butyl acrylate latexes with various monomer ratios", *ACI Materials Journal*, **88**, No. 1 pp. 56-61.

Okada, K. & Ohama, Y. (1990), "Current status and trend of concrete-polymer composites in Japan", *The 6th International Congress of Polymers in Concrete*, Shanghai, pp. 28-35.

Oye, B. A. (1989), *Repair systems for concrete-polymer cement mortars*, PhD thesis, Institute For Uorganisk Kjemi Trondheim, Norway.

Page, C. L., Short, N. R. & Tarras, A. E. (1981), "Diffusion of chloride ions in hardened cement pastes", *Cement and Concrete Research*, **11** pp. 395-406.

Patel, R. G., Killoh, D.C., Parrott, D. J. & Gutteridge, W. A. (1988), "Influence of curing at different relative humidities upon compound reactions and porosity in portland cement paste", *Materials and Structure*, **21**, pp. 192-197.

Perkins, P. H. (1984), "The use of SBR/cement slurry for bonding coats", *Concrete*, **18**, No.3

Plum, D. R. (1990), "The behaviour of polymer materials in concrete repair, and factors influencing selection", *The Structural Engineer*, **68**, NO. 17 pp. 337-345.

Ramachandran, V. S. (1969), *Applications of Differential Thermal Analysis in Cement Chemistry*, Chemical Publishing Company, INC. New York.

Ramachandran, V. S. & Sereda, P. J. (1973), "Differential thermal studies of polymethyl methacrylate-impregnated cement pastes", *Thermochimica Acta.*, **5**, pp. 443-450.

Ramachandran, V. S. & Sereda, P. J. (1977), "A discussion of the paper, 'Differential thermal analysis of premixpolymer cement materials' by Cook, D. J., Morgan, D. R., Sirivivatnanon, V. & Chplin, R. P. (1976)", *Cement and Concrete Research*, **7**, pp. 355-356.

Salbin, M. (1996) "*Properties and performance of polymer modified cements and mortars*" PhD thesis, Aston University, Birmingham.

Sandrolini, F. Saccant, A. and Motori, A. (1992), "Influence of polymer phase distribution on the mechanical properties of premix PMC materials", *The 7th International Congress of Polymers in Concrete*, pp. 153-165.

Sergi, G., Yu, S. W. & Page, C. L. (1992), "Diffusion of chloride and hydroxyl ions in cementitious materials exposed to a saline environment", *Magazine of Concrete Research*, **44**, No.158, Mar. pp. 63-69.

Shaw, I. M. (1989), *Interactions between organic polymers and cement hydration products*. PhD thesis, Aston University, Birmingham.

Shi, D. & Winslow, D. N. (1985) "*Contact angle and damage during mercury intrusion into cement paste*" *Cement and Concrete Research*, **15**, pp. 645-654.

Skalny, J. & Young, J. F. (1980), "Mechanisms of portland cement hydration", *7th International Symposium on the Chemistry of Cement*, **1**, II-1/3.

Smutzer, R.K. & Hockett, R.B. (1981), "Latex modified portland cement concrete-A laboratory investigation of plastic and hardened properties of concrete mixture containing three formulations used in bridge deck overlays", Indian State Highway Commission.

Soroushian, P., Aouadi, F. & Nagi, M. (1991), "Latex-modified carbon fiber reinforced mortar", *ACI Materials Journal*, **88**, No.1, pp. 1-17.

Steinor, H. A. (1952), "Discussion of paper by Hansen, W. C.", *Third International Symposium on the Chemistry of Cement*, London, pp. 627-631.

Su, Z., Bijen, J. J. & Larbi, J. A. (1991), "Influence of polymer modification on the hydration of portland cement", *Cement and Concrete Research*, **21**, pp 535.

Swamy, R. N. (1979), "Review polymer reinforcement of cement systems", *Journal of Materials Science*, **14**, pp 1521-1553.

Tang, L & Nilsson, L. O. (1993), "Chloride binding capacity and binding isotherms of OPC pastes and mortars", *Cement and Concrete Research*, **23**, pp. 247-253.

Taylor, H. F. W. & Turner, A. B. (1987), "Reactions of tricalcium silicate paste with organic liquids", *Cement and Concrete Research*, **17**, pp. 613-623.

Taylor, H. F. W. (1990), *Cement Chemistry*, Academic Press Harcourt Brace Jovanovich, Publisher London.

Teichman, H. (1976), "Polymer Dispersion for cement and concrete", *The first International Congress of Polymers in Concrete*, London, pp. 112-124.

Wagner, H. B. (1965) "Polymer-modified hydraulic cements" I&EC Product research and Development. Editor Hader, R. N. **4**, pp. 191-197.

Tritthart, J. (1989), "Chloride binding in cement", *Cement and Concrete Research*, **17**, pp. 586-584.

Wagner, H. B. (1967), "Hydration-limited, Polymer-modified hydraulic cements", in Hader, R. N. (ed), *I&EC Product research and Development.*, **6**, pp. 223-231.

Wagner, H. B. & Grenley, D. (1978), "Interphase effects in polymer-modified hydraulic cement", *Journal of Applied Polymer Science*, **22**, pp. 813-822.

Walters, D. G. (1987), "What are latexes?", *Concrete International*, pp. 44-47.

Walters, D. G. (1988), "Latex Hydraulic cement additives", *Transportation Research Board*, Session 195.

Walters, D. G. (1990), "Composition of latex-modified portland cement mortars", *ACI Materials Journal*, **87**, No.4 pp. 371-377..

Wexham Developments Ltd. (1988), *JAF Conduction calorimeter operating manual*, Slough.

Wu X., Roy, D. M. & Langton, C. A. (1983), "Early stage hydration of slag - cement", *Cement and Concrete Research*, **13**, pp. 277-286.

Yu, S. W. & Page, C. L. (1991), "Diffusion in cementitious materials: 1. Comparative study of chloride and oxygen diffusion in hydrated cement pastes", *Cement and Concrete Research*, **21**, pp. 581-588..

APPENDIX A

X-RAY POWDER DIFFRACTION FILE OF CEMENT-BASED MATERIALS

Calcium Hydroxide Ca(OH)_2

2.63-x 1.93-4 1.80-4 1.69-2 1.48-1 1.45-1 4.90-7 3.11-2

Calcium Carbonate CaCO_3

3.40-x 3.27-5 2.70-5 2.48-3 2.37-4 2.34-3 1.98-7 1.88-3
 3.04-x 2.50-1 2.29-2 2.10-2 1.91-2 1.88-2 1.60-1 3.86-1
 3.30-x 2.73-x 2.07-6 1.86-3 1.82-7 1.65-3 4.23-2 3.57-6

Dicalcium Silicate C_2S

2.71-x 2.81-5 1.96-5 2.22-4 1.58-4 3.90-2 1.56-2 .00-1
 2.75-9 2.80-7 2.79-x 2.92-3 2.32-2 3.20-2 2.77-2 2.87-1
 2.74-x 2.80-x 2.78-9 2.61-7 2.19-7 2.73-4 2.72-4 2.88-4
 2.74-x 3.01-5 1.90-5 1.80-3 1.63-3 4.32-2 3.80-2 1.75-2

$\gamma\text{C}_2\text{S}$

2.74-x 3.04-8 2.77-6 1.92-5 3.83-4 4.36-3 2.48-2 1.65-2

$\beta\text{C}_2\text{S}$

2.72-x 2.79-9 2.75-x 2.61-8 2.19-6 2.73-5 2.28-4 2.04-3

Tricalcium Silicate C_3S

2.77-7 2.79-x 2.6-9 3.02-7 2.75-7 3.06-6 2.74-6 2.62-6
 2.76-x 2.74-9 2.59-9 2.18-9 1.76-9 1.49-9 3.02-8 1.62-8

Silicate Hydrate: Calcium $\text{Ca}_2\cdot\text{SiO}_4\cdot\text{H}_2\text{O}$

3.04-x 2.84-6 2.70-8 2.47-6 1.90-8 1.80-6 1.66-6 1.26-6

$\text{CaO}\cdot\text{SiO}_2\cdot\text{H}_2\text{O}$

3.07-x 2.97-x 2.81-x 2.28-7 1.83-x 1.67-x 11.0-8 5.50-7

$x\text{CaO}\cdot\text{SiO}_2\cdot y\text{H}_2\text{O}$

3.07-9 5.53-8 14.0-x 2.98-8 2.81-8 1.83-8 3.25-7 2.72-7

Calcium Alumium Oxide Hydrate
CaO.Al₂O₃.10H₂O

14.2-9 3.56-1 7.16-x 2.56-1 2.27-1 4.73-1 5.37-1 3.70-1

3CaO.Al₂O₃.8-12H₂O

7.65-x 3.77-9 2.86-7 1.65-7 2.46-6 2.31-6 2.10-3 1.43-5

CaO.Al₂O₃.xH₂O

7.73-x 4.02-8 8.33-x 3.88-8 2.87-8 2.45-8 1.65-8 2.69-6

Etringite

3CaO.Al₂O₃.3CaSO₄.31H₂O

9.73-x 5.61-8 3.88-5 2.56-5 2.21-5 2.77-4 4.69-4 3.84-3

Monosulphate

3CaO.Al₂O₃.CaSO₄.12H₂O

8.9-x 4.45-9 2.23-3 3.99-2 2.42-2 2.19-2 2.07-2 2.88-1

3CaO.Al₂O₃.CaSO₄.13H₂O

8.92-x 2.87-7 4.46-6 3.99-6 2.45-6 2.41-5 1.66-5 2.73-4

Calcium Alumium Chloride Sulphate Hydrate

6CaO.2Al₂O₃.CaSO₄.CaCl.24H₂O

8.32-x 4.18-x 2.87-5 3.35-4 2.39-3 2.37-3 2.44-2 2.24-2

APPENDIX B CALIBRATION OF HYDRATION CURVES AND CALCULATION OF TOTAL HYDRATION HEAT

The theory of calibration of hydration curves has been described in Chapter 4. Here provides an example of the procedure of calibration by using a computer. The calculations include the calculation of calorimeter constants k_1 and k_2 , total hydration heat Q_t and hydration degree a .

To enter the experimental program, type in

C:/cd QBX and RETURN

C:/QBE/WEX and RETURN

and then enter the following experimental parameters which are asked on the screen:

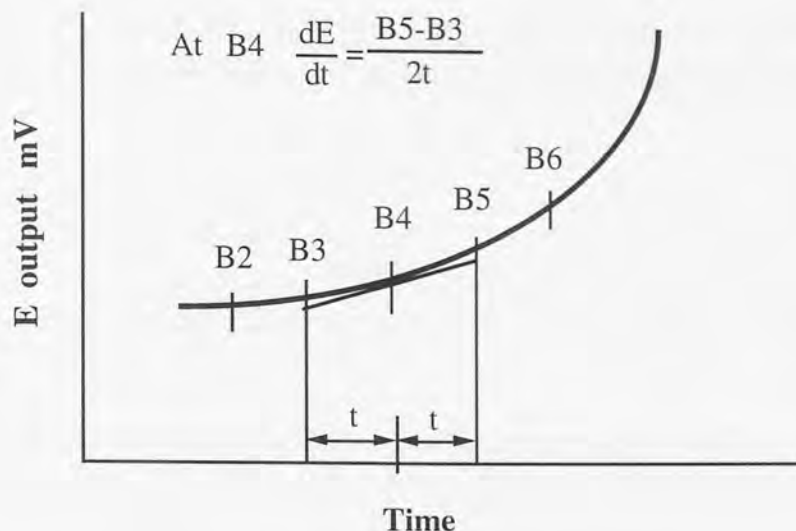
File name for channel one: 10%SBR 1
How mang readings for channel one? 580
Time interval between readings (min.)? 5

File name for channel two:
.....
.....

Press space bar to start

Determination of the rate of change of output (dE/dt) and Calculation of the calorimeter constants (k_1 and k_2)

The rate of change of output (dE/dt) at a particular time may be estimated from the output chart as shown below:



For example, if the output values B2 to B6 mV taken at intervals of time t (saying 5 min), then at point B4:

$$\frac{dE}{dt} = \frac{B5-B3}{2t}$$

If using a computer, this is easy to be done. Input the experimental data into an Excel worksheet (see Table B. 1). In Cell C4 enter formula, $\frac{B5-B3}{2 \times 5 \times 60}$ and fill down. This column gave the values of $\frac{dE}{dt}$ in the equation : $W=k_1E+k_2\frac{dE}{dt}$. In order to get k_1 and k_2 , block B520:C540 and do regression analysis. It should be noted that B520 is the point where the calorimeter output rises up (ignoring first few readings) and B540 is the point where the output reaches the maximum. From the regression line (see Fig.4.4), we got the slope of the line, thus, the calorimeter constants k_1 and k_2 .

In Column D, enter formula $\frac{k_1 \times B + k_2 \times C}{30}$ to transfer mV/g to w/kg. Plot Column A against Column D, we got the calibrated hydration curve.

Calculation of total hydration heat (Q) and hydration degree (a)

The total hydration heat over experimental period is the area under the hydration curve, which can be obtained by and suitable numerical integration technique, such as Trapezoidal Rule. In Column E, enter formula $5 \times 60 \times D$ (since time interval is 5 min). In Cell F4, enter formula $E4 + E3$, and in Cell F5 enter $E5 + F4$ and fill down. The hydration heat (Qt) at any time is shown in Column F. It should be mentioned that the heat evolved by the the heater during the calibration should be deducted from the total heat. The total heat over 72 hours (Q72) can be obtained by extending the tail of hydration

curve. In order to calculate the hydration degree (α) at various time, enter $G/Q72$ in Column **G**. The hydration degree (α) is used in the calculation of hydration kinetics parameters.

TABLE B. 1

A worksheet of Excel for calibration of hydration curve and calculation of total heat

1	A	B	C	D	E	F	G
2	time	readings (mV)	dE/dt	W/kg		Qt (kJ)	α
3	0	6.3270		7.3167	2194.999	2.1950	0.0152
4	5	1.3100	-4.52E-04	2.0012	600.431	2.7950	0.0194
5	10	1.0390	-2.96E-04	0.4515	135.4617	2.9305	0.0203
6	15	0.8613	-1.99E-04	0.4587	137.6136	3.0681	0.0212
7	20	0.7418	-1.39E-04	0.4552	136.5684	3.2046	0.0222
8	25	0.6585	-9.88E-05	0.4465	133.9482	3.3386	0.0231
9	30	0.5993	-7.87E-05	0.4325	129.7512	3.4683	0.0240
...
520	2585	0.2650	-1.67E-06	0.2433	73.0011	123.0394	0.8520
521	2590	0.2640	5.05E-04	0.5844	175.3296	123.2147	0.8532
522	2595	0.5668	7.20E-04	1.3529	405.8652	123.6206	0.8561
523	2600	0.9988	4.83E-04	1.7370	521.1021	124.1417	0.8597
524	2605	1.2888	3.13E-04	1.7283	518.4972	124.6602	0.8633
525	2610	1.4763	2.03E-04	1.7112	513.3669	125.1735	0.8668
526	2615	1.5980	1.37E-04	1.7044	511.3068	125.6848	0.8704
527	2620	1.6800	9.29E-05	1.7054	511.6326	126.1965	0.8739
528	2625	1.7358	6.54E-05	1.7086	512.5731	126.7091	0.8774
529	2630	1.7750	4.42E-05	1.7117	513.5226	127.2226	0.8810
530	2635	1.8015	3.21E-05	1.7136	514.0785	127.7367	0.8846
531	2640	1.8208	2.46E-05	1.7181	515.4237	128.2521	0.8881
532	2645	1.8355	1.75E-05	1.7218	516.5403	128.7686	0.8917
534	2650	1.8460	1.37E-05	1.7241	517.2435	129.2859	0.8953
535	2655	1.8543	8.75E-06	1.7258	517.7475	129.8036	0.8989
536	2660	1.8595	7.08E-06	1.7261	517.8447	130.3215	0.9025
537	2665	1.8638	5.00E-06	1.7275	518.2584	130.8397	0.9060
538	2670	1.8668	3.75E-06	1.7280	518.4108	131.3581	0.9096
539	2675	1.8690	2.08E-06	1.7281	518.4405	131.8766	0.9132
540	2680	1.8703	2.50E-06	1.7284	518.5323	132.3951	0.9168
541	2685	1.8718	1.67E-06	1.7295	518.8626	132.9140	0.9204
...

APPENDIX C AN ESTIMATION OF POLYMER LAYERS COVERING CEMENT GRAINS

Polymer particle layers, which surrounded the cement grains can be estimated by the following calculations. Take SBR latex as an example and let its particle diameter be 0.17 μm and specific gravity of latex be 1.01. Assume that specific area of cement is 3500 cm^2/g . When SBR addition is 20%, there are 0.2g SBR solid particles in 1g cement.

$$\begin{aligned} \text{Volume of 0.2g SBR} &= \frac{0.2}{1.01} \text{ cm}^3 \\ &= 19.802 \times 10^{10} \mu\text{m}^3 \end{aligned}$$

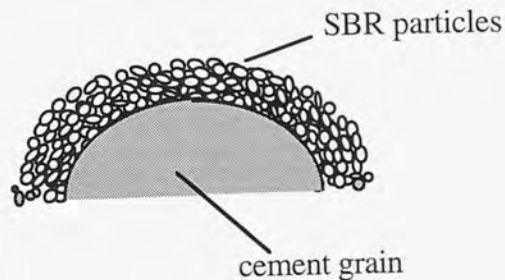
$$\text{number of particles in 0.2g SBR} = \frac{19.802 \times 10^{10}}{\frac{4\pi}{3} \cdot \left(\frac{0.17}{2}\right)^3}$$

$$\text{area covered by SBR particles} = \pi \cdot \left(\frac{0.17}{2}\right)^2 \cdot \frac{19.802 \times 10^{10}}{\frac{4\pi}{3} \cdot \left(\frac{0.17}{2}\right)^3}$$

$$\begin{aligned} &= 174.72 \times 10^{10} \mu\text{m}^2 \\ &\approx 17500 \text{ cm}^2 \end{aligned}$$

$$\text{possible layers of SBR particles} = \frac{17500}{3500} = 5$$

Thus, with 20% SBR addition cement grains may be covered by up to 5 layers of SBR particles as shown below.



APPENDIX D PAPERS PUBLISHED AND SUBMITTED FROM THE STUDY

1. Zeng, S. Short, N. R. and Page, C. L. (1996) "Early Age Hydration Kinetics of Polymer modified Cement" *Advances in Cement Research*. **8**. No.29 Jan. pp1-9
2. Short, N. R. Zeng, S. and Page, C. L. "Steady and Non-Steady State Diffusion of Chloride Ions in Polymer Modified cement" Submitted to *Cement and Concrete Research*.



Aston University

Content has been removed for copyright reasons



Aston University

Content has been removed for copyright reasons



Aston University

Content has been removed for copyright reasons